

Cover Page



Universiteit Leiden



The handle <http://hdl.handle.net/1887/25830> holds various files of this Leiden University dissertation.

Authors: Bovenberg, Maria Sarah Sophie & Degeling, Marja Hannah

Title: Cancer and glioma : an integrated approach of gene therapy and bioluminescence imaging

Issue Date: 2014-05-27

Cancer and Glioma

An integrated approach of Gene Therapy and
Bioluminescence Imaging



Sarah Bovenberg and Hannah Degeling

SUBSIDIES

Sarah Bovenberg: Fulbright, Huygens Scholarship Program, VSB fonds, Jo Keur fonds, Saal van Zwanenberg Stichting, en het Afdelingsfonds Neurochirurgie Leiden.

Hannah Degeling: Fulbright, Saal van Zwanenberg Stichting, VSB fonds, Dr. Hendrik Muller Vaderlandschfonds, KWF Kankerbestrijding, Hersenstichting, Jo Keur fonds, Massachusetts General Hospital, en het Afdelingfonds Neurochirurgie Leiden.

CANCER AND GLIOMA

An integrated approach of Gene Therapy and Bioluminescence Imaging

Proefschrift

ter verkrijging van de graad van Doctor aan de Universiteit Leiden, op gezag van
Rector Magnificus prof. mr. C.J.J.M. Stolker, volgens besluit van het College voor
Promoties te verdedigen op dinsdag 27 mei 2014

klokke 15.00 uur

door

Maria Sarah Sophie Bovenberg
geboren te Utrecht in 1987

klokke 16.15 uur

door

Marja Hannah Degeling
geboren te Amsterdam in 1986

Promotiecommissie

Promotor

Prof. dr. W.C. Peul

Co-promotores

Dr. C.L.A.M. Vleggeert-Lankamp

Dr. B.A. Tannous, verbonden aan Harvard University

Overige leden promotiecommissie

Prof. dr. R.C. Hoeben

Prof.dr. S. Leenstra, verbonden aan de Erasmus universiteit Rotterdam

Prof.dr. M. J. B. Taphoorn, verbonden aan de Vrije universiteit Amsterdam

Dr. T. Wurdinger, verbonden aan de Vrije universiteit Amsterdam

The scientific theory I like best is that the rings of Saturn are composed entirely of lost airline luggage.

-Mark Russell

TABLE OF CONTENTS

Chapter 1	Introduction to Glioma	p11
Chapter 2	Introduction to the Tannous Lab	p31
Chapter 3	Enhanced <i>Gaussia</i> Luciferase based blood assay for monitoring of <i>in vivo</i> biological processes	p71
Chapter 4	Multiplex blood reporters for simultaneous monitoring of cellular processes	p83
Chapter 5	Novel triple bioluminescence imaging system for monitoring of Glioma response to combined soluble TRAIL and Lanatoside C therapy	p97
Chapter 6	Directed molecular evolution reveals <i>Gaussia</i> Luciferase variants with enhanced light output stability	p123
Chapter 7	Codon-optimized <i>Luciola italica</i> luciferase variants for mammalian gene expression in culture and <i>in vivo</i>	p143
Chapter 8	A simple and sensitive assay for mycoplasma detection in mammalian cell culture	p161
Chapter 9	<i>Gaussia</i> Luciferase-based mycoplasma detection assay in mammalian cell culture	p177
Chapter 10	Multimodal targeted high relaxivity thermosensitive liposome for <i>in vivo</i> imaging	p191

Chapter 11	Advances in stem cell therapy against glioma	p217
Chapter 12	Cell-based immunotherapy against glioma: from bench to bedside	p249
Chapter 13	Discussion: future perspectives of Sarah Bovenberg (I) and Hannah Degeling (II)	p275
Chapter 14	Summary	p303
Chapter 15	Nederlandse samenvatting	p311
	Acknowledgements	p323
	Curriculum vitae and list of publications Sarah Bovenberg	p328
	Curriculum vitae and list of publications Hannah Degeling	p330

CHAPTER I



INTRODUCTION TO CANCER AND GLIOMA

1. CANCER

In 2008 (most recent data) 0.5% of the 304,059,724 people in the United States developed an invasive form of cancer. Breast cancer (inc. 184,450 , † 40,930), colon and rectum cancer (inc. 148,810, † 49,960), lung cancer (inc. 215,000, † 161,840), and prostate cancer (inc.186,320, †28,660) appear to be the most common forms. Of the 1,437,180 people who developed cancer, around 21,810 got brain and/or other central nervous system tumors with a corresponding death rate of 13,070; which is more than half of the incidence in that year. When studying these numbers, one can see that apart from central nervous tumors, lung cancer too has a relatively high death rate. However, one should take into consideration that lung cancer often occurs at a higher age than brain cancer cases.¹

In 2008 in The Netherlands an incidence of 90,182 (0.5%) of invasive cancer cases was reported on a population of 16,446,000 people in total. The most common type of cancer was breast cancer, with an incidence of 13,121 and a death rate of 3357. Similar to the US the other most common types of cancers were lung cancer (11,507, † 10,339), prostate cancer (10,512, † 2,476), and colon cancer (19,654, † 12,202). Cancer of the central nervous system had an incidence of 1156 and a death rate of 992.² As one can see, the numbers in The Netherlands reflect those of the United States.^{2,3,1} The conclusion that can be drawn from these numbers is that in order to prevent death extensive research is needed for early diagnosis and treatment of invasive cancer in general. A particular high focus is necessary for the deadly central nervous system tumors.

Table 1.: Cancer incidence and death rates for the USA and The Netherlands (2008).

<i>USA</i>	<i>Incidence</i>	<i>Death</i>	<i>% Death</i>	<i>The Netherlands</i>	<i>Incidence</i>	<i>Death</i>	<i>% Death</i>
Breast	184,450	40,930	22.19030	Breast	13,121	3,357	25.58494
Colon	148,810	49,960	33.57301	Colon	19,654	12,202	62.08405
Lung	215,000	161,840	75.27442	Lung	11,507	10,339	89.84966
Prostate	186,320	28,660	15.38214	Prostate	10,512	2,476	23.55403
CNS	21,810	13,070	59.92664	CNS	1,156	992	85.81315

Abbreviations: USA, United States of America; CNS, Central Nervous System.

Cancer is simply stated by the transformation of a healthy cell into a malignant cancer cell. This malignant transformation can be predisposed by genetic factors, but

environmental influences mostly underlie the process of cancer. When environmental factors are the cause, think of certain chemicals, radiation or biological causes such as bacteria and viruses. It is important to take a closer look at the development of cancer cells, namely, which genes are involved? We can separate at least four groups of genes involved in this malignant transformation: oncogenes, tumor suppressor genes, DNA repair genes, and the gene encoding telomerase. The first oncogenes were discovered ironically with the help of viruses. It was rationalized that if a virus could be held responsible for the onset of cancer, then the genome of that virus should contain the responsible sequences for that onset. Furthermore, in the 70's Bishop and Varmus discovered that normal human cells too could have these similar gene sequences without the process of any malignancy. Nevertheless, these genes were as a matter of fact involved in the regulation of cell growth and differentiation and could therefore be defined as pro-oncogenes. Sometimes, numerous copies of those oncogenes occur in a cancer cell such as the c-erb-B2 gene which is repeated in a certain type of breast cancer or N-myc which can have an important role in the development of the neuroblastoma. Other processes associated with these oncogenes are chromosomal translocation, point mutations and viral infection, with the latter due to the incorporation of a virus into the human genome.

Tumor suppressor genes can be held responsible for the onset of a cancer cell when the expression of these genes is suppressed in response to different stimuli, for example a point mutation or a genetic cause; hence cell growth is no longer limited. DNA repair genes are not directly responsible for cancer formation, however, since they are the care takers of the DNA, their absence or inadequate function will lead to instability in the genome and thus leading to a higher chance of cancer formation. A lot of research on telomerase expression resulted recently in the discovery that telomerase is present in almost all carcinoma cells; therefore, telomerase could have a great diagnostic and maybe even therapeutic value.⁴

The transcription factor Nuclear Factor kappa B (NF- κ B), will be discussed shortly to give a quick impression of the complexity and interaction chains involved in the onset of cancer. The NF- κ B complex in the cytoplasm of the cell is usually bound to the I κ B family making it impossible for NF- κ B to travel to the cell nucleus and bind to the DNA for further action. Many different signals, such as growth factor and hormones, can result in the activation of I κ B kinase responsible for phosphorylation of I κ B and

thereby releasing NF- κ B dimers. These dimers are then translocated to the nucleus where they bind to the κ B location in the promoter or enhancer region of the target genes controlling the expression of this gene. When NF- κ B is activated, the transcription of many genes is induced. Moreover, NF- κ B seems to be a key mediator in inflammation, tumor onset and growth and the formation of blood vessels. NF- κ B activation is also known to be associated with numerous types of cancer.⁵ This example should give us an understanding of how important it is to reveal the function of these molecular factors in cancer and by further exploring some of these processes. This is exactly where the field of molecular imaging has been indispensable. By revealing these biological processes step by step, each discovery is a step closer to better cancer diagnostics and treatment.

One can also think about the biological processes of metastatic cells, which involve numerous genes and proteins. The journey of metastasis is nonetheless not easy for a cancer cell. The estimation is that around 0.01% of the tumor cells will be able to depart from the original site, survive the blood stream, attach to a suitable tissue and manipulate normal cells for the malignant transformation. However, once a cancer cell is able to metastasize, the new colonies are more resistant to the standard treatment than the original tumor due to their genetic alternations.

To overcome this problem research focuses on different theories of metastasis. One can see cancer for example as an inflammatory disease that uses immune cells for its spread and therefore the metastasis can be limited by the inhibition of the immune system. Or one can see metastasis as an embryonic process and the traveling cancer cells are in fact cancer stem cells that use the properties of a stem cell to migrate.

Recently, individual tumor cells were detected in the blood stream of patients with early-stage cancer, suggesting that the onset of metastasis might even take place in the beginning of the cancer formation. This would open the doors for early-stage cancer detection by simple blood assays.

Nevertheless, the facts that some tumor cells need years to spread whereas others go out immediately and that metastatic tumor cells look different in every organ, remain a barrier for early detection and treatment. Besides, what if the cancer cells that are not killed by the chemotherapeutic obtain mutations, which transform them into even more resistant killers?⁶

2. GLIOMA

Gliomas account for 31% of all tumors in the Central Nervous System (CNS) and for 78% of all CNS malignancies (www.Cbtrus.org). Malignant gliomas are classified as astrocytoma, oligodendroglioma, or oligo-astrocytoma and histologically graded as WHO grade II, III (anaplastic) or IV.⁷ Grade II tumors are associated with a survival time of 5 to 15 years, while grade III gliomas often predict a survival time of less than 3 years. Glioblastoma Multiforme (GBM, or astrocytoma grade IV) is the most malignant of all glial tumors and has an extreme poor prognosis, with an average 5 years survival of only 3.3% and the majority of patients dying within a year. Without treatment median survival is 4-6 months.⁸ The characteristics of this malignancy include uncontrolled cellular proliferation, invasiveness with both long root like processes and single invasive cells, areas of necrosis, and extensive angiogenesis.⁹ ¹⁰ Furthermore, the GBM cells are resistant to apoptosis, and possess multiple genetic alterations.¹¹ Primary GBM occurs de novo, without a pre-existing less malignant precursor lesion, and comprises over 90% of the GBM cases. Secondary GBM occurs through progression of a low grade astrocytoma or anaplastic astrocytoma and generally occurs in younger patients.¹²

The current standard of care treatment for GBM consists of surgical macroscopic debulking of the tumor mass, followed by both radiation and chemotherapy.^{13, 14} Progression free survival in the first 6 months appears to be directly related to the amount of tumor mass removed, with a more extensive resection corresponding to a better outcome (41 vs. 21%).^{15, 16} Combined treatment with radiation and temozolomide further increases median survival to 12-14 months, which is significantly better than the results achieved with radiation alone (median survival: 9 months).^{8, 15, 17} However, regardless of treatment most patients die within a year from new secondary tumor foci forming within 2 cm of the resected area.^{18, 19}

2.1 Factors complicating GBM treatment

Evidently, GBM is difficult to treat. Average survival increased with months instead of years, while researchers worldwide are working hard to find a cure. The aggressive

behavior of GBM tumor cells is caused by an array of tools that are specifically designed to escape eradication. The distinct tumor heterogeneity, the ability to escape the cellular immune response, the resistance to therapy, the interaction between the tumor cells and the microenvironment, and the inability of treatment to reach all tumor cells make GBM such a challenge to treat.

2.1.1 Tumor heterogeneity

One of the hallmarks of GBM is its heterogeneity. Cells differ in morphology, behavior and genetics²⁰ and consequently it is very difficult to grade the tumors, measure response to therapy and understand the mechanisms of resistance. Not one GBM tumor is similar to another. Primary and secondary GBM appear morphologically the same, but genetically, differences are profound.²¹ It is thus unlikely that one standard therapy aimed to cure all tumors diagnosed as GBM can be developed.

Necrosis is one of the features of GBM and is thought to play an important role in the development of the heterogeneity of the cell population. First, hypoxia is likely to appear in tumor regions where metabolic demands exceed the supply or as a result of thrombolytic events that are often seen in glioma patients. As a result, migratory genes are triggered and cells start to move away from the hypoxic site, whereas necrosis ensues in the hypoxic center. A lining of palisade cells develops around this necrotic core, expressing an abundance of angiogenic and growth factors and thereby facilitating angiogenesis and tumor proliferation.^{22, 23} At the same time, a clonal selection takes place selecting highly malignant tumor cells that are resistant to apoptosis by inactivation of p53.²⁴ The selection of more highly malignant cells may then again lead to a higher metabolic demand, causing a vicious cycle of hypoxia, necrosis, selection and proliferation; resulting in a very heterogeneous population of cells, which are highly resistant to conventional therapy. Therefore, necrosis is a very powerful predictor of a bad outcome.¹⁰

2.1.2 Tumor invasion in the microenvironment

Gliomas are known for their tendency to infiltrate the surrounding brain parenchyma, which makes it very difficult to rely on locally applied treatment, like surgery. After initial surgery, tumor reoccurrence usually takes place within 2 cm of the original tumor site, suggesting that at the time of surgery individual cells already invaded the surrounding brain tissue. This is one of the major challenges in GBM treatment and makes a better understanding of both tumor cell biology and tumor microenvironment highly desired.

Tumor invasion is a very intricate process involving a combination of the ability to migrate (cell motility) and the ability to modulate the extracellular matrix (ECM). These abilities are present in both low and high grade gliomas, suggesting they are acquired early in tumorigenesis.⁹ Preferential patterns of migration can be discerned, including migration along the white matter tracts, around neurons in the gray matter (a phenomenon known as perineural satellitosis), perivascular growth and subpial spread.⁹ These patterns suggest the existence of some sort of tropism or a restricted ability of GBM to invade specific regions between certain cell combinations and also show that interactions with the tumor microenvironment play an important role in the process of invasion.²⁵

To facilitate invasion, GBM cells display a wide array of tools. First, a variety of proteases such as cysteines, serines and matrix metalloproteinases (MMP's) is secreted by the tumor cells to degrade the ECM in order to allow migration, and to remodel the ECM in a way that facilitates tumor growth.²⁶ Expression of these proteases increases with tumor grade. Further, an increase of integrin receptors can be observed, facilitating the interaction of the cells with the ECM molecules and thereby modifying the cell cytoskeleton towards locomotion. Kinases such as the cytosolic Focal Adhesion Kinase (FAK) are activated by epidermal growth factor receptor (EGFR) which in turn activates downstream pathways involved in proliferation, survival and migration.^{27, 28} Growth factors as fibroblast growth factor (FGF), epidermal growth factor (EGF), vascular endothelial growth factor (VEGF), platelet derived epidermal growth factor (PDEGF) and their receptors are upregulated and promote both proliferation and migration. EGFRVIII mutation is often

found in GBM and is known to upregulate expression of genes responsible for MMP and collagen production, thereby further facilitating invasion.²⁹

The final tool GBM cells display in their attempt to remodel the ECM into an optimal niche for growth and development is the creation of a zone of local immune suppression. Immunosuppression is facilitated by cell-to-cell contact and by the secretion of various cytokines. This strategy leads to T cell activation inhibition and the initiation of T cell apoptosis, and thereby prevents the immunessystem form actively attacking the tumor cells.³⁰

2.1.3 Angiogenesis in GBM

In order to adapt to hypoxic conditions once the tumor mass increases, GBM cells release pro inflammatory agents. Also, GBM cells have the ability to transdifferentiate in tumor derived endothelial cells (TDEC).³¹ These TDEC are capable of forming vascular structures within the tumor, reestablishing oxygen and nutrient flow and making GBM one of the most vascularized tumors. However, anti-angiogenesis treatment with anti-VEGF receptor inhibition does not seem to affect the TDEC's.

2.1.4 Blood Brain Barrier

Since extra-neural spread of GBM is very rare, the most convenient method of treatment would be local in the CNS. However, the delivery of therapeutics is challenging due to a natural filtering mechanism, the blood-brain-barrier. Most chemotherapeutics are unable to cross this barrier, or are cleared very rapidly out of the brain extracellular space. The integrity of the blood-brain-barrier varies per region and this affects the locally available drug concentration.³² GBM cells are capable of pumping out drugs after uptake, by means of P-glycoprotein and other pumps.³³ The high intratumoral pressure further complicates delivery of therapeutic agents. Damage to healthy brain tissue, due to the limited intracranial space, is another point of concern.

2.1.5 Cancer Stem Cells

The “old” stochastic model on tumor growth proclaims that all cells in a tumor are biologically equivalent and are able to initiate or drive tumor formation, due to accumulation of mutations.^{34, 35} In contrast, the Cancer Stem Cell (CSC) theory suggests that a rare population of tumor cells is responsible for tumor growth, resistance and recurrence.³⁶ These cells are named Cancer Stem Cells because of their “normal stem cell” like properties; they share important characteristics with stem cells, including their ability of limitless self-renewal and differentiation.³⁷ They are capable of generating a diverse population of cells, both tumorigenic and non-tumorigenic, present in tumors. They seem to exclusively drive tumor growth and to give rise to a diverse progeny.³⁸ Once implanted in immunogenic mice, CSC are capable of generating a photocopy of the original malignancy of which they were extracted.³⁹ Both models are depicted in figure 1.

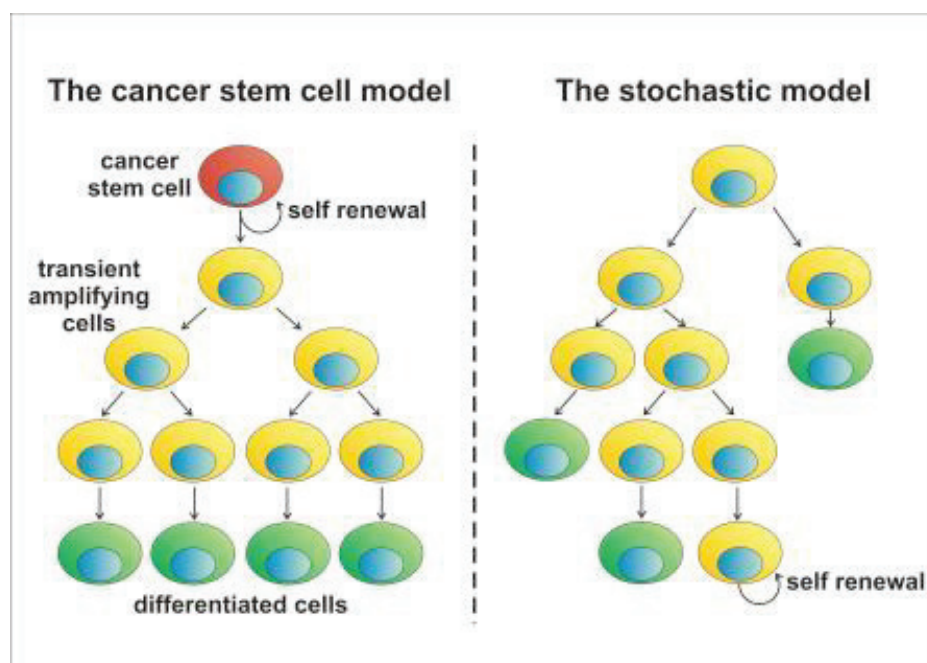


Figure 1. Model of cancer theories. The CSC theory suggests a strong hierarchical pattern within the tumor. Cancer stem cells are the only cells capable of self-renewal and proliferation. They initiate and drive tumor growth. The stochastic model describes tumor

growth as a random process. Accumulation of genetic alterations and mutations drives tumor growth and all cells can contribute to this process. Red: CSC. Yellow: transient amplifying cells. These cells are slowly maturing and lose their ability of self-renewal along the way. Green: fully differentiated tumor cells that are no longer capable of self-renewal. Image adapted from www.eurostemcell.org

The CSC theory implies that indiscriminate killing of all cancer cells may be an inefficient and ineffective way to treat cancer, since it is not targeted to eliminate the few CSC that actually drive the cancer. In this scenario the treatment will kill the proliferating “innocent” cell population, and since these cells consists of the majority of the tumor, treatment will seem effective. However, CSC are known to be very resistant to chemo- or radiotherapy due to their stem cell-like properties and their relative quiescence, and will remain at the tumor site (unless surgically removed), eventually causing a relapse (Figure 2).^{33, 40, 41} Selective targeting of CSC might be a better approach.

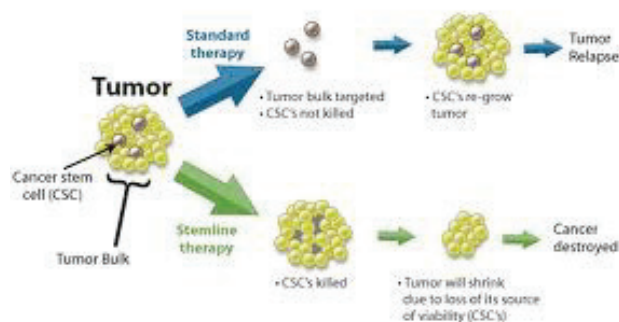


Figure 2 The effect of two different therapeutic approaches on CSC. If standard therapy is used, CSC will escape elimination and start the process of tumor initiation and proliferation all over again. Tumor relapse seems inevitable. If however, tumor therapy is aimed at CSC directly, CSC will die and the remaining tumor bulk, with no tumorigenic capacities of its own, will shrink and disappear, and no recurrence will occur. Image adapted from Lui et al. Cancer Research, 2011.

In GBM, glioma stem cells (GSC) have shown similarities to normal stem cells and progenitor cells, expressing the markers CD133 and Nestin.³⁷ This leads to concern of toxicity when using these markers to design drugs targeted to GSCs. Since glioma stem cells produce vascular endothelial growth factor (VEGF), promoting

angiogenesis, and since they appear to need a vascular niche for optimal functioning,⁴²⁻⁴⁴ the use of anti-angiogenic therapy to inhibit glioma CSC functioning might be a better strategic approach. There is ongoing discussion over the exact role of CSC and their characteristics,⁴⁵ but nonetheless CSC are believed to play an important role in GBM tumor initiation, progression and angiogenesis, making GBM so complicated to treat.

2.1.6 Genetic alterations and resistance to apoptosis

Resistance to apoptosis of GBM cells is very common. Genetic alterations that upregulate oncogenes and inactivate tumor-suppressor genes (including retinoblastoma protein (RB) and p53) are found in the majority of GBM cells.^{46, 47} This, combined with the natural selection of highly malignant clones, and the stem cell-like properties of a subgroup of the GBM cells, make that GBM cells are highly resistant to apoptosis.³³ In addition, GBM cells express a variety of molecules affecting both intrinsic and extrinsic apoptotic pathways. They secrete soluble decoy death receptors aimed at the natural defense mechanisms and often the Bcl2 family of anti-apoptotic genes is upregulated. Crosstalk between the anti apoptotic pathways further contributes to the difficulty of finding an effective treatment.

3. WHAT ARE THE CURRENT STRATEGIES FOR TREATING GBM?

3.1 Current treatment

The National Comprehensive Cancer Network states that standard treatment of GBM consists of maximal surgical removal of the tumor mass, 6 weeks postoperative radiotherapy, and concomitant systemic chemotherapy with temozolomide followed by 6 months of adjuvant treatment with temozolomide (NCCN guidelines version 2.2011: CNS Cancers, www.nccn.org).^{48, 49} Advances in both surgical and imaging techniques permit safer and more extensive removal of the tumor, but due to the highly invasive nature of GBM surgery is not intended to be curative. The prognosis after recurrence is very poor, and recommendations for adjuvant treatment strategies are ill defined. Current options include surgery with or

without camustine wafer placement (if the recurrence is local), radiotherapy, chemotherapy, anti-angiogenic agents (monoclonal antibody bevacizumab), or experimental therapies (www.nccn.org). Surgery seems to prolong survival up to a limited degree. The benefits of repeated radiotherapy remain unclear.⁵⁰⁻⁵² Due to toxicity to normal cells, high enough doses can't be delivered. Resistance to chemotherapy can be overcome by changes in dose regimen and by combining temozolomide with the cyclo-oxygenase 2 (COX-2) inhibitor rofecoxib, leading to an anti-angiogenic effect.⁵² Interestingly enough, not all anti-angiogenic agents seem to enhance the efficacy of temozolomide treatment. Combined temozolomide and bevacizumab regimens resulted in inferior outcomes than seen after treatment with bevacizumab or temozolomide monotherapy.⁵³ This may be partially explained by many patients with CNS tumors however require dexamethasone or anti-epileptic drugs, which in combination with temozolomide or other anti-cancer agents, may lead to drug-drug interactions with a reduced efficacy and an increase of side effects.⁵⁴

Genotyping for personalized medicine is slowly starting to influence treatment options. 60% of GBM tumors with chromosomal 1p loss respond to a chemotherapy regimen of PVC (procarbazine, CCNU and vincristine) combined with temozolomide, while 'regular' GBM tumors are not sensitive to this specific regimen. GBMs with EGFR amplification rarely respond to chemotherapy at all. O6-methylguanine DNA transferase or MGMT, a DNA repair enzyme that protects cells from damage caused by ionizing radiation and alkylating agents, is another powerful molecular predictor.^{55, 56} The MGMT promoter is methylated in 40 to 45% of GBMs, which means that cells are unable to properly repair DNA damage.^{57, 58} MGMT methylation is currently the strongest predictor of outcome and benefit of temozolomide treatment.⁵⁹ Simple genotyping assays screening patients for chromosomal 1p loss, EGFRIII mutation and MGMT promoter methylation can therefore not only increase quality of life (only exposing those patients to treatment that have a high chance of good response), but can further result in higher survival rates, since no time is wasted on the 'wrong' type of therapy.

Since GBMs are highly vascularized tumors, **anti-angiogenesis strategies** have received a great deal of attention. VEGF expression levels correlate with tumor

malignancy levels and many angiogenic factors are secreted (VEGF, PDGF, fibroblast growth factor 2 (FGF2), Hepatocyte Growth Factor).⁶⁰ Monoclonal antibodies directed against VEGF or its receptor (e.g. Bevacizumab) are FDA approved and currently in use, although treatment did not prove to be more effective than standard therapy (www.nccn.org)⁶¹ However, quality of life seemed to improve.^{62, 63} Side effects related to toxicity, resistance, and progression to a more invasive type of tumor are reported. Other strategies including small molecule inhibitors (Cediranib) designed to inhibit VEGFR2 Tyrosine Kinase activity, or soluble decoy receptors identical to VEGFR1 (Aflibercept) are currently under investigation in clinical trials.^{64, 65}

3.2 New foci of research

Due to the limited success of therapies discussed above, new foci of research have emerged. As discussed earlier, GBM tumors are highly heterogeneous, display all kinds of anti-apoptotic escape routes, suppress the immune system, invade the surrounding parenchyma with unmatched aggressiveness and possess a whole array of tools to rearrange the extra tumoral environment to their advantage. Integrins, the cell surface receptors responsible for cell adhesion to the ECM, are known to play a crucial role in the recruitment of the ECM by activating intracellular pathways responsible for cell survival, migration, and angiogenesis in both GBM cells and cells in their direct environment (fibroblasts, vascular endothelial cells, bone marrow derived cells).⁶⁶ Further, interaction between GBM cells and ECM molecules results in modification of the GBM cytoskeleton and locomotion. In a Phase II clinical trial, Cilengitide, a synthetic cyclic peptide that blocks the binding of integrin to its receptors, showed moderately positive results.⁶⁷ This drug is also being tested in combination with other anti cancer agents (www.clinicaltrials.gov).

Other targeted therapies aimed at disrupting the interactions between GBM and ECM include receptor tyrosine kinase inhibitors (blocking the activation of intracellular pathways associated with cell proliferation and migration) and small non-coding RNA's, which are used to inhibit cell to cell signal transduction and activation of stem cell pathways. The latter approach is believed to directly target cancer stem cells and, since this population is thought to be the driving source of tumor

proliferation and metastasis, should result in less aggressive behavior of the tumor as a whole. Unfortunately, so far the results of these strategies have been poor, with no survival benefit in GBM patients.

The fact that many of the single agent targeted therapies seem to fail is most likely attributable to the complexity of the interactions between GBM and ECM and to the crosstalk between the different intra- and extra cellular pathways, allowing tumor cells to overcome interventions and to escape cell death over and over again. The relatively low number of patients diagnosed with GBM makes recruitment for clinical trials and testing of new agents even more problematic. Further advances in surgery, genomics, proteomics, genetics and imaging modalities will be needed to get more insight in GBM tumor biology and to find diagnostics, predictive biomarkers, and targeted strategies to treat GBM successfully.

REFERENCES

1. society Ac. *Global Cancer Facts & Figures*. 2011. No.861811.
2. IKZ. IKZ integraal kankercentrum Zuid. Available at: http://www.ikz.nl/page.php?id=3146&nav_id=17&menu_id=3146. Accessed 01-19-2012.
3. SERVICES USDOHAH, Health Nio. *SEER Surveillance, Epidemiology, and End Results Program*. NIH Publication No. 05-4772; 2005.
4. Van de Velde e. *Oncologie*. Bohn Stafleu van Loghum; 2006.
5. Badr CE, Niers JM, Tjon-Kon-Fat LA, Noske DP, Wurdinger T, Tannous BA. (2009). Real-time monitoring of nuclear factor kappaB activity in cultured cells and in animal models. *Mol Imaging*.8(5):278-290.
6. Slomski A. *Metastasis: The Killing Fields*. protomag; 2009.
7. Cha S. (2006). Update on brain tumor imaging: from anatomy to physiology. *AJNR Am J Neuroradiol*.27(3):475-487.
8. Grossman SA, Ye X, Piantadosi S, Desideri S, Nabors LB, Rosenfeld M, et al. (2010). Survival of patients with newly diagnosed glioblastoma treated with radiation and temozolomide in research studies in the United States. *Clin Cancer Res*.16(8):2443-2449.
9. Louis DN. (2006). Molecular pathology of malignant gliomas. *Annu Rev Pathol*.1:97-117.
10. Louis DN, Ohgaki H, Wiestler OD, Cavenee WK, Burger PC, Jouvet A, et al. (2007). The 2007 WHO classification of tumours of the central nervous system. *Acta Neuropathol*.114(2):97-109.
11. Furnari FB, Fenton T, Bachoo RM, Mukasa A, Stommel JM, Stegh A, et al. (2007). Malignant astrocytic glioma: genetics, biology, and paths to treatment. *Genes Dev*.21(21):2683-2710.
12. Ohgaki H, Kleihues P. (2007). Genetic pathways to primary and secondary glioblastoma. *Am J Pathol*.170(5):1445-1453.
13. Sathornsumetee S, Rich JN, Reardon DA. (2007). Diagnosis and treatment of high-grade astrocytoma. *Neurol Clin*.25(4):1111-1139, x.
14. Walker MD, Green SB, Byar DP, Alexander E, Jr., Batzdorf U, Brooks WH, et al. (1980). Randomized comparisons of radiotherapy and nitrosoureas for the treatment of malignant glioma after surgery. *N Engl J Med*.303(23):1323-1329.
15. Stummer W. (2006). Perspectives in central nervous system malignancies. *IDrugs*.9(6):412-414.
16. Stummer W, Pichlmeier U, Meinel T, Wiestler OD, Zanella F, Reulen HJ. (2006). Fluorescence-guided surgery with 5-aminolevulinic acid for resection of malignant glioma: a randomised controlled multicentre phase III trial. *Lancet Oncol*.7(5):392-401.
17. Stupp R, Mason WP, van den Bent MJ, Weller M, Fisher B, Taphoorn MJ, et al. (2005). Radiotherapy plus concomitant and adjuvant temozolomide for glioblastoma. *N Engl J Med*.352(10):987-996.
18. Hochberg FH, Pruitt A. (1980). Assumptions in the radiotherapy of glioblastoma. *Neurology*.30(9):907-911.
19. Okamoto Y, Di Patre PL, Burkhard C, Horstmann S, Jourde B, Fahey M, et al. (2004). Population-based study on incidence, survival rates, and genetic alterations of low-grade diffuse astrocytomas and oligodendrogliomas. *Acta Neuropathol*.108(1):49-56.

20. Bonavia R, Inda MM, Cavenee WK, Furnari FB. (2011). Heterogeneity maintenance in glioblastoma: a social network. *Cancer Res.*71(12):4055-4060.
21. Wen PY, Kesari S. (2008). Malignant gliomas in adults. *N Engl J Med.*359(5):492-507.
22. Brat DJ, Van Meir EG. (2004). Vaso-occlusive and prothrombotic mechanisms associated with tumor hypoxia, necrosis, and accelerated growth in glioblastoma. *Lab Invest.*84(4):397-405.
23. Brat DJ, Castellano-Sanchez AA, Hunter SB, Pecot M, Cohen C, Hammond EH, et al. (2004). Pseudopalisades in glioblastoma are hypoxic, express extracellular matrix proteases, and are formed by an actively migrating cell population. *Cancer Res.*64(3):920-927.
24. Graeber TG, Osmanian C, Jacks T, Housman DE, Koch CJ, Lowe SW, et al. (1996). Hypoxia-mediated selection of cells with diminished apoptotic potential in solid tumours. *Nature.*379(6560):88-91.
25. Zlatescu MC, TehraniYazdi A, Sasaki H, Megyesi JF, Betensky RA, Louis DN, et al. (2001). Tumor location and growth pattern correlate with genetic signature in oligodendroglial neoplasms. *Cancer Res.*61(18):6713-6715.
26. Rao JS. (2003). Molecular mechanisms of glioma invasiveness: the role of proteases. *Nat Rev Cancer.*3(7):489-501.
27. Uhm JH, Gladson CL, Rao JS. (1999). The role of integrins in the malignant phenotype of gliomas. *Front Biosci.*4:D188-199.
28. Natarajan M, Hecker TP, Gladson CL. (2003). FAK signaling in anaplastic astrocytoma and glioblastoma tumors. *Cancer J.*9(2):126-133.
29. Lal A, Glazer CA, Martinson HM, Friedman HS, Archer GE, Sampson JH, et al. (2002). Mutant epidermal growth factor receptor up-regulates molecular effectors of tumor invasion. *Cancer Res.*62(12):3335-3339.
30. Wei J, Barr J, Kong LY, Wang Y, Wu A, Sharma AK, et al. (2010). Glioma-associated cancer-initiating cells induce immunosuppression. *Clin Cancer Res.*16(2):461-473.
31. Soda Y, Marumoto T, Friedmann-Morvinski D, Soda M, Liu F, Michiue H, et al. (2011). Transdifferentiation of glioblastoma cells into vascular endothelial cells. *Proc Natl Acad Sci U S A.*108(11):4274-4280.
32. Neuwelt EA, Bauer B, Fahlke C, Fricker G, Iadecola C, Janigro D, et al. (2011). Engaging neuroscience to advance translational research in brain barrier biology. *Nat Rev Neurosci.*12(3):169-182.
33. Haar CP, Hebbar P, Wallace GC, Das A, Vandergrift WA, 3rd, Smith JA, et al. (2012). Drug Resistance in Glioblastoma: A Mini Review. *Neurochem Res.*
34. Fearon ER, Vogelstein B. (1990). A genetic model for colorectal tumorigenesis. *Cell.*61(5):759-767.
35. Hanahan D, Weinberg RA. (2000). The hallmarks of cancer. *Cell.*100(1):57-70.
36. Visvader JE, Lindeman GJ. (2008). Cancer stem cells in solid tumours: accumulating evidence and unresolved questions. *Nat Rev Cancer.*8(10):755-768.
37. Singh SK, Clarke ID, Terasaki M, Bonn VE, Hawkins C, Squire J, et al. (2003). Identification of a cancer stem cell in human brain tumors. *Cancer Res.*63(18):5821-5828.
38. Visvader JE, Lindeman GJ. (2010). Stem cells and cancer - the promise and puzzles. *Mol Oncol.*4(5):369-372.

39. Barnett SC, Robertson L, Graham D, Allan D, Rampling R. (1998). Oligodendrocyte-type-2 astrocyte (O-2A) progenitor cells transformed with c-myc and H-ras form high-grade glioma after stereotactic injection into the rat brain. *Carcinogenesis*.19(9):1529-1537.
40. Hirschmann-Jax C, Foster AE, Wulf GG, Nuchtern JG, Jax TW, Gobel U, et al. (2004). A distinct "side population" of cells with high drug efflux capacity in human tumor cells. *Proc Natl Acad Sci U S A*. 101(39):14228-14233.
41. Cheng L, Wu Q, Huang Z, Guryanova OA, Huang Q, Shou W, et al. (2011). L1CAM regulates DNA damage checkpoint response of glioblastoma stem cells through NBS1. *EMBO J*.30(5):800-813.
42. Bao S, Wu Q, Sathornsumetee S, Hao Y, Li Z, Hjelmeland AB, et al. (2006). Stem cell-like glioma cells promote tumor angiogenesis through vascular endothelial growth factor. *Cancer Res*.66(16):7843-7848.
43. Folkins C, Shaked Y, Man S, Tang T, Lee CR, Zhu Z, et al. (2009). Glioma tumor stem-like cells promote tumor angiogenesis and vasculogenesis via vascular endothelial growth factor and stromal-derived factor 1. *Cancer Res*.69(18):7243-7251.
44. Calabrese C, Poppleton H, Kocak M, Hogg TL, Fuller C, Hamner B, et al. (2007). A perivascular niche for brain tumor stem cells. *Cancer Cell*.11(1):69-82.
45. Dietrich J, Diamond EL, Kesari S. (2010). Glioma stem cell signaling: therapeutic opportunities and challenges. *Expert Rev Anticancer Ther*.10(5):709-722.
46. Vousden KH, Lu X. (2002). Live or let die: the cell's response to p53. *Nat Rev Cancer*.2(8):594-604.
47. Weinberg RA. (1995). The retinoblastoma protein and cell cycle control. *Cell*.81(3):323-330.
48. Stupp R, Hegi ME, Mason WP, van den Bent MJ, Taphoorn MJ, Janzer RC, et al. (2009). Effects of radiotherapy with concomitant and adjuvant temozolomide versus radiotherapy alone on survival in glioblastoma in a randomised phase III study: 5-year analysis of the EORTC-NCIC trial. *Lancet Oncol*.10(5):459-466.
49. Stupp R, Pica A, Mirimanoff RO, Michielin O. (2007). [A practical guide for the management of gliomas]. *Bull Cancer*.94(9):817-822.
50. Barker FG, 2nd, Chang SM, Gutin PH, Malec MK, McDermott MW, Prados MD, et al. (1998). Survival and functional status after resection of recurrent glioblastoma multiforme. *Neurosurgery*.42(4):709-720; discussion 720-703.
51. Butowski NA, Sneed PK, Chang SM. (2006). Diagnosis and treatment of recurrent high-grade astrocytoma. *J Clin Oncol*.24(8):1273-1280.
52. Tuettenberg J, Grobholz R, Korn T, Wenz F, Erber R, Vajkoczy P. (2005). Continuous low-dose chemotherapy plus inhibition of cyclooxygenase-2 as an antiangiogenic therapy of glioblastoma multiforme. *J Cancer Res Clin Oncol*.131(1):31-40.
53. Desjardins A, Reardon DA, Coan A, Marcello J, Herndon JE, 2nd, Bailey L, et al. (2012). Bevacizumab and daily temozolomide for recurrent glioblastoma. *Cancer*.118(5):1302-1312.
54. Yap KY, Chui WK, Chan A. (2008). Drug interactions between chemotherapeutic regimens and antiepileptics. *Clin Ther*.30(8):1385-1407.

55. Cairncross G, Macdonald D, Ludwin S, Lee D, Cascino T, Buckner J, et al. (1994). Chemotherapy for anaplastic oligodendroglioma. National Cancer Institute of Canada Clinical Trials Group. *J Clin Oncol.*12(10):2013-2021.
56. Louis DN, Pomeroy SL, Cairncross JG. (2002). Focus on central nervous system neoplasia. *Cancer Cell.*1(2):125-128.
57. Esteller M, Garcia-Foncillas J, Andion E, Goodman SN, Hidalgo OF, Vanaclocha V, et al. (2000). Inactivation of the DNA-repair gene MGMT and the clinical response of gliomas to alkylating agents. *N Engl J Med.*343(19):1350-1354.
58. Brandes AA, Franceschi E, Tosoni A, Benevento F, Scopece L, Mazzocchi V, et al. (2009). Temozolomide concomitant and adjuvant to radiotherapy in elderly patients with glioblastoma: correlation with MGMT promoter methylation status. *Cancer.*115(15):3512-3518.
59. Hegi ME, Liu L, Herman JG, Stupp R, Wick W, Weller M, et al. (2008). Correlation of O6-methylguanine methyltransferase (MGMT) promoter methylation with clinical outcomes in glioblastoma and clinical strategies to modulate MGMT activity. *J Clin Oncol.*26(25):4189-4199.
60. Schmidt NO, Westphal M, Hagemann C, Ergun S, Stavrou D, Rosen EM, et al. (1999). Levels of vascular endothelial growth factor, hepatocyte growth factor/scatter factor and basic fibroblast growth factor in human gliomas and their relation to angiogenesis. *Int J Cancer.*84(1):10-18.
61. Norden AD, Drappatz J, Muzikansky A, David K, Gerard M, McNamara MB, et al. (2009). An exploratory survival analysis of anti-angiogenic therapy for recurrent malignant glioma. *J Neurooncol.*92(2):149-155.
62. Henriksson R, Asklund T, Poulsen HS. (2011). Impact of therapy on quality of life, neurocognitive function and their correlates in glioblastoma multiforme: a review. *J Neurooncol.*104(3):639-646.
63. Nagpal S, Harsh G, Recht L. (2011). Bevacizumab improves quality of life in patients with recurrent glioblastoma. *Chemother Res Pract.*2011:602812.
64. Brandsma D, van den Bent MJ. (2007). Molecular targeted therapies and chemotherapy in malignant gliomas. *Curr Opin Oncol.*19(6):598-605.
65. de Groot JF, Lamborn KR, Chang SM, Gilbert MR, Cloughesy TF, Aldape K, et al. (2011). Phase II study of aflibercept in recurrent malignant glioma: a North American Brain Tumor Consortium study. *J Clin Oncol.*29(19):2689-2695.
66. Eliceiri BP, Cheresh DA. (1999). The role of alphav integrins during angiogenesis: insights into potential mechanisms of action and clinical development. *J Clin Invest.*103(9):1227-1230.
67. Gilbert MR, Kuhn J, Lamborn KR, Lieberman F, Wen PY, Mehta M, et al. (2012). Cilengitide in patients with recurrent glioblastoma: the results of NABTC 03-02, a phase II trial with measures of treatment delivery. *J Neurooncol.*106(1):147-153.

CHAPTER II



INTRODUCTION TO THE TANNOUS LAB

an integrated approach of bioluminescence imaging and gene therapy

1. GENE THERAPY

Gene therapy (GT) is based on the idea to use nucleic acid (DNA or RNA) as a pharmaceutical agent to treat disease.^{1,2} This idea came to life as soon as Watson and Clark unraveled the mysteries of DNA in the 1950's. In 1972 Friedman and Roblin published a paper in *Science* titled "Gene Therapy for Human Genetic Disease?" formulating the first concrete concept of the field.⁶ It would take another 20 years before the FDA approved the use of gene therapy in the United States, but then in 1992 Ashanti da Silva, a four years old girl, became the first person in history to receive gene therapy.⁷ She suffered from X-linked SCID, a single genetic defect resulting in immune deficiencies. Treatment was successful, however the effects were temporally. Since then, over 2000 clinical trials with gene therapy have been conducted (www.clinicaltrials.gov) and now this field seems to hold one of the promises of modern medicine.

In contrast to drug-based therapies, that are administered exogenously and repeatedly, gene therapy aims to heal from within. DNA recombination techniques allow pieces of DNA (or RNA) to be created from scratch, resulting in genes with desirable characteristics. These newly created genes can be incorporated in the genome of the cells of choice, where they'll start producing the tools for the intended intervention. Since integration in the host genome will theoretically result in long-term expression of the therapeutic gene, there's no need for repeated administration. Virtually any type of intervention can be programmed into DNA, allowing the cell's original genes to be inactivated or upregulated, nonfunctioning genes to be replaced, and genes with desirable characteristics to be introduced.

1.1 Viral vectors

Viral vectors are the vehicles of choice for transgene delivery in the gene therapy field. Viruses are characterized by their ability to introduce their genetic material into host cells as part of their replication cycle, while to a certain extent avoiding immunosurveillance. When the host cells are attacked by the virus, introduction of the viral genetic material takes place. As soon as this newly introduced information is translated, hijacking of the host replication machinery is initiated. The host cell will

carry out the instructions of the viral genetic material, creating more and more virus to invade surrounding cells. This way, viruses are capable of surrendering large populations of cells.

In gene therapy several types of viruses are redesigned in such a manner that, instead of their own genetic material, they carry therapeutic genes into the host cells. Each type of virus has its own characteristics (Table 1), making it suited for different appliances. For the projects in this thesis, we mainly worked with adeno-associated viruses (AAV) and Lentivirus.

Adeno-associated virus (AAV) is the virus of choice for the treatment of many neurological disorders. Several serotypes exist (2,4,5,7,8), with 2 being the one most often used in the brain, due to its preference for neuronal cells.⁸ AAV is capable of infecting both dividing and non-dividing cells and long time stable gene expression is achieved. Wild type AAV is known to integrate its DNA on a specific locus on chromosome 19, but this specificity is lost with the different serotypes, which usually maintain their DNA in a linear configuration in the cytoplasm (episomally).⁹ AAV is associated with very low toxicity and does not seem to evoke an immune response. Due to all these features, it is currently used in clinical trials for neurological disorders. A disadvantage of AAV is its low genomic capacity. A maximum of 5 kb can be packaged into AAV vectors, which makes it often impossible to deliver both a transgene and its reporter.¹⁰

Lentivirus (HIV-based) is a subgroup of the retroviridae family. It can deliver significant amounts of DNA and is capable of integrating its DNA permanently into the host genome, resulting in long-term stable gene expression.¹¹ This might lead to a risk of oncogenic mutagenesis when integration happens at the site of e.g. a tumor suppressor gene.¹² This is the reason that lentiviruses are primarily used for in vitro systems or in animal models after ex vivo infection. Some clinical trials are testing lentivirus safety in humans.¹³

	Adenovirus	Adeno-associated virus	Alphavirus	Herpesvirus	Retrovirus / Lentivirus	Vaccinia virus	
Particle characteristics	Genome	dsDNA	ssDNA	ssRNA (+)	dsDNA	ssRNA (+)	
	Capsid	Icosahedral	Icosahedral	Icosahedral	Icosahedral	Icosahedral	Complex
	Coat	Naked	Naked	Enveloped	Enveloped	Enveloped	Enveloped
	Virion polymerase	Negative	Negative	Negative	Negative	Positive	Positive
	Virion diameter	70 - 90 nm	18 - 26 nm	60 - 70 nm	150 - 200nm	80 - 130 nm	170 - 200 X 300 - 450nm
	Genome size	39 - 38 kb	5 kb	12 kb	120 - 200 kb	3 - 9 kb	130 - 280 kb
							
Family	<i>Adenoviridae</i>	<i>Parvoviridae</i>	<i>Togaviridae</i>	<i>Herpesviridae</i>	<i>Retroviridae</i>	<i>Poxviridae</i>	
Gene Therapy Properties	Infection / tropism	Dividing and non-dividing cells	Dividing and non-dividing cells	Dividing and non-dividing cells	Dividing cells*	Dividing and non-dividing cells	
	Host genome interaction	Non-integrating	Non-integrating*	Non-integrating	Non-integrating	Integrating	Non-integrating
	Transgene expression	Transient	Potential long lasting	Transient	Potential long lasting	Long lasting	Transient
	Packaging capacity	7.5 kb	4.5 kb	7.5 kb	> 30 kb	8 kb	25 kb

Table 1 Characteristics of the most commonly used viral vectors for gene therapy. Image www.genethrapy.net1.3 Gene therapy for GBM

1.2 Gene therapy and cancer

Gene therapy against cancer is based on the delivery of cytotoxic genes to the tumor cells to achieve cell death directly, or by delivering “replacement genes” to overcome the resistance to therapeutics that is seen in many cancer types.^{1,14} The most studied direct cytotoxic transgene in GBM is the Herpes Simplex Type 1 Thymidine Kinase (TK).¹⁵ This gene enables the conversion of the prodrug ganciclovir into the highly toxic deoxyguanosine triphosphate, resulting in early chain termination of nascent DNA strands. The advantage of this approach is that only cells expressing the TK gene will convert ganciclovir (intracellular) into its lethal counterpart, while regular cells will remain unharmed. A modest increase in survival is reported in several studies. Another commonly used transgene is the E. Coli cytosine deaminase (CD) which converts 5-fluorocytine (5-FC) into its toxic variant 5-fluorouracil (5-FU).¹⁶

After successful introduction of the gene and administration of 5-FU, extensive cell death could be observed. Unlike TK, the CD therapeutic strategy has the advantage of excellent bystander effect since the 5-FU can travel from cell-to-cell via gap junctions.

Instead of introducing drug-activating genes into cells, it is also possible to deliver genes coding for immunotoxins. An example of such an approach is an AAV encoding transgenes for PE (pseudomonas exotoxin).¹⁷ Expression of the PE gene leads to disruption of the cellular protein translation and causes cell death. To prevent elimination of normal non-tumor cells, the PE toxin is linked to human IL 13R α 2, a variant of the IL13 receptor that is overexpressed by 50-80% of GBM cells, but not by normal cells. This approach is still in an experimental phase¹⁸, but tumor regression and long-term survival was observed in ~70% of the animals.

Despite some success stories, gene therapy is not living up to its full promise yet. It appears to be very difficult to achieve a high enough percentage of transduced cells, limiting the effectiveness of the therapy.¹⁹ GBM cells prove to be particular difficult to transduce, due to the characteristic intra-tumoral heterogeneity and high intracranial pressure. Bystander effect of the transgene, in which the neighboring non-transduced cells are also killed, is needed to ensure effective therapy. Another problem is caused by the short-lived nature of this approach. Whereas theoretically integration of DNA in the host genome will result in long-term expression, this seems to be problematic to achieve in real life. After initial transduction, loss of transgene expression can be observed over time. Due to problems with integration of viral vector DNA into the genome and rapidly dividing cells, no permanent expression can be acquired so that patients require multiple rounds of gene therapy. Other concerns for viral therapy include toxicity of the gene or its vector to normal tissue, the host immune-response, tissue targeting, gene control, virus safety and the chance of inducing tumors by insertional mutagenesis. As of today, it is still impossible to exactly pinpoint the spot in the DNA where the new gene is to be integrated. Chances are the new gene integrates at the wrong place along the DNA strand, could disrupt a tumor suppressor gene and there slowly activates the process of cancer.

As mentioned above one of the challenges of using gene therapy in GBM is the achievement of a high enough yield of viral expression. Most approaches are focused on direct intratumoral injection of the virus to achieve expression of the therapeutic protein by the tumor cells themselves. Besides the fact that it is very difficult to establish consistent transduction of this heterogeneous cell population, another problem arises. Once the virus delivers its therapeutic gene to the tumor cells, production of the desired anti tumor proteins begins. Anti tumor proteins are designed to be highly lethal in order to be as effective in eliminating tumor growth as possible. However, since the tumor cells express the drug themselves, the therapeutic reservoir is rapidly depleted once the drug gets effective and the cells start dying, allowing for the escape of residual cells. To overcome this problem, Maguire et al designed a different approach in which not the tumor cells but the surrounding healthy brain parenchyma was engineered to express and anti-cancer agent, creating a 'zone of resistance.'²⁰ Using an AAV8 vector expressing interferon beta (INF β) to transduce the normal brain, tumor growth in orthotopic xenograft models was completely prevented, even in the contralateral hemisphere and complete eradication of established tumors was achieved. These results open new possibilities for a more effective treatment of GBM with gene therapy.

All the above strategies are aimed at the elimination of tumor cells. This is however not the only way gene therapy can be of use in GBM. A very important role is reserved for its attribution to the knowledge of GBM tumor biology. Combining gene therapy and molecular imaging has lead to major discoveries in tumor signaling pathways, behavior, response to therapy and the role of the microenvironment, allowing the development of more effective treatment options.

1.3 An alternative approach: Liposomes

To enhance the diagnostics and treatment of many disorders, including cancer, one should think of disease-specific-targeting strategies. Most conventional chemotherapeutics lack the ability to deliver the therapeutic content specifically to the target tissues, which results in toxicity to healthy structures and often inadequate levels of therapeutic agents at the targeted tissue. Furthermore, gene therapy by use

of viral vectors is not yet at the level where we can 100% specifically target a specific group of cells. Liposomes might provide an interesting alternative for selective target delivery of therapeutics. Since many liposomes are currently widely used for pharmaceutical therapy and thereby approved for clinical purposes, they are of great interest for further exploration and applications.

About 45 years ago, Alec Bangham observed that phospholipids form closed bilayered structures when put in aqueous solutions, which were named liposomes. In short, liposomes are spherical, self-closed structures formed by one or several concentric lipid bilayers with an aqueous phase inside and between the lipid bilayers.²¹ A real breakthrough occurred around 20 years ago when several liposomal drugs were approved and thereby many biomedical products and technologies were developed. The ideal liposome has 1. a size of around 80-120 nm to minimize phagocytosis of the liposome particles in the blood ²², 2. a coat of for example PEG to slow down liposome recognition by the immune system and the resulting clearance of liposomes ²¹, and 3. target specificity such as immunoliposomes, foliate-mediated targeted liposomes, transferrin-mediated liposomes or biotin-streptavidin liposomes. Furthermore, liposomes are often PH-sensitive for efficient release of their contents inside the acidic endosome of the cell or the liposomes can be thermo-sensitive for ultra sound release of their therapeutic content.^{23,24}

Besides the use of liposomes for therapy, they are also suitable for the delivery of imaging agents, which can be detected with most of the imaging modalities described in the next paragraph. For gamma-scintigraphy and MRI, the liposomes require respectively a sufficient quantity of radionuclide or paramagnetic metal. CT-contrast agents also can be incorporated into either the inner water compartment of the liposomes or in the liposomal membrane, as well as the incorporation of gas bubbles, which are sound reflectors, for the use of ultra sound.^{21,25} The use of MRI for liposomal therapy and delivery of imaging agents has a great advantage due to its non-invasive character, the lack of radiation and its high spatial resolution. On the other hand, the sensitivity of MRI can often be disappointing, which fortunately can be overcome by a good contrast agent. Liposomes are known to be useful carriers of these contrast agents.

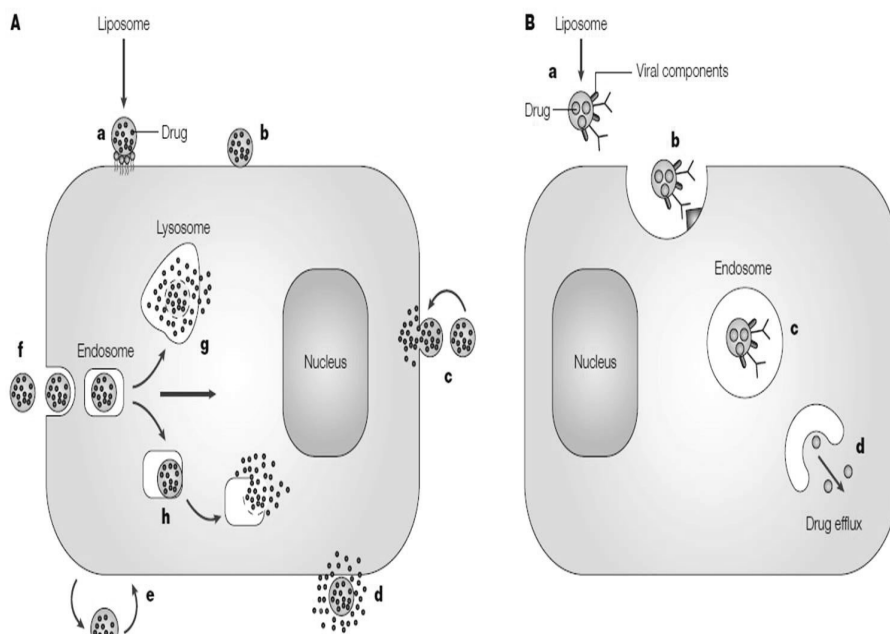


Figure 1: Liposome cell interaction. A) Drug loaded liposomes can specifically (a) or non-specifically (b) adsorb onto the cell surface. Liposomes can also fuse with the membrane (c) and release their contents into the cytoplasm, or can be destabilized by certain cell membrane components when adsorbed on the surface (d) so that the released drug can enter the cell via micropinocytosis. Liposomes can undergo the direct or transfer-protein mediated exchange of lipid components with the cell membrane (e) or be subjected to specific or non-specific endocytosis (f). In case of endocytosis, a liposome can be delivered by the endosome into the lysosome (g), or, en route to the lysosome the liposome can provoke endosome destabilization (h), which results in drug liberation into the cell cytoplasm. B) Liposome modified with viral components (a) and loaded with a drug can specifically interact with cells (b), provoke endocytosis, and via the interaction of viral components with the inner membrane of the endosome (c), allow for drug efflux into the cell cytoplasm (d).²¹

2. MOLECULAR IMAGING

Molecular Imaging (MI), defined by the Center of Molecular Imaging Innovation and Translation as ‘the visualization, characterization, and measurement of biological processes at the molecular and cellular levels in humans and other living systems,’ was developed in the early 21st century and has since rapidly evolved as a useful tool in the biomedical research field.²⁶ MI has provided the opportunity to visualize

and monitor biological processes at both cellular and subcellular level without disturbing the living organism itself, thereby allowing the *in vivo* monitoring of specific molecular and cellular processes as gene expression, multiple simultaneous molecular events, progression or regression of cancer, and drug- and gene therapy.²⁷

Currently disease is seen as the development of anatomic changes or physiologic changes, but unquestionably molecular changes underlie these developments. Direct imaging of these molecular changes will allow for detection of the disease in a much earlier stage. Further, the effects of the chosen treatment can be monitored.²⁸ Molecular Imaging is especially getting more and more essential in the cancer field. Our assessment of tumor type and diagnosis, prognostic markers, gene expressions, behavioral predictions, location, infiltration and response to therapy, e.g. our complete anti-tumor toolbox almost entirely relies on the (combined) use of various imaging modalities. Since Molecular Imaging allows for real time *in vivo* monitoring, understanding of the complicated and dynamic intra-tumoral processes becomes possible. Biological processes can be studied in their own physiologically authentic environment, instead of in laboratory-designed models. This is in huge contrast with the *ex vivo* techniques such as histology that we had to rely on before. Only a single static point in time could be measured, showing the end effects of molecular alterations, but not how and why those alterations took place. This 'how' and 'why' can now be visualized with molecular imaging and this knowledge can be directly applied to new treatment strategies.

In order to successfully visualize these biological processes *in vivo*, specific and sensitive molecular imaging probes are needed. These probes are molecules such as radiolabeled ligands, substrates, antibodies or cytokines, which can be used to differentiate between the different molecular events. Often it is useful to create inactive probes that require a substrate-enzyme interaction or the unquenching of a fluorophor to become active. Molecular Imaging consists of a wide array of these probes to produce imaging signals. Nuclear medicine relies on the decay of radioactive molecules (tracers), while sound (ultrasound), magnetism (MRI) and light (optical techniques; fluorescence and bioluminescence) are other key players (Table 2).²⁹ The required common characteristics of all these techniques is the availability of

a stable, non toxic high affinity probe or reporter, their ability to overcome physiological barriers (blood-brain-barrier), the use of amplification techniques to increase the signal to noise ratio, and the availability of high resolution fast imaging modalities.²⁸

Whereas techniques such as positron emission tomography (PET), single photon emission computed tomography (SPECT), computed tomography (CT), magnetic resonance imaging (MRI), and ultrasound are widely used in the clinical setting, they all have different shortcoming for pre-clinical small animal imaging. On the other hand, optical imaging including bioluminescence imaging (BLI) and fluorescence imaging (FLI) are valuable for pre-clinical small animal imaging.³⁰ Application of multimodality imaging using probes which can be imaged with a combination of either one of the above techniques results in fast validation in animal models (e.g. BLI) and translation into the clinic (e.g. MRI/PET).³¹

2.1 Overview of different imaging modalities

To gain insight into the different modalities used in molecular imaging and to obtain better understanding of the following chapters, a brief overview of the most commonly used imaging modalities will be provided.

Nuclear Imaging. Nuclear medicine gained recognition as a medical specialty in the 50's.^{32,33} This specialism makes use of radiation to image biological processes for medical purposes. To explain the different modalities that are often used in nuclear medicine, one should first know the concept of a gamma camera. A **gamma camera**, also known **scintigraphy** or an Anger camera, counts the gamma photons absorbed by the crystal of the camera. When a gamma photon radiates from the patient (originating from an administered pharmaceutical) and reaches the camera, an electron is released from the iodine in the crystal of the camera, which upon finding its minimal energy state produces a faint flash of light. Thereby a 2-dimensional image is created. Both **PET** and **SPECT** scanners are based on the principle of a gamma camera. A PET scanner can detect gamma photons that are the result of a hit between a positron, emitted by the molecular probe administered, and an electron. The molecular probe consists of a decaying nucleotide such as

Carbon-11, Fluorine-18, Oxygen-15, or Iodine-124. A PET scanner can thereby reconstruct an image of the positron-emitting radionucleotide tagged to a specific molecule, which is recognized by enzymes or prone to binding to receptors, to visualize for example the expression of a therapeutic gene of interest.^{34,35,36,37} The PET technique is widely used to visualize molecular processes and a majority of these are related to tumor cell growth.³⁸ Whereas PET uses the collision of positrons and electrons, SPECT tracks the position of gamma radiation directly by a rotation process around the body. Therefore, SPECT acquires information of the concentration of gamma emitting radionuclide, such as Technetium-99m, Indium-111 and Iodine-131, instead of a volumetric distribution that can be acquired by PET. Since PET uses this indirect radiation for a real-time image in time and space it is more sensitive than SPECT. SPECT on the other hand is significantly less expensive.²⁷ PET and SPECT are both used in the clinic and for small animal imaging.

X-ray and CT imaging. An **X-ray** is an image of electromagnetic radiation sent through the body and recorded on a film. Dense structures will appear as white on the image by blocking most of the radiation, whereas black displays the opposite namely air. X-ray images are commonly used for the evaluation of anatomical structures and are easy and relatively cheap to acquire.^{39,40} **CT**, also known as CAT scanning (Computerized Axial Tomography) uses the same X-ray absorption as simple X-rays but it acquires different type of images by rotating the source and the detector around the body, resulting in multiple serial images and volumetric data.^{27,41} CT is applied both in the clinical settings and for small animal research, although the utility of the CT technique for molecular imaging remains controversial mainly because of the difficulty in designing adequate contrast agents and probes for this modality.^{28,42}

Ultrasound (US). This technique of high-frequency sound waves transmitted through tissues and then reflected back and detected, is often used to observe perfusion and anatomical characteristics.

Currently, contrast agents detectable by US and useful for molecular imaging are tested in animals. These contrast agents consists of microbubbles to which proteins and antibodies can be attached. When these microbubbles are linked to a

therapeutic agent the ultrasound can be used to release this therapeutic agent at the specific disease site, leading to therapy. ^{43,44,26}

Magnetic resonance imaging. MRI stands for high resolution imaging without ionizing radiation. When a temporary radiofrequency pulse is given to the hydrogen atoms in the body, whose spins are aligned because of a strong magnetic field, they temporarily change their alignment of spinning and get into an excited state, creating a pulse of radio wave the moment they switch back to ground state. These radio waves are detected and quantified. The major advantage of MRI is that it is suitable for high-resolution tissue images and contrast agents that can even enhance the signal, such as paramagnetic gadolinium, are available making MRI an important imaging modality. ^{27,45} Nevertheless, certain drawbacks remain for the use of MRI including longer image acquisition time, often large amounts of contrast agent ⁴⁶, difficulty in delivery of those contrast agents, and poor sensitivity due to lack of accumulation of the contrast agent at the targeted site. ⁴⁵ In order to make MRI more suited for molecular imaging, it is unnecessary to explain the importance of exploring new contrast techniques with higher sensitivity and specificity for targeted imaging and treatment.

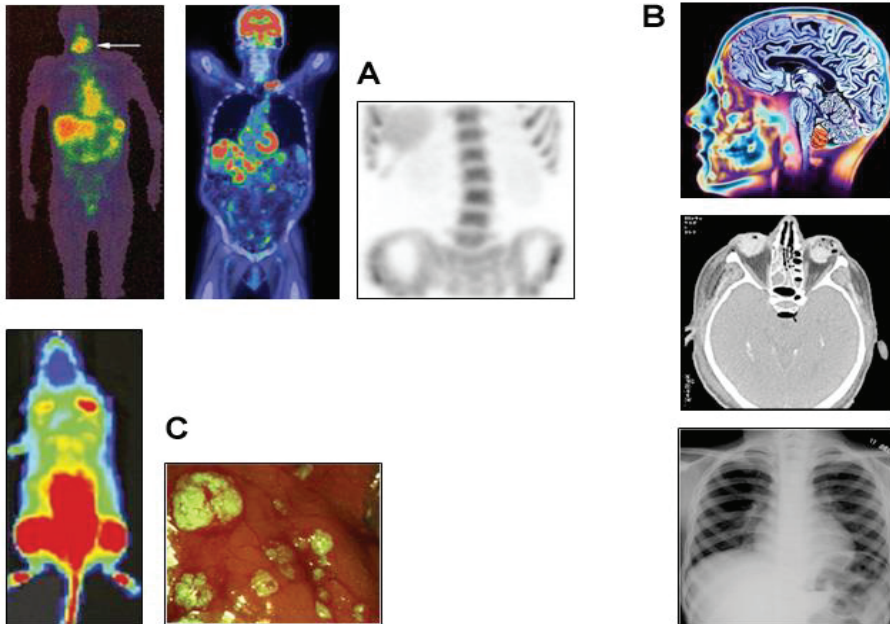


Figure 2: Imaging Modalities, adapted from ^{47,48,49,50,51,52,53}. A) Nuclear medicine, from left to right: Gamma scintigraphy, PET and SPECT scan. B) From top to bottom: MRI, CT and X-ray. C) Optical imaging, from left to right: BLI in a mouse and FLI during surgery.

Imaging Technique	EM Radiation Spectrum Used In Image Generation	Advantages	Disadvantages
Positron emission tomography (PET)	High energy gamma rays	High sensitivity; isotopes can substitute for naturally occurring atoms; quantitative; translational research	PET cyclotron or generator needed; relatively low spatial resolution; radiation of subject
Single photon emission computed tomography (SPECT)	Lower energy gamma rays	Many molecular probes available; can image multiple probes simultaneously; may be adapted to clinical imaging systems	Relatively low spatial resolution; radiation
Optical bioluminescence imaging	Visible light	Highest sensitivity; quick, easy, low cost, and relatively high throughput	Low spatial resolution; current 2-D imaging only; relatively surface-weighted; limited translational research
Optical fluorescence imaging	Visible light or near-infrared	High sensitivity; detects fluorochrome in live and dead cells	Relatively low spatial resolution; relatively surface-weighted
Magnetic resonance imaging (MRI)	Radio waves	Highest spatial resolution; combines morphologic and functional imaging	Relatively low sensitivity; long scan and postprocessing time; mass quantity of probe may be needed
Computed tomography (CT)	X-rays	Bone and tumor imaging; anatomic imaging	Limited 'molecular' applications; limited soft tissue resolution; radiation
Ultrasound	High-frequency sound	Real time; low cost	Limited spatial resolution; mostly morphologic although targeted microbubbles under development

Table 2 Characteristics of the main techniques used in Molecular Imaging. Copyright Center for Molecular Imaging Innovation and Translation

2.2 Optical Imaging

Optical imaging is specific type of molecular imaging. The basis of optical imaging techniques consists of photons travelling through tissue and interacting with tissue components.²⁹ Genes encoding fluorescent proteins or luciferases can be engineered, transferred into host cells and/or living animals and their light output can be measured with sensitive cameras. Optical imaging is highly sensitive for contrast agents and reporter molecules *in vivo*, meaning that even small signals can be detected. Further, it proved to be an excellent tool for use *in vitro* and in small animal models. It is inexpensive, highly sensitive, and the procedure is not very time consuming. The only disadvantage of optical imaging is the limited transmission of light through animal tissues, resulting in a decreased signal quantitation. Fluorescence imaging and Bioluminescence imaging are the two optical imaging techniques used in this thesis.

2.2.1 Fluorescence Imaging

Fluorescence refers to the property of certain molecules to absorb light at a particular wavelength and to emit light of a longer wavelength after a brief interval known as the fluorescence lifetime.²⁹ The most commonly used fluorescent reporter is the green fluorescent protein (GFP). GFP is a 27 kDa protein derived from the jellyfish *Aequorea Victoria* and it emits green light upon illumination with ultraviolet light.⁵⁴ The GFP gene is easily introduced to virtually any cell type and is extensively used as a reporter of expression or as a biosensor. When fused to other proteins, it becomes possible to monitor specific cell compartments, protein trafficking and all kind of cellular dynamic processes.⁵⁵ Since GFP expression is not harmful to cells, it has become a very powerful tool for fluorescence microscopy to observe cellular processes over time. Using mutagenesis at the chromophore region of the GFP gene, several variants were engineered.⁵⁶ With the creation of BFP (blue), YFP (yellow) and CFP (cyan), each using a different excitation and emission wavelength, simultaneous measurements became possible. In 2008 the discovery of GFP was awarded the Nobel Prize for Chemistry.

So far, the use of fluorescence has mostly been in *in vitro* setting due to its emission peak in the 500 nm wavelength (green light) leading to poor tissue penetration. *In vivo*, only 1-2 mm depth can be detected, and often surgical exposure is needed before visualization of the reporter is possible. Further, an external light source is needed for excitation, leading to high background signals due to tissue auto-fluorescence. Current research focuses on overcoming these limitations. Proteins that emit light in the far-red region of the spectrum or that show brighter light emission might improve the *in vivo* use of fluorescence. Due to a spectrum shift towards a wavelength longer than 600-610 nm, signals from red fluorescent (RFP) can be detected for several millimeters to centimeters in tissues, without the attenuation that occurs with other fluorescent proteins.^{57,58,59,60,61,62} Recently new imaging technologies have made it possible to acquire 3D fluorescence images, resulting in further improvement of sensitivity.⁶³ This and several other developments in the fluorescence imaging field cleared the road for the use of this technique in the clinic. At the moment FLI is near to serving as a highly useful tool for breast imaging as well as for intraoperative guidance.^{45,64}

2.2.2 Bioluminescence imaging

Bioluminescence Imaging (BLI) is a technique based on converting chemical energy into visible light in living animals. For centuries seamen and fishermen had seen lights in the waters and realized that these lights were emitted by organisms living in the water; this phenomenon was called **bioluminescence**. Only about 45 years ago, these organisms began to be characterized.^{65,66,67} It was discovered that their light reaction depends on a luciferase (an enzyme), and its substrate (called a luciferin); coupling of enzyme and substrate causes a chemical conversion of the substrate resulting in light emission as is depicted in figure 3.⁶⁸ All known luciferases use molecular oxygen to catalyze this reaction, and some luciferases require the presence of co-factors such as ATP and Mg²⁺ for activity. Since no external light source is needed, BLI has virtually no background. Luciferases comprise a wide range of enzymes; usually they are found in lower organisms such as insects, fungi, bacteria and marine crustaceans, but no shared sequence homology exists.⁶⁸ Luciferase have proved to be very useful reporters in mammalian cells, since they are easily introduced in virtually all cell types by means of viral vectors, and they can provide real time, non-invasive measurements of in situ biological events, thereby giving a complete picture of the kinetics of an entire process.⁶⁸⁻⁷⁰ With the current techniques, as few as a 10 cells expressing a luciferase can be detected in deep tissue of some animal models using a cooled charge-coupled device (CCD) camera.

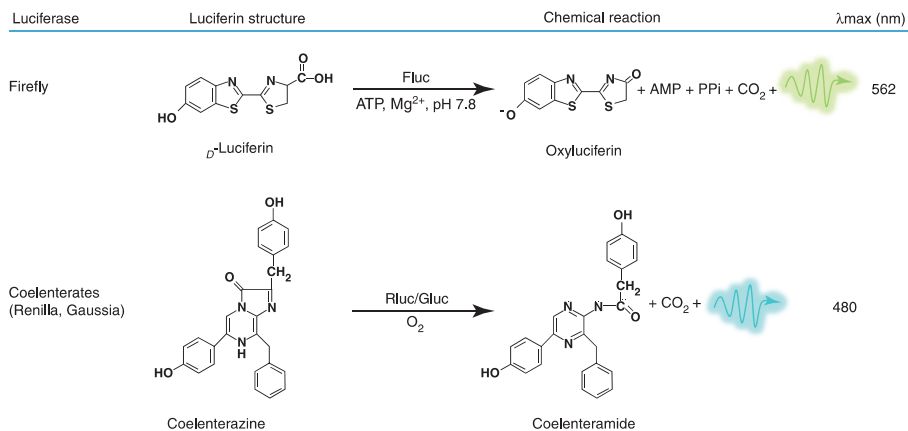


Figure 3. The Bioluminescent reactions of Firefly luciferase (Fluc), Renilla reniformis (Rluc) and Gaussia luciferase (Gluc). The chemical structure, the chemical reaction and the peak light emission (λ_{max}) are depicted for each luciferase. Adapted from Badr and Tannous, Trends in Biotechnology, 2011.

American Firefly Luciferase, or Fluc, is derived from the light emitting organ of the *Photinus Pyralis* and is one of the most commonly used luciferases. This 62 kDa protein has a very high quantum yield (>88%) and emits green light (562 nm peak with a broad shoulder) upon oxidation of its substrate D -luciferin (Figure 4). The presence of ATP and Mg²⁺ is required for this reaction to take place. Fluc is expressed in the cytoplasm and therefore is cell-associated. Fluc displays a glow-type light emission kinetics with a half-life of 10 minutes, making it one of the best luciferases available to yield stable light output.⁷¹⁻⁷³

The luciferase from the sea pansy *Renilla Reniformis* (Rluc) is another commonly used reporter. Rluc is a 34kDa protein, which uses coelenterazine as a substrate, and emits blue light with a peak at 480 nm (Figure 4). No ATP is needed for Rluc activity, however the enzymatic turnover and quantum yield of this reaction is only 6% making it not very suited as a reporter.⁷⁴

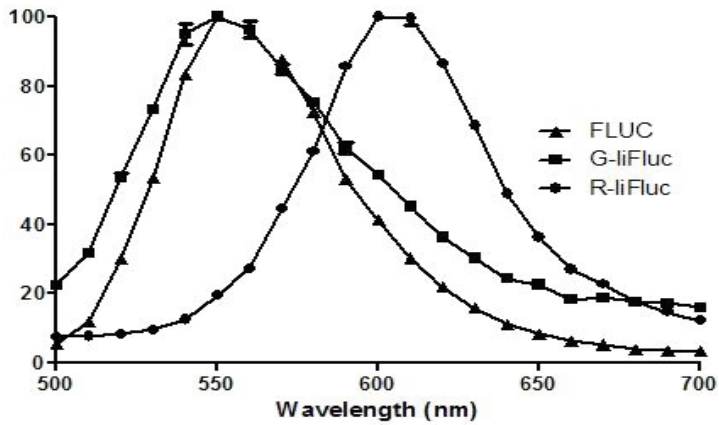
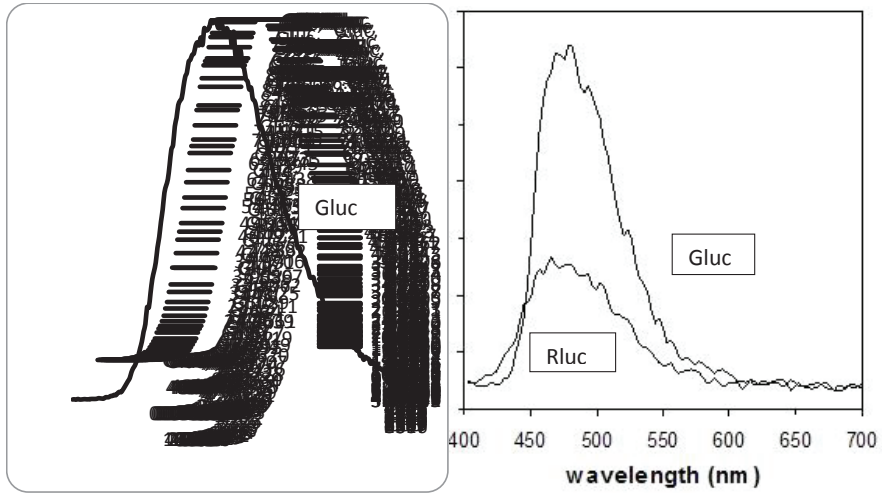
The luciferase from the marine copepod *Gaussia Princeps* (Gluc) is the smallest luciferase (19.9 kDa) known. Similar to Rluc, Gluc uses coelenterazine for its chemical reaction, resulting in blue light emission with a peak at 480 nm. Gluc is over 2000-fold more sensitive than either Fluc or Rluc when expressed in mammalian

cells culture and therefore has become the reporter of choice.⁶⁸ While most luciferases are retained in the cell, *Gaussia* Luciferase is unique as its cDNA possesses a natural signal sequence and therefore is secreted upon expression in mammalian cells. While this causes a certain loss of signal at the site of origin, it does allow Gluc to report both from the cells themselves as well as their environment. Therefore, the Tannous Lab developed Gluc as a blood reporter. Since Gluc is naturally secreted, the level of Gluc in the blood correlates with the specific biological process (cell number, viral transduction, tumor volume, etc).^{75,76} Despite its secretion, Gluc still emits over 200-fold higher signal than Rluc, and is comparable in signal intensity to Fluc when imaged *in vivo*⁶⁸. A Gluc-variant that is expressed on the cell surface was recently designed and showed to be a sensitive reporter for tracking T-cells *in vivo*.⁷⁷ Gluc is currently the reporter of choice for monitoring of different biological phenomena and in different fields including gene expression, tumor volume, cell viability in high throughput screening for drug discovery, protein-protein interactions in BRET.⁷⁸⁻⁸⁴

The luciferase from the *Vargula hilgendorfi* (Vluc), a marine ostracod, is one of the few other naturally secreted luciferases⁸⁵. In the presence of Vargulin, Vluc emits a blue light (462nm). However, the in-availability of the Vluc substrate limited its use. Recently, Vargulin became commercially available, so that use at a larger scale can be initiated.

Table 3: Different luciferases and their origin, substrate, wavelength and emission type.

Luciferase	Origin	Substrate	Wave length	Flash/Glow
Firefly (Fluc)	<i>Photinus pyralis</i> American Firefly	Beetle D-luciferin Mg ²⁺ , ATP	562nm	Flash
Renilla (Rluc)	<i>Renilla reniformis</i>	Coelenterazine	480nm	Flash
Gaussia (Gluc)	<i>Gaussia princeps</i>	Coelenterazine	480nm	Flash
<i>Vargula hilgendorfi</i> (Vluc)	<i>Vargula hilgendorfi</i>	Vargullin	467nm	Glow
<i>Luciola italica</i>	<i>Luciola italica</i>	Beetle D-luciferin	550nm GliFluc	Flash



Vargula (463nm), Green Renilla (527nm) and Red Italice (613nm)

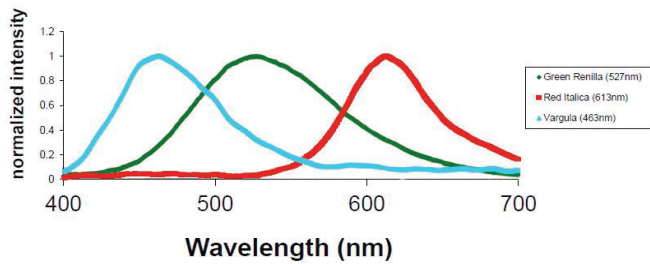


Figure 4: Emission spectra of different luciferases, adapted from chapter VII, ^{3,5}

Aside from light emission characteristics these luciferases have different kinetics of light output, sensitivity and enzymatic stability. Rluc and Gluc both display a flash-type kinetic reaction, in which the emitted light decays to background level within minutes. Fluc on the other hand displays a glow type kinetic that decays over a longer period of time.⁶⁸ Further, Fluc has a half-life of 4 hours in contrast to the half-life of Gluc, which is around 5 days.⁶⁸ These different characteristics make each reporter suitable for a different type of application. Whereas the glow kinetics of Fluc is favorable for high throughput screening *in vitro*, the absence of natural secretion makes the real-time monitoring from the same cells impossible. Gluc on the contrary is perfect as a secreted reporter, but its flash characteristics make it unsuitable for high throughput screening.

For *in vivo* applications, we can point out a comparable dilemma: Fluc is more sensitive due to its emission towards the red side of the spectrum, however, unlike Gluc, its activity cannot be monitored in the blood and therefore is not suited for monitoring of few circulating cells. Since Fluc and Rluc/Gluc utilize different substrates, they can be used together for dual BLI to monitor two different processes simultaneously.

2.3 Secreted blood reporters

Traditional enzyme-based reporter systems using cytosolic markers have been successfully used in different fields; however, they generally require tissue lysis and are therefore not suited for frequent imaging.⁸⁶ On the other hand, reporter proteins which are naturally secreted and can be detected in the cell-free conditioned medium in culture or in animal body fluids (blood/urine) were shown to be useful tools for non-invasive and real-time monitoring of different biological processes including tumor development, growth and response to different therapies, time-course embryo development, viral dissemination, gene transfer as well as the fate of genetically engineered cells in animal models.^{68,87,88} The most commonly used blood reporters are the secreted alkaline phosphatase (SEAP), soluble marker peptides derived from

human carcinoembryonic antigen and human chorionic gonadotropin, as well as *Gaussia* luciferase.⁸⁶

SEAP was the first described blood reporter; Berger et al.⁸⁹ used SEAP for quantification experiments in cell culture and created a fully active secreted protein by introducing a termination codon. Thereafter, this reporter was applied for *ex vivo* analysis of gene transfer in a mouse model.⁹⁰ SEAP can be constitutively expressed and efficiently released from transfected cells and is the most common reporter to monitor biological processes *ex vivo*.⁸⁶ Bettan et al.⁹⁰ and Cullen and Malim⁹¹ observed that changes in SEAP levels in medium of Chinese hamster ovary cells are directly proportional to changes in intracellular SEAP mRNA and cell number and hereby they initiated the widely use of SEAP as a secreted serum reporter.^{86,92} Its use has been extended to the clinic, where its serum levels have been used to monitor systemic and cervical antibodies after vaccination with HPV16/18 AS04-adjuvant vaccine.⁹²

Due to its high molecular weight (64kDA) expression level in the blood is low, requiring relatively large samples to be measured. Further, most blood samples contain naturally occurring serum alkaline phosphatases, which can interfere with the SEAP assay.⁹³

Soluble marker peptides are of great use in cancer virotherapy studies since they can be introduced into a virus to monitor its spread and elimination *in vivo*. Furthermore, they can even measure the profile of viral gene expression as well as the kinetics over time.^{86,87} An optimal soluble marker peptide should lack biological activity, the half-life should be constant in the circulation, it should have a limited immunogenicity and a validated assay should be available.⁸⁷

Edmonston vaccine strain of measles virus (MV-Edm) has been effectively engineered to express different soluble marker peptides, including human carcinoembryonic antigen (hCEA) and the β subunit of human chorionic gonadotropin (β hCG).^{94,95} Recently strains of this virus have been used to infect and destroy cancerous cells without affecting the surrounding tissues. This specificity can be explained by an over expression of CD46, a measles virus receptor, on the tumor cells. Simultaneously, these strains were modified to express certain soluble marker

peptides, such as CEA, and thereby the viral gene expression and replication could be monitored *in vivo*.⁸⁷

Recently, *Gaussia* luciferase has been characterized as a blood reporter. The major advantage of using Gluc as a secreted blood reporter is that its *ex vivo* blood analysis can complement *in vivo* bioluminescence imaging. Thereby Gluc assay has the ability to localize the signal *in vivo* while monitoring the tumor response *ex vivo*.⁷⁵ This multifaceted approach gives Gluc great advantage as a blood reporter. Furthermore, Gluc also has a much shorter assay time with increased sensitivity and linear range over other secreted blood reporters.^{75,68,80}

Gluc has been used extensively as a blood reporter. The Gluc blood assay was for instance used to monitor the response to treatment and metastasis of human breast cancer in animal models. Besides the good correlation between the primary tumor volume and the Gluc level in the blood and urine, more importantly the Gluc assay revealed early detection of tumor growth and metastasis in these animal models which was not accomplished by typical *in vivo* imaging techniques.⁸²

In addition, Gluc can be used for the evaluation of transcriptional regulation associated with signaling pathways. These pathways can be dysregulated in many human disorders including cancer.

2.4 BLI in cancer: strategic approaches

BLI has shown to be a valuable tool in the understanding of tumor biology and the intricate processes associated with tumorigenesis. Its ability to report from the subcellular level, to track both proteins and cells, to visualize gene activation and to monitor responses to cancer therapies has allowed the development of many new research strategies. Its key roles in cancer are summarized below.

Imaging of apoptosis. Apoptosis, or programmed cell death is executed through activation of cysteine aspartyl proteases (caspases) and is very often disrupted in cancer. This process has recently been monitored by fusing an inactive luciferase reporter gene to a caspase cleavage site. An example of such a reporter is the caspase 3 – Gluc reporter. Gluc is fused to the estrogen receptor (ER) regulating domain and is thereby rendered inactive. Since the two genes are separated by a

caspase cleavage site (DEVD), Gluc will be released in the presence of caspase 3, resulting in light emission when apoptosis occurs.⁹⁶⁻⁹⁸

Imaging of tumor therapy. BLI allows for the quantitative measurement of tumor growth and response to therapy. The amount of luciferase expression correlates directly to the amount of tumor cells.⁹⁹ First, luciferase reporter genes are *ex vivo* introduced in GBM cells for stable expression. Upon transplantation, tumor signal can be measured by cooled CCD camera or in the blood using the luciferin substrate; making it possible to track growth, metastasis and response to therapy in animal models of GBM.^{100,101}

Drug discovery. The screening of drug libraries is a very time consuming process. BLI allows for sensitive and relatively quick readout of photon emission. This way screening of thousands of compounds can be done in an effective way, using a cell-based assay. Luciferases are used as cell viability markers and by interpreting their light output, molecules with specific toxicity towards cancer cells can be identified.¹⁰² Gluc is especially useful in this setting, since it is secreted. Sampling aliquots of conditioned medium over time allows noninvasive evaluation of cell fate in real time.¹⁰³ Luciferases can also be used for the screening of gene-targeted drugs. Reporter genes containing a DNA binding sequence of the gene of interest (GOI) driving the expression of a luciferase can be introduced. P53, the most studied tumor suppressor gene, is an important target for drugs. By using a p53 reporter vector, small molecules that affect the transcriptional activation can be identified.

Imaging of (Cancer) Stem Cells. Cancer Stem Cells are thought to play a major role in the initiation and progression of GBM. Understanding and tracking of these cells could provide new insights in tumor biology. Further, a variety of 'regular' stem cells (mesenchymal, neural, embryonic, hematogenic) can be used as drug delivery vehicles, since they are known to "home" to the tumor site upon iv administration.^{104,105} This way, delivery issues related to the use of viral vectors (low transduction percentage, targeting) can be circumvented. An RFP-luciferase-thymidine kinase reporter protein has been used to label mesenchymal stem cells and track them in mice using BLI and PET.¹⁰⁶ Other stem cell tracking assays based on Gluc have been validated in animal models for several stem cell lines.

Imaging of hypoxia and angiogenesis. Hypoxia and angiogenesis are very closely related; they are two of the hallmarks of GBM. Upon hypoxic circumstances, different growth factors, transcription factors and cytokines are induced (as described in the GBM section). The main transcription factor found in a hypoxic state is the hypoxia-inducing factor (HIF1). HIF1 binds to HRE (HIF responsive element) to maintain transcription factor activation. Reporter luciferases coupled to the HRE element are designed to allow the visualization of hypoxic areas in the tumor and to help developing HIF targeted therapies.^{107,108} A similar system exists to measure angiogenesis. These luciferase reporters are coupled to VEGFR2, allowing visualization of areas high in angiogenic activity upon activation of the receptor.¹⁰⁹

BLI and gene therapy. Gene therapy is a promising approach in the battle against cancer and many other diseases. BLI reporter luciferases allow the evaluation of viral tropism, transduction efficiency and replication^{110,111}, providing the tools to further optimize this method. Since the efficacy of gene therapy mediated approaches is dependent on proper transduction, it is important to validate whether or not enough expression has been established. Otherwise, a lack of effect will be blamed on the chosen strategy, and a potential successful approach is rendered ineffective for the wrong reasons.

2.5 BLI and cancer: hot topics and limitations

The ability of BLI to give insight in both interactions between cells and their environment and intracellular processes makes BLI a very important tool in cancer research. Furthermore, it can facilitate the identification of cancer treatment by validating novel drugs in animal models, bridging the gap between the laboratory and the clinic. However, some limitations need to be overcome to further increase the value of BLI in (cancer) research. As for this moment, the use of BLI is limited to animal models, due to its relatively weak light emission (due to signal quenching and scattering through tissue) and potential substrate-associated toxicity).

Light emission and signal quenching. Both Gluc and Rluc emit light in the blue range of the spectrum. This causes that part of their light is absorbed by pigmented molecules as hemoglobin and melanin and is scattered through tissue, limiting its *in*

in vivo sensitivity. Still, sufficient signal can escape these barriers and is detected by a cooled CCD camera or in the blood. Current research is focusing on the engineering of luciferase variants emitting light in the red region of the spectrum or with an even brighter intensity.

Signal Stability. Gluc emits light in a flash type bioluminescence reaction, resulting in a peak signal as soon as substrate is added, followed by rapid light decay. This is favorable for readings with a CCD camera, since accumulation of signal over time is limited, allowing for several reads in a relatively short amount of time. Since Gluc is secreted, it is also very suitable as a cell viability marker in drug screens. Aliquots of the conditioned medium can be assayed over time, allowing functional analysis of drug kinetics. However, due to the rapid light decay, the use of a luminometer with a built-in injector is essential for immediate reading of signal once substrate is added, one well at a time. Too much time delay will be accompanied by a drop in Gluc signal, not caused by efficacy of the drug, but by kinetic instability, potentially confounding results. Therefore, a Gluc variant with a more stable light output would be highly desirable for use in drug screens. A more stable type of Gluc has recently been discovered; however, this luciferase only exhibits its increased stability in the presence of the detergent Triton-X100. Interactions between the detergent and the to be tested drugs cannot be excluded, limiting the value of the assay.

Measuring interaction. One limitation to current bioluminescence imaging is that typically only one luciferase reporter is used to measure one parameter of tumor development. As a highly malignant form of brain tumor, GBM progression is a complex process involving communication between tumor cells, surrounding “normal” cells, and the vasculature.¹¹² Simultaneous measurement of multiple factors of tumor growth as well as the tumor’s response to therapeutic agents would be extremely helpful in getting insight in the complex interactions of cancer growth. Since Fluc and Gluc/Rluc use different substrates, recently a combination of these luciferases has been used for dual reporting allowing the simultaneous monitoring of two events.¹¹³

TRAIL. TRAIL (tumor necrosis factor related apoptosis inducing ligand) is a member of the TNF family and is one of the most commonly explored cancer therapeutics,

because it binds to death receptors found specifically on tumor cells. Therefore, TRAIL is able to cause a widespread apoptotic effect with minimal cytotoxic effects on normal tissues.^{114,115} In preclinical studies, impressive growth inhibition and cytotoxicity against malignant tumor cells of various origin was observed, including lung, breast, colon, bladder, brain and T cell malignancies.¹¹⁶ However, there also appears to be a group of tumors, including GBM, that is resistant to TRAIL-mediated apoptosis. Upregulation of the Bcl2 associated Athanoge (BAG3) genes and multiple other genes have been described, causing resistance at various points along the apoptotic pathway. The second issue in the use of TRAIL for glioma therapy is its inability to cross the blood brain barrier. In a recent Gluc-based drug screen of the Tannous lab, molecules were identified that sensitized GBM cells for TRAIL. This resulted in the selection of Lanatoside C, an FDA approved cardiac glycoside that is capable of crossing the blood-brain barrier.¹⁰³ Lanatoside C on its own was found to induce a non-apoptotic necroptosis-like cell death. The combination of the dual cell death mechanisms displayed by TRAIL (apoptotic) and Lanatoside C (necroptotic) appeared to be very successful and provides a basis for the development of new glioma therapy.¹⁰³

2.6 *In vitro* Glioma Research and Mycoplasma

Mycoplasma species are the smallest organisms known and thereby not seen by microscope. Mycoplasma are resistant to commonly used antibiotics and therefore are frequent contaminants in regular cell culture with an incidence up to 70%.^{4,117,118} These contaminants have been shown to affect different pathways in cell culture yielding to false interpretation of data. Whether *in vitro* or *in vivo*, all molecular techniques described above can be severely affected by mycoplasma contamination with almost all cellular processes.^{117,119,120} Logically, these facts underlie the importance of detecting and clearing Mycoplasma contamination in all experimental research laboratories.

While many different species of mycoplasma have been isolated, only few are responsible for 90-95% of mammalian cell contaminations, namely: *M. orale*, *M. hyorhinitis*, *M. arginini*, *M. fermentans*, *M. hominis* or *A. laidlawii*. The most common

form of Mycoplasma is the *M. orale*, found in the oral cavity of healthy humans and accounts for 20-40% of all mycoplasma infections in cell cultures (Table 5).⁴ With the knowledge of this widespread contamination and its disastrous effects, one can understand that a detection method which is simple, sensitive, specific and inexpensive is needed.

Currently a wide range of detection methods are being used, of which the classical culture assay with the polymerase chain reaction (PCR) is known to be the most reliable nonetheless complex and time-consuming approach. PCR is based on the amplification of mycoplasma DNA, it has the advantage to distinguish different species of Mycoplasma and it provides a sensitive and specific method to quickly identify contamination and monitor growing cell cultures. Nevertheless PCR requires careful preparation of the sample, attention to polymerase inhibitors in the cell cultures and often has false positive contaminants.¹²¹ Traditional bacterial culture has the advantage of actually observing the colonies in combination with a high sensitivity and inexpensiveness. However this assay disqualifies itself by being even more time consuming; expertise is required and simply not all common Mycoplasma species can be cultured.⁴ In addition to culture and PCR, other assays have been described, such as fluorescent DNA staining, enzyme-linked immunosorbent assays and RNA amplification, with each having significant drawbacks. Fluorescence DNA staining lacks the ability to reveal all the common species, enzyme-linked immunosorbent assays have a low sensitivity and RNA amplification requires a rather complex protocol.^{4,117,121} Currently a simple bioluminescence-based mycoplasma detection kit is commercially available, but it has low sensitivity and its use for larger stocks of cell culture is limited due to high cost.

Table 5: Most common mycoplasma contaminations. ⁴

Species	Frequency	Natural host
<i>M. orale</i>	20 – 40%	Human
<i>M. hyorhinis</i>	10 – 40%	Swine
<i>M. arginini</i>	20 – 30%	Bovine
<i>M. fermentans</i>	10 – 20%	Human
<i>M. hominis</i>	10 – 20%	Human
<i>A. laidlawii</i>	5 – 20%	Bovine

3. AIMS AND OUTLINE

The aim of this thesis is to combine the strengths of gene-therapy and BLI for the development of novel reporter systems in order to study glioma tumor biology and its response to therapeutic compounds. We further tried to optimize the currently available BLI luciferases (*Gaussia* luciferase, *Vargula hilgendorfi*) and assays (Gluc blood assay, Mycoplasma detection assay). We explored a new multimodal targeted liposome formulation with increased relaxivity for the treatment and imaging of cancer. Finally we combined the newly developed and enhanced reporters to test a new therapeutic combination for the treatment of Glioma (TRAIL, Lanatoside C). The research as described above is divided into ten chapters (**chapter III to XII**). Sarah Bovenberg takes responsibility for **chapter III, IV, V, and XI**, and Hannah Degeling takes responsibility for **chapter VI until X and chapter XII**.

Secreted blood reporters are valuable tools for sensitive and fast detection, quantification and noninvasive monitoring of in vivo biological processes.^{75,80} The level of these secreted reporters can be measured over time to generate multiple data sets without the need to sacrifice the animal, since only a small amount of blood is required. In **Chapter III** we enhanced the sensitivity of Gluc as a blood-reporter by designing an alternative Gluc blood assay. The enormous advantage of capturing Gluc in a blood-based assay instead of by CCD camera is the ability to follow intracellular processes in real time. Whereas CCD camera obtained pictures show luciferase signal (and thereby reporter gene activation) at a static point in time, the blood assay allows for a dynamic approach, in which a drop of blood can be collected every 5 minutes. The CCD camera does not share this characteristic, since the procedure is time consuming and the BLI reaction takes place inside the animal. Therefore, one has to wait until the previous BLI signal has died out, before a new (reliable) measurement can be made. In the new assay, Gluc is captured from the blood by an antibody-mediated reaction before bioluminescence reaction takes place. This procedure prevents signal quenching by pigmented molecules like hemoglobin, resulting in an over one order in magnitude increase in sensitivity, allowing the detection of few circulating cells and metastases.

In **Chapter V** the development of a triple reporter system based on *Vargula*, *Gaussia* and *Firefly* luciferases for sequential imaging of three different biological processes is described. We applied this system to monitor the effect of the apoptosis-inducing ligand sTRAIL (soluble Tumor necrosis factor-Related Apoptosis-Inducing Ligand) on GBM tumor cells using an adeno-associated viral AAV vector. As explained earlier, TRAIL is only toxic to cancer cells, since only these cells overexpress TRAIL death receptors. Unfortunately, GBM cells seem to be resistant to TRAIL-mediated apoptosis. To overcome this limitation, in a drug screen a molecule sensitizing GBM cells for TRAIL, called Lanatoside C, was identified. Lanatoside C is a known, FDA approved, cardiac glycoside. We designed a triple luciferase reporter system, to measure the activation patterns and outcome of combined treatment of TRAIL and Lanatoside C in GBM. Since TRAIL cannot cross the blood brain barrier, we circumvented this problem by delivering sTRAIL directly to brain tumor environment by AAV-mediated gene delivery. By engineering the normal brain to synthesize and secrete sTRAIL, it can form a zone of resistance against newly developed glioma, which can be treated with lanatoside C therapy. We used Vluc to monitor AAV gene delivery of sTRAIL, Gluc to monitor the binding of sTRAIL to the glioma death receptor and the consequential activation of downstream events, and Fluc to measure tumor response to combined sTRAIL and Lanatoside C treatment. This work is the first demonstration of triple *in vivo* bioluminescence imaging and will have broad applicability in different fields.

In **Chapter IV** we describe the development of a first of its kind multiplex blood reporter that allows the *ex vivo* evaluation of *in vivo* processes. Since tumorigenesis is an intricate and dynamic process and GBM cells in particular are known for their ability to escape cell death and change characteristics, we developed the first multiplex blood reporter based on secreted alkaline phosphatase (SEAP), *Gaussia* and *Vargula* luciferases. This multiplex system differs from the triple imaging system as described in Chapter V in that here all reporters are secreted. As a result, tumor changes can be followed in real time (by simply taking an aliquot of blood), whereas the reporter from chapter V does not allow for real time imaging. Since *Vargula* has not been previously used as a blood reporter, first we characterized it as a secreted blood reporter. As a proof of concept the response of three different subsets of glioma cells to the chemotherapeutic agent Temozolomide (TMZ) in the same animal

was monitored. No signal bleeding or substrate cross reaction was observed, proving that these 3 reporters can be used simultaneously in the same animal. This new multiplex reporter system can be extended and applied to many different fields for simultaneous monitoring of multiple biological parameters in real time.

One of the current limitations of BLI for *in vivo* imaging applications is the emission of light in the blue range of the spectrum. As discussed above, pigmented molecules like melanin and hemoglobin absorb the emitted light, while tissue further scatters the signal. Therefore, little signal remains to be picked up by CCD camera, decreasing the sensitivity of BLI for *in vivo* applications. Red light on the other hand, does not get absorbed, and would therefore be an ideal characteristic for a sensitive *in vivo* BLI reporter. Another issue is the flash type bioluminescence of Gluc when used in high throughput drug screens, limiting the numbers of drugs that can be screened.¹⁰³ A Gluc variant that catalyzes a glow-type reaction would be extremely helpful in the field of drug discovery allowing for high-throughput approach without the risk of confounding results due to kinetic instability (wildtype Gluc) or to interactions with detergents such as TritonX-100 (GucM43I). Therefore, in **Chapter VI** we used directed molecular evolution to optimize *Gaussia* luciferase for high throughput applications and *in vivo* work. We screened for variants with a higher light intensity, glow-type luminescence and shift in emission spectrum, resulting in the identification of several variants with 10-15nm shifts in emission spectrum and one variant with a glow-type of bioluminescence that remained stable for over 10 minutes.

The exploration for new luciferases hasn't come to an end yet. So far liFluc has only been used for cell-based assays and has only been expressed in bacteria. Therefore, in **Chapter VII** we developed and characterized a codon-optimized variant of liFluc for mammalian gene expression and used it for *in vivo* imaging of tumors.

Since glioma research relies heavily on tissue culture, and since almost every single intracellular biological processes can be influenced by Mycoplasma contamination – severely confounding results- the use for Gluc as a Mycoplasma detection sensor was explored in **Chapter VIII**. We developed a simple and cost-effective

mycoplasma detection assay using the *Gaussia* luciferase reporter and showed it to be much more sensitive than other bioluminescence-based assays.

In **Chapter IX** we describe the step-by-step protocol for Gluc Mycoplasma assay as created in **Chapter VIII**. Further, we point out critical steps and potential pitfalls regarding the assay for other users.

In **Chapter X**, we developed a new type of liposome as a contrast agent for MRI with a higher efficiency than the conventional liposome. We showed that this new liposome can be used for MRI guided therapeutic delivery to targeted cells due to its biotin inclusion and for ultrasound guided release of its contents due to its thermo-sensitivity.

In **Chapter XI and XII** we provide an overview of the Glioma research field, placing the work developed in this thesis in a broader setting. We review current research strategies, both in experimental setting and in the clinic, discuss the translational gap that exists between those two worlds and reflected on possible future directions.

In **Chapter XIII** we both discuss our own work and suggest what following steps should be taken in order to translate our findings into a clinical setting.

REFERENCES

- 1 Fulci, G. & Chiocca, E. A. The status of gene therapy for brain tumors. *Expert opinion on biological therapy* **7**, 197-208, doi:10.1517/14712598.7.2.197 (2007).
- 2 Robbins, P. D. & Ghivizzani, S. C. Viral vectors for gene therapy. *Pharmacology & therapeutics* **80**, 35-47 (1998).
- 3 Maguire, C. A., van der Mijn, J. C., Degeling, M. H., Morse, D. & Tannous, B. A. Codon-Optimized *Luciola italica* Luciferase Variants for Mammalian Gene Expression in Culture and In Vivo. *Molecular imaging*, doi:10.2310/7290.2011.00022 (2011).
- 4 Drexler, H. G. & Uphoff, C. C. Mycoplasma contamination of cell cultures: Incidence, sources, effects, detection, elimination, prevention. *Cytotechnology* **39**, 75-90, doi:10.1023/A:1022913015916 (2002).
- 5 systems, T. *Triple Luciferase Assay Reagent for Renilla, Cypridina (Vargula), and Red Firefly Luciferases*, <http://www.targetingsystems.net/pdf/TLAR-1_brochure.pdf> (
- 6 Friedmann, T. & Roblin, R. Gene therapy for human genetic disease? *Science* **175**, 949-955 (1972).
- 7 Sheridan, C. Gene therapy finds its niche. *Nature biotechnology* **29**, 121-128, doi:10.1038/nbt.1769 (2011).
- 8 Bartlett, J. S., Samulski, R. J. & McCown, T. J. Selective and rapid uptake of adeno-associated virus type 2 in brain. *Human gene therapy* **9**, 1181-1186, doi:10.1089/hum.1998.9.8-1181 (1998).
- 9 Samulski, R. J. Adeno-associated virus: integration at a specific chromosomal locus. *Current opinion in genetics & development* **3**, 74-80 (1993).
- 10 Muzyczka, N. Use of adeno-associated virus as a general transduction vector for mammalian cells. *Current topics in microbiology and immunology* **158**, 97-129 (1992).
- 11 Naldini, L. *et al.* In vivo gene delivery and stable transduction of nondividing cells by a lentiviral vector. *Science* **272**, 263-267 (1996).
- 12 Davidson, B. L. & Breakefield, X. O. Viral vectors for gene delivery to the nervous system. *Nature reviews. Neuroscience* **4**, 353-364, doi:10.1038/nrn1104 (2003).
- 13 Escors, D. & Breckpot, K. Lentiviral vectors in gene therapy: their current status and future potential. *Archivum immunologiae et therapiae experimentalis* **58**, 107-119, doi:10.1007/s00005-010-0063-4 (2010).
- 14 Kroeger, K. M. *et al.* Gene therapy and virotherapy: novel therapeutic approaches for brain tumors. *Discovery medicine* **10**, 293-304 (2010).
- 15 Beltinger, C. *et al.* Herpes simplex virus thymidine kinase/ganciclovir-induced apoptosis involves ligand-independent death receptor aggregation and activation of caspases. *Proceedings of the National Academy of Sciences of the United States of America* **96**, 8699-8704 (1999).
- 16 Hiraoka, K. *et al.* Therapeutic efficacy of replication-competent retrovirus vector-mediated suicide gene therapy in a multifocal colorectal cancer metastasis model. *Cancer research* **67**, 5345-5353, doi:10.1158/0008-5472.CAN-06-4673 (2007).
- 17 Wykosky, J., Gibo, D. M., Stanton, C. & Debinski, W. Interleukin-13 receptor alpha 2, EphA2, and Fos-related antigen 1 as molecular denominators of high-grade astrocytomas and specific targets for combinatorial therapy.

- Clinical cancer research : an official journal of the American Association for Cancer Research* **14**, 199-208, doi:10.1158/1078-0432.CCR-07-1990 (2008).
- 18 Candolfi, M. *et al.* Gene therapy-mediated delivery of targeted cytotoxins for glioma therapeutics. *Proceedings of the National Academy of Sciences of the United States of America* **107**, 20021-20026, doi:10.1073/pnas.1008261107 (2010).
- 19 Brenner, M. K. & Okur, F. V. Overview of gene therapy clinical progress including cancer treatment with gene-modified T cells. *Hematology / the Education Program of the American Society of Hematology. American Society of Hematology. Education Program*, 675-681, doi:10.1182/asheducation-2009.1.675 (2009).
- 20 Maguire, C. A. *et al.* Preventing growth of brain tumors by creating a zone of resistance. *Molecular therapy : the journal of the American Society of Gene Therapy* **16**, 1695-1702, doi:10.1038/mt.2008.168 (2008).
- 21 Torchilin, V. P. Recent advances with liposomes as pharmaceutical carriers. *Nature reviews. Drug discovery* **4**, 145-160, doi:10.1038/nrd1632 (2005).
- 22 PharmaEngine. *PharmaEngine*, <<http://www.pharmaengine.com/>> (
- 23 Tagami, T., Ernsting, M. J. & Li, S. D. Optimization of a novel and improved thermosensitive liposome formulated with DPPC and a Brij surfactant using a robust in vitro system. *Journal of controlled release : official journal of the Controlled Release Society* **154**, 290-297, doi:10.1016/j.jconrel.2011.05.020 (2011).
- 24 Buse, J. & El-Aneed, A. Properties, engineering and applications of lipid-based nanoparticle drug-delivery systems: current research and advances. *Nanomedicine (Lond)* **5**, 1237-1260, doi:10.2217/nnm.10.107 (2010).
- 25 Dagar, S., Rubinstein, I. & Onyuksel, H. Liposomes in ultrasound and gamma scintigraphic imaging. *Methods in enzymology* **373**, 198-214, doi:10.1016/S0076-6879(03)73013-4 (2003).
- 26 Miller, J. C. & Thrall, J. H. Clinical molecular imaging. *Journal of the American College of Radiology : JACR* **1**, 4-23, doi:10.1016/S1546-1440(03)00025-5 (2004).
- 27 Shah, K., Jacobs, A., Breakefield, X. O. & Weissleder, R. Molecular imaging of gene therapy for cancer. *Gene therapy* **11**, 1175-1187, doi:10.1038/sj.gt.3302278 (2004).
- 28 Weissleder, R. & Mahmood, U. Molecular imaging. *Radiology* **219**, 316-333 (2001).
- 29 Weissleder, R. & Pittet, M. J. Imaging in the era of molecular oncology. *Nature* **452**, 580-589, doi:10.1038/nature06917 (2008).
- 30 Massoud, T. F. & Gambhir, S. S. Molecular imaging in living subjects: seeing fundamental biological processes in a new light. *Genes & development* **17**, 545-580, doi:10.1101/gad.1047403 (2003).
- 31 Ray, P. Multimodality molecular imaging of disease progression in living subjects. *Journal of biosciences* **36**, 499-504 (2011).
- 32 Peterson, T. E. & Furenlid, L. R. SPECT detectors: the Anger Camera and beyond. *Physics in medicine and biology* **56**, R145-182, doi:10.1088/0031-9155/56/17/R01 (2011).
- 33 Patton, J. A. Instrumentation for coincidence imaging with multihead scintillation cameras. *Seminars in nuclear medicine* **30**, 239-254 (2000).
- 34 Reader, A. J. & Zweit, J. Developments in whole-body molecular imaging of live subjects. *Trends in pharmacological sciences* **22**, 604-607 (2001).

- 35 Herholz, K., Wienhard, K. & Heiss, W. D. Validity of PET studies in brain
tumors. *Cerebrovascular and brain metabolism reviews* **2**, 240-265 (1990).
- 36 Price, P. PET as a potential tool for imaging molecular mechanisms of
oncology in man. *Trends in molecular medicine* **7**, 442-446 (2001).
- 37 Gambhir, S. S. Molecular imaging of cancer with positron emission
tomography. *Nature reviews. Cancer* **2**, 683-693, doi:10.1038/nrc882 (2002).
- 38 Jacobs, A. H., Dittmar, C., Winkeler, A., Garlip, G. & Heiss, W. D. Molecular
imaging of gliomas. *Molecular imaging* **1**, 309-335 (2002).
- 39 Mettler, F. A. *Essentials of Radiology*. Vol. 2 chapter 1 (Saunders Elsevier,
2005).
- 40 Medicine, U. S. N. L. o. *MedlinePlus*,
<<http://www.nlm.nih.gov/medlineplus/sitemap.html>> (2012).
- 41 Administration, U. S. F. a. D. *FDA U.S. Food and Drug Administration*,
<<http://www.fda.gov/>> (2012).
- 42 Tjuvajev, J. G. *et al.* A general approach to the non-invasive imaging of
transgenes using cis-linked herpes simplex virus thymidine kinase. *Neoplasia*
1, 315-320 (1999).
- 43 Leong-Poi, H., Christiansen, J., Klibanov, A. L., Kaul, S. & Lindner, J. R.
Noninvasive assessment of angiogenesis by ultrasound and microbubbles
targeted to alpha(v)-integrins. *Circulation* **107**, 455-460 (2003).
- 44 Lindner, J. R. *et al.* Ultrasound assessment of inflammation and renal tissue
injury with microbubbles targeted to P-selectin. *Circulation* **104**, 2107-2112
(2001).
- 45 Hildebrandt, I. J. & Gambhir, S. S. Molecular imaging applications for
immunology. *Clin Immunol* **111**, 210-224, doi:10.1016/j.clim.2003.12.018
(2004).
- 46 Bulte, J. W., Duncan, I. D. & Frank, J. A. In vivo magnetic resonance tracking
of magnetically labeled cells after transplantation. *Journal of cerebral blood
flow and metabolism : official journal of the International Society of Cerebral
Blood Flow and Metabolism* **22**, 899-907, doi:10.1097/00004647-200208000-
00001 (2002).
- 47 *cancernetwork*. *cancernetwork*, <<http://www.cancernetwork.com/home>> (
48 *aztechradiology*. *aztechradiology*, <<http://aztechradiology.com/>> (
49 *BBC*. *BBC mobile*, <<http://www.bbc.co.uk/>> (
50 *MIE*. *MIE Medical Imaging Electronics*, <<http://www.miegermany.de/>> (
51 *Radiologists*, C. A. o. *Radiology for patients*, 2004).
- 52 *Engineers*, S. o. P. *Society of Petroleum Engineers*,
<<http://www.spe.org/index.php>> (
53 *Berkerly lab*, A. U. S. D. o. E. N. L. O. b. t. U. o. C. *News Center*,
<<http://newscenter.lbl.gov/>> (
54 *Chalfie*, M., Tu, Y., Euskirchen, G., Ward, W. W. & Prasher, D. C. Green
fluorescent protein as a marker for gene expression. *Science* **263**, 802-805
(1994).
- 55 Gerdes, H. H. & Kaether, C. Green fluorescent protein: applications in cell
biology. *FEBS letters* **389**, 44-47 (1996).
- 56 Ellenberg, J., Lippincott-Schwartz, J. & Presley, J. F. Dual-colour imaging with
GFP variants. *Trends in cell biology* **9**, 52-56 (1999).
- 57 Zacharakis, G. *et al.* Volumetric tomography of fluorescent proteins through
small animals in vivo. *Proceedings of the National Academy of Sciences of*

- the United States of America* **102**, 18252-18257, doi:10.1073/pnas.0504628102 (2005).
- 58 Zacharakis, G., Shih, H., Ripoll, J., Weissleder, R. & Ntziachristos, V. Normalized transillumination of fluorescent proteins in small animals. *Molecular imaging* **5**, 153-159 (2006).
- 59 Turchin, I. V. *et al.* Fluorescence diffuse tomography for detection of red fluorescent protein expressed tumors in small animals. *Journal of biomedical optics* **13**, 041310, doi:10.1117/1.2953528 (2008).
- 60 Shaner, N. C. *et al.* Improved monomeric red, orange and yellow fluorescent proteins derived from *Discosoma* sp. red fluorescent protein. *Nature biotechnology* **22**, 1567-1572, doi:10.1038/nbt1037 (2004).
- 61 Shcherbo, D. *et al.* Bright far-red fluorescent protein for whole-body imaging. *Nature methods* **4**, 741-746, doi:10.1038/nmeth1083 (2007).
- 62 Weissleder, R., Tung, C. H., Mahmood, U. & Bogdanov, A., Jr. In vivo imaging of tumors with protease-activated near-infrared fluorescent probes. *Nature biotechnology* **17**, 375-378, doi:10.1038/7933 (1999).
- 63 Ntziachristos, V., Ripoll, J., Wang, L. V. & Weissleder, R. Looking and listening to light: the evolution of whole-body photonic imaging. *Nature biotechnology* **23**, 313-320, doi:10.1038/nbt1074 (2005).
- 64 Bremer, C., Tung, C. H., Bogdanov, A., Jr. & Weissleder, R. Imaging of differential protease expression in breast cancers for detection of aggressive tumor phenotypes. *Radiology* **222**, 814-818 (2002).
- 65 Greer, L. F., 3rd & Szalay, A. A. Imaging of light emission from the expression of luciferases in living cells and organisms: a review. *Luminescence : the journal of biological and chemical luminescence* **17**, 43-74, doi:10.1002/bio.676 (2002).
- 66 McElroy, W. D., Seliger, H. H. & White, E. H. Mechanism of bioluminescence, chemiluminescence and enzyme function in the oxidation of firefly luciferin. *Photochemistry and photobiology* **10**, 153-170 (1969).
- 67 Johnson, F. H. & Shimomura, O. Enzymatic and nonenzymatic bioluminescence. *Photophysiology*, 275-334 (1972).
- 68 Tannous, B. A., Kim, D. E., Fernandez, J. L., Weissleder, R. & Breakefield, X. O. Codon-optimized *Gussia* luciferase cDNA for mammalian gene expression in culture and in vivo. *Molecular therapy : the journal of the American Society of Gene Therapy* **11**, 435-443, doi:10.1016/j.ymthe.2004.10.016 (2005).
- 69 McCaffrey, A., Kay, M. A. & Contag, C. H. Advancing molecular therapies through in vivo bioluminescent imaging. *Molecular imaging* **2**, 75-86 (2003).
- 70 Gross, S. & Pivnicka-Worms, D. Spying on cancer: molecular imaging in vivo with genetically encoded reporters. *Cancer cell* **7**, 5-15, doi:10.1016/j.ccr.2004.12.011 (2005).
- 71 DeLuca, M. Firefly luciferase. *Advances in enzymology and related areas of molecular biology* **44**, 37-68 (1976).
- 72 de Wet, J. R., Wood, K. V., Helinski, D. R. & DeLuca, M. Cloning firefly luciferase. *Methods in enzymology* **133**, 3-14 (1986).
- 73 Palomares, A. J., DeLuca, M. A. & Helinski, D. R. Firefly luciferase as a reporter enzyme for measuring gene expression in vegetative and symbiotic *Rhizobium meliloti* and other gram-negative bacteria. *Gene* **81**, 55-64 (1989).
- 74 Lorenz, W. W. *et al.* Expression of the *Renilla reniformis* luciferase gene in mammalian cells. *Journal of bioluminescence and chemiluminescence* **11**, 31-

- 37, doi:10.1002/(SICI)1099-1271(199601)11:1<31::AID-BIO398>3.0.CO;2-M (1996).
- 75 Wurdinger, T. *et al.* A secreted luciferase for ex vivo monitoring of in vivo processes. *Nature methods* **5**, 171-173, doi:10.1038/nmeth.1177 (2008).
- 76 Bovenberg, M. S., Degeling, M. H. & Tannous, B. A. Enhanced gaussia luciferase blood assay for monitoring of in vivo biological processes. *Analytical chemistry* **84**, 1189-1192, doi:10.1021/ac202833r (2012).
- 77 Santos, E. B. *et al.* Sensitive in vivo imaging of T cells using a membrane-bound *Gaussia princeps* luciferase. *Nature medicine* **15**, 338-344, doi:10.1038/nm.1930 (2009).
- 78 Tannous, B. A. *Gaussia* luciferase reporter assay for monitoring biological processes in culture and in vivo. *Nature protocols* **4**, 582-591, doi:10.1038/nprot.2009.28 (2009).
- 79 Maguire, C. A. *et al.* *Gaussia* luciferase variant for high-throughput functional screening applications. *Analytical chemistry* **81**, 7102-7106, doi:10.1021/ac901234r (2009).
- 80 Badr, C. E., Hewett, J. W., Breakefield, X. O. & Tannous, B. A. A highly sensitive assay for monitoring the secretory pathway and ER stress. *PLoS one* **2**, e571, doi:10.1371/journal.pone.0000571 (2007).
- 81 Badr, C. E. *et al.* Real-time monitoring of nuclear factor kappaB activity in cultured cells and in animal models. *Molecular imaging* **8**, 278-290 (2009).
- 82 Chung, E. *et al.* Secreted *Gaussia* luciferase as a biomarker for monitoring tumor progression and treatment response of systemic metastases. *PLoS one* **4**, e8316, doi:10.1371/journal.pone.0008316 (2009).
- 83 Nakanishi, H., Higuchi, Y., Kawakami, S., Yamashita, F. & Hashida, M. piggyBac transposon-mediated long-term gene expression in mice. *Molecular therapy : the journal of the American Society of Gene Therapy* **18**, 707-714, doi:10.1038/mt.2009.302 (2010).
- 84 Badr, C. E. *et al.* Suicidal gene therapy in an NF-kappaB-controlled tumor environment as monitored by a secreted blood reporter. *Gene therapy* **18**, 445-451, doi:10.1038/gt.2010.156 (2011).
- 85 Thompson, E. M., Nagata, S. & Tsuji, F. I. Cloning and expression of cDNA for the luciferase from the marine ostracod *Vargula hilgendorffii*. *Proceedings of the National Academy of Sciences of the United States of America* **86**, 6567-6571 (1989).
- 86 Tannous, B. A. & Teng, J. Secreted blood reporters: insights and applications. *Biotechnology advances* **29**, 997-1003, doi:10.1016/j.biotechadv.2011.08.021 (2011).
- 87 Msaouel, P., Dispenzieri, A. & Galanis, E. Clinical testing of engineered oncolytic measles virus strains in the treatment of cancer: an overview. *Current opinion in molecular therapeutics* **11**, 43-53 (2009).
- 88 Maelandsmo, G. M. *et al.* Use of a murine secreted alkaline phosphatase as a non-immunogenic reporter gene in mice. *The journal of gene medicine* **7**, 307-315, doi:10.1002/jgm.666 (2005).
- 89 Berger, J., Hauber, J., Hauber, R., Geiger, R. & Cullen, B. R. Secreted placental alkaline phosphatase: a powerful new quantitative indicator of gene expression in eukaryotic cells. *Gene* **66**, 1-10 (1988).
- 90 Bettan, M., Dartel, R. & Scherman, D. Secreted human placental alkaline phosphatase as a reporter gene for in vivo gene transfer. *Analytical biochemistry* **271**, 187-189, doi:10.1006/abio.1999.4144 (1999).

- 91 Cullen, B. R. & Malim, M. H. Secreted placental alkaline phosphatase as a eukaryotic reporter gene. *Methods in enzymology* **216**, 362-368 (1992).
- 92 Kemp, T. J. *et al.* Evaluation of systemic and mucosal anti-HPV16 and anti-HPV18 antibody responses from vaccinated women. *Vaccine* **26**, 3608-3616, doi:10.1016/j.vaccine.2008.04.074 (2008).
- 93 Hiramatsu, N. *et al.* Alkaline phosphatase vs luciferase as secreted reporter molecules in vivo. *Analytical biochemistry* **339**, 249-256, doi:10.1016/j.ab.2005.01.023 (2005).
- 94 Peng, K. W. *et al.* Intraperitoneal therapy of ovarian cancer using an engineered measles virus. *Cancer research* **62**, 4656-4662 (2002).
- 95 Pham, L. *et al.* Concordant activity of transgene expression cassettes inserted into E1, E3 and E4 cloning sites in the adenovirus genome. *The journal of gene medicine* **11**, 197-206, doi:10.1002/jgm.1289 (2009).
- 96 Ray, P., De, A., Patel, M. & Gambhir, S. S. Monitoring caspase-3 activation with a multimodality imaging sensor in living subjects. *Clinical cancer research : an official journal of the American Association for Cancer Research* **14**, 5801-5809, doi:10.1158/1078-0432.CCR-07-5244 (2008).
- 97 Laxman, B. *et al.* Noninvasive real-time imaging of apoptosis. *Proceedings of the National Academy of Sciences of the United States of America* **99**, 16551-16555, doi:10.1073/pnas.252644499 (2002).
- 98 Niers, J. M., Kerami, M., Pike, L., Lewandrowski, G. & Tannous, B. A. Multimodal in vivo imaging and blood monitoring of intrinsic and extrinsic apoptosis. *Molecular therapy : the journal of the American Society of Gene Therapy* **19**, 1090-1096, doi:10.1038/mt.2011.17 (2011).
- 99 Suzuki, T., Usuda, S., Ichinose, H. & Inouye, S. Real-time bioluminescence imaging of a protein secretory pathway in living mammalian cells using Gaussia luciferase. *FEBS letters* **581**, 4551-4556, doi:10.1016/j.febslet.2007.08.036 (2007).
- 100 Hamstra, D. A. *et al.* Real-time evaluation of p53 oscillatory behavior in vivo using bioluminescent imaging. *Cancer research* **66**, 7482-7489, doi:10.1158/0008-5472.CAN-06-1405 (2006).
- 101 Edinger, M. *et al.* Revealing lymphoma growth and the efficacy of immune cell therapies using in vivo bioluminescence imaging. *Blood* **101**, 640-648, doi:10.1182/blood-2002-06-1751 (2003).
- 102 Nogawa, M. *et al.* Monitoring luciferase-labeled cancer cell growth and metastasis in different in vivo models. *Cancer letters* **217**, 243-253, doi:10.1016/j.canlet.2004.07.010 (2005).
- 103 Badr, C. E., Wurdinger, T. & Tannous, B. A. Functional drug screening assay reveals potential glioma therapeutics. *Assay and drug development technologies* **9**, 281-289, doi:10.1089/adt.2010.0324 (2011).
- 104 Prins, R. M. *et al.* Anti-tumor activity and trafficking of self, tumor-specific T cells against tumors located in the brain. *Cancer immunology, immunotherapy : CII* **57**, 1279-1289, doi:10.1007/s00262-008-0461-1 (2008).
- 105 Swijnenburg, R. J. *et al.* In vivo imaging of embryonic stem cells reveals patterns of survival and immune rejection following transplantation. *Stem cells and development* **17**, 1023-1029, doi:10.1089/scd.2008.0091 (2008).
- 106 Wang, X. *et al.* Dynamic tracking of human hematopoietic stem cell engraftment using in vivo bioluminescence imaging. *Blood* **102**, 3478-3482, doi:10.1182/blood-2003-05-1432 (2003).

- 107 Harada, H., Kizaka-Kondoh, S. & Hiraoka, M. Optical imaging of tumor hypoxia and evaluation of efficacy of a hypoxia-targeting drug in living animals. *Molecular imaging* **4**, 182-193 (2005).
- 108 Shibata, T., Giaccia, A. J. & Brown, J. M. Development of a hypoxia-responsive vector for tumor-specific gene therapy. *Gene therapy* **7**, 493-498, doi:10.1038/sj.gt.3301124 (2000).
- 109 Faley, S. L. *et al.* Bioluminescence imaging of vascular endothelial growth factor promoter activity in murine mammary tumorigenesis. *Molecular imaging* **6**, 331-339 (2007).
- 110 Luker, K. E., Hutchens, M., Schultz, T., Pekosz, A. & Luker, G. D. Bioluminescence imaging of vaccinia virus: effects of interferon on viral replication and spread. *Virology* **341**, 284-300, doi:10.1016/j.virol.2005.06.049 (2005).
- 111 Cook, S. H. & Griffin, D. E. Luciferase imaging of a neurotropic viral infection in intact animals. *Journal of virology* **77**, 5333-5338 (2003).
- 112 Gilbertson, R. J. & Rich, J. N. Making a tumour's bed: glioblastoma stem cells and the vascular niche. *Nature reviews. Cancer* **7**, 733-736, doi:10.1038/nrc2246 (2007).
- 113 Bhaumik, S., Lewis, X. Z. & Gambhir, S. S. Optical imaging of Renilla luciferase, synthetic Renilla luciferase, and firefly luciferase reporter gene expression in living mice. *Journal of biomedical optics* **9**, 578-586, doi:10.1117/1.1647546 (2004).
- 114 Pan, G. *et al.* The receptor for the cytotoxic ligand TRAIL. *Science* **276**, 111-113 (1997).
- 115 Zhang, L. & Fang, B. Mechanisms of resistance to TRAIL-induced apoptosis in cancer. *Cancer gene therapy* **12**, 228-237, doi:10.1038/sj.cgt.7700792 (2005).
- 116 Chaudhari, B. R., Murphy, R. F. & Agrawal, D. K. Following the TRAIL to apoptosis. *Immunologic research* **35**, 249-262, doi:10.1385/IR:35:3:249 (2006).
- 117 Hay, R. J., Macy, M. L. & Chen, T. R. Mycoplasma infection of cultured cells. *Nature* **339**, 487-488, doi:10.1038/339487a0 (1989).
- 118 Rottem, S. & Barile, M. F. Beware of mycoplasmas. *Trends in biotechnology* **11**, 143-151 (1993).
- 119 Logunov, D. Y. *et al.* Mycoplasma infection suppresses p53, activates NF-kappaB and cooperates with oncogenic Ras in rodent fibroblast transformation. *Oncogene* **27**, 4521-4531, doi:10.1038/onc.2008.103 (2008).
- 120 Zinocker, S. *et al.* Mycoplasma contamination revisited: mesenchymal stromal cells harboring Mycoplasma hyorhinis potently inhibit lymphocyte proliferation in vitro. *PloS one* **6**, e16005, doi:10.1371/journal.pone.0016005 (2011).
- 121 Uphoff, C. C. & Drexler, H. G. Detection of mycoplasma in leukemia-lymphoma cell lines using polymerase chain reaction. *Leukemia : official journal of the Leukemia Society of America, Leukemia Research Fund, U.K* **16**, 289-293, doi:10.1038/sj.leu.2402365 (2002).

CHAPTER III



Enhanced *Gaussia* luciferase based blood assay for monitoring of *in vivo* biological processes

M. Sarah S. Bovenberg^{1,2,3*}, M. Hannah Degeling^{1,2,3*} and Bakhos A. Tannous^{1,2}

¹Experimental Therapeutics and Molecular Imaging Laboratory, Neuroscience Center, Department of Neurology,
²Program in Neuroscience, Harvard Medical School, Boston, MA 02114 USA. ³Department of Neurosurgery,
Leiden University Medical Center, Leiden, The Netherlands. * These authors contributed equally

ABSTRACT

Secreted *Gaussia* Luciferase (Gluc) has been shown to be a useful tool for *ex vivo* monitoring of *in vivo* biological processes. The Gluc level in the blood was used to detect tumor growth, metastasis and response to therapy, gene transfer, circulating cells viability, as well as transcription factors activation, complementing *in vivo* bioluminescence imaging. The sensitivity of the Gluc blood assay is limited due to the absorption of blue light by pigmented molecules such as hemoglobin resulting in quenching of the signal and therefore lower sensitivity. To overcome this problem, we designed an alternative microtiter well-based binding assay in which Gluc is captured first from blood using a specific antibody followed by the addition of coelenterazine and signal acquisition using a luminometer. This assay showed to be over one order of magnitude more sensitive in detecting Gluc in the blood as compared to the direct Gluc blood assay enhancing *ex vivo* monitoring of biological processes.

INTRODUCTION

Secreted blood reporters are valuable tools for sensitive and fast detection, quantification and non-invasive monitoring of *in vivo* biological processes¹⁻⁵. The level of these secreted reporters can be measured over time to generate multiple data sets without the need to sacrifice the animal, since only a small amount of blood is required. *Gaussia* Luciferase (Gluc) has been recently shown to be a promising blood reporter for *ex vivo* monitoring of *in vivo* biological processes⁴⁻⁶. This small luciferase (19.9 kDa) emits a blue flash light (480 nm) upon catalyzing the oxidation of its substrate coelenterazine⁷. Gluc cDNA possesses a signal sequence and therefore is naturally secreted in an active form upon expression in mammalian cells⁷. Further, the level of secreted Gluc in blood is linear with respect to cell number, growth and proliferation, and therefore can be used as a marker for monitoring of biological processes including tumor growth, metastasis and response to therapy^{6,8,9}, gene transfer^{6,9-11}, viral infection¹², circulating cells viability⁶, as well as transcription factors activation^{13,14}, complementing *in vivo* bioluminescence imaging. Compared to other widely used secreted blood reporters such as the

secreted alkaline phosphatase or SEAP, Gluc has several advantages including a much shorter assay time, an increased sensitivity and linear range as well as shorter half life in circulation allowing multiple measurements within a short period of time without accumulation of signal^{4,5}.

One of the major disadvantages of using Gluc as a blood reporter is the absorption of its blue light by pigmented molecules such as hemoglobin resulting in quenching of the signal and therefore lower sensitivity. To overcome this problem, we designed an alternative microtiter well-based assay in which Gluc is captured first from blood using a specific antibody followed by the addition of coelenterazine and signal acquisition using a luminometer. This optimized microtiter well-based assay showed to be over one order of magnitude more sensitive than the typical direct Gluc blood assay. This optimized assay is useful for the detection of subtle luciferase levels *in vivo* facilitating non-invasive *ex vivo* monitoring of various biological processes.

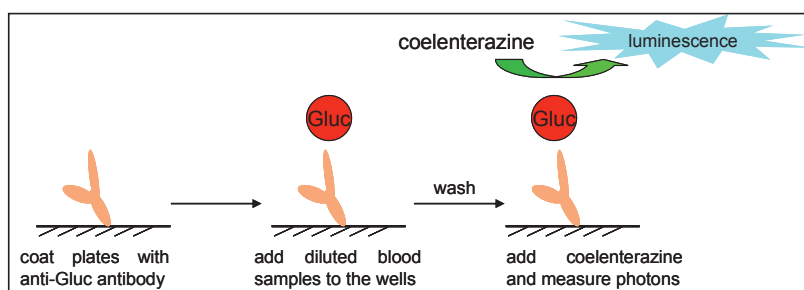


Figure 1. Gluc is captured from the blood in an antibody-mediated reaction, before bioluminescence measurement takes place

EXPERIMENTAL SECTION

Animal studies and blood collection. All animal studies were approved by the Massachusetts General Hospital Review Board. U87 human glioma cells (ATCC) were transduced by a lentivirus vector to stably express Gluc as we previously described⁶. To generate tumors, 1 million of these cells (in 50 μ l) were mixed with equal volume of Matrigel and injected subcutaneously in the flanks of athymic nude

mice. Blood samples were collected from these mice as well as mice with no tumors by making a small incision in the tail and directly adding it to an eppendorf tube containing EDTA as an anti-coagulant (10 mM final concentration).

Microtiter well-based Gluc assay. High binding microtiter 96 well plates (Thermo Fisher Scientific, Rochester, NY) were coated overnight with different amounts of polyclonal rabbit anti-Gluc antibody (Nanolight, Pinetop, AZ) or monoclonal mouse anti-Gluc (generated through the Massachusetts General Hospital antibody production facility¹⁵) diluted in 100 mM carbonate buffer pH 9.6 [or phosphate-buffer saline (PBS) or 50 mM Tris-HCl, pH 7.8 in the presence of 0.5 g/l NaN₃ for optimization studies] in a total volume of 50 µl (unless otherwise stated). Eighteen to twenty four hours later, the plates were washed 2x with 200 mM Tris-HCl pH 7.8 (or PBS or 100 mM carbonate pH 9.6 for optimization studies). Blood samples were then mixed in 200 mM Tris pH 7.8 to a final volume of 50 µl, centrifuged at 200x g, and the supernatants were added to the coated wells, incubated for one hour (unless otherwise stated) at room temperature with shaking. The plates were then washed once with 200 mM Tris-HCl, pH 7.8 (PBS or 100 mM carbonate buffer, pH 9.6) and analyzed by injecting 50 µl 50 µg/ml (unless otherwise stated) coelenterazine diluted in PBS (or 200 mM Tris-HCl pH 7.8 in the presence or absence of 5 mM NaCl) and acquiring photon counts for 10 sec using a microplate luminometer (Dynex, Chantilly, Va).

Direct Gluc blood assay. Five µl (unless otherwise stated) of Gluc-containing blood or Gluc negative blood were added directly to a 96-well white microtiter plate and the Gluc activity was detected by injecting 50 µl 50 µg/ml (unless otherwise stated) coelenterazine and acquiring photon counts for 10 sec using a microplate luminometer as described⁴.

Statistical Analysis. All experiments were repeated at least 3 times to achieve statistical significance. Data are presented as the mean relative light units (RLU) ± standard deviation (SD) from 5 different replicates in each experiment. P values were calculated using Student's t-test. Reproducibility was assessed by calculating the % coefficient of variation (%CV) at 3 different Gluc concentrations.

RESULTS AND DISCUSSION

We performed several optimization steps for the microtiter well-based Gluc binding assay. Two Gluc specific antibodies are available, a polyclonal rabbit anti-Gluc antibody and a monoclonal mouse anti-Gluc antibody. We first compared these two antibodies by coating the microtiter plates with 50 μ l (diluted 1:100 in 50 mM Tris-HCl pH 7.8) with either of these antibodies. Twenty-four hours later, plates were washed with Tris-HCl buffer and 5 μ l blood (Gluc positive and negative) were mixed with 45 μ l Tris-HCl, centrifuged for 5 min at 200x g and the supernatant was added to each well (in triplicates) and incubated for 1 hour at room temperature with shaking. Wells were then washed with Tris-HCl buffer and analyzed with 50 μ l 50 μ g/ml (diluted in PBS) coelenterazine using a luminometer. The polyclonal antibody showed to have higher binding capacity of Gluc from the blood and therefore was used for all subsequent studies (Fig. 1A).

We next checked the optimum amount of polyclonal antibody for coating the microtiter plates. Polyclonal Gluc antibody was serially diluted in 50 mM Tris-HCl, pH 7.8 and added to all wells. Twenty-four hours later, the Gluc assay was performed as above. A 1:500 dilution of the antibody yielded the highest Gluc binding (Fig. 1B) without any effect on the noise defined as the signal obtained from the Gluc negative blood samples (data not shown). Several buffers were then tested for coating the microtiter wells with the Gluc polyclonal antibody including PBS, 50 mM Tris-HCl pH 7.8 and 100 mM carbonate pH 9.6. The carbonate buffer showed the highest signal and the lowest background yielding around 2-fold higher signal-to-noise ratio (calculated by dividing the signals obtained from Gluc-positive blood to Gluc-negative blood) as compared to all other buffers tested (Fig. 1C). Therefore, the polyclonal antibody diluted 1:500 in carbonate buffer was used for all subsequent studies.

We also optimized the assay time for binding Gluc on antibody-coated plates. The optimum coating protocol above was used to capture 5 μ l Gluc-containing blood in Tris-HCl buffer for different time points ranging from 5 min to 24 hours. One hour incubation time gave high binding of Gluc, which even increased further by 2-fold over 24 hours (Fig. 1D). For simplicity purposes, one hour binding time can be used. We also compared the assay volume, in which all assay steps including coating, binding and detection were performed, in 50 or 100 μ l. No statistical significance

differences were observed between the two volumes tested and therefore the lowest 50 μ l volume was chosen for further studies (Fig. 1E).

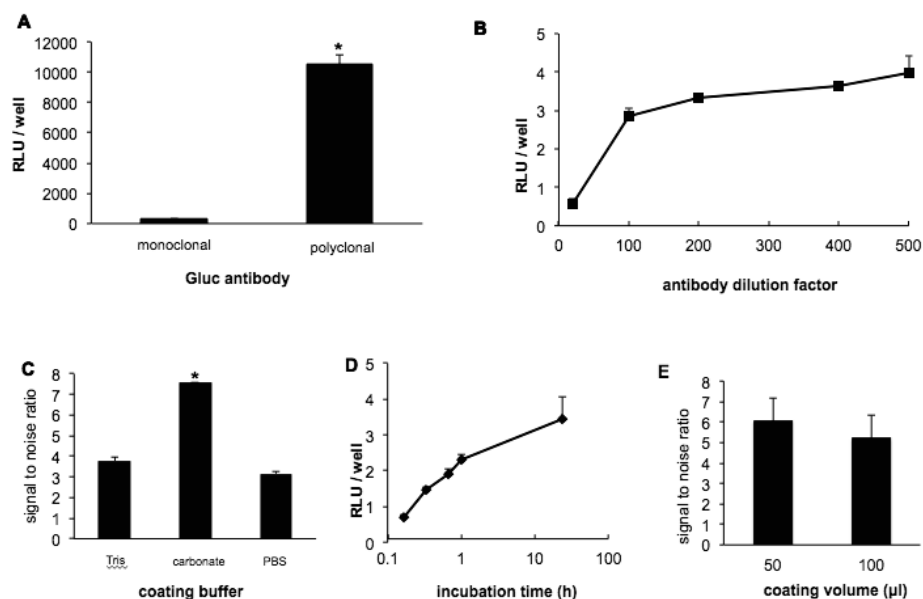


Figure 1. Optimization of the Gluc blood-binding assay. (A) Polyclonal or monoclonal anti-Gluc antibody diluted 1:100 in 50 mM Tris-HCl, pH 7.8 were used to coat the microtiter plates. Twenty-four hours later, plates were washed and 5 μ l blood containing Gluc or negative blood (mixed with 45 μ l 200 mM Tris pH 7.8) were added to each well in triplicates, incubated for 1 hour, and analyzed after the addition of 50 μ l 50 μ g/ml coelenterazine using a luminometer. (B-C) Different dilutions of the polyclonal anti-Gluc antibody diluted in 50 mM Tris-HCl buffer (B) or the same antibody diluted 1:500 in different buffers (C) were used to detect 5 μ l of blood-containing Gluc as in (A). (D) 5 μ l blood (mixed with 45 μ l Tris-HCl buffer) were added to the microtiter wells pre-coated with anti-Gluc antibody and incubated at different time points. Plates were then washed and analyzed as in (A). (E) Different volume of the polyclonal anti-Gluc antibody (diluted 1:500 in carbonate buffer) was used to coat the microtiter wells and was used to detect 5 μ l of blood as in (A). Data presented as average \pm SD from 3 independent experiments with 5 replicates per experiment. * $p < 0.001$.

After optimizing the assay conditions, we focused on improving the bioluminescent-detection step. Different volumes and concentrations of coelenterazine, the Gluc substrate, were tested using the optimized protocol above. A concentration of 50 μ g/ml in a total volume of 50 μ l was found to give the best signal-to-noise ratio (Fig.

2A and B). We then compared different buffers to dilute the coelenterazine for the detection of Gluc. We used PBS or 50 mM Tris-HCl in the presence or absence of NaCl, since this salt is known to enhance the Gluc reaction. We found that PBS resulted in the highest signal-to-noise ratio and therefore was chosen for final analysis (Fig. 2C).

Previously, we showed that 5 μ l of blood gives the highest Gluc signal which is substantially decreased when using higher volumes due to quenching of the bioluminescence signal by hemoglobin and other molecules⁸. Further, detecting Gluc in serum did not show an increased sensitivity due to auto-oxidation of coelenterazine yielding higher noise^{6,8}. We confirmed these data using the direct Gluc blood assay and compared them to our optimized microtiter plate-based Gluc blood assay. Different volumes of Gluc-containing blood (or Gluc negative blood) were analyzed with both assays. As expected, using the direct assay, a linear decrease of Gluc signal with increasing amount of blood was observed showing quenching of light by hemoglobin. On the other hand, a linear increase in signal reaching a plateau at around 40 μ l was observed with the microtiter plate-based binding assay showing that this assay can be used to detect higher blood volume (Fig. 2D). The background noise for the binding assay did not change with increasing blood volume (average 0.186 RLU). On the other hand, the direct assay showed a decrease in background RLUs ranging from 0.136 RLU for 5 μ l blood to 0.08 RLU for 80 μ l blood. More importantly, higher signal-to-noise ratio was obtained with all different blood volumes tested yielding around 20-fold higher ratio when assaying 40 μ l blood using the microtiter plate binding assay as compared to the typical 5 μ l direct detection of Gluc (Fig. 2D).

Finally, using the optimized protocol above, we compared the sensitivity of the microtiter plate-based binding assay to the typical direct assay for detecting Gluc in the blood. Blood was collected from nude mice bearing tumors expressing Gluc, serially diluted with Gluc-negative blood and analyzed with both assays. The microtiter well-based binding assay showed to be over 16-fold more sensitive in detecting Gluc in the blood as compared to the direct standard approach showing that our optimized protocol could be used for detection of subtle luciferase levels *in vivo* facilitating non-invasive monitoring of various biological processes (Fig. 2E). To assess reproducibility, we analyzed 3 different dilutions (1:1, 1:10, 1:100) of Gluc-

containing blood (n=9) using both the binding and direct assays. We found that the %CV to be $\leq 9\%$ for the binding assay and $\leq 15\%$ for the direct assay.

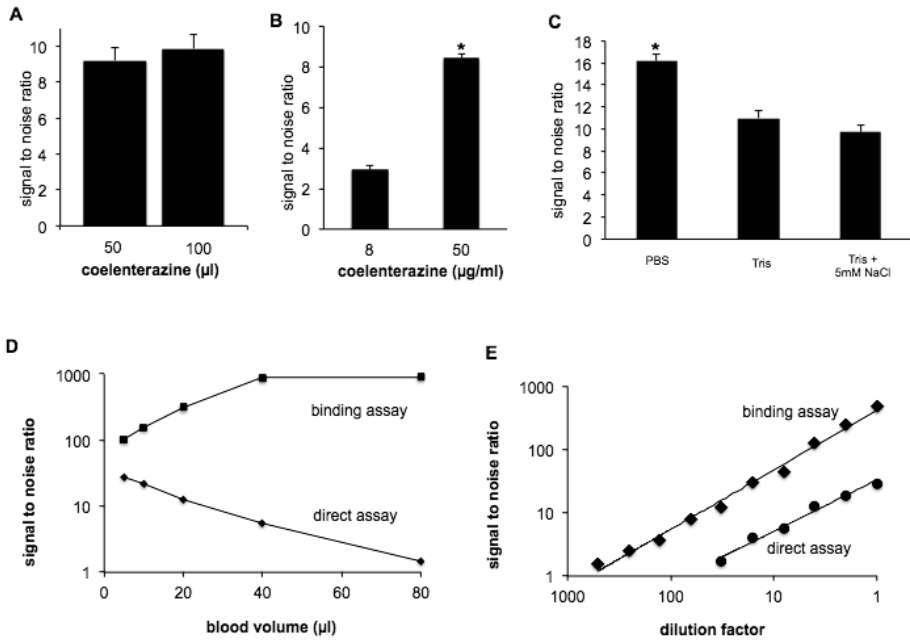


Figure 2. Microtiter plate-based binding assay for the detection of Gluc in blood. Microtiter wells were coated with 50 µl of the polyclonal rabbit anti-Gluc antibody diluted 1:500 in carbonate buffer. **(A-C)** Five µl blood-containing Gluc or negative blood (mixed with 45 µl 200 mM Tris pH 7.8) were added to each well in triplicates, incubated for 1 hour and analyzed with different volumes of 50 µg/ml (a) or amounts (b) of coelenterazine diluted in PBS or in 50 mM Tris-HCl pH 7.8 in the presence or absence of 5 mM NaCl (c). **(D)** Different amounts of blood-containing Gluc or negative blood (background noise) were mixed with 200 mM Tris pH 7.8 and added to each well in triplicates. One hour later, plates were washed and analyzed with 50 µl 50 µg/ml coelenterazine (diluted in PBS) using a luminometer. The same samples were also analyzed using the standard direct Gluc blood assay. The signal (RLUs from Gluc-positive cells) over noise (RLUs from Gluc-negative cells) ratio with respect to blood volume is showing. **(E)** Blood-containing Gluc was serially diluted with Gluc-free blood and analyzed by both the microtiter plate-based binding assay as well as the direct assay. Data presented as average \pm SD from 3 independent experiments with 5 replicates per experiment. * $p < 0.001$.

In conclusion, we developed a microtiter plate-based binding assay and showed it to be more sensitive in detecting Gluc in the blood as compared to the typical direct measurement. This assay is suited for the detection of Gluc in any sample including conditioned medium from mammalian cell cultures as well as urine from small animals. The optimized assay is very useful for *ex vivo* monitoring of *in vivo* biological processes where high sensitivity is required such as detecting few circulating cells, early tumor metastasis and apoptosis^{6,8,16}.

REFERENCES

- 1 Berger, J., Hauber, J., Hauber, R., Geiger, R. & Cullen, B. R. Secreted placental alkaline phosphatase: a powerful new quantitative indicator of gene expression in eukaryotic cells. *Gene* **66**, 1-10 (1988).
- 2 Hiramatsu, N., Kasai, A., Hayakawa, K., Yao, J. & Kitamura, M. Real-time detection and continuous monitoring of ER stress in vitro and in vivo by ES-TRAP: evidence for systemic, transient ER stress during endotoxemia. *Nucleic Acids Res* **34**, e93 (2006).
- 3 Peng, K. W., Fecteau, S., Wegman, T., O'Kane, D. & Russell, S. J. Non-invasive in vivo monitoring of trackable viruses expressing soluble marker peptides. *Nat Med* **8**, 527-531 (2002).
- 4 Tannous, B. A. Gaussia luciferase reporter assay for monitoring biological processes in culture and in vivo. *Nat Protoc* **4**, 582-591 (2009).
- 5 Tannous, B. A. & Teng, J. Secreted blood reporters: Insights and applications. *Biotechnol Adv* **29**, 997-1003, doi:S0734-9750(11)00153-4 [pii] 10.1016/j.biotechadv.2011.08.021 (2011).
- 6 Wurdinger, T. *et al.* A secreted luciferase for ex vivo monitoring of in vivo processes. *Nat Methods* **5**, 171-173 (2008).
- 7 Tannous, B. A., Kim, D. E., Fernandez, J. L., Weissleder, R. & Breakefield, X. O. Codon-optimized Gaussia luciferase cDNA for mammalian gene expression in culture and in vivo. *Mol Ther* **11**, 435-443 (2005).
- 8 Chung, E. *et al.* Secreted Gaussia luciferase as a biomarker for monitoring tumor progression and treatment response of systemic metastases. *PLoS One* **4**, e8316 (2009).
- 9 Griesenbach, U. *et al.* Secreted Gaussia luciferase as a sensitive reporter gene for in vivo and ex vivo studies of airway gene transfer. *Biomaterials* **32**, 2614-2624 (2011).
- 10 Badr, C. E. *et al.* Suicidal gene therapy in an NF-kappaB-controlled tumor environment as monitored by a secreted blood reporter. *Gene Ther* (2010).
- 11 Nakanishi, H., Higuchi, Y., Kawakami, S., Yamashita, F. & Hashida, M. piggyBac transposon-mediated long-term gene expression in mice. *Mol Ther* **18**, 707-714 (2010).
- 12 Marquardt, A. *et al.* Single cell detection of latent cytomegalovirus reactivation in host tissue. *J Gen Virol* (2011).
- 13 Badr, C. E. *et al.* Real-time monitoring of nuclear factor kappaB activity in cultured cells and in animal models. *Mol Imaging* **8**, 278-290 (2009).
- 14 Yang, J. & Richmond, A. J. Monitoring NF-kappaB mediated chemokine transcription in tumorigenesis. *Methods Enzymol* **460**, 347-355 (2009).
- 15 Badr, C. E., Hewett, J. W., Breakefield, X. O. & Tannous, B. A. A highly sensitive assay for monitoring the secretory pathway and ER stress. *PLoS One* **2**, e571 (2007).
- 16 Niers, J. M., Kerami, M., Pike, L., Lewandrowski, G. & Tannous, B. A. Multimodal in vivo imaging and blood monitoring of intrinsic and extrinsic apoptosis. *Mol Ther* **19**, 1090-1096 (2011).

CHAPTER IV



Multiplex blood reporters for simultaneous monitoring of cellular processes

M. Sarah S. Bovenberg^{1,2,3}, M. Hannah Degeling^{1,2,3}, Sayedali Hejazi^{1,2}, Romain Amante^{1,2},
Marte van Keulen^{1,2,4}, Carmen L.A. Vleggeert-Lankamp³, Marie Tannous⁵, Christian Badr^{1,2},
and Bakhos A. Tannous^{1,2}

¹Experimental Therapeutics and Molecular Imaging Laboratory, Neuroscience Center, Department of Neurology,
²Program in Neuroscience, Harvard Medical School, Boston, MA 02114 USA. ³Department of Neurosurgery,
Leiden University Medical Center, Leiden, The Netherlands. ⁴Neuro-oncology Research Group, Department of
Neurosurgery, VU Medical Center, Cancer Center Amsterdam, 1007 MB Amsterdam, The Netherlands. ⁵Faculty
of Natural and Applied Sciences, Notre Dame University, Barsa, Lebanon.

INTRODUCTION

Secreted blood reporters are valuable tools for sensitive and fast detection, quantification and non-invasive *ex vivo* monitoring of *in vivo* biological processes.¹ Currently, the three most commonly used secreted blood reporters are the secreted alkaline phosphatase (SEAP)²⁻⁵, soluble peptides derived from human carcinoembryonic antigen (hCEA) and human chorionic gonadotropin (β HCG)⁶⁻⁹ and *Gaussia* luciferase (Gluc)¹⁰⁻¹⁴. The level of these secreted reporters can be measured over time in blood, serum and/or urine to generate multiple data sets without the need to sacrifice the animal, since only a small amount of fluid is required. In contrast to other tools for monitoring of cellular processes, secreted blood reporters are suitable to follow biological parameters along the way, providing new insights in the factors contributing to disease development and progression¹. During the last 20 years, secreted blood reporters have proven their value in a wide variety of medical fields, including embryo development, viral dissemination, fate of (stem) cells, gene transfer and tumorigenesis and response to therapy.¹⁴⁻¹⁶ The contribution of secreted blood reporters to understanding of these complicated processes would increase even further, if instead of one, multiple parameters could be measured simultaneously and over time.

The discovery of new secreted reporters with different substrate specificities, emission spectra and/or detection assays will allow the development of multiplex assays that are capable in monitoring several processes, given that their separate reactions remain distinguishable. Here, we characterized the naturally secreted luciferase from the marine ostracod *Vargula (Cypridina) hilgendorfi* (Vluc)^{17,18} as a blood reporter and multiplexed it with Gluc and SEAP to develop a triple blood reporter system to monitor three distinct biological processes. As a proof of concept, we successfully monitored the response of three different subsets of glioma cells to the chemotherapeutic agent temozolomide¹⁹ in the same animal. This multiplex system can be extended and applied to many different fields for simultaneous monitoring of multiple biological parameters in the same biological system.

RESULTS

We first characterized a codon-optimized Vluc variant for mammalian gene expression as a blood reporter. Different amounts of U87 human glioma cells stably expressing Vluc and the mcherry red fluorescent protein (RFP) were implanted subcutaneously in nude mice. Three days post-implantation, 5 μ l blood samples (in triplicates) were withdrawn, mixed with EDTA (as an anti-coagulant), and assayed for Vluc activity using a luminometer after addition of the vargulin substrate. Several optimization steps for the detection of Vluc in the blood were first performed using different concentrations of the vargulin substrate in blood and serum. We found that 100 μ l of 0.25 μ g/ml vargulin (diluted in PBS) gave the best signal-to-background (S/B) ratio (supplementary Fig. 1a). Since hemoglobin in whole blood is known to interfere with bioluminescence, we compared the activity of Vluc in blood versus serum and observed that serum gave higher S/B ratio at a concentration of 0.2 μ g/ml (supplementary Fig. 1a). EDTA did not have any effect on the Vluc activity (Supplementary Fig. 1b). Using these optimized conditions, we observed that Vluc activity in blood is linear with respect to cell number in a range covering at least 3 orders of magnitudes (Fig. 1a). We then checked the possibility of detecting Vluc in urine, similar to Gluc^{14,13}. We found that Vluc activity in urine was also linear with respect to cell number, albeit less sensitive, showing that Vluc is cleared by the kidneys (Fig. 1a). We next evaluated the half-life of Vluc in circulation by intravenously injecting Vluc-containing conditioned medium of cells in nude mice and assaying blood for Vluc activity at different time points. We found that the Vluc half-life in circulation to be around 3 hours (Fig. 1b).

Since it is of utmost importance that the chemical reaction of the individual reporters used for multiplex application can be distinguished, we determined the specificity of each reporter to its substrate in the blood. U87 glioma cells stably expressing Gluc, Vluc or SEAP (all under the control of CMV promoter) were implanted subcutaneously in different nude mice. Three days later, 5 μ l blood was assayed for each reporter activity using coelenterazine, vargulin or SEAP substrate. Significant signal from blood was obtained only when the proper reporter/substrate combination was used, showing no substrate overlap or cross reaction among the

different reporters, and indicating that Gluc, Vluc and SEAP can be used together for multiplex applications (Fig. 1c).

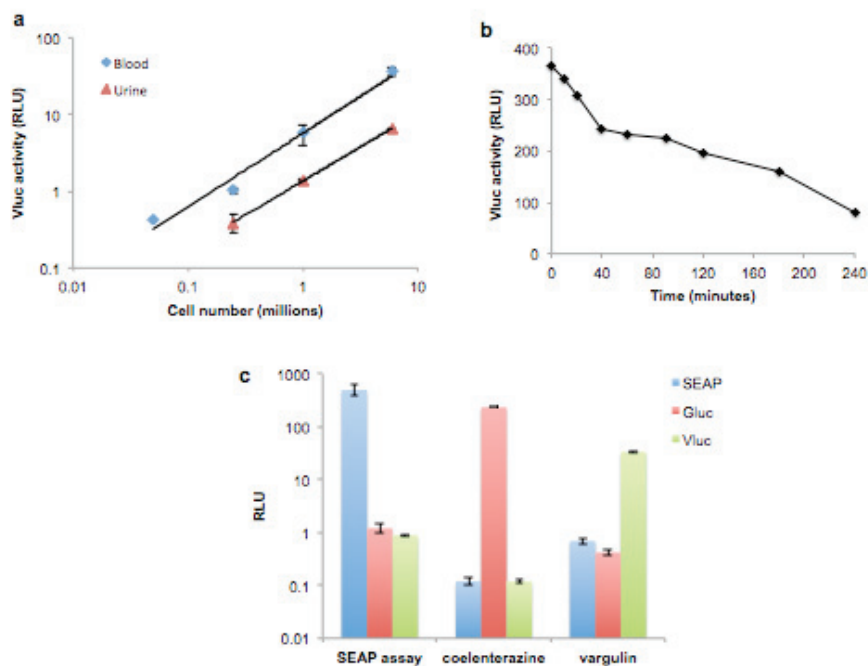


Figure 1. Triple secreted reporter system. (a) Linearity of Vluc blood reporter with respect to cell number. Different U87 glioma cells expressing Vluc were implanted subcutaneously in nude mice (n=4/group). One week later, 5 μ l blood or urine (in triplicates) was assayed for Vluc activity using 100 μ l of the vargulin substrate. (b) half-life of Vluc in circulation. Conditioned medium from U87 cells expressing Vluc were filtered, and 150 μ l was i.v. injected in nude mice (n=4). At different time points, 5 μ l blood (in triplicates) was assayed for Vluc activity. Specificity of each reporter for its substrate. Mice were injected subcutaneously with U87 cells expressing either Gluc, Vluc or SEAP (n=4/group). One week later, 5 μ l blood or serum (in triplicates) were assayed for Gluc, Vluc, and SEAP activity. A significant signal is obtained in blood/serum only with the proper reporter/substrate combination.

Finally, we applied the triple reporter system for non-invasive monitoring of three different subsets of U87 glioma cells in response to temozolomide (TMZ), the chemotherapeutic agent of choice for the treatment of grade IV glioma¹⁹. We used U87 parent cells as well as two TMZ-resistant subclones of these cells, U87R1 and U87R2. U87 parent cells (sensitive to TMZ) were engineered by a lentivirus vector to

express Gluc (U87-Gluc), while U87R1 were engineered to express Vluc (U87R1-Vluc) and U87R2 to express both SEAP and Fluc (U87R2-SEAP/Fluc). Fluc here is used for in vivo localization of U87R2 cells with bioluminescence imaging (since SEAP cannot be imaged in vivo) while Gluc and Vluc are used to localize U87 and U87R1 cells respectively. First, the triple secreted reporter system was confirmed in culture by plating 5,000 of either U87-Gluc, U87R1-Vluc, U87-R2-SEAP/Fluc (singleplex) or combination of all three cells (2,000 cells of each line; multiplex) in a 96-well plate. Aliquots of the conditioned medium were then assayed for each luciferase activity every day over 4 days. Using the singleplex assay, we observed that U87-Gluc cells responded very well to TMZ (>50% cell death) while this drug had no significant effect on U87R1-Vluc and U87-R2-SEAP/Fluc as expected (Fig. 2).

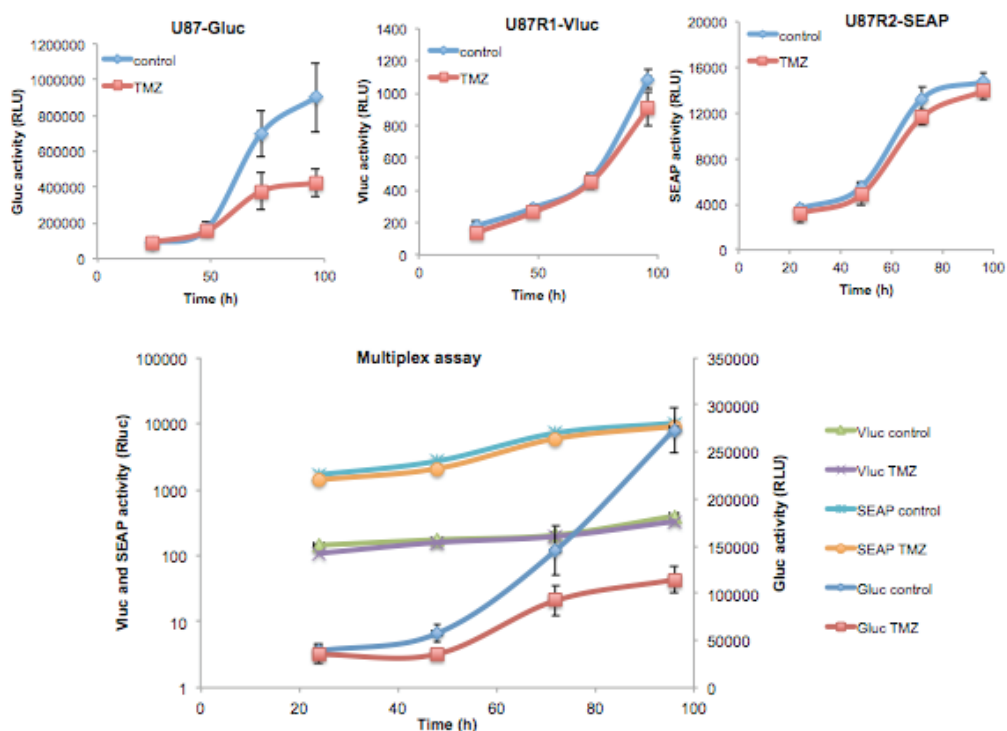


Figure 2. Triple secreted reporter system in vitro. U87-Gluc, U87R1-Vluc, U87R2-SEAP/Fluc cells or a combination of all three cell lines (multiplex) were plated in a 96-well

plate and treated with either TMZ (100 nM) or DMSO control. At different time points, aliquots of conditioned medium were assayed for Gluc, Vluc or SEAP reporters. Only U87 parent cells responded to TMZ (as observed by Gluc assay) but not U87R1 or U87R2 cells with both singleplex and multiplex assay.

The multiplex assay showed the exact same phenomena proving that these three reporters can be used together for simultaneous monitoring of three distinct biological processes over time. We then mixed these three cell lines equally and intracranially implanted 75,000 cells (25,000 of each line) in the brain of nude mice. One week later (time zero), a sample of blood was withdrawn and a group of mice (n=6) was injected with 10 mg/kg TMZ, while the other group was injected with DMSO (control). Blood was collected at different time points and 5 μ l of blood (for Gluc) or serum (for Vluc and SEAP) was assayed for each luciferase activity using coelenterazine, vargulin or SEAP assay respectively. As expected, a continuous decrease in Gluc level in the blood in response of parent U87 cells to TMZ was observed over time in the treated group, while an increase in Gluc signal was observed in the control group (Fig. 3). On the other hand, both Vluc and SEAP levels increased in serum over time in both treated and control groups showing that U87R1 and U87R2 cells are resistant to TMZ (Fig. 3). Before and 10 days post-treatment, mice were imaged for Gluc, Vluc and Fluc after injection of coelenterazine, vargulin and D -luciferin confirming the blood assays (Fig. 3). All together, these results show that Gluc, Vluc and SEAP can be multiplexed together as blood reporters for non-invasive monitoring of biological processes, in real time.

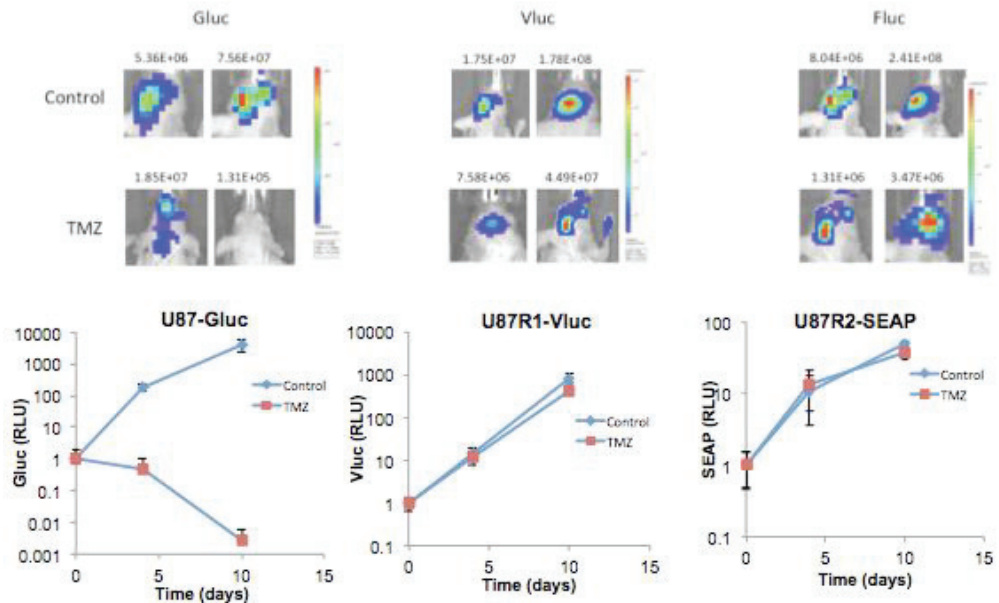


Figure 3. Multiplex blood reporter systems. A mixture of U87-Gluc, U87-Vluc and U87-SEAP/Fluc cells (25,000 of each cell line) were intracranially injected in the brain of nude mice. One week later, mice were randomized in 2 groups, which received either 10mg/kg TMZ or DMSO vehicle (n=6/group). Before and at different time points post-treatment, 5 μ l blood was assayed for Gluc activity. Likewise, 5 μ l of serum was assayed for Vluc and SEAP activity. Before and at day 10 post-TMZ treatment, signal was localized to tumors by in vivo bioluminescence imaging of Gluc, Vluc and Fluc after injection of coelenterazine, vargulin and β -luciferin substrates respectively.

In summary, we have developed a multiplexed blood reporter system for simultaneous monitoring of multiple biological parameters in the same experimental animal. This system could be applied in many different fields facilitating the understanding of disease development and expedites findings of novel therapeutics and translation into the clinic.

EXPERIMENTAL SECTION

Lentivirus vectors. *Lentivirus vectors expressing CMV-SEAP, CMV-Gluc and CMV-Fluc were previously described*¹⁴. Codon-optimized Vluc cDNA for mammalian gene expression was amplified by polymerase chain reaction (PCR) from pCMV-Vluc

(Targeting Systems) and cloned in a similar vector backbone as CMV-SEAP creating CMV-Vluc. Lentivirus vectors were packaged as previously described.¹⁴

Cell culture and reagents. U87 human glioma cells were obtained from ATCC. U87R1 and U87R2 cells were generated by repeated exposure of U87 cells to low doses of TMZ (a kind gift from Dr. Peter Wesseling, VU University Medical Center, Cancer Center, Amsterdam, the Netherlands). All cells were grown in Dulbecco's modified Eagle's medium (DMEM) supplemented with 10% fetal bovine serum (Sigma, St. Louis, MO, USA), 100 U penicillin, and 0.1 mg streptomycin (Sigma) per milliliter, at 37 °C and 5% CO₂ in a humidified atmosphere. Temozolomide was obtained from Sigma.

Reporter substrates. Coelenterazine was obtained from NanoLight™ Technology (Pinetop, AZ) and resuspended at 5 mg/ml in acidified methanol. Vargulin substrate was obtained from NanoLight™ Technology and was resuspended at 5 mg/ml in acidified methanol. *D*-luciferin was purchased from Gold Biotechnology® (St. Louis, MO) and resuspended at 25 mg/ml in PBS. SEAP was detected using the the Great EscAPe SEAP kit (Clontech) as per manufacturer's instructions.

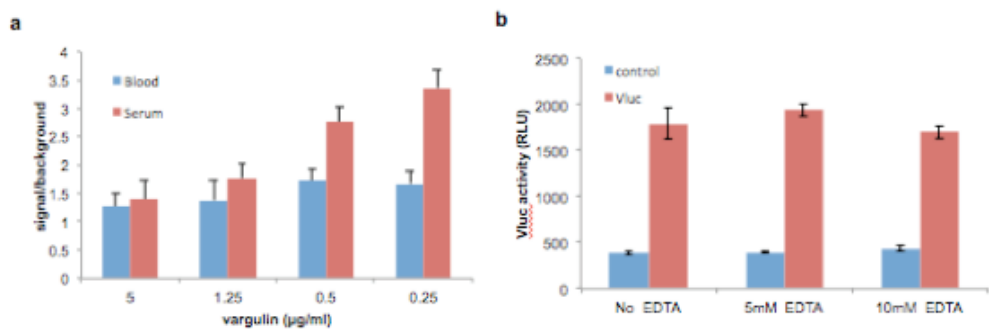
In vitro experiments. U87-Gluc, U87R1-Vluc and U87R2-SEAP/Fluc cells were plated in a 96 well plate (5000 cells/well) in a total volume of 50 and 24 hours later treated with either temozolomide (100 nM) or DMSO vehicle. At different time points, 10 µl aliquot (in triplicates) of cell-free conditioned medium was collected and assayed for either Gluc, Vluc or SEAP using either coelenterazine (5 µg/ml in PBS), vargulin (1 µg/ml in PBS) or the Great EscAPe respectively. We refreshed the media of cells 6 hours before measurements to avoid accumulation of the reporter.

Animal studies and blood collection. All animal studies were approved by the Massachusetts General Hospital Review Board. U87 human glioma cells, U87R1 and U87R2 were transduced with each lentivirus vector for stable expression by adding the vector directly to the cells using 10 transducing units of each vector per cell. To generate tumors, different amount of these cells (in 50 µl) were mixed with equal volume of Matrigel and injected subcutaneously in the flanks of athymic nude mice. For brain tumor model, a mixture of these cells (25,000 per cell line, in 2 µl

Opti-MEM) were intracranially injected in the left midstriatum of nude mice using the following coordinates from bregma in mm: anterior-posterior +0.5, medio-lateral +2.0, dorso-ventral -2.5. These injections were performed using a Micro 4 Microsyringe Pump Controller (World Precision Instruments, Sarasota, FL) attached to a Hamilton syringe with a 33-gauge needle (Hamilton, Rena, NV) at a rate of 0.2 μ L/min. One week later, mice were randomized in 2 groups (n=6/group) and treated with either 10mg/kg temozolomide or DMSO vehicle. Blood samples were collected from these mice as well as from mice with no tumors (negative control) by making a small incision in the tail and directly adding it to an eppendorf tube containing EDTA as an anti-coagulant (10 mM final concentration).

Ex vivo multiplex blood reporter assays. For Gluc assay, activity was measured by injecting 100 μ l 100 μ M coelenterazine (nanolight, pinetop, AZ) to 5 μ l of blood and acquiring photon counts over 10 seconds using a luminometer (Dynex). The SEAP chemiluminescence activity was measured in 5 μ l serum using the Great EscAPE SEAP kit (Clontech) as per manufacturer's instructions. For Vluc assay, activity was measured in 5 μ l blood or serum after injecting 100 μ l 0.25 μ g/ml of vargulin (diluted in PBS) and acquiring photon counts using a luminometer.

Triple in vivo imaging. For Fluc imaging, mice were injected i.p. with 200 mg/kg body weight of *D*-luciferin solution and imaging was performed 10 min later. For Gluc imaging, mice were injected i.v. (through retro-orbital route) with 5 mg/kg body weight of coelenterazine solution diluted in PBS and imaging was performed immediately. For Vluc *in vivo* imaging, mice were injected i.v. with 4 mg/kg body weight (diluted in PBS) and imaging was performed immediately. For sequential imaging of all three reporters, we imaged Gluc on day 1, Vluc 4 hrs later and Fluc on Day 2 to allow enough time for the signal to reach background levels between different imaging sessions. Imaging was performed using an IVIS® Spectrum optical imaging system fitted with an XGI-8 Gas Anesthesia System (Caliper Life Sciences, Hopkinton, MA). Bioluminescent images were acquired using the auto-exposure function. Data analysis for signal intensities and image comparisons were performed using Living Image® software (Caliper Life Sciences).



Supplementary Figure 1: optimization of Vluc assay. (a) Blood was withdrawn from mice bearing subcutaneous U87-Vluc tumors and 5µl blood or serum (in triplicates) was assayed for Vluc activity using different concentrations of vargulin (in 100 µl). (b) conditioned medium of U87 cells expressing Vluc or Fluc (control) were assayed for Vluc activity in the presence and absence of EDTA.

REFERENCES

1. Tannous, B.A. & Teng, J. Secreted blood reporters: insights and applications. *Biotechnology advances* **29**, 997-1003 (2011).
2. Blacklock, J., You, Y.Z., Zhou, Q.H., Mao, G. & Oupicky, D. Gene delivery in vitro and in vivo from bioreducible multilayered polyelectrolyte films of plasmid DNA. *Biomaterials* **30**, 939-950 (2009).
3. Cutrera, J., *et al.* Discovery of a Linear Peptide for Improving Tumor Targeting of Gene Products and Treatment of Distal Tumors by IL-12 Gene Therapy. *Mol Ther* (2011).
4. Hiramatsu, N., Kasai, A., Hayakawa, K., Yao, J. & Kitamura, M. Real-time detection and continuous monitoring of ER stress in vitro and in vivo by ES-TRAP: evidence for systemic, transient ER stress during endotoxemia. *Nucleic Acids Res* **34**, e93 (2006).
5. Hughes, T.S., *et al.* Intrathecal injection of naked plasmid DNA provides long-term expression of secreted proteins. *Mol Ther* **17**, 88-94 (2009).
6. Galanis, E., *et al.* Phase I trial of intraperitoneal administration of an oncolytic measles virus strain engineered to express carcinoembryonic antigen for recurrent ovarian cancer. *Cancer Res* **70**, 875-882 (2010).
7. Iankov, I.D., Hillestad, M.L., Dietz, A.B., Russell, S.J. & Galanis, E. Converting tumor-specific markers into reporters of oncolytic virus infection. *Mol Ther* **17**, 1395-1403 (2009).
8. Liu, C., *et al.* Combination of measles virus virotherapy and radiation therapy has synergistic activity in the treatment of glioblastoma multiforme. *Clin Cancer Res* **13**, 7155-7165 (2007).
9. Peng, K.W., Fecteau, S., Wegman, T., O'Kane, D. & Russell, S.J. Non-invasive in vivo monitoring of trackable viruses expressing soluble marker peptides. *Nat Med* **8**, 527-531 (2002).
10. Griesenbach, U., *et al.* Secreted Gaussia luciferase as a sensitive reporter gene for in vivo and ex vivo studies of airway gene transfer. *Biomaterials* **32**, 2614-2624 (2011).
11. Nakanishi, H., Higuchi, Y., Kawakami, S., Yamashita, F. & Hashida, M. piggyBac transposon-mediated long-term gene expression in mice. *Molecular therapy : the journal of the American Society of Gene Therapy* **18**, 707-714 (2010).
12. Niers, J.M., Kerami, M., Pike, L., Lewandrowski, G. & Tannous, B.A. Multimodal In Vivo Imaging and Blood Monitoring of Intrinsic and Extrinsic Apoptosis. *Mol Ther* (2011).
13. Tannous, B.A. Gaussia luciferase reporter assay for monitoring biological processes in culture and in vivo. *Nat Protoc* **4**, 582-591 (2009).
14. Wurdinger, T., *et al.* A secreted luciferase for ex vivo monitoring of in vivo processes. *Nat Methods* **5**, 171-173 (2008).
15. Maelandsmo, G.M., *et al.* Use of a murine secreted alkaline phosphatase as a non-immunogenic reporter gene in mice. *J Gene Med* **7**, 307-315 (2005).
16. Msaouel, P., Dispenzieri, A. & Galanis, E. Clinical testing of engineered oncolytic measles virus strains in the treatment of cancer: an overview. *Curr Opin Mol Ther* **11**, 43-53 (2009).
17. Thompson, E.M., Nagata, S. & Tsuji, F.I. Cloning and expression of cDNA for the luciferase from the marine ostracod *Vargula hilgendorffii*. *Proc Natl Acad Sci U S A* **86**, 6567-6571 (1989).

18. Thompson, E.M., Nagata, S. & Tsuji, F.I. Vargula hilgendorffii luciferase: a secreted reporter enzyme for monitoring gene expression in mammalian cells. *Gene* **96**, 257-262 (1990).
19. Stupp, R., *et al.* Radiotherapy plus concomitant and adjuvant temozolomide for glioblastoma. *The New England journal of medicine* **352**, 987-996 (2005).

CHAPTER V



Novel triple bioluminescence imaging system for monitoring of Glioma response to combined soluble TRAIL and Lanatoside C therapy

Casey A. Maguire^{1,3}, M. Sarah S. Bovenberg^{1,3,4}, Matheus HW Crommentuijn^{1,3,5}, Johanna M. Niers^{1,3,5}, Mariam Kerami^{1,3,5}, Jian Teng^{1,3}, Miguel Sena-Estevés⁶, Christian E. Badr^{1,3}, and Bakhos A. Tannous^{1,2,3,*}

¹Experimental Therapeutics and Molecular Imaging Laboratory, Neuroscience Center, Department of Neurology, ²Center for Molecular Imaging Research, Department of Radiology, Massachusetts General Hospital, and ³Program in Neuroscience, Harvard Medical School, Boston, USA. ⁴Department of Neurosurgery, Leiden University Medical Center, Leiden, The Netherlands. ⁵Neuro-oncology Research Group, Department of Neurosurgery, VU Medical Center, Cancer Center Amsterdam, 1007 MB Amsterdam, The Netherlands. ⁶Department of Neurology, University of Massachusetts Medical School, Worcester, MA.

ABSTRACT

We developed a triple reporter system based on Vargula, Gaussia and firefly luciferases for sequential imaging of three different biological processes. We applied this system to monitor the effect of soluble tumor necrosis factor-related apoptosis-inducing ligand (sTRAIL-delivered using an adeno-associated viral AAV vector), in combination with the cardiac glycoside lanatoside C, in different orthotopic glioma models. Binding of sTRAIL on tumor cells activated downstream events leading to an initial decrease in glioma proliferation, followed by tumor re-growth through resistant cells. Co-treatment with lanatoside C sensitized the resistant subpopulation of glioma to sTRAIL-induced apoptosis as monitored by the triple reporter system. Since AAV vectors, TRAIL, and cardiac glycosides have been used in the clinic separately, this therapeutic strategy could be easily adapted to humans. This work is the first demonstration of triple *in vivo* bioluminescence imaging and will have broad applicability in different fields.

INTRODUCTION

Bioluminescence imaging (BLI) using luciferase reporters has been indispensable for non-invasive monitoring of different biological processes in cancer such as tumor volume and transcriptional activation during tumor development/therapy, as well as immune cell infiltration into the tumor environment¹. The major advantage of using BLI compared to endpoint analysis is that it provides real-time, non-invasive measurements of *in situ* biological events, giving a complete “picture” of the kinetics of an entire process. Great strides have been made since the seminal study by Contag et al. published in 1995 which was the first demonstration of *in vivo* BLI². For example, as few as 10 cells expressing firefly luciferase can be detected in deep tissue in some animal models³. This study followed by the discovery and molecular construction of different luciferases with a multitude of properties including secreted luciferases⁴, multi-color light emission spectras for better tissue penetrance *in vivo* and spectral deconvolution⁵, increased thermostability⁶, and light output (sensitivity)⁷. One limitation to current bioluminescence imaging is that typically only one and at most two luciferase reporters are used to measure one or two parameters⁸. As

tumor formation is a complex process, concurrent measurement of several processes will be important for the development of novel therapeutics and their transition to the clinic.

Tumor necrosis factor apoptosis-inducing ligand (TRAIL) is regarded as a potential anti-cancer agent, however, considerable numbers of cancer cells, especially adult gliomas, are resistant to apoptosis induction by TRAIL^{9,10}. Another major disadvantage of using TRAIL for glioma therapy is its inefficient transport across the blood-brain barrier¹¹. Through drug screening, we have identified lanatoside C, an FDA approved cardiac glycoside, to sensitize primary GBM cells to TRAIL-induced apoptosis¹². Cardiac glycosides including lanatoside C have been recently shown to provide neuroprotection against ischemic stroke showing that these drugs penetrate the brain efficiently^{13, 14}.

In this study, we explored the use of adeno-associated viral vector (AAV) to deliver soluble TRAIL (sTRAIL) to brain tumors in combination with its sensitizer, lanatoside C for glioma therapy. The AAV vector serotype chosen (AAVrh.8) efficiently transduces the normal brain (primarily neurons) to synthesize and secrete sTRAIL, which in turn binds to death receptors found specifically on glioma cells, and kill them upon lanatoside C treatment. We first developed and optimized triple bioluminescence imaging system using three different luciferases, each specific to its own substrate, from the marine copepod *Gaussia princeps* (Gluc-uses coelenterazine as a substrate), the American firefly *photinus pyralis* (Fluc,_{-D}-luciferin substrate), and ostracod *Vargula (Cypridina) hilgendorffii* (Vluc-uses vargulin as a substrate). We then applied this system to monitor sequentially (1) AAV gene delivery; (2) sTRAIL binding to glioma death receptors and activation of downstream events; and (3) tumor response to the combined sTRAIL/lanatoside C therapy. We showed that glioma cells are somewhat resistant to sTRAIL monotherapy and the combined sTRAIL/lanatoside C therapy yields significant delay in tumor growth. This combined therapy could potentially be translated to humans since all its components have been used in clinical trials separately. Further, this study is the first demonstration of triple *in vivo* BLI, which would be applicable to many disease/therapeutic pre-clinical models.

RESULTS

Characterization of a codon-optimized Vargula luciferase for mammalian gene expression. We first cloned the Vluc cDNA, codon-optimized for mammalian gene expression into a lentivirus vector under the control of the CMV promoter (Lenti-Vluc). This vector also expresses the mCherry fluorescent protein under an internal ribosomal entry site (IRES), used to monitor transduction efficiency. Since Vluc cDNA carries a natural signal sequence,¹⁵ it is secreted to the conditioned medium once expressed in mammalian cells. We first compared the level of Vluc secretion by transducing 293T cells with this lentivirus vector and evaluating cell lysates and conditioned medium for Vluc activity using the vargulin substrate. We observed that the majority of Vluc activity (78%) was contained in the medium fraction showing efficient secretion (**Fig. 1a**). Next, we checked the light emission kinetics of Vluc after substrate addition over 5 minutes. We observed a slow decay in light emission with 44% of the initial signal remaining 5 minutes post substrate addition (**Fig. 1b**). To further characterize Vluc as a mammalian cell reporter, we measured the stability of the enzyme over time at 37°C. Conditioned medium from cells expressing Vluc was incubated at 37°C in a humidified cell incubator. Aliquots were taken at different time points and assayed for Vluc activity. We observed that Vluc levels did not drop below initial levels over 12 days indicating high enzyme stability in cells conditioned medium (**Fig. 1c**), similar to that reported for the secreted *Gaussia* luciferase¹⁶. We next evaluated Vluc as a reporter to monitor cell viability and proliferation over time. U87 glioma cells transduced with Lenti-Vluc were plated and aliquots of media were collected at different time points. In parallel a commercially available Fluc-based viability assay was performed for comparison. We observed a high correlation ($r^2=0.98$) between the Vluc viability assay and the established viability assay (**Fig. 1d**).

Figure 1

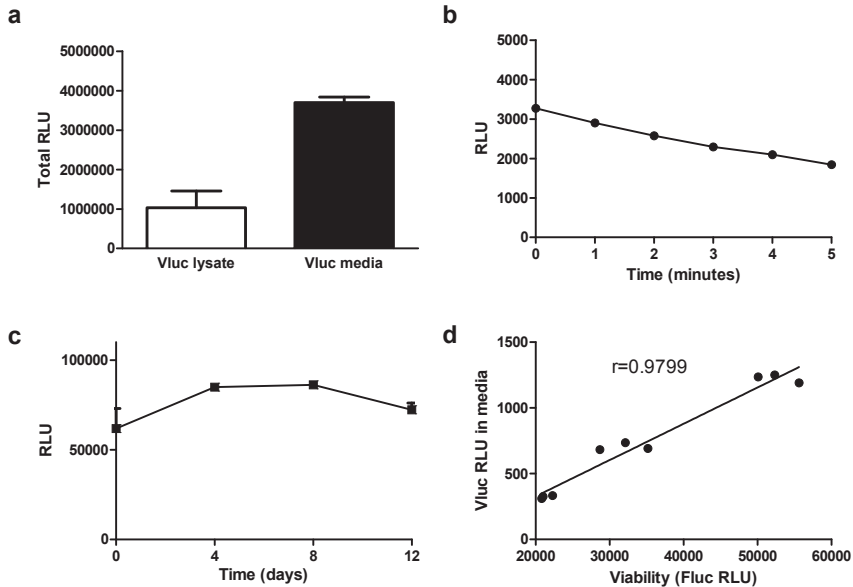


Figure 1. *In vitro* characterization of Vluc-catalyzed luminescence. (a) A Vluc assay was performed on conditioned medium as well as cell lysates from 293T cells transduced with a lentivirus vector encoding Vluc to determine the fraction (in RLU) of Vluc being secreted. (b) Vluc light emission kinetics was performed by adding vargulin to Vluc-containing media and acquiring signal over time. (c) Stability of Vluc enzyme was determined by assaying an aliquot of Vluc-containing cell-free conditioned medium, incubated at 37 °C, at different time points. (d) Vluc-based viability assay. 10^5 U87 cells expressing Vluc were seeded in a 12-well plate and an aliquot of conditioned medium was assayed for Vluc activity over time. For comparison, a commercially available Fluc-based viability assay (CellTiter Glo; Promega) was performed.

Optimization of the triple *in vivo* bioluminescence imaging system. In order to validate Vluc as a reporter for *in vivo* imaging, we first characterized its bioluminescence properties in a quantitative tumor model. Nude mice were injected subcutaneously with 2×10^6 U87 cells stably expressing Vluc (through transduction with Lenti-Vluc). Ten days later, mice were injected intravenously (i.v.- through retro-ocular route) with vargulin (4 mg/kg body weight) and imaged using a cooled charge-coupled device (CCD) camera at different time points post-vargulin injection. We observed the peak luminescent signal immediately upon injection of vargulin, which rapidly declined to 25% of starting signal by 6 minutes and down to 10% by 26

minutes (**Fig. 2a**). Next, we compared i.v. versus intraperitoneal (i.p.) injection of the vargulin substrate for Vluc imaging and observed that the peak signal occurred 10 minutes after i.p. injection (**Supplementary Fig. 1**), with the i.v. injection yielding an 8-fold higher photons/min compared to the i.p. injection (**Fig. 2b**). Therefore, the i.v. injection route was used throughout the study.

We then evaluated the potential of Vluc to be multiplexed with Gluc and Fluc for sequential triple bioluminescence imaging by testing luciferase/substrate specificity *in vivo*. U87 stably expressing either Vluc, Gluc or Fluc (under control of the CMV promoter) were implanted subcutaneously in nude mice at three different sites. Ten days later, mice were imaged first for Gluc-mediated bioluminescence imaging by i.v. injection of coelenterazine (5 mg/kg body weight) and acquiring photon counts immediately. Intense luminescence was detected only from tumors expressing Gluc (**Fig. 2c**). Next, mice were imaged after i.v. injection of vargulin (4 mg/kg body weight) and again signal was obtained only from tumor-expressing Vluc. Finally, mice were i.p. injected with Δ -luciferin (150 mg/kg body weight) and imaged 10 min later which showed signal only in tumor-expressing Fluc (**Fig. 2c**). Fluc was imaged last since it is known to have glow-type kinetics in mice. These results show that each of these luciferases is specific to its own substrate and can be multiplexed together in the same biological system to monitor three distinct biological processes sequentially.

Figure 2

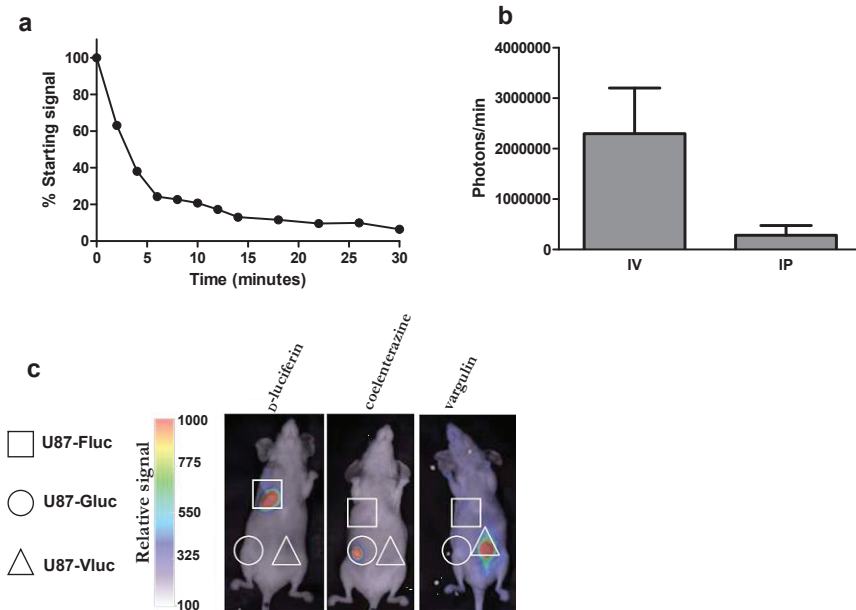


Figure 2. Triple in vivo bioluminescence imaging. (a,b) 2×10^6 U87-Vluc glioma cells were implanted subcutaneously in nude mice. Tumor-associated Vluc bioluminescence signal was imaged after i.v. injection of vargulin over time (a). Tumor associated Vluc signal after i.v. or i.p. injection of vargulin was measured (b). U87 glioma cells stably expressing Gluc, Vluc or Fluc (all under CMV promoter) were injected subcutaneously in nude mice at different sites. Ten days later, Sequential imaging of Gluc, Vluc and Fluc was performed after injection of coelenterazine, vargulin and *D*-luciferin, respectively (c).

Monitoring of glioma therapy using triple in vivo bioluminescence imaging. We used the triple luciferase reporter system to monitor the effect of glioma to a secreted soluble variant of the anti-cancer agent TRAIL (sTRAIL¹⁷) in combination with its sensitizer lanatoside C. We first cloned sTRAIL under control of the constitutively active chicken beta-actin (CBA) promoter into an AAV2 ITR-flanked transgene cassette and pseudotyped it with an AAVrh.8 capsid (AAV-sTRAIL; **Fig. 3a**). As a control, we packaged a similar vector expressing GFP driven by the CBA promoter. We chose to use AAVrh.8 as we have previously shown that this serotype yields excellent transduction efficiency of murine normal brain¹⁸. Injection of AAVrh.8 into the tumor using convection-enhanced delivery results in transduction of primarily

neuronal cells surrounding the tumor¹⁸. The transduced neurons form a therapeutic zone around the tumor by synthesizing and secreting sTRAIL, which in turn will find and bind its death receptor present specifically on glioma cells. Co-treatment with lanatoside C should allow sensitization of glioma cells to TRAIL's pro-apoptotic effects¹².

To determine the functionality of the AAV-sTRAIL construct, we transduced U87 cells with 10^4 genome copy (g.c.)/cell of AAV-sTRAIL vector or AAV-GFP as a control. Three days later, conditioned media from these cells were harvested and analyzed for TRAIL using an ELISA kit. We observed a TRAIL concentration of 124 ng/ml from conditioned medium of AAV-sTRAIL infected cells while it was undetectable in the media from AAV-GFP control cells, showing the proper expression and secretion of sTRAIL into the conditioned medium of cells. Transfer of conditioned media from AAV-sTRAIL transduced cells along with lanatoside C onto U87 cells provided robust cell killing as expected (**Supplementary Fig. 2**).

We next cloned V_{luc} cDNA under control of CBA promoter in another AAV2 vector pseudotyped with AAVrh.8 capsid (AAV-V_{luc}; **Fig. 3a**). V_{luc} was used as a marker for efficient gene transfer. We then engineered U87 glioma cells to stably express Fluc and the mCherry fluorescent protein (U87Fluc) under control of CMV promoter, using a lentivirus vector (**Fig. 3a**). Fluc was used as a marker for tumor volume. Since TRAIL is known to activate a series of events including the nuclear factor kappa B (NF- κ B) pathway, we engineered a lentivirus vector expressing Gluc under the control of tandem repeats of NF- κ B responsive elements (**Fig. 3a**)¹⁹, and used it to transduce the U87Fluc cells generating U87Fluc/NF-Gluc cells. We initially used U87 glioma cells as a model since these cells are partially resistant to the pro-apoptotic effects of TRAIL²⁰.

We stereotactically implanted 10^5 U87Fluc/NF-Gluc cells into the striatum of nude mice and allowed tumors to form. Two weeks later, mice were randomly divided into two groups (n=5). The first group was infused into the same tumor implanted site with 10^{10} g.c. of both AAV-V_{luc} + AAV-GFP (AAV-V_{luc}/GFP; serving as a negative control for tumor therapy and for imaging of gene delivery) and the second group was infused with 10^{10} g.c. of both AAV-V_{luc} (to monitor successful transgene delivery) and AAV-sTRAIL (anti-tumor therapy; AAV-V_{luc}/sTRAIL). As a negative control for V_{luc} imaging, a group of mice received similar injection of AAV-GFP

alone. Ten days post-vector injection, we monitored AAV gene delivery by injecting (i.v.) mice with vargulin substrate and immediately imaging using a CCD camera. Evident bioluminescent signal (average radiance of 7.5×10^5 p/s/cm²/sr \pm 2.3E4) was seen at the injection site of all AAV-Vluc injected mice (and not the AAV-GFP control) showing successful gene delivery (**Fig. 3b**). Mice were also imaged at 1, 2, and 3 weeks post-vector injection for tumor-associated Fluc-signal, and therefore tumor size, after i.p. injection of *D*-luciferin substrate. We observed that AAV-mediated sTRAIL expression slowed the tumor growth as compared to control mice. For example, at week 1 post-vector injection, Fluc imaging showed an average radiance for AAV-Vluc/GFP control mice of 1.03×10^6 photons/s/cm²/sr while it was only 2.38×10^4 photons/s/cm²/sr for AAV-Vluc/sTRAIL treated mice (**Fig. 3c,d**). The average bioluminescent signal remained high (1.28×10^6 photons/s/cm²/sr) for AAV-Vluc/GFP control mice at week 2 and by week 3, 70% of mice were sacrificed due to advanced tumor progression (**Fig. 3c,d**). In contrast, at two weeks post-vector injection, the average signal remained very low (1.8×10^4 photons/s/cm²/sr) for the AAV-Vluc/sTRAIL injected group (**Fig. 3c,d**). Interestingly, in this group the radiance increased by 214-fold between the two and three week post-vector injection presumably due to gained-resistance to sTRAIL therapy (**Fig. 3c,d**).

TRAIL binding to its death receptors recruits TNFR1-associated death domain protein (TRADD) leading to NF- κ B activation²¹, we therefore sought to detect NF- κ B induction and therefore sTRAIL binding to glioma cells in our model. Mice in both the AAV-Vluc/GFP (control) and AAV-Vluc/sTRAIL groups were imaged 3-4 days post-viral injection for Fluc (tumor size) and for Gluc after retro-orbital injection of coelenterazine. Fluc bioluminescence at the tumor location was detectable in both groups of mice as expected but visible specific Gluc signal detected only in mice injected with AAV-Vluc/sTRAIL and not AAV-Vluc/GFP control animals indicating binding of sTRAIL to glioma cells and induction of the downstream NF- κ B pathway (**Fig. 3e**). In two separate experiments, we compared the relative NF- κ B induction between the AAV-Vluc/GFP and AAV-Vluc/sTRAIL groups by normalizing the Gluc levels to the tumor size (quantitated by Fluc imaging). In both experiments, we observed a much higher normalized Gluc signal (15-142-fold) in the mice treated with AAV-sTRAIL compared to the control group indicating induction of NF- κ B (**Fig. 3f**). These results were reproduced in three independent experiments and shows

that our triple luciferase system could be used to image three independent processes.

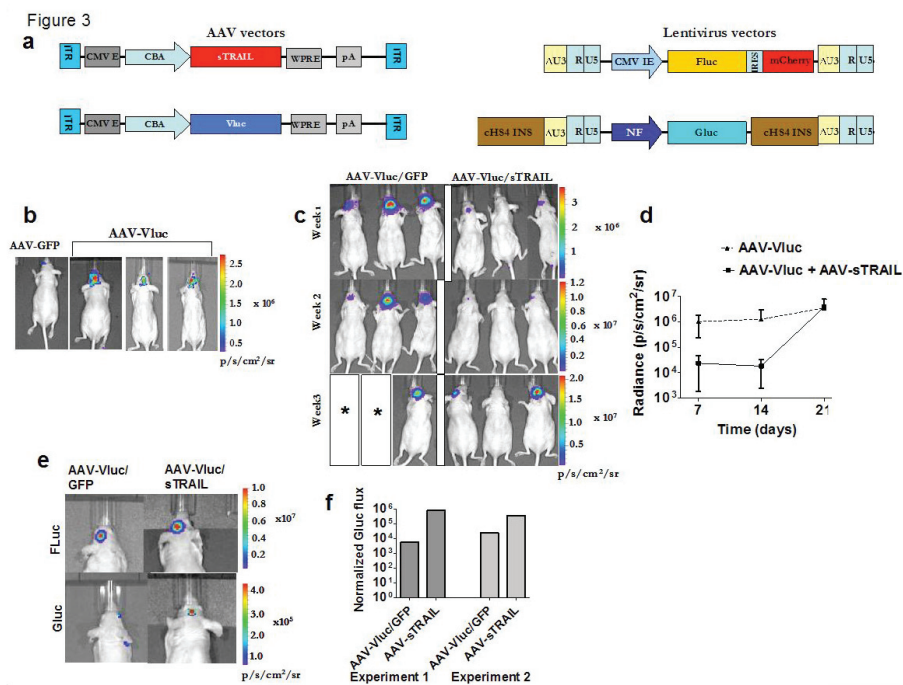


Figure 3. Monitoring of TRAIL-mediated cancer gene therapy with triple bioluminescence imaging. (a) Schematic diagram for the different AAV (left) and lentivirus vector (right) constructs used in this study. AAV vectors: **CMV E**, cytomegalovirus enhancer; **CBA**, chicken beta actin promoter; **WPRE**, woodchuck hepatitis virus posttranscriptional regulatory element; **pA**, bGH poly A signal. Lentivirus vectors: Diagrams shown represent integrated provirus. **CMV IE**, cytomegalovirus immediate early promoter; **cHS4 INS**, chicken β globin hypersensitive site 4 insulator sequence; **NF**, NF- κ B inducible promoter. (b-f) 10^5 U87Fluc/NF-Gluc glioma cells were implanted intracranially in nude mice. (b) Two weeks later, the mice brain were infused at the same tumor injection site with 10^{10} g.c. of either AAV-GFP, AAV-Vluc/GFP or AAV-Vluc/sTRAIL (as noted). Vluc bioluminescence imaging was performed 10 days post-vector injection confirming AAV-mediated gene delivery. Representative mice from AAV-Vluc/sTRAIL and AAV-GFP are shown. (c) Tumor volume was monitored by Fluc bioluminescence imaging at different time points. (d) Quantitation of tumor-associated Fluc signal in c. (e) Fluc imaging, a marker for tumor volume, as well as Gluc imaging, a marker for TRAIL binding on glioma cells, was performed. (f) Gluc signal normalized to Fluc signal in (e) to account for tumor size from two separate experiments is shown.

We have previously discovered that a cardiac glycoside, lanatoside C (LanC), sensitizes glioma cells to recombinant TRAIL, thus overcoming their resistance to TRAIL-mediated killing, both in cultured cells and in a subcutaneous model¹². We then tested the effect of this combined therapy in our orthotopic glioma model using AAV vector to deliver sTRAIL. Nude mice were again implanted into the striatum with 10^5 U87Fluc/NF-Gluc cells as above. Two weeks post-injection (when tumor was formed as monitored by Fluc imaging), mice were randomly divided into two groups, which received injection of either AAV-Vluc/GFP or AAV-Vluc/sTRAIL. Each group was then divided into two subgroups (n=10) which either received i.p. injection of DMSO (vehicle) or LanC (7.5 mg/kg body weight). This resulted in the following four groups: (1) AAV-Vluc/GFP, (2) AAV-Vluc/GFP + LanC, (3) AAV-Vluc/sTRAIL, (4) AAV-Vluc/sTRAIL+LanC. Lanatoside C was injected daily for 3 weeks starting one-day post-vector injection. Gene transfer as well as TRAIL binding to glioma cells was imaged as above, using Vluc and Gluc, which showed similar results to figure 3. Tumor volume was imaged over time with Fluc bioluminescence imaging. At two weeks post-injection, AAV-Vluc/GFP and AAV-Vluc/GFP + LanC treated mice had an average radiances of 1.04×10^6 and 3.6×10^6 photons/s/cm²/sr, respectively (**Fig. 4a,c**). On the other hand, both AAV-Vluc/sTRAIL and AAV-Vluc/sTRAIL+LanC treated mice had similar radiances to one another, which were significantly lower (>18-fold; p<0.05) than AAV-Vluc/GFP and AAV-Vluc/GFP+LanC control groups (**Fig. 4a,c**). Between 2 and 3 weeks post-vector injection, all mice in the AAV-Vluc/GFP and AAV-Vluc/GFP+LanC were sacrificed due to tumor progression whereas mice from AAV-Vluc/sTRAIL and AAV-Vluc/sTRAIL+LanC remained alive. Imaging of mice in the AAV-Vluc/sTRAIL and AAV-Vluc/sTRAIL+LanC groups at week 3 post-vector injection revealed a 6.7-fold lower mean radiance (p<0.05) in the combination treated group as compared to AAV-Vluc/sTRAIL alone showing that LanC had a sensitization effect on glioma cells to sTRAIL when co-delivered (**Fig 4,b-d**).

Figure 4

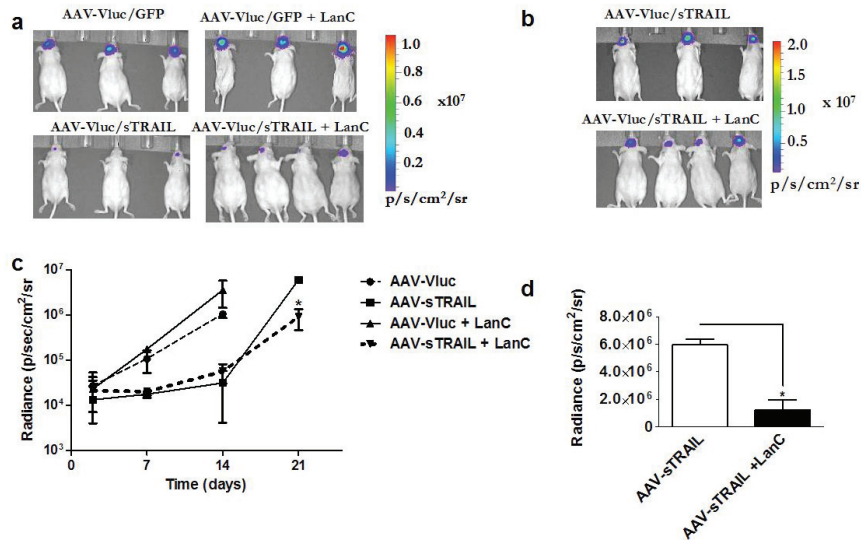


Figure 4. Lanatoside C enhances TRAIL-mediated therapy against intracranial gliomas. Mice bearing U87Fluc/NF-Gluc gliomas received an infusion of AAV-Vluc/GFP or AAV-Vluc/sTRAIL. Each group was divided into 2 subgroups, which either received vehicle or LanC. Tumor growth was monitored over time by Fluc bioluminescence imaging. (a,b) Bioluminescence images from representative mice in each group at week 2 (a) and 3 (b). (c) Quantitation of tumor-associated bioluminescence of the different treatment groups over time. (d) Quantitation of Fluc signal in the AAV-Vluc/sTRAIL and AAV-Vluc/sTRAIL+LanC groups at week 3. Mice in AAV-Vluc/GFP and AAV-Vluc/GFP+LanC had been sacrificed prior to week 3 imaging due to tumor progression.

To check whether lanatoside C could re-sensitize TRAIL-resistant cell population to its apoptotic effects, mice bearing established U87Fluc/NF-Gluc were injected with AAV-Vluc/sTRAIL as above. Sixteen days post-vector injection, mice were treated for 6 consecutive days with LanC. At day 22, Fluc imaging revealed a 17-fold decrease in tumor volume confirming sensitization (**Fig. 5a**). These mice were then left off the drug for 7 days. At day 29, Fluc imaging revealed a 60-fold increase in tumor-associated signal indicating that U87 glioma cells regained TRAIL resistance in the absence of LanC (**Fig. 5a**). Placing the mice back on this drug from day 29 to day 36 again showed re-sensitization of glioma tumors to TRAIL (**Fig. 5a**). These data suggest that LanC could re-sensitize resistant glioma cells to TRAIL-induced cell death. In another group of mice, we allowed the glioma cells to gain resistance to TRAIL before treating with one cycle of LanC (given at day 29). U87Fluc/5NF-Gluc

were implanted in the brain of mice, injected with AAV-Vluc/sTRAIL or AAV-Vluc/GFP as above and imaged for tumor-associated Fluc signal over time, which showed tumor re-growth. Fluc imaging at day 36 showed a 1.6-fold decrease in Fluc signal and therefore sensitization of resistant glioma cells to TRAIL in the AAV-Vluc/sTRAIL injected group (**Fig. 5b**). On the other hand, the control group injected with AAV-Vluc/GFP+LanC showed a 6.3-fold-increase in tumor volume between day 29 and 36 (**Fig. 5c**), proving that the observed anti-tumor effect is due to the combined sTRAIL and LanC Therapy.

Figure 5

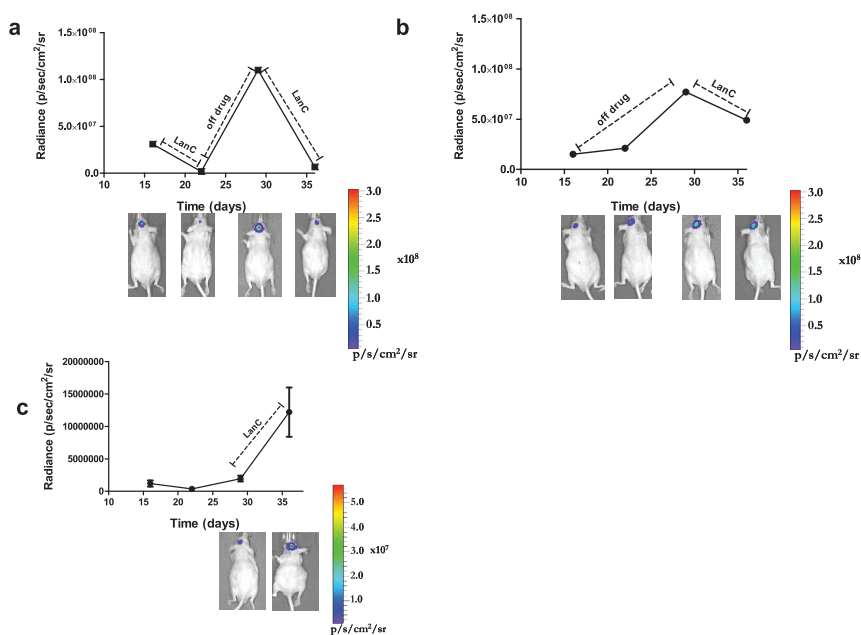


Figure 5. Lanatoside C re-sensitizes glioma tumors to TRAIL. (a) Mice brains bearing U87Fluc/NF-Gluc gliomas were infused with AAV-Vluc/sTRAIL. Sixteen days later, mice were treated with two 6-days cycle of LanC with a 7 days period off drug between each cycle. Tumor volume was monitored by Fluc bioluminescence imaging. (b) Similar treatment as (a) except mice received only one cycle of LanC treatment 30 days post-vector injection. (c) Control experiment in which mice bearing U87Fluc/NF-Gluc gliomas were injected with AAV-Vluc/GFP vectors and then subjected to one cycle of LanC treatment. Tumor volume was imaged at the beginning and end of drug treatment. Representative mouse from each group is shown under each time point.

We next evaluated our AAV-sTRAIL+LanC therapy in an invasive primary glioma orthotopic xenograft model using human GBM8 tumor stem-like cells²² stably expressing Fluc. These cells are cultured as neurospheres and we observed that they are semi-sensitive to monotherapy of TRAIL and LanC, However, combined therapy induces >95% cell death (**Supplementary Fig. 3**). GBM8-Fluc cells were implanted into the striatum of nude mice. At day 14 post-tumor injection, mice were imaged for Fluc signal (tumor volume) and then divided into 4 different groups (n=8), such that the mean bioluminescence of each group was similar to one another. At day 22, when imaging showed no significant difference in tumor volume between groups (p=0.9955, **Supplementary Fig. 4**), each group of mice was treated as follows: (1) AAV-Vluc/GFP, (2) AAV-Vluc/GFP+LanC, (3) AAV-Vluc/sTRAIL, (4) AAV-Vluc/sTRAIL+LanC. Tumor volume was monitored once/week using Fluc BLI over 4 weeks. One week post-treatment, the Fluc signal in the AAV-Vluc/GFP and AAV-Vluc/GFP+LanC group increased by 8.5-fold and 17-fold, respectively (Fig. 6a). In contrast, groups of mice treated with AAV-Vluc/sTRAIL or AAV-Vluc/sTRAIL+LanC showed a 4-fold and 7.2-fold decrease in Fluc signal, and therefore tumor volume, respectively (**Fig. 6a**). The AAV-Vluc/GFP and AAV-Vluc/GFP+LanC groups reached a maximum signal between 2 and 3 weeks post-treatment. Mice treated with AAV-Vluc/sTRAIL continued to have a lower signal compared to the control group, although the signal increased 20-fold between weeks 1-4 (**Fig. 6a**). On the other hand, mice in the co-treatment group which received AAV-Vluc/sTRAIL+LanC group only increased 1.6-fold between weeks 1-4 (**Fig. 6a**). Histological analysis of brains from mice in the different treatment groups was performed at the time of sacrifice. Mice treated with the control AAV-Vluc/GFP vector showed large multi-lobed tumors that were easily visualized by Hematoxylin and Eosin (H&E) stain (**Fig. 6b**). Large tumors at the injected side were also apparent in the control AAV-Vluc/GFP+LanC treated mice (**Fig. 6b**). In contrast, mice treated with AAV-Vluc/sTRAIL had more diffuse tumor with “ring like” phenotype around the site of vector injection (striatum), with secondary tumor masses away from injection site, and tumor cell infiltration along the corpus callosum (**Fig. 6b,c**). In mice treated with both AAV-Vluc/sTRAIL+LanC, no visible tumor masses were observed at the site of vector injection showing efficient therapy of the primary tumor mass (**Fig. 6b**). However, tumor cells migration away from the therapeutic zone was also observed (**Fig. 6c**).

Figure 6

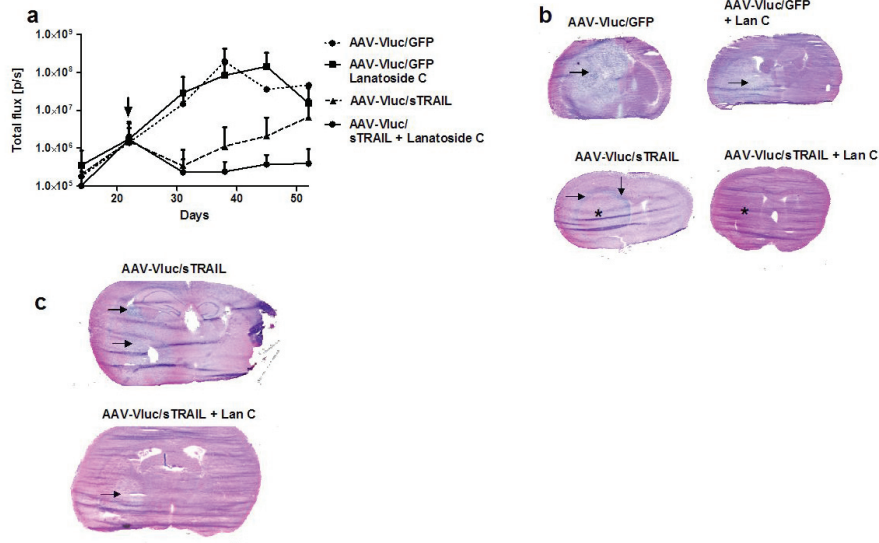


Figure 6. Combined AAV-sTRAIL and lanatoside C therapy slows invasive primary glioma growth. (a) Mice were stereotactically injected with human GBM8 tumor stem-like cells stably expressing Fluc. Three weeks later, mice were divided into 4 different treatment groups as noted. Fluc imaging for tumor size was performed over time. Arrow indicates the start of the treatment. (b-c) H&E histological analysis of a representative mouse from each group at the site of vector injection (b) and distal from the tumor/vector injection site (c) are shown. * indicates tumor/vector injection site. Arrows indicate tumor cells migration away from injection site.

DISCUSSION

Luciferases have played a major role in advancing our understanding of biological processes. A broader array of biocompatible, non-toxic and efficiently- expressed reporters that can be used together with existing luciferases can serve to expand this potential. The present study demonstrates for the first time a triple luciferase reporter system suitable for *in vivo* bioluminescence imaging. We showed that *Vargula* luciferase can be multiplexed together with *Gaussia* and firefly luciferases for sequential monitoring of three distinct biological phenomena. We also showed that this triple bioluminescence imaging yield specific, detectable bioluminescence signal

deep within the brain (with intact skull, ~3.5 mm) of mice. Importantly, we successfully employed this reporter system to monitor three different biological processes in an orthotopic brain tumor model, thus validating the system for different applications.

Since the cloning and sequencing of *Vargula* (formerly *Cypridina*) *hilgendorffii* (Vluc) cDNA in 1989¹⁵, several reports have demonstrated the usefulness of this enzyme for luminescence assays²³⁻²⁶. However, to our knowledge, no reports have applied it for *in vivo* imaging probably due to the unavailability of its substrate, vargulin, which is now commercially available. Vluc cDNA possess a signal sequence and therefore is naturally secreted from cells allowing real time, multi-time point analysis from the same cells^{23, 27}. In this study, we characterized a codon-optimized Vluc cDNA for mammalian gene expression and showed Vluc to be very stable with no significant decline in activity over 12 days in cell-free conditioned media at 37 °C. Despite the fact that the majority of Vluc was found in the conditioned media of mammalian cells, the intracellular Vluc level was efficient for *in vivo* imaging. In applications where higher sensitivity is required, a membrane-bound variant of Vluc²⁷ could be used which should yield higher cellular activity similar to a recent report for *Gaussia* luciferase^{28, 29}.

Systems for multi-modal imaging exist which incorporate different technologies such as fluorescence, bioluminescence, positron emission tomography (PET), and magnetic resonance imaging (MRI)³⁰. While substantial multi-parameter information can be gained by these systems, they have several drawbacks including high cost (e.g. MRI), logistical concerns such as short half-life of some PET probes, and broad technical expertise. While fluorescent reporter-based imaging as well as luciferases emitting at different wavelengths can be used for multi-imaging applications, they require expensive and complicated instrumentation with spectral deconvolution for visualizing of each biological parameter of interest^{31,32}. Furthermore, fluorescence-based imaging is limited by a high background due to tissue autofluorescence as well as single animal analysis. On the other hand, BLI has low background noise and is thus more sensitive for deep tissue imaging applications¹. The triple *in vivo* bioluminescence imaging system described here yields multi-parameter information distinguished by sequential imaging using different specific substrates, while remaining both cost effective and highly sensitive, as well as being user friendly

since only a simple CCD camera is required with no need for sophisticated instrument hardware/software. This same system can be extended and applied to any field to monitor three distinct biological phenomena, allowing one to obtain maximal information in animal models

TRAIL has been regarded as an anti-cancer agent, however, significant cancer types, including gliomas, are resistant to TRAIL-induced cell death⁹. Mechanisms of resistance include downregulation of death receptors³³, decoy receptor expression³⁴, as well as overexpression of the caspase-8 inhibitor, c-FLIP, due to deregulation of the mTOR signaling pathway³⁵. Additionally NF- κ B induction by TRAIL has been reported as a tumor cell resistance mechanism^{10,36}. Through drug screening, we have previously shown that the family of cardiac glycosides, including lanatoside C, sensitizes glioma cells to TRAIL-induced cell death partially through upregulation of death receptors^{12,37}. Cardiac glycosides have been recently shown to provide neuroprotection against ischemic stroke^{13,14} and therefore penetrate the brain efficiently. Another disadvantage of using TRAIL for brain tumor therapy is its inability to cross the blood-brain barrier. In this study, we circumvented this problem by delivering sTRAIL directly to brain tumor environment by AAV-mediated gene delivery. By engineering the normal brain to synthesize and secrete sTRAIL, it can form a zone of resistance against newly developed glioma, which can be treated with lanatoside C therapy. Since TRAIL, AAV vectors, and lanatoside C have been used separately in clinical trials, this therapeutic approach can be potentially translated to humans. In addition to the more traditional U87 glioma model in which sTRAIL and LanC showed a therapeutic benefit, we tested this therapy against an invasive human glioma model, GBM8²². While AAV-sTRAIL showed a therapeutic response compared to the controls, mice eventually succumbed to tumor burden. H&E staining revealed a ring-like tumor formation around the vector injection site (highest concentration of sTRAIL), as well as secondary tumor formation away from injection site due to tumor cell migration. On the other hand, the combined AAV-sTRAIL+LanC group showed significantly lower bioluminescent signal over the course of treatment, as compared to AAV-sTRAIL alone, with practically no tumor at the injection site as shown by H&E staining. However, tumor cell migration away from the injection site was also observed which eventually lead to animal death. To enhance this combined therapy against invasive tumor cells, a multi-injection

approach of the vector may be required. Alternatively, systemic injection of an AAV vector which can lead to global gene delivery (e.g. AAV9) may allow for widespread sTRAIL expression in the brain³⁸.

METHODS

Cells: U87 human glioblastoma cell line and 293T human kidney fibroblast cells were obtained from the American Type Culture Collection (Manassas, VA). Both cell lines were cultured in high glucose Dulbecco's modified Eagle's medium (Invitrogen, Carlsbad, CA) supplemented with 10% fetal bovine serum (Sigma, St Louis, MO) and 100 U/ml penicillin, 100 µg/ml streptomycin (Invitrogen) in a humidified atmosphere supplemented with 5% CO₂ at 37°C. GBM8 tumor stem-like cells were grown as neurospheres as previously described²². Briefly, spheres were cultured in Neurobasal medium (Invitrogen) supplemented with 3mM L-Glutamine (Mediatech), 1x B27 supplement (Gibco), 0.5x N2 supplement (Gibco), 2 µg/ml heparin (Sigma), 20 ng/ml recombinant human EGF (R & D systems), 20 ng/ml recombinant human FGF2 (Peprotech) and 0.5x penicillin G/streptomycin sulfate/amphotericin B complex (Mediatech).

Adeno-associated viral vectors and lentivirus vectors. The AAV-Vluc vector was constructed by replacing EGFP in AAV-CBA-EGFP³⁹ with the human codon optimized Vluc cDNA (a kind gift from Dr. Rampyari Walia, Targeting Systems, El Cajon, CA). AAV-sTRAIL vector consists of a transgene cassette for soluble, secreted TRAIL carrying amino acid (a.a.) 1-150 from human Flt3L, an isoleucine zipper domain, and the extracellular domain (a.a. 114-281) of the human TRAIL designed based on previously reported h-Flex-zipper-TRAIL¹⁷. In all these AAV vectors, gene expression is controlled by a hybrid cytomegalovirus enhancer/chicken beta actin promoter (CBA). All vectors carry a woodchuck hepatitis virus post-transcriptional regulatory element (WPRE) downstream of the transgene. AAV vector pseudotyped with AAVrh.8 capsids were produced by co-transfection of 293T cells using calcium phosphate precipitation of vector plasmid, a mini-adenovirus helper plasmid pFΔ6 (from Dr. Weidong Xiao, Univ. Penn. Med. Ctr., Philadelphia, PA), and AAVrh.8 helper plasmid pAR8 as described³⁹. AAV vectors were purified and titered, as described³⁹, yielding typical titers of 10¹³ g.c. per ml¹⁸. For sTRAIL

expression in culture, AAV vectors were packaged as AAV2 since this serotype is known to transduce cells in culture much more efficiently as compared to AAV2 genome pseudotyped with AAVrh.8.

U87 cells stably expressing Fluc and mCherry were generated by transduction of these cells with CSCW2-Fluc-ImCherry lentivirus vector at a multiplicity of infection of 10 transducing units/cell as described¹⁸. These cells were subsequently transduced with Lenti-NF-Gluc, a lentivirus vector encoding a Gluc under the control of 5 tandem repeats of NF- κ B-responsive elements¹⁹. These double-transduced U87 cells are referred to as U87Fluc/NF-Gluc cells. The lentivirus vector encoding VLuc was constructed by replacing the Fluc insert in CSCW2-Fluc-ImCherry with the human codon-optimized VLuc cDNA. The lentivirus vector expressing Gluc was previously described¹⁶. U87 cell lines stably expressing VLuc or Gluc were generated in a similar manner to Fluc. GBM8 cells stably expressing Fluc and mCherry were generated by transduction of these cells with CSCW2-Fluc-ImCherry as above.

In vivo tumor models. All animal experiments were approved by the Massachusetts General Hospital Subcommittee on Research Animal Care following guidelines set forth by the National Institutes of Health Guide for the Care and Use of Laboratory Animals. Six-eight weeks athymic nude mice were anesthetized with a mixture of Ketamine (100 mg/kg) and Xylazine (5 mg/kg) in 0.9% sterile saline. For subcutaneous tumors, mice were injected with 100 μ L of a 50:50 mixture of Matrigel™ Basement Membrane Matrix (BD Biosciences, Franklin Lakes, NJ) and 1-2 million U87 cells expressing either Gluc, VLuc or Fluc resuspended in Opti-MEM. For the brain tumor model, 10⁵ U87Fluc/5NF-Gluc cells (in 2 μ L Opti-MEM) were intracranially injected in the left midstriatum of nude mice using the following coordinates from bregma in mm: anterior-posterior +0.5, medio-lateral +2.0, dorso-ventral -2.5. These injections were performed using a Micro 4 Microsyringe Pump Controller (World Precision Instruments, Sarasota, FL) attached to a Hamilton syringe with a 33-gauge needle (Hamilton, Reno, NV) at a rate of 0.2 μ L/min. For implantation of GBM8-Fluc spheres in mice, cells were dissociated with Accutase (Innovative Cell Technologies, San Diego, CA) 2 days before injection. On the day of injection the majority of spheres were of medium size of approximately 100 cells/sphere, which were left intact for implantation. Approximately 3x10⁵ cells (3000

spheres) were injected per mouse in a volume of 3 μ l at 0.3 μ l/min using the microsyringe pump and a 33-gauge needle as above.

For AAV vector injection, mice were anesthetized as above and injected intracranially using the same coordinates as for tumor injections. AAV vectors were infused at a rate of 0.2 μ L/min using a Micro 4 Microsyringe Pump Controller attached to a Hamilton syringe with a 33-gauge needle.

In vitro and in vivo luciferase imaging. *D*-luciferin was purchased from Gold Biotechnology® (St. Louis, MO) and resuspended at 25 mg/ml in PBS. For Fluc imaging, mice were injected i.p. with 200 mg/kg body weight of *D*-luciferin and imaging was performed 10 min later. Coelenterazine was obtained from NanoLight™ Technology (Pinetop, AZ) and resuspended at 5 mg/ml in acidified methanol. For Gluc imaging, mice were injected i.v. (through retro-orbital sinus) with 5 mg/kg body weight of coelenterazine solution diluted in PBS and imaging was performed immediately. Vargulin substrate (*Cypridina* luciferin) was obtained from NanoLight™ Technology and was resuspended at 5 mg/ml in acidified methanol or from Targeting Systems, sold as a solution. For Vluc as a marker for cell proliferation, and since Vluc was shown to be stable in the conditioned medium, we refreshed the media of cells 4 hours before measurements to avoid accumulation of the reporter. For Vluc *in vivo* imaging, mice were injected i.v. (unless otherwise noted) with 4 mg/kg body weight (diluted in PBS) and imaging was performed immediately. Imaging was performed using an IVIS® Spectrum optical imaging system fitted with an XGI-8 Gas Anesthesia System (Caliper Life Sciences, Hopkinton, MA). Bioluminescent images were acquired using the auto-exposure function. Data analysis for signal intensities and image comparisons were performed using Living Image® software (Caliper Life Sciences).

TRAIL ELISA. The functionality of the AAV-sTRAIL vector was tested by transducing U87 cells with 10^4 g.c./cell with AAV2-sTRAIL or a negative control vector AAV2-GFP. Three days later, media was harvested from all wells and a Quantikine Human TRAIL ELISA (R&D Systems, Minneapolis, MN) was performed per manufacturer's instructions.

Statistical analysis. Statistical analysis was performed using GraphPad Prism version 5.01 software (LaJolla, CA). For comparisons between two samples, an unpaired two-tailed t test was performed. A p value of < 0.05 was considered to be statistically significant. For analysis between multiple groups, a one-way analysis of variance (ANOVA) was performed followed by a Bonferroni's Multiple Comparison Test to compare 2 groups.

ACKNOWLEDGEMENTS

This work was supported by grant from 1R01NS064983 (BAT) and by a Fellowship from the American Brain Tumor Association (CM). We thank Dr. Hiroaki Wakimoto and Samuel Rabkin for the GBM8 cells. We would like to acknowledge the MGH Nucleic Acid Quantitation Core, the Neuroscience Image Analysis Core, and the MGH Vector Core supported by NIH/NINDS P30NS04776.

REFERENCES

1. Badr CE, Tannous BA. Bioluminescence imaging: progress and applications. *Trends Biotechnol.* Dec;29(12):624-633.
2. Contag CH, Contag PR, Mullins JI, Spilman SD, Stevenson DK, Benaron DA. Photonic detection of bacterial pathogens in living hosts. *Mol Microbiol.* Nov 1995;18(4):593-603.
3. Rabinovich BA, Ye Y, Etto T, Chen JQ, Levitsky HI, Overwijk WW, et al. Visualizing fewer than 10 mouse T cells with an enhanced firefly luciferase in immunocompetent mouse models of cancer. *Proc Natl Acad Sci U S A.* Sep 23 2008;105(38):14342-14346.
4. Tannous BA, Kim DE, Fernandez JL, Weissleder R, Breakefield XO. Codon-optimized *Gussia* luciferase cDNA for mammalian gene expression in culture and in vivo. *Mol Ther.* Mar 2005;11(3):435-443.
5. Branchini BR, Southworth TL, Khattak NF, Michelini E, Roda A. Red- and green-emitting firefly luciferase mutants for bioluminescent reporter applications. *Anal Biochem.* Oct 1 2005;345(1):140-148.
6. Branchini BR, Ablamsky DM, Murtiashaw MH, Uzasci L, Fraga H, Southworth TL. Thermostable red and green light-producing firefly luciferase mutants for bioluminescent reporter applications. *Anal Biochem.* Feb 15 2007;361(2):253-262.
7. Kim SB, Suzuki H, Sato M, Tao H. Superluminescent variants of marine luciferases for bioassays. *Anal Chem.* Nov 15;83(22):8732-8740.
8. Vilalta M, Jorgensen C, Degano IR, Chernajovsky Y, Gould D, Noel D, et al. Dual luciferase labelling for non-invasive bioluminescence imaging of mesenchymal stromal cell chondrogenic differentiation in demineralized bone matrix scaffolds. *Biomaterials.* Oct 2009;30(28):4986-4995.
9. Ricci MS, Kim SH, Ogi K, Plastaras JP, Ling J, Wang W, et al. Reduction of TRAIL-induced Mcl-1 and cIAP2 by c-Myc or sorafenib sensitizes resistant human cancer cells to TRAIL-induced death. *Cancer Cell.* Jul 2007;12(1):66-80.
10. Zhang L, Fang B. Mechanisms of resistance to TRAIL-induced apoptosis in cancer. *Cancer Gene Ther.* Mar 2005;12(3):228-237.
11. Xiang H, Nguyen CB, Kelley SK, Dybdal N, Escandon E. Tissue distribution, stability, and pharmacokinetics of Apo2 ligand/tumor necrosis factor-related apoptosis-inducing ligand in human colon carcinoma COLO205 tumor-bearing nude mice. *Drug Metab Dispos.* Nov 2004;32(11):1230-1238.
12. Badr CE, Wurdinger T, Nilsson J, Niers JM, Whalen M, Degterev A, et al. Lanatoside C sensitizes glioblastoma cells to tumor necrosis factor-related apoptosis-inducing ligand and induces an alternative cell death pathway. *Neuro Oncol.* Nov;13(11):1213-1224.
13. Marx J, Pretorius E, Bornman MS. The neurotoxic effects of prenatal cardiac glycoside exposure: a hypothesis. *Neurotoxicol Teratol.* Jan-Feb 2006;28(1):135-143.
14. Wang JK, Portbury S, Thomas MB, Barney S, Ricca DJ, Morris DL, et al. Cardiac glycosides provide neuroprotection against ischemic stroke: discovery by a brain slice-based compound screening platform. *Proc Natl Acad Sci U S A.* Jul 5 2006;103(27):10461-10466.

15. Thompson EM, Nagata S, Tsuji FI. Cloning and expression of cDNA for the luciferase from the marine ostracod *Vargula hilgendorffii*. *Proc Natl Acad Sci U S A*. Sep 1989;86(17):6567-6571.
16. Wurdinger T, Badr C, Pike L, de Kleine R, Weissleder R, Breakefield XO, et al. A secreted luciferase for ex vivo monitoring of in vivo processes. *Nat Methods*. Feb 2008;5(2):171-173.
17. Wu X, He Y, Falo LD, Jr., Hui KM, Huang L. Regression of human mammary adenocarcinoma by systemic administration of a recombinant gene encoding the hFlex-TRAIL fusion protein. *Mol Ther*. Mar 2001;3(3):368-374.
18. Maguire CA, Meijer DH, LeRoy SG, Tierney LA, Broekman ML, Costa FF, et al. Preventing growth of brain tumors by creating a zone of resistance. *Mol Ther*. Oct 2008;16(10):1695-1702.
19. Badr CE, Niers JM, Tjon-Kon-Fat LA, Noske DP, Wurdinger T, Tannous BA. Real-time monitoring of nuclear factor kappaB activity in cultured cells and in animal models. *Mol Imaging*. Sep-Oct 2009;8(5):278-290.
20. Yang B, Wu X, Mao Y, Bao W, Gao L, Zhou P, et al. Dual-targeted antitumor effects against brainstem glioma by intravenous delivery of tumor necrosis factor-related, apoptosis-inducing, ligand-engineered human mesenchymal stem cells. *Neurosurgery*. Sep 2009;65(3):610-624; discussion 624.
21. Chaudhary PM, Eby M, Jasmin A, Bookwalter A, Murray J, Hood L. Death receptor 5, a new member of the TNFR family, and DR4 induce FADD-dependent apoptosis and activate the NF-kappaB pathway. *Immunity*. Dec 1997;7(6):821-830.
22. Wakimoto H, Kesari S, Farrell CJ, Curry WT, Jr., Zaupa C, Aghi M, et al. Human glioblastoma-derived cancer stem cells: establishment of invasive glioma models and treatment with oncolytic herpes simplex virus vectors. *Cancer Res*. Apr 15 2009;69(8):3472-3481.
23. Inouye S, Ohmiya Y, Toya Y, Tsuji FI. Imaging of luciferase secretion from transformed Chinese hamster ovary cells. *Proc Natl Acad Sci U S A*. Oct 15 1992;89(20):9584-9587.
24. Thompson EM, Nagata S, Tsuji FI. *Vargula hilgendorffii* luciferase: a secreted reporter enzyme for monitoring gene expression in mammalian cells. *Gene*. Dec 15 1990;96(2):257-262.
25. Thompson EM, Adenot P, Tsuji FI, Renard JP. Real time imaging of transcriptional activity in live mouse preimplantation embryos using a secreted luciferase. *Proc Natl Acad Sci U S A*. Feb 28 1995;92(5):1317-1321.
26. Tanahashi Y, Ohmiya Y, Honma S, Katsuno Y, Ohta H, Nakamura H, et al. Continuous measurement of targeted promoter activity by a secreted bioluminescence reporter, *Vargula hilgendorffii* luciferase. *Anal Biochem*. Feb 15 2001;289(2):260-266.
27. Ura S, Ueda H, Kazami J, Kawano G, Nagamune T. Single cell reporter assay using cell surface displayed *Vargula* luciferase. *J Biosci Bioeng*. 2001;92(6):575-579.
28. Santos EB, Yeh R, Lee J, Nikhamin Y, Punzalan B, Punzalan B, et al. Sensitive in vivo imaging of T cells using a membrane-bound Gaussia princeps luciferase. *Nat Med*. Mar 2009;15(3):338-344.
29. Niers JM, Chen JW, Lewandrowski G, Kerami M, Garanger E, Wojtkiewicz G, et al. Single reporter for targeted multimodal in vivo imaging. *J Am Chem Soc*. Mar 21;134(11):5149-5156.

30. Weissleder R, Pittet MJ. Imaging in the era of molecular oncology. *Nature*. Apr 3 2008;452(7187):580-589.
31. Gammon ST, Leevy WM, Gross S, Gokel GW, Piwnica-Worms D. Spectral unmixing of multicolored bioluminescence emitted from heterogeneous biological sources. *Anal Chem*. Mar 1 2006;78(5):1520-1527.
32. Ntziachristos V. Fluorescence molecular imaging. *Annu Rev Biomed Eng*. 2006;8:1-33.
33. Ding L, Yuan C, Wei F, Wang G, Zhang J, Bellail AC, et al. Cisplatin restores TRAIL apoptotic pathway in glioblastoma-derived stem cells through up-regulation of DR5 and down-regulation of c-FLIP. *Cancer Invest*. Oct;29(8):511-520.
34. Chamuleau ME, Ossenkuppele GJ, van Rhenen A, van Dreunen L, Jirka SM, Zevenbergen A, et al. High TRAIL-R3 expression on leukemic blasts is associated with poor outcome and induces apoptosis-resistance which can be overcome by targeting TRAIL-R2. *Leuk Res*. Jun;35(6):741-749.
35. Panner A, James CD, Berger MS, Pieper RO. mTOR controls FLIPS translation and TRAIL sensitivity in glioblastoma multiforme cells. *Mol Cell Biol*. Oct 2005;25(20):8809-8823.
36. Ibrahim SM, Ringel J, Schmidt C, Ringel B, Muller P, Koczan D, et al. Pancreatic adenocarcinoma cell lines show variable susceptibility to TRAIL-mediated cell death. *Pancreas*. Jul 2001;23(1):72-79.
37. Badr CE, Wurdinger T, Tannous BA. Functional drug screening assay reveals potential glioma therapeutics. *Assay Drug Dev Technol*. Jun;9(3):281-289.
38. Foust KD, Nurre E, Montgomery CL, Hernandez A, Chan CM, Kaspar BK. Intravascular AAV9 preferentially targets neonatal neurons and adult astrocytes. *Nat Biotechnol*. Jan 2009;27(1):59-65.
39. Broekman ML, Comer LA, Hyman BT, Sena-Estevés M. Adeno-associated virus vectors serotyped with AAV8 capsid are more efficient than AAV-1 or -2 serotypes for widespread gene delivery to the neonatal mouse brain. *Neuroscience*. 2006;138(2):501-510.

CHAPTER VI



Directed molecular evolution reveals *Gaussia* luciferase variants with enhanced light output stability

M. Hannah Degeling^{1,2,3*}, M. Sarah S. Bovenberg^{1,2,3*}, Grant K. Lewandrowski^{1,2*}, Mark C. de Gooijer^{1,2,4}, Carmen L.A. Vleggeert-Lankamp⁴, Marie Tannous⁵, Casey A. Maguire^{1,2}, and Bakhos A. Tannous^{1,2}

¹Experimental Therapeutics and Molecular Imaging Laboratory, Neuroscience Center, Department of Neurology, ²Program in Neuroscience, Harvard Medical School, Boston, MA 02114 USA. ³Department of Neurosurgery, Leiden University Medical Center, Leiden, The Netherlands. ⁴Neuro-oncology Research Group, Department of Neurosurgery, VU Medical Center, Cancer Center Amsterdam, 1007 MB Amsterdam, The Netherlands. ⁵ Faculty of Natural and Applied Sciences, Notre Dama University, Barsa, Lebanon. * These authors contributed equally

ABSTRACT

Gaussia Luciferase (Gluc) has proven to be a powerful mammalian cell reporter for monitoring numerous biological processes in immunology, virology, oncology and neuroscience. Current limitations of Gluc as a reporter include its emission of blue light, which is absorbed by mammalian tissues, limiting its use *in vivo*, and a flash-type bioluminescence reaction, making it unsuited for high-throughput applications. To overcome these limitations, a library of Gluc variants was generated using directed molecular evolution and screened for relative light output, a shift in emission spectrum, and glow-type light emission kinetics. Several variants with a 10-15 nm shift in their light emission peak were found. Further, a Gluc variant that catalyzes a glow-type bioluminescence reaction yielding over 10 minutes of stable light output, suited for high-throughput applications, was also identified. These results indicate that molecular evolution could be used to modulate Gluc bioluminescence reaction characteristics.

INTRODUCTION

Bioluminescence imaging (BLI) is currently one of the most valued and widely used techniques in basic biomedical research.¹⁻³ Bioluminescence relies on the conversion of chemical energy into visible light in culture or in living animals. This reaction is dependent on a luciferase enzyme which, in the presence of oxygen, causes a biochemical conversion of the luciferin substrate resulting in emission of light.¹ In the past decade, bioluminescence imaging has become indispensable for non-invasive monitoring of biological processes including gene expression,^{4, 5} protein-protein interactions,⁶⁻⁸ T-cell and stem cell trafficking,^{9, 10} tumorigenesis and response to therapy,^{4, 11, 12} and has further been used as a read-out for high-throughput screening assays in drug discovery.^{13, 14} Although many luciferases exist, only a few are currently in use. As a mammalian cell reporter, luciferase needs to meet certain criteria including a distinct emission spectrum ideally with a significant red component (for *in vivo* applications), and a high quantum yield without intracellular accumulation of substrate to allow for real-time monitoring of enzyme expression¹⁻³. Examples of frequently used luciferases are from the American firefly

Photinus Pyralis (Fluc), *Renilla reniformis* (Rluc), *Gaussia princeps* (Gluc) and *Vargula hilgendorfi* (Vluc)¹. Recently, differences between properties of these luciferases including specificity to different substrates, spectral emission, or bioluminescence half-life, were used to develop multiplex reporter systems by which several cellular processes can be monitored simultaneously.¹⁵⁻¹⁷ The next step to further improve the field of bioluminescence is to generate more stable, brighter and variants with different light emission properties suited for different applications.

Gaussia luciferase from the marine copepod *Gaussia princeps* has many advantageous properties over other luciferases including high signal intensity, a favorable enzyme stability, and a secretion signal, making it suitable for real time *ex vivo* monitoring of biological processes in medium of cultured cells and blood or urine in animals.¹⁸⁻²⁰ Gluc is a monomeric protein composed of 185 aa (19.9 kDa) that uses coelenterazine as a substrate. It is the smallest luciferase known with a peak light emission at around 470 nm and a broad spectrum extending up to 600 nm.¹⁹ Since Gluc does not require ATP for activity, in contrast to the commonly used Fluc, it can be used as a reporter from cells as well as their immediate environment.

Current limitations of Gluc include signal quenching and absorption of its blue light by pigmented molecules when used *in vivo* and its rapid light decay, making the use of a luminometer with a built-in injector essential for immediate reading of signal once substrate is added, one well at a time. Several successful attempts have been made to optimize Gluc as a mammalian cell reporter. To overcome signal quenching when measuring Gluc in the blood *ex vivo*, we have developed an alternative microtiter well-based binding assay in which Gluc is captured from the blood before coelenterazine is added leading to around 10-fold increased sensitivity¹⁸. We have also characterized a Gluc mutant, GlucM43I, which catalyzes stable light output in the presence of Triton-X 100 detergent, suited for high-throughput applications.²¹ Gluc was also shown to potentially contain 2 catalytic domains, the first covering amino acids 27-97 and the second domain covering amino acids 98-168.²² Recently, Kim and colleagues developed a semi-rational consensus sequence driven mutagenesis strategy to synthesize potent mutant Gluc by comparing sequence similarities between the chromophore region of *Aequorea* green fluorescent protein (GFP) and coelenterazine.²³ Using this rational and hydrophobicity search, they

hypothesized that Gluc active site is between amino acids 71-140, the most hydrophilic domain. Site-directed mutagenesis of this active core, similar to those performed for GFP, lead to efficient alteration of Gluc properties including variants with a shift in emission spectrum [Y97W, I90L and Monsta (combination of F89W, I90L, H95E and Y97W mutations)], and enhanced light output (I90L). In this study, we used directed molecular evolution to create a Gluc library based on the sequence of wild type Gluc and screened around 5000 newly generated clones for increased activity, a shift in the emission spectrum, and increased light emission stability. Several variants were selected and sequenced for their mutations. One of these mutants carrying three different mutations (L30S, L40P, M43V; Gluc4) showed a glow-type bioluminescence reaction (as compared to flash reaction for wild-type Gluc) with stable light output up to 10 minutes without the need of a detergent, suited for high-throughput applications.

EXPERIMENTAL SECTION

Construction of Gluc library. A library of Gluc variants was created by shuffling cDNA fragments using error-prone PCR. First, the humanized codon-optimized cDNA sequence encoding *Gaussia* luciferase¹⁹ (Nanolight, Pinetop, AZ) was amplified by PCR (without the Gluc signal sequence) using Taq polymerase (5 PRIME, Fisher Scientific, Pittsburgh, PA) and two flanking primers, which introduced an EcoRI (upstream primer) and XhoI (downstream primer) restriction sites, using the following conditions: 1 cycle of 94 °C-2 min; 35 cycles of: 94 °C-30 s, 58 °C-30 s and 72 °C-30 s; 1 cycle of 72 °C -7 min. The PCR product was then digested using 0.3 Units of DNaseI (New England Biolabs, Ipswich, MA) for 10 min at room temperature followed by heat inactivation at 75°C for 15 min after the addition of EDTA. The digested DNA was separated on a 2% agarose gel by electrophoresis. DNA fragments from ~50–150 base pairs were carefully excised using a sterile scalpel. The gel slice was placed in 3,500 MWCO dialysis tubing (Fisher Scientific, Pittsburgh, PA) and the DNA was eluted into TBE by electrophoresis for 15 min at 120V. The DNA was then ethanol precipitated and re-suspended in nuclease-free water. The PCR fragments were reassembled into the full-sized product using Extensor Hi-Fidelity PCR enzyme mix (Thermo Scientific, Portsmouth, NH) without

primers using the following conditions: 1 cycle, 94 °C-2 min; 40 cycles of: 94 °C-30 s, 45 °C-30 s and 68 °C-30 s. One microliter from this reaction then served as a template for a second PCR using the same primers as for error prone PCR above and the following conditions: 1 cycle, 94 °C-2 min; 25 cycles of: 94 °C-30 s, 58 °C-30 s and 68 °C-30 s; 1 cycle, 68 °C-7 min. The PCR product was gel extracted after electrophoresis, digested with EcoRI and XhoI and ligated into a similarly digested pHGCx expression vector.¹⁹

Screening procedure. HMS174 bacterial cells were transformed with the newly created Gluc library by electroporation and spread on ampicillin agar plates. The next day, different colonies were collected by a Hudson RapidPick colony picker (Hudson Robotics, Inc., Springfield, NJ) and grown for 12 hours in 1 ml of LB media at 37 °C in deep 96 well plates. The bacterial cell culture media was then used directly to screen for emission spectrum shift using the Flexstation III plate reader (Molecular Devices, Sunnyvale, CA). Samples of 50 µl were transferred to regular white 96 well plates and read with 50 µl 40 µM coelenterazine (CTZN). The remaining bacterial media in the deep 96 well plates were mixed with glycerol and frozen at -80 °C. The clones showing differential spectrum shift as compared to wild-type (wt) Gluc were selected, sequenced for mutations, and cloned into a CSCW lentivirus mammalian expression backbone under the control of CMV promoter²⁰ using upstream primers which re-introduced the signal sequence to the cDNA. 293T cells (obtained from ATCC) were then transfected with the different Gluc variants using calcium phosphate protocol and two days later, the cell-free conditioned medium was collected and used for the different bioluminescent assays. Lentivirus vectors were packaged as previously described.¹⁸⁻²⁰

Bioluminescence assays. The emission spectrum for the different Gluc variants was confirmed using a Cary Eclipse Fluorescence Spectrophotometer (Varian, Inc., Palo Alto, CA) that reads the full spectrum within milliseconds (averaging reading time per sample of 5 msec). Emission spectrum analysis was performed using 100 µl of conditioned medium brought up to 500 µl in 1X PBS in a cuvette followed by addition of 500 µl CTZN (8 µg/ml diluted in PBS). The emission slit (nm) was set to 10-round, under a 400-600 nm emission wavelength window, using the bio/chemiluminescence setting. For relative activity comparison, 293T cells were

plated in 6-well plates and co-transfected with 0.5 µg of different Gluc variants and a similar amounts of a plasmid expressing firefly luciferase and mCherry fluorescent protein under control of CMV promoter (CSCW-Fluc-ImCherry)²⁰ as above. Forty-eight hours later, cells were analyzed by fluorescent microscopy for mCherry expression for transfection efficiency. Ten microliter aliquots (in 5-plicates) of the conditioned medium were assayed for Gluc activity as above. Cells were then lysed in 200 µl 1xRLB lysis buffer (Promega) and 20 µl aliquots of lysates (in triplicates) were assayed for Fluc activity using 80 µl of FLAR reagent (Targeting Systems, El Cajon, CA) and a luminometer (Model MLX, Dynex Technologies) that was set to read for 10 sec and integrate the signal for 2 sec. Fluc reads were used to normalize for transfection efficiency between wells. The enzymatic activities of different Gluc mutants over multiple coelenterazine injections were determined by reading 10 µl samples of conditioned medium in a 96 well microtiter plate using the Dynex luminometer while multiple injections of 20 µl of CTZN (8 µg/ml, in PBS) was added to the same wells and signal was recorded immediately after each injection; we used a 1 sec reading time and 10 different injections of CTZN per well, resulting in a total of 10 reads. The kinetic assay was performed by transferring 10 µl aliquots of conditioned medium (in 5-plicates) to a 96 well white plate, automatically injecting 40 µl 8 µg/ml CTZN in PBS (with or without 0.01% Triton) and recording kinetic intervals of 14 seconds over 10 min using the Flexstation III instrument (Molecular Devices). For validation of Gluc4 for high-throughput applications, 15 µl aliquots of conditioned medium from cells expressing wt Gluc, GlucM43I or Gluc4 were first transferred to a 384 well plate (in triplicates) using an automated dispenser (Multidrop Combi, Thermo Scientific). In a similar fashion, 45 µl 8 µg/ml CTZN diluted in PBS was also dispensed into each well and the plate was then analyzed using the Flexstation III that was set to read for 50 msec/well. In another experiment, U87 human glioma cells (ATCC) expressing either Gluc4 or wt Gluc were plated in a 96-well plate. The next day, several wells/plate were marked and treated with 1 mM temozolomide (Sigma). Seventy-two hours later, 10 µl aliquot of conditioned medium was transferred to a white plate followed by the addition of 45 µl 8 µg/ml CTZN/well using an automated dispenser and acquiring photon counts using the Dynex luminometer which was set to read for 1sec/well column by column.

Cloning multiple mutations. All mutations derived from the screen were located in the first catalytic domain of Gluc as described.²² Mutations were then transferred to the second catalytic domain by site directed mutagenesis, using PCR to create the desired point mutations for GlucL40P, GlucM43V, and GlucL40S variants, resulting in Gluc1 (L40S, E111S), Gluc2 (L30S, M43V, I114V), Gluc3 (L40P, E111P) and Gluc4 (L40P, M43V, L30S). For each Gluc variant, the desired mutation was incorporated using an overlapping PCR strategy. Using the screen derived Gluc variant cDNA as a template, two flanking Gluc primers which introduce a 5' NheI site and a 3' XhoI site were used for direct cloning of the final PCR product into CSCW plasmid. Two complementary inner primers were designed with a desired sequence mismatch to alter the codon of interest. Three different PCR reactions were performed to incorporate the mutation using specific primer sets (Supplementary Table 2): PCR 1 used Gluc variant cDNA as template and the forward flanking NheI primer combined with the reverse mutagenic primer. PCR 2 using the reverse flanking XhoI primer and the forward mutagenic primer. Specific bands for PCR 1 and 2 were gel extracted and 2 μ l of PCR product from PCR 1 and 2 were then used as template for overlapping PCR (PCR 3) using the flanking primers. All PCR reactions were performed using Phusion high fidelity polymerase (New England Biolabs). Correct incorporation of specific mutations was confirmed using DNA sequencing at the Massachusetts General Hospital DNA core facility. The full length PCR product was digested with NheI and XhoI and ligated with similarly digested CSCW lentivirus plasmid. The PCR primer sequences used in this study can be found in Supplementary Tables 1 and 2.

Statistical Analysis. All experiments were repeated at least 5 times to achieve statistical significance. Data are presented as the mean relative light units (RLU) \pm standard deviation (SD) from 5 different replicates in each experiment. P values were calculated using Student's t-test. Relative reaction kinetics, turnover rates, and Drug screening results are shown as representative data of 5 independent experiments.

RESULTS AND DISCUSSION

Recently, through hydrophobicity search and by comparing sequence similarities between the chromophore region of *Aequorea* green fluorescent protein (GFP) and coelenterazine, Kim et al suggested that the Gluc active core ranges between amino acids 71-140.²³ We took an alternative strategy and used directed molecular evolution to shuffle Gluc cDNA to find potent Gluc variants. Table 1 shows potential Gluc variants and their corresponding mutations derived from our screen.

Name	Mutation
GlucL40P	L40P
GlucL40S	L40S
GlucL30S, M43V	L30S, M43V
Gluc1	L40S, E111S
Gluc2	L30S, M43V, I114V
Gluc3	L40P, E111P
Gluc4	L30S, L40P, M43V
Gluc5	S16K, M43V, V159M

Table 1. Overview of the different Gluc variants and corresponding mutations.

Interestingly, all these Gluc variants were not part of the active core discovered by Kim et al., suggesting that Gluc could have another potential putative core region. Importantly, none of these mutations were found in 10 random clones from the original Gluc plasmid library showing that our library is fairly diverse (data not shown). Another study suggested that Gluc contains two catalytic domains and therefore two coelenterazine binding pockets.²² According to this study, all mutations derived from our screen are found in the first catalytic domain (amino acids 27-97; Fig. 1). We therefore attempted to enhance our mutants by also changing the corresponding amino acids in the second catalytic domain (amino acids 98-168) creating Gluc1, Gluc2 and Gluc3 variants (Fig. 1 and Table 1). Finally, we attempted to amplify our mutants by combining different mutations into a single Gluc cDNA creating Gluc4 (Fig. 1 and Table 1).

Figure 1

```

SS
MGVKVLFALICIAVAEA

1)
Gluc wt      KPTENNEDFNIVAVASNFATTDLDAD
GlucL40P    KPTENNEDFNIVAVASNFATTDLDAD
GlucL40S    KPTENNEDFNIVAVASNFATTDLDAD
GlucL30S, M43V KPTENNEDFNIVAVASNFATTDLDAD
Gluc1       KPTENNEDFNIVAVASNFATTDLDAD
Gluc2       KPTENNEDFNIVAVASNFATTDLDAD
Gluc3       KPTENNEDFNIVAVASNFATTDLDAD
Gluc4       KPTENNEDFNIVAVASNFATTDLDAD
Gluc5       KPTENNEDFNIVAVASNFATTDLDAD

27)
Gluc wt      RGKLPGKKLPLEVLKEMEANARKAGCTRGCLICLSHIKCTPKMKKFI PGRCHTYEGDKESAQQGIGEAIVD
GlucL40P    RGKLPGKKLPLEVPEKEMEANARKAGCTRGCLICLSHIKCTPKMKKFI PGRCHTYEGDKESAQQGIGEAIVD
GlucL40S    RGKLPGKKLPLEVSKEMEANARKAGCTRGCLICLSHIKCTPKMKKFI PGRCHTYEGDKESAQQGIGEAIVD
GlucL30S, M43V RGKSPGKKLPLEVLKEVEANARKAGCTRGCLICLSHIKCTPKMKKFI PGRCHTYEGDKESAQQGIGEAIVD
Gluc1       RGKLPGKKLPLEVSKEMEANARKAGCTRGCLICLSHIKCTPKMKKFI PGRCHTYEGDKESAQQGIGEAIVD
Gluc2       RGKSPGKKLPLEVLKEVEANARKAGCTRGCLICLSHIKCTPKMKKFI PGRCHTYEGDKESAQQGIGEAIVD
Gluc3       RGKLPGKKLPLEVPEKEMEANARKAGCTRGCLICLSHIKCTPKMKKFI PGRCHTYEGDKESAQQGIGEAIVD
Gluc4       RGKSPGKKLPLEVPEKVEANARKAGCTRGCLICLSHIKCTPKMKKFI PGRCHTYEGDKESAQQGIGEAIVD
Gluc5       RGKLPGKKLPLEVLKEVEANARKAGCTRGCLICLSHIKCTPKMKKFI PGRCHTYEGDKESAQQGIGEAIVD

98)
Gluc wt      IPEIPGFKDLEPMEQFIAQVDLCVDCTGCLKGLANVQCSDLLKKWLPQRCATFASKIQGQVDKIKGAGGD
GlucL40P    IPEIPGFKDLEPMEQFIAQVDLCVDCTGCLKGLANVQCSDLLKKWLPQRCATFASKIQGQVDKIKGAGGD
GlucL40S    IPEIPGFKDLEPMEQFIAQVDLCVDCTGCLKGLANVQCSDLLKKWLPQRCATFASKIQGQVDKIKGAGGD
GlucL30S, M43V IPEIPGFKDLEPMEQFIAQVDLCVDCTGCLKGLANVQCSDLLKKWLPQRCATFASKIQGQVDKIKGAGGD
Gluc1       IPEIPGFKDLEPMSQFIAQVDLCVDCTGCLKGLANVQCSDLLKKWLPQRCATFASKIQGQVDKIKGAGGD
Gluc2       IPEIPGFKDLEPMSQFIAQVDLCVDCTGCLKGLANVQCSDLLKKWLPQRCATFASKIQGQVDKIKGAGGD
Gluc3       IPEIPGFKDLEPMSQFIAQVDLCVDCTGCLKGLANVQCSDLLKKWLPQRCATFASKIQGQVDKIKGAGGD
Gluc4       IPEIPGFKDLEPMEQFIAQVDLCVDCTGCLKGLANVQCSDLLKKWLPQRCATFASKIQGQVDKIKGAGGD
Gluc5       IPEIPGFKDLEPMEQFIAQVDLCVDCTGCLKGLANVQCSDLLKKWLPQRCATFASKIQGQVDKIKGAGGD

```

Figure 1. Gluc variants and corresponding mutations in the second active domain characterized in this study. Shown, the Gluc signal peptide covering amino acids 1-27, first active domain covering amino acids 27-97, and second active domain covering amino acids 98-168.

Variants were first screened for a shift in emission spectrum using the Flexstation III device which is a slow reader requiring several minutes to read the full spectrum. Results could therefore be confounded by the kinetic properties of each clone (e.g. flash versus glow emission). All our shifted clones were confirmed using a Cary Eclipse Fluorescence Spectrophotometer, which reads the full spectrum in milliseconds. Upon conformational analysis, we found that GlucL40P, GlucL40S and Gluc4 (L30S, L40P, M43V) showed a 10-15 nm shift in light emission peak as compared to wild-type (wt) Gluc (Supplementary Fig. 1). Mutating the corresponding amino acid in the second active domain (Gluc1, Gluc2 and Gluc3) did not have an additional effect on the emission spectrum (data not shown). These results suggest that this strategy could be used to find Gluc mutants with different emission spectra suited for different applications.

We then compared the relative activities of different Gluc variants to wt Gluc. 293T cells were co-transfected with an expression plasmid for Fluc and each of the Gluc variants, or wt Gluc. Forty-eight hours later, aliquots of conditioned medium were assayed for Gluc activity. Cell lysates were assayed for Fluc activity, which was used to normalize for transfection efficiency. Gluc5 (S16K, M43V, V159M) showed to have around 2-fold enhanced activity as compared to wt Gluc (Fig. 2a). Further, Gluc4 carrying multiple mutations and all variants with corresponding mutations in the second active domain (Gluc1, Gluc2, Gluc3) showed to have 10-100x less activity as compared to wt (Fig. 2a). These results suggest that these amino acids in the second active domain are important for Gluc activity.

To further characterize these new Gluc variants, we compared their light output to wt Gluc after several substrate injection/read intervals to gain insight into enzymatic turnover rate of these variants. GlucL30S/M43V and GlucL40P with similar activity to wt Gluc (Fig. 2a) showed increasing activities after each substrate injection, reaching a plateau after 2-3 rounds of injections (Fig. 2b). Interestingly, the combination of these two variants (Gluc4) showed even higher turnover rate where the signal continued to increase even after 6 rounds of substrate addition, proving that these mutations are important for this characteristic (Fig. 2b). Gluc3 variant containing the corresponding mutation in the second Gluc active domain also showed higher activities over multiple injections as compared to wt Gluc (Fig. 2b). These properties suggest a higher turnover rate of these Gluc variants.

Next, we determined the bioluminescent reaction kinetics of all Gluc variants. Since our laboratory previously reported on a Gluc variant which catalyzes a stable light output in the presence of TritonX-100 (GlucM43I),²¹ we decided to include this variant and assay all variants in the presence and absence of this detergent. Remarkably, all Gluc variants, with the exception of Gluc5 (S16K, M43V and V159M) and GlucM43I, showed higher stable light output as compared to wt Gluc, which typically catalyzes a flash-type reaction in the absence of the detergent (Fig. 2c). Gluc variants containing corresponding mutations in the second active domain [Gluc1 (L40S and E111S); Gluc3 (L40P and E111P)], having lower relative activity, showed enhanced light output stability. More importantly, the Gluc4 variant carrying multiple mutations which had lower activity and higher turnover rate (Fig. 2a, b)

displayed a glow-type reaction with ~20% loss in signal over 10 minutes without the need of a detergent (Fig. 2c). All variants including the wt Gluc showed higher stable light output in the presence of TritonX-100, however, L40P, L40S, Gluc1, Gluc2, Gluc3 and Gluc4 exhibited the highest stability (Fig. 2c). As expected, the addition of the detergent decreased the light output of all variants and native Gluc by around one log of magnitude²¹ (data not shown).

Figure 2

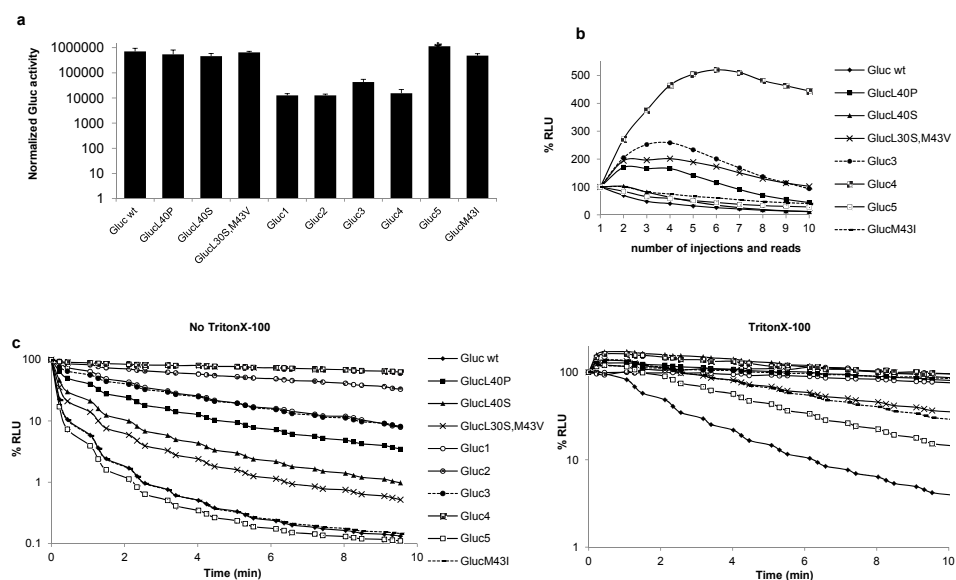


Figure 2. Characterization of different Gluc variants. 293T cells were transfected with different Gluc variants or wt Gluc and 48 hours later, aliquots of the conditioned medium were assayed for different properties. (a) Relative activity of each Gluc variant normalized to Fluc signal, a marker for transfection efficiency. (b) Enzymatic activity over repeated injections of coelenterazine (diluted in PBS) followed by signal acquisition using a plate luminometer with a built-in injector. (c) Bioluminescence light emission kinetics for each Gluc variant was analyzed by adding coelenterazine (diluted in PBS in the presence or absence of TritonX-100) and acquiring photon counts every 14 seconds over a period of 10 minutes using a luminometer.

Since Gluc4 showed to have the most stable light output without the need of TritonX-100, and since detergents could interfere with some assays such as live cell analysis, protein assays, or enzymatic activities, we decided to evaluate this variant for high-throughput applications. Our laboratory developed a drug screening assay

using Gluc as a cell viability marker.¹³ Since Gluc is secreted, aliquots of the conditioned medium can be assayed over time, allowing functional analysis of drug kinetics. In this study, we have used the native Gluc as a viability marker and therefore measurements of one well at a time using a luminometer with a built-in injector was essential due to the flash-type reaction kinetics of this reporter, limiting the numbers of drugs that can be screened.¹³ A Gluc variant that catalyzes a glow-type reaction would be extremely helpful in the field of drug discovery allowing for high-throughput approach without the risk of confounding results due to kinetic instability (wt Gluc) or to interactions with detergents such as TritonX-100 (GucM43I). 293T Cells were infected with a lentivirus vector carrying the expression cassette for wt Gluc, GlucM43I or Gluc4 under the control of CMV promoter. Aliquots of conditioned medium from these cells were transferred to a 384 well plate and read under high throughput conditions by adding coelenterazine (diluted in PBS) to all wells simultaneously and acquiring photon counts for 50 msec/well, resulting in a read-time of <1 minute per plate. As expected, the signal from wt Gluc and GlucM43I variant decreased over the course of measurements of different columns in the 384-well plate, with around 50% signal loss between the first and last columns (Fig. 3a,b and Supplementary Fig. 2). On the other hand, there was no significant signal loss of Gluc4 activity among all columns showing the usefulness of this variant for high-throughput applications (Fig. 3a,b). During this experiment, we noticed that the emission of blue light and the stable light emission of Gluc4 is so sensitive that we can simply visualize it by naked eye in the dark. Further, despite the fact that Gluc4 is 100x less sensitive than wt Gluc, this mutant yields 2 logs of magnitude more light output when expressed in mammalian cells under our assay conditions, as compared to firefly luciferase, the most commonly used mammalian cell reporter (Supplementary Fig. 3a). To confirm that this change in relative activity is not due to simply different amounts of protein production/expression or secretion levels, conditioned medium as well as lysates from cells expressing Gluc4 or wt Gluc were analyzed for Gluc protein level by western blotting using anti-Gluc antibody which showed nearly equal Gluc protein levels being produced and secreted (Supplementary Fig. 3b)

To further evaluate Gluc4 mutant for high-throughput screening, we plated U87 glioma cells stably expressing Gluc4 or wt Gluc in 96-well plates in triplicate. We

deliberately added temozolomide, a known chemotherapeutic agent against glioma, to 12 selected wells that were marked. Seventy-two hours later, 10 μ l aliquots of conditioned medium were transferred to a new 96-well plate, to which coelenterazine was added to all wells simultaneously using an automated injector, followed by Gluc signal acquisition (column by column) using a plate luminometer. The Gluc4 mutant showed signal stability across all columns in the plate. Upon data analysis for positive hits defined as >50% decrease in Gluc activity and therefore cell viability, Gluc4 revealed 100% of the “true” hits (selected wells to which the drug was added) without any false-positives (Fig. 3c,d). On the other hand, the wt Gluc signal decreased across all columns; the last column of the plate had >80% lower signal compared to the first column. In this case, wt Gluc revealed 51 false positive hits, which is more than half of the screened plate (Fig. 3c,d). These data suggests that Gluc4 is a strong useful reporter for high-throughput applications.

Figure 3

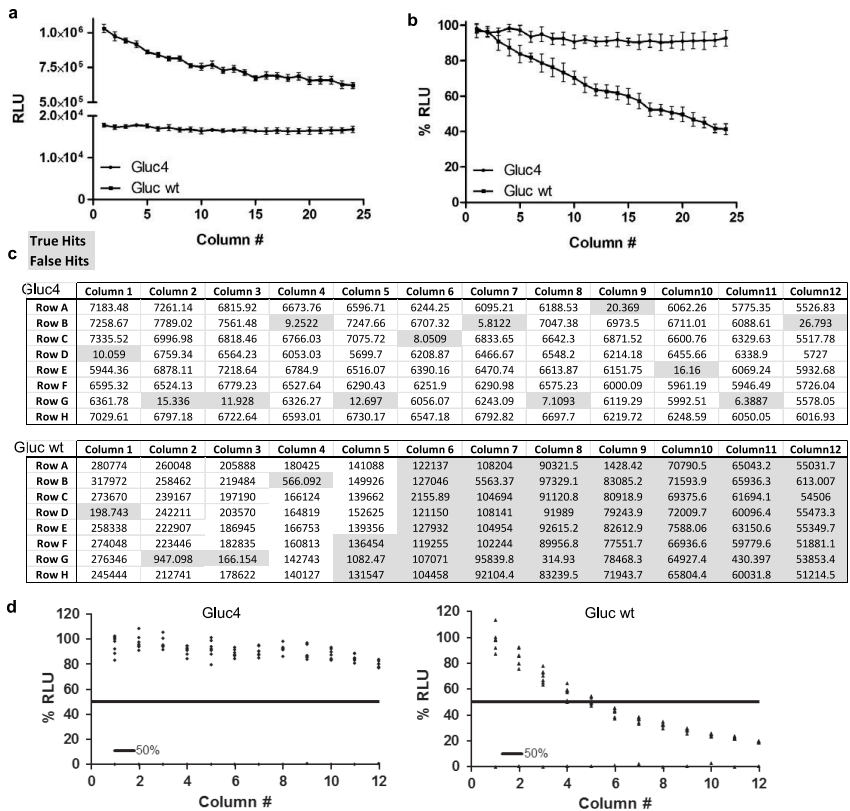


Figure 3. Gluc4 variant displays a glow-type reaction suited for high-throughput applications. (a-b) Aliquots from conditioned medium of cells expressing wt Gluc, or Gluc4 were dispensed in 3 different 384-well plates in a high-throughput fashion followed by addition of coelenterazine (diluted in PBS) to all wells and signal acquisition (50 msec/well) using the Flexstation III device. Data presented in (a) as average raw RLU/column \pm SD and in (b) as average %RLU/column \pm SD in which the first well was set at 100%. (c-d) U87 human glioma cells expressing Gluc4 or wt Gluc were plated in a 96-well plate and 12 wells/plate were marked and treated with 1 mM temozolomide. Seventy-two hours later, 10 μ l aliquots of conditioned medium were transferred to a new 96-well plate to which 45 μ l of coelenterazine was added to all wells simultaneously and signal was acquired using the Dynex luminometer column by column. Raw data is showing in (c) highlighting the “true” hits and false-positives using the Gluc4 or wt Gluc. (d) Scatter plot of each plate in which data are presented as %RLU where the first well of the first column was set at 100%.

In conclusion, using directed molecular evolution, we identified several Gluc variants with a shift in emission spectrum (up to 15 nm) and enhanced light-output stability. We showed that mutations in the second active domain of Gluc could have dramatic effect on light emission intensity, but have advantages with respect to turnover rate

and bioluminescence reaction kinetics. We also discovered a Gluc variant (Gluc4) that catalyzes a glow-type reaction with <20% decrease in signal over 10 min, suited for high-throughput applications. Interesting, all these mutations were not part of the Gluc active core recently discovered by Kim et al.,²³ suggesting another potential Gluc putative core domain. Aside from the given useful improvements of the current repertoire of available Gluc variants, these clones and their mutations shed new light on the structure and biophysical characteristics of Gluc giving insight towards the development of potent Gluc variants for different applications.

ACKNOWLEDGEMENTS

This work was supported by grants from NIH/NINDS P30NS045776 and [1R01NS064983](#) (BAT). Casey Maguire is supported by a Fellowship from the American Brain Tumor Association. We thank John Darga of the Center for Computational and Integrative Biology, Massachusetts General Hospital, for performing the bacteria colony picking and growth of the Gluc plasmid library.

REFERENCES

1. Badr CE, Tannous BA. (2011). Bioluminescence imaging: progress and applications. *Trends Biotechnol.*29(12):624-633.
2. Prescher JA, Contag CH. (2010). Guided by the light: visualizing biomolecular processes in living animals with bioluminescence. *Curr Opin Chem Biol.*14(1):80-89.
3. Weissleder R, Pittet MJ. (2008). Imaging in the era of molecular oncology. *Nature.*452(7187):580-589.
4. Bhang HE, Gabrielson KL, Lattera J, Fisher PB, Pomper MG. (2011). Tumor-specific imaging through progression elevated gene-3 promoter-driven gene expression. *Nat Med.*17(1):123-129.
5. Subramaniam D, Natarajan G, Ramalingam S, Ramachandran I, May R, Queimado L, et al. (2008). Translation inhibition during cell cycle arrest and apoptosis: Mcl-1 is a novel target for RNA binding protein CUGBP2. *Am J Physiol Gastrointest Liver Physiol.*294(4):G1025-1032.
6. Pichler A, Prior JL, Luker GD, Piwnicka-Worms D. (2008). Generation of a highly inducible Gal4-->Fluc universal reporter mouse for in vivo bioluminescence imaging. *Proc Natl Acad Sci U S A.*105(41):15932-15937.
7. Iyer M, Wu L, Carey M, Wang Y, Smallwood A, Gambhir SS. (2001). Two-step transcriptional amplification as a method for imaging reporter gene expression using weak promoters. *Proc Natl Acad Sci U S A.*98(25):14595-14600.
8. Stefan E, Aquin S, Berger N, Landry CR, Nyfeler B, Bouvier M, et al. (2007). Quantification of dynamic protein complexes using Renilla luciferase fragment complementation applied to protein kinase A activities in vivo. *Proc Natl Acad Sci U S A.*104(43):16916-16921.
9. Sacco A, Doyonnas R, Kraft P, Vitorovic S, Blau HM. (2008). Self-renewal and expansion of single transplanted muscle stem cells. *Nature.*456(7221):502-506.
10. Santos EB, Yeh R, Lee J, Nikhamin Y, Punzalan B, Punzalan B, et al. (2009). Sensitive in vivo imaging of T cells using a membrane-bound Gaussia princeps luciferase. *Nat Med.*15(3):338-344.
11. Niers JM, Kerami M, Pike L, Lewandrowski G, Tannous BA. (2011). Multimodal In Vivo Imaging and Blood Monitoring of Intrinsic and Extrinsic Apoptosis. *Mol Ther.*
12. McMillin DW, Delmore J, Weisberg E, Negri JM, Geer DC, Klippel S, et al. (2010). Tumor cell-specific bioluminescence platform to identify stroma-induced changes to anticancer drug activity. *Nat Med.*16(4):483-489.
13. Badr CE, Wurdinger T, Tannous BA. (2011). Functional drug screening assay reveals potential glioma therapeutics. *Assay Drug Dev Technol.*9(3):281-289.
14. Feng Y, Mitchison TJ, Bender A, Young DW, Tallarico JA. (2009). Multi-parameter phenotypic profiling: using cellular effects to characterize small-molecule compounds. *Nat Rev Drug Discov.*8(7):567-578.
15. Bhaumik S, Gambhir SS. (2002). Optical imaging of Renilla luciferase reporter gene expression in living mice. *Proc Natl Acad Sci U S A.*99(1):377-382.
16. Michelini E, Cevenini L, Mezzanotte L, Ablamsky D, Southworth T, Branchini B, et al. (2008). Spectral-resolved gene technology for multiplexed bioluminescence and high-content screening. *Anal Chem.*80(1):260-267.

17. Michelini E, Cevenini L, Mezzanotte L, Ablamsky D, Southworth T, Branchini BR, et al. (2008). Combining intracellular and secreted bioluminescent reporter proteins for multicolor cell-based assays. *Photochem Photobiol Sci.*7(2):212-217.
18. Bovenberg MS, Degeling MH, Tannous BA. (2012). Enhanced Gaussia luciferase blood assay for monitoring of in vivo biological processes. *Anal Chem.*84(2):1189-1192.
19. Tannous BA, Kim DE, Fernandez JL, Weissleder R, Breakefield XO. (2005). Codon-optimized Gaussia luciferase cDNA for mammalian gene expression in culture and in vivo. *Mol Ther.*11(3):435-443.
20. Wurdinger T, Badr C, Pike L, de Kleine R, Weissleder R, Breakefield XO, et al. (2008). A secreted luciferase for ex vivo monitoring of in vivo processes. *Nat Methods.*5(2):171-173.
21. Maguire CA, Deliolanis NC, Pike L, Niers JM, Tjon-Kon-Fat LA, Sena-Esteves M, et al. (2009). Gaussia luciferase variant for high-throughput functional screening applications. *Anal Chem.*81(16):7102-7106.
22. Inouye S, Sahara Y. (2008). Identification of two catalytic domains in a luciferase secreted by the copepod *Gaussia princeps*. *Biochem Biophys Res Commun.*365(1):96-101.
23. Kim SB, Suzuki H, Sato M, Tao H. (2011). Superluminescent variants of marine luciferases for bioassays. *Anal Chem.*83(22):8732-8740.

CHAPTER VII



Codon-optimized *Luciola italica* luciferase variants for mammalian gene expression in culture and *in vivo*

Casey A. Maguire^{1,3}, Johannes C. van der Mijn⁴, M. Hannah Degeling^{1,5}, Danielle Morse¹,
Bakhos A. Tannous^{1,2,3}

¹Neuroscience Center, Department of Neurology, and ²Center for Molecular Imaging Research, Department of Radiology, Massachusetts General Hospital, and ³Program in Neuroscience, Harvard Medical School, Boston, USA. ⁴Department of Neurosurgery, VU Medical Center Cancer Center, 1007 MB Amsterdam, The Netherlands. ⁵University of Leiden, Leiden, The Netherlands

ABSTRACT

Luciferases have proven to be useful tools in advancing our understanding of biological processes. Having a multitude of bioluminescent reporters with different properties is highly desirable. Here, we characterized codon-optimized thermostable green- and red-emitting luciferase variants from the Italian firefly *Luciola italica* for *in vivo* imaging. Using lentivirus vectors to deliver and stably express these luciferases in mammalian cells, we showed that both variants displayed similar levels of activity and protein half-lives as well as similar light-emission kinetics. Further, we characterized the red-shifted variant for *in vivo* bioluminescence imaging. Intramuscular injection of tumor cells stably expressing this variant into nude mice yielded a robust luciferase activity. Light emission peaked at 10 minutes post-D-luciferin injection and retained >60% of signal after 1 hr. Similarly, luciferase activity from intracranially-injected glioma cells expressing the red-shifted variant was readily detected and used as a marker to monitor tumor growth over time. Overall, our characterization of these codon-optimized luciferases lays the groundwork for their further utilization as bioluminescent reporters in mammalian cells.

INTRODUCTION

Bioluminescence imaging (BLI) using luciferase reporters has provided crucial information regarding many biological processes including tumorigenesis, bacterial pathogenesis, and transcription factor activation¹⁻³. The major advantage of BLI compared to endpoint analysis is that it provides real time, non-invasive analysis of *in situ* biological events, thereby giving a complete “picture” of the kinetics of an entire process. Great strides have been made since the seminal study by Contag et al. published in 1995 which was the first demonstration of *in vivo* BLI⁴. For example, as few as 10 cells expressing an optimized American firefly luciferase can be detected in mice⁵. Additional progress has been made by the discovery and codon optimization of the naturally secreted *Gaussia princeps* luciferase, allowing for sensitive detection of *in vivo* biological processes by simple blood sampling⁶. The discovery of luciferases as well as the genetic engineering of existing luciferases

which emit light at longer wavelengths, thus reducing tissue absorption of light, has enhanced the sensitivity of *in vivo* BLI^{7,8,9}.

The luciferase with the most biochemical characterization is from the North American firefly *Photinus pyralis* (Fluc). Fluc catalyzes a two-step reaction in which luciferin is first adenylated through an ATP-dependent mechanism. Next, molecular oxygen is used to oxidize the adenylated intermediate yielding oxyluciferin, a molecule in an excited energy state. Upon decay of excited state oxyluciferin, a photon of light is emitted¹⁰. Due to the high quantum yield of the luminescence reaction, Fluc was pursued as a reporter enzyme. Since its cloning and expression in mammalian cells in 1987¹¹, Fluc has become the “workhorse” of the molecular biology lab as a reporter for gene expression and ATP levels in cells^{12, 13} as well as non-invasive monitoring of *in vivo* processes using bioluminescence imaging technology¹⁴.

Subsequently, other luciferases have been cloned and characterized for bioluminescence imaging in an attempt to increase detection sensitivity as well as dual parameter measurement. Luciferases which catalyze red-shifted light (emission peak >600nm)¹⁵ or mutations of existing luciferases to a red-shifted emission spectra¹⁶ have improved the sensitivity of detection as light absorption by mammalian tissues and hemoglobin decreases greatly above 600 nm¹⁷. *Renilla reniformis* luciferase (Rluc) and *Gaussia princeps* luciferase (Gluc) utilize coelenterazine as a substrate, in contrast to Fluc, and therefore sequential imaging of Fluc and Gluc or Rluc *in vivo* can be used to monitor two different biological processes¹⁸. Recently, the cDNA encoding the green-emitting luciferase from the Italian firefly *Luciola italica* (liFluc) was cloned by Branchini et al. which has 64% amino acid identity with the luciferase from *Photinus pyralis*¹⁹. This luciferase has several advantages over Fluc including thermostability and higher enzyme turnover leading to approximately 2-fold higher light output¹⁹. Further, using standard mutagenesis, a red-shifted variant was characterized²⁰. liFluc has been expressed and purified from bacteria and was used for cell based assays²⁰, however, a codon-optimized variant for mammalian gene expression has not been established for *in vivo* imaging. In the current study, we characterize codon-optimized variants of both the green- and red-emitting liFluc for mammalian gene expression and use the ladder for *in vivo* bioluminescence imaging in small animals.

MATERIALS AND METHODS

Cell culture and reagents. 293T human kidney fibroblasts cells, U87 human glioma cells (both from American Type Culture Collection, Manassas, VA) and Gli36 human glioma cells (kindly provided by Dr. Anthony Capanogni, University of California at Los Angeles, Los Angeles, CA), were maintained in Dulbecco's modified Eagle's medium (DMEM) supplemented with 10% fetal bovine serum (Sigma, St. Louis, MO), 100 U/ml penicillin, and 0.1 mg/ml streptomycin (Sigma), referred to as complete DMEM. All cells were grown at 37 °C in a 5% CO₂ humidified atmosphere.

Lentivirus vector construction. Human codon optimized cDNA variants of both green emitting *Luciola italica* luciferase (G-liFluc) and red emitting (R-liFluc) were kindly provided by Dr. Rampyari Walia (Targeting Systems, El-Cajon, CA). These cDNAs were cloned into a lentivirus vector plasmid, CSCW²¹. Transgene expression in this plasmid is driven by a cytomegalovirus (CMV) promoter with the inclusion of an internal ribosomal entry site (IRES) for co-expression of mCherry red fluorescent proteins to allow for titering and transduction confirmation⁶. Both G-liFluc and R-liFluc coding sequences were PCR-amplified using Pfu polymerase (Agilent technologies, Santa Clara, CA) and the following primers: Forward primer, 5' ATAGCTAGCGATCCATGGAAACAGAAAG3'; reverse primer, 5'TACTCGAGACTACCCACCTGCTTGAGGT 3'. The thermalcycler conditions were 1 cycle of 94°C for 2 min; 30 cycles of 94 °C for 45s, 60 °C for 45s, 72 °C for 90s; 1 cycle of 72 °C for 10 min. The forward primer was synthesized with an NheI site and the reverse with an XhoI restriction site for ligation with similarly-digested CSCW-ImCherry plasmid. Constructs were named CSCW-GliFluc-ImCherry and CSCW-R-liFluc-ImCherry. A lentivirus vector encoding the Gaussia luciferase (Gluc) and the Cerulean fluorescent protein (CFP) separated by an IRES (CSCW-Gluc-ICFP) was described previously²². Lentivirus vectors were produced as described before²¹ and vector titers (transducing units/ml) were determined by performing serial dilutions of vector stocks on 293T cells followed by counting the number of mCherry or CFP positive 293T cells 3 days later using fluorescence microscopy.

Lentivirus vector transduction. For side by side comparison of G-liFluc and R-liFluc luciferases, Gli36 and U87 human glioma cells were engineered to stably express both Gluc and either one of these luciferases. Around 350,000 cells were plated in a 6 well plate. The Next day, cells were first transduced with the CSCW-Gluc-ICFP

lentivirus using a multiplicity of infection (MOI) of 50 in the presence of 10 µg/mL Polybrene in 3 mL. The plate was centrifuged at 1800 rpm for 1 hr at room temperature. Afterwards, cells were cultured overnight. Seventy-two hrs later, the same protocol was applied to transduce the same cells with either CSCW-RliFluc-ImCherry or CSCW-GliFluc-ImCherry. The CFP (a marker for cell number) and mCherry (marker for transduction efficiency) fluorescence intensities in both cell lines was quantified using a FlexStation® 3 microplate reader (Molecular devices, Sunnyvale, CA).

In vitro Gaussia luciferase assay. 10^4 cells/well were plated in a 96 well plate. After 24 h, cells were washed once with 50 µL PBS and lysed on the plate in 50 µL lysis buffer (Targeting systems, El Cajon, CA). From each well, 20 µL cell lysates were transferred to a standard white opaque 96 wells plate for endpoint luminescence measurement using the FlexStation® 3 microplate reader. 50 µL 10 µM coelenterazine in PBS was injected into each well and photon count was measured immediately for 500 ms.

In vitro Luciola italica luciferase assays. A 20 µL aliquot from cell lysates was transferred to a white opaque 96 well plate. 80 µL FLAR-1 Luciferase Assay Kit reagent (Targeting systems, El Cajon, CA) was added and total luminescence was measured for 500 ms.

Luciferin dosing studies. 80 µL of different *D*-luciferin concentrations (Gold biotechnology, St Louis, MO; diluted in PBS containing 2 mM ATP) ranging from 0.5 µM to 50 mM were added into wells containing 20 µL of lysates from Gli36 cells expressing either G-liFluc or R-liFluc. Photon count was acquired for 500 ms using the microplate reader.

Stability of luciferases. 5×10^5 cells plated in a well of a 6 well plate were lysed in 500 µL of cell lysis buffer. A 65 µL aliquot of cell lysates was frozen immediately. Lysates were incubated for 30 min, 1h, 2h, 4h and 6h at 37 °C. In triplicate, 20 µL aliquots from each time point was transferred into an opaque 96 well plate and 80 µL FLAR reagent was injected per well. Luminescence was acquired as above.

Kinetic assays. 20 µL aliquots of lysates from Gli36 cells stably expressing G-liFluc or R-liFluc (10^4 cells lysed in 50 µL) were mixed with 80 µL 830 µM *D*-Luciferin (in PBS containing 2 mM ATP). Luminescence was acquired for 500 ms every 20 seconds for 4 minutes using the microplate reader.

Spectral analysis of G-liFluc and R-liFluc light emission. 80 μL of FLAR reagent was added to 20 μL of cell lysates and light emission was measured using the microplate reader every 10 nm using the device's emission monochromator.

In vivo experiments. All animal experiments were approved by the Massachusetts General Hospital Subcommittee on Research Animal Care. Athymic nude mice were anesthetized with a mixture of Ketamine (100 mg/kg) and Xylazine (5 mg/kg) in 0.9% sterile saline. For intramuscular injection ($n=4$), 3×10^6 (in 25 μL) Gli36 cells expressing R-liFluc and Gluc were mixed with equal volume of MatrigelTM (BD Biosciences, San Jose, CA) and injected using an insulin syringe. For the brain tumor model, 10^5 U87 cells expressing R-liFluc and Gluc (in 1 μL PBS) were intracranially injected in the left midstriatum of nude mice ($n=4$) using the following coordinates from bregma in mm: anterior-posterior +0.5, medio-lateral +2.0, dorso-ventral -2.5. These injections were performed using a Micro 4 Microsyringe Pump Controller (World Precision Instruments, Sarasota, FL) attached to a Hamilton syringe with a 33-gauge needle (Hamilton, Rena, NV) at a rate of 0.2 $\mu\text{L}/\text{min}$.

In vivo bioluminescence imaging. Bioluminescence images were obtained at different time points post-implantation of tumor cells. Mice were anesthetized as above. Initially, 20 μL blood was drawn from the tail vein of each mouse and mixed with 2 μL 20 mM EDTA which was stored on ice until assayed. Mice were then intraperitoneally (i.p.) injected with 150 μL of *D*-luciferin (150 mg/kg body weight). Ten min later, photon count was acquired using a cryogenically-cooled CCD camera for 1 min as described²³. For *in vivo* light emission kinetics, imaging was performed every 5 minutes for 1h, starting immediately upon substrate injection. CMIR-Image software, developed by the Center for Molecular Imaging Research at the Massachusetts General Hospital, was used to process the data and quantify signal intensity. Total bioluminescent signals, representing the sum of 1 minute photon counts, are shown in a pseudo-color photon count manner. Images were fused with a gray-scale white light image to allow anatomic localization.

Gluc blood assay. The Gluc-blood assay was performed as described²⁴. Briefly, 5 μL blood was transferred into a white opaque 96-well plate and 100 μL 100 μM coelenterazine was injected to each well and the total luminescence was acquired for 10 sec using a luminometer (Dynex, Richfield, MN).

RESULTS

Expression of codon-optimized variants of the *Luciola italica* luciferase in mammalian cells

To ascertain the utility of the codon-optimized green- and red-emitting variants of the *Luciola italica* luciferase as mammalian cell reporters, we cloned the cDNA of either variant into a lentivirus vector plasmid. Cells were first transduced with a lentivirus vector encoding *Gaussia princeps* luciferase (Gluc) and the Cyan fluorescent protein expressed using an internal ribosomal entry site (IRES) element (**Fig. 1A & B**). The expression of Gluc and CFP is used as an internal control to normalize for cell number both *in vitro* and *in vivo* as previously described⁶. These cells were then engineered using lentivirus vectors to stably express either the green-emitting G-liFluc or red-shifted R-liFluc as well as the mCherry Red fluorescent protein separated by an IRES element (**Fig. 1A**). mCherry is used as a marker for transduction efficiency for the liFluc construct (**Fig 1B**). Two weeks post-transduction, cells were plated in a 96-well plate. First, the mCherry fluorescence intensity was measured using a microplate reader which showed that Gli36 cells had 1.5-fold higher transduction efficiency with R-liFluc as compared to G-liFluc (**Fig. 1C**). Then, aliquots of lysates from same cells were assayed for Gluc activity to normalize for cell number (**Fig. 1D**). Finally, the same lysates were analysed for liFluc activity. Luciferase activity was 3.6×10^4 RLU for G-liFluc and 4.4×10^4 RLU for R-liFluc (**Fig 1E**). When the liFluc values were normalized to transduction efficiency (mCherry, Fig. 1C) and cell number (Gluc, Fig 1D), we obtained 2.2×10^4 RLU for G-liFluc and 1.2×10^4 RLU for R-liFluc (**Fig. 1F**). This 1.83-fold difference was found to be statistically significant ($P=0.018$).

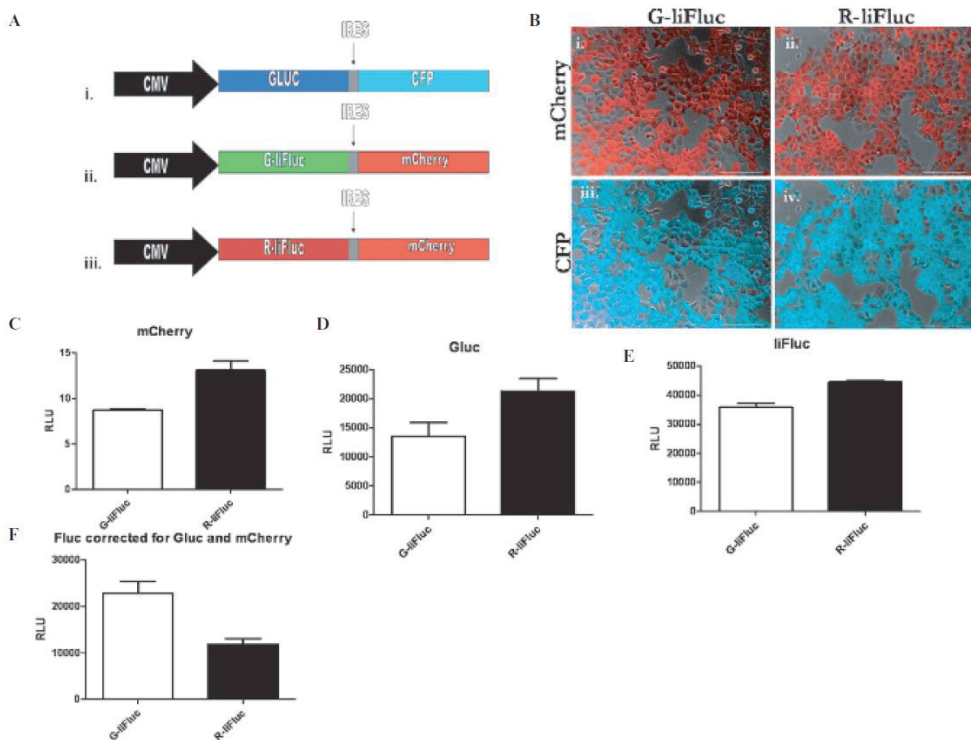


Figure 1. Expression of the codon-optimized *Luciola italica* luciferase green-emitting (G-liFluc) and red-shifted (R-liFluc) variants in mammalian cells. (A) Lentivirus expression cassettes used in this study. Gli36 human glioma cells were first transduced with a lentivirus vector encoding *Gaussia* luciferase (Gluc) and CFP (i.) followed by either G-liFluc (ii.) or R-liFluc (iii.) and mCherry encoding vectors. (B) Confirmation of successful transduction with these vectors using fluorescence microscopy. Shown are overlays of bright field and mCherry fluorescence (i., ii.) and bright field and CFP fluorescence (iii.-iv.). Scale bar, 100 μ m. (C) Transduction efficiency of Gli36 with vectors encoding G-liFluc or R-liFluc was determined by assaying for mCherry fluorescence using a microplate reader. (D) Gluc assay from lysates of same cells using coelenterazine as a substrate. (E) *Luciola italica* luciferase assay on separate aliquot of the same cellular lysates in (D) using ρ -luciferin as a substrate. (F) *Luciola italica* luciferase activity normalized for transduction efficiency (mCherry levels from C) and cell number (Gluc levels from D).

Emission and stability of liFluc variants

We first confirmed the spectrum of light output from G-liFluc and R-liFluc in mammalian cells. As expected, we obtained an emission spectra with a peak at 550 nm and 610 nm for G-liFluc and R-liFluc respectively, which are similar to values reported for non-codon optimized variants purified from bacteria²⁰ (Fig. 2A). Stability

assays were then performed for these variants and were compared to the North American firefly luciferase (Fluc). Both G-liFluc and R-liFluc showed an increased thermostability compared to Fluc (5.3 h and 2 h vs 0.5 h; **Fig. 2B**).

Dose response of green and red-emitting liFluc to *D*-luciferin

To gain insight into the performance of each variant under different substrate concentrations, we carried out a dose response analysis of *D*-luciferin ranging from 1 μ M to 50 mM on lysates from Gli36 cells expressing either liFluc. Both G-liFluc and R-liFluc displayed a similar dose/activity profile, although at lower doses the G-liFluc displayed a substantially higher activity than R-liFluc (**Fig. 2C**). For example at a *D*-luciferin dose of 5 μ M, G-liFluc displayed a 5.1-fold higher RLU value than R-liFluc. This difference was reduced to 1.27-fold at the 0.5 mM dose (**Fig. 2C**). At the higher *D*-luciferin doses of 5 and 50 mM, we observed an apparent inhibition of enzyme activity.

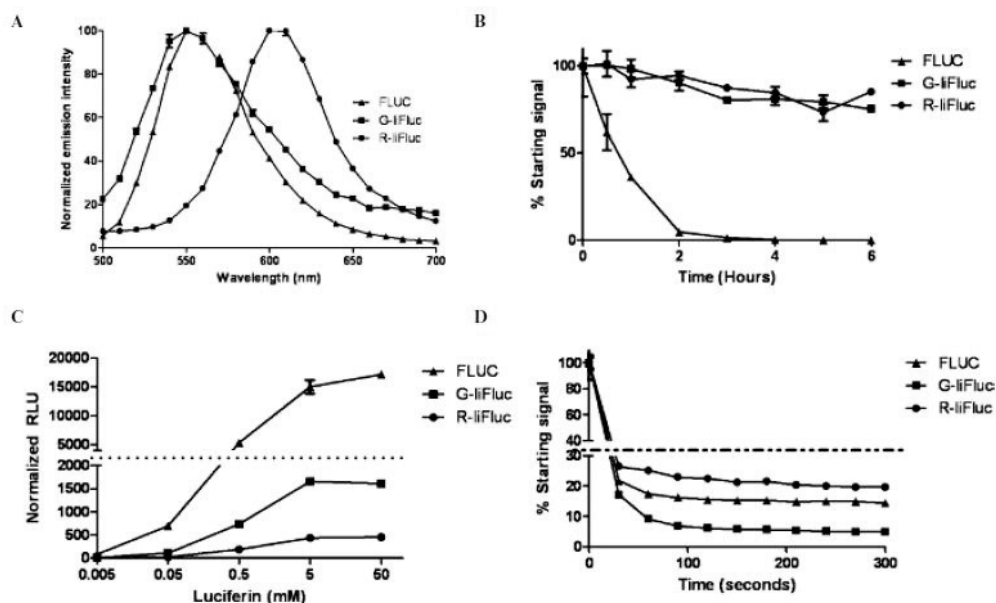


Figure 2. Characterization of *Luciola italica* luciferase activity in mammalian cells. (A) Emission spectra of G-liFluc and R-liFluc and the North American firefly luciferase Fluc. **(B)** *Luciola italica* luciferase stability at 37°C. Lysates from cells expressing either G-liFluc, R-

liFluc or Fluc, were incubated at 37 °C and assayed for luciferase activity at different time points. **(C)** *D*-luciferin dose response of G-liFluc, R-liFluc, and Fluc was assayed on lysates from B.. **(D)** light emission kinetics of liFluc variants. *D*-luciferin was added to a well containing lysates from cells expressing either G-liFluc, R-liFluc or Fluc. Light emission was measured every 30 seconds for 5 minutes.

Light emission kinetics for liFluc variants

Light emission kinetics after substrate *D*-luciferin addition was determined for both G-liFluc and R-liFluc in lysates from cells expressing either luciferases. The relative light units declined to 50% of starting values at 1 minute for G-liFluc and 46 sec for R-liFluc variant (**Fig. 2D**). Interestingly, luminescence signal stabilized for R-liFluc at 2 minutes to 10 minutes post-substrate addition (16% of starting signal) while the luminescence continued to decay for G-liFluc (from 20% to 6%).

In vivo imaging of R-liFluc

Since light of longer wavelengths is known to have much lower absorption by pigmented molecules such as hemoglobin and melanin as well as scattering by mammalian tissues, we characterized the red-shifted *Luciola italica* luciferase R-liFluc for *in vivo* deep tissue bioluminescence imaging. Nude mice were injected into the hamstring with 3×10^6 Gli36 cells expressing R-liFluc. Fourteen-days post-injection, mice were injected intraperitoneally (i.p.) with 150 mg/kg *D*-luciferin and imaged using a cooled CCD camera. Light emission was readily detected from these muscle tissues (4.03×10^5 photons/min; **Fig. 3A**). To determine the optimum acquisition time for imaging R-liFluc in deep tissues, we imaged mice immediately and at 5 min interval for 1 hr after *D*-luciferin injection. Bioluminescence signal was detected immediately after injection and peaked at 10 minutes post-substrate injection (**Fig. 3B**). Signal began to slowly decline at 30 minutes, although never dropped below 48% for the 1 hour duration (**Fig. 3B**).

Having confirmed its utility for imaging in muscle tissues, we next tested R-liFluc as a reporter to image brain tumors, which requires adequate light to pass through 2.5 mm of brain tissue as well as ~1mm of skull. 10^5 U87 glioma cells stably expressing R-liFluc-ImCherry and Gluc-ICFP were injected into the striatum of nude mice. At two and three weeks post injection, mice were anesthetized and blood was collected and assayed for Gluc activity⁶, and then mice were i.p. injected with 150 mg/kg *D*-luciferin and imaged for R-liFluc 10 min later. At two weeks post tumor cells

implantation, luminescence was detected at an average of 1.23×10^3 photons/min (**Fig. 4A**). This signal increase to 8.58×10^3 photons/min at week 3 post tumor injection (**Fig. 4A**) resulting in a 7-fold increase in signal between the two time points proving that R-liFluc can be used as a reporter to monitor biological processes including tumor growth over time. A similar fold increase was observed for Gluc in the tumor as assessed by Gluc-blood assay at the same time points (**Fig. 4B**).

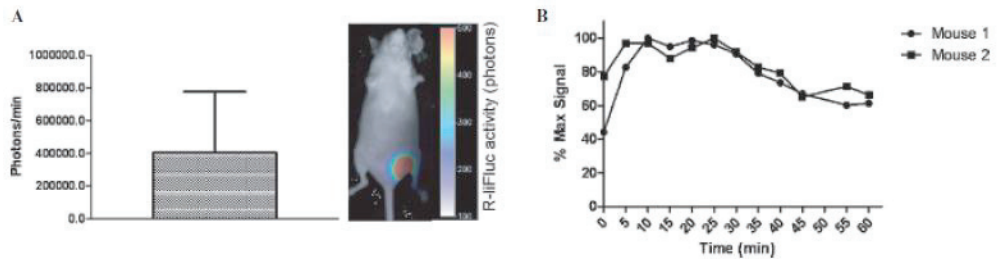


Figure 3. Red-emitting *Luciola italica* luciferase variant for *in vivo* imaging. 3×10^6 Gli36 cells expressing R-liFluc were injected into the hamstring of nude mice. **(A)** Two weeks later, mice were injected i.p with *D*-luciferin (150 mg/kg body weight) and imaged 10 min later using a cooled CCD camera. Signal from tumor was quantified using CMIRimage program. Data shown are mean \pm SD (n=4). **(B)** Light emission kinetics after injection of *D*-luciferin. Same experiment in (A) was repeated but the luciferase activity was acquired immediately and every 5 min for 1 hr post-substrate injection. Data shown from 2 representative animals.

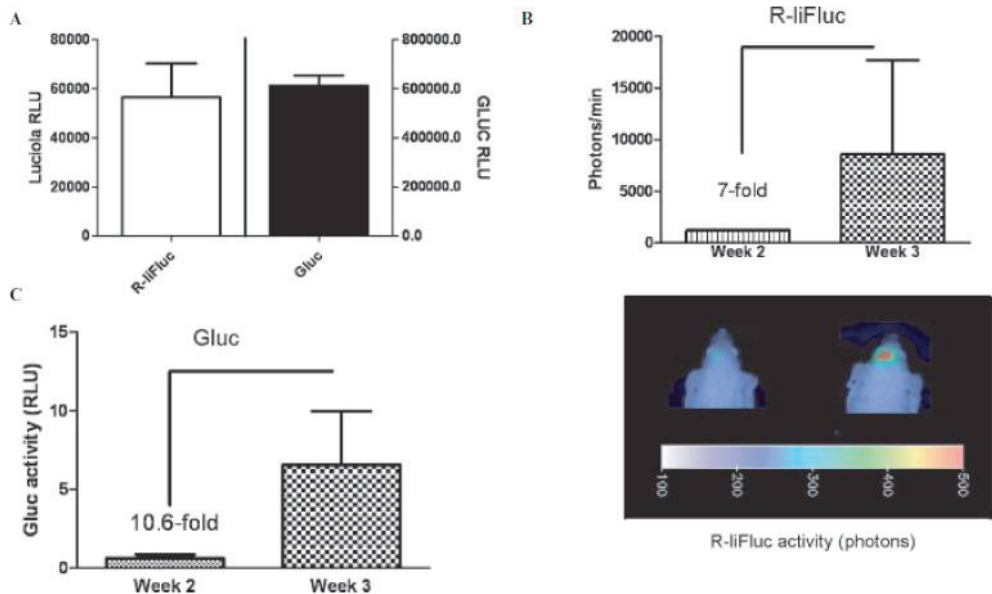


Figure 4. Bioluminescence imaging of brain tumors expressing Red-emitting *Luciola italica* luciferase. A. Luciferase activity from U87 cells stably expressing R-liFluc and Gluc. B. The striatum of nude mice were stereotactically injected with 10^5 U87 human glioma cells expressing both R-liFluc and Gluc. At 2 and 3 weeks post-tumor implantation, mice were intraperitoneally injected with D-luciferin (150mg/kg body weight) and imaged for *Luciola Italica* luciferase activity 10 minutes later using a cooled CCD camera. Intracranial brain tumor associated R-liFluc signal (bottom) as quantified using the CMIR-image program (top). C. Prior to D-luciferin injection, 5uL blood was collected and assayed for Gluc activity after addition of 100uL of 100uM coelenterazine and acquiring photon counts using a luminometer. Data shown are mean +/- SD (n=4).

DISCUSSION

Luciferases catalyze light producing chemical reaction by oxidizing their substrates, luciferin, while emitting photons. This process, known as bioluminescence, is a natural phenomenon found in many lower forms of life including fungi, bacteria, insects and marine cutaneous. The North American firefly luciferase from *Photinus pyralis* (Fluc) is the best characterized luciferase for luminescence applications and has proven invaluable as a biological reporter protein^{25, 26}. Oxidation of *D*-luciferin by Fluc results in a high quantum yield of light emission leading to a sensitive detection. Less than 10^4 molecules of Fluc protein can be detected using a standard luciferase

assay²⁷. However, the yellow-green color of light emission is suboptimal for *in vivo* imaging. Although there is single report of a red-shifted variant of Fluc with enhanced *in vivo* luminescence properties¹⁶, the availability of other luciferases expands the potential of advancing our understanding of biological processes. Our results broaden the characterization of the *Luciola italica* luciferase as a promising biological reporter in mammalian cells. Using green and red-emitting codon-optimized, liFluc variants, we observed a robust luciferase activity in cultured mammalian cells. Additionally, we found that the red-emitting variant was a valuable tool for *in vivo* bioluminescence imaging of tumors in deep tissues.

One important characteristic of luciferases for molecular biological applications is thermostability. For measurement of luciferase activity in cultured cells or tissue homogenates, cells are lysed and the luciferase protein is subject to degradation/inactivation by proteases, pH changes, and temperature fluctuations^{28, 29}. This has implications for storage conditions of samples post cell lysis. We found that both the G-liFluc and R-liFluc variants had a 10 and 4-fold increase in half-life activity compared to Fluc. This may lower the amount of signal decay between sample harvest and freezing/assaying, allowing for higher number of samples to be processed simultaneously. Interestingly, at a lower substrate dose, the green-emitting liFluc had a higher activity than R-liFluc, most likely due to a lower K_M for the green-peaked variant. This characteristic may be desirable for *in vitro* assays in the case that lower substrate concentrations are used.

For a luciferase/luciferin combination to be suited for *in vivo* imaging, they need to overcome certain barriers such as light absorption by pigmented molecules (e.g. hemoglobin and melanin) and scattering by deep tissues. Since most light below 600 nm cannot penetrate mammalian tissues, red-emitting luciferases would be highly beneficial for *in vivo* imaging. The codon-optimized red-emitting liFluc characterized here with a peak emission at 610 nm showed to be a robust tool for imaging tumor cells injected intramuscularly or in the brain of nude mice.

Aside from *in vivo* imaging, having multiple luciferases utilizing the same substrate but yielding different emission properties could be highly useful for multicolor applications using spectral unmixing^{9, 30}. Since the codon-optimized green and red-emitting liFluc variants have a distinct emission maximum, they can be used together to monitor dual biological processes simultaneously. Further, they can be

combined with other luciferases utilizing different substrates, such as *Gaussia* or *Renilla* luciferase, for triple reporter systems²⁰.

In conclusion, we have characterized two human codon-optimized *Luciola italica* thermostable variants for bioluminescence applications in mammalian cells and showed that the red-emitting variant is useful for deep tissue imaging. These variants may be useful alternative luciferases where increased thermostability is desired.

Acknowledgments

This work was supported partly by grants from the National Cancer Institute (P50 CA86355; BT) and the National Institute of Neurological Disorders (P30 NS045776; BT) and the American Brain Tumor Association Fellowship program (CM). We would like to thank Dr. Ralph Weissleder, Director of the Center for Molecular Imaging Research at the Massachusetts General Hospital for the use of the cooled CCD camera.

REFERENCES

1. Klerk, C.P. et al. Validity of bioluminescence measurements for noninvasive in vivo imaging of tumor load in small animals. *Biotechniques* **43**, 7-13, 30 (2007).
2. Badr, C.E. et al. Real-time monitoring of nuclear factor kappaB activity in cultured cells and in animal models. *Molecular imaging* **8**, 278-290 (2009).
3. Andreu, N. et al. Optimisation of bioluminescent reporters for use with mycobacteria. *PLoS One* **5**, e10777.
4. Contag, C.H. et al. Photonic detection of bacterial pathogens in living hosts. *Mol Microbiol* **18**, 593-603 (1995).
5. Rabinovich, B.A. et al. Visualizing fewer than 10 mouse T cells with an enhanced firefly luciferase in immunocompetent mouse models of cancer. *Proc Natl Acad Sci U S A* **105**, 14342-14346 (2008).
6. Wurdinger, T. et al. A secreted luciferase for ex vivo monitoring of in vivo processes. *Nature methods* **5**, 171-173 (2008).
7. Branchini, B.R. et al. Thermostable red and green light-producing firefly luciferase mutants for bioluminescent reporter applications. *Anal Biochem* **361**, 253-262 (2007).
8. Branchini, B.R., Southworth, T.L., Khattak, N.F., Michelini, E. & Roda, A. Red- and green-emitting firefly luciferase mutants for bioluminescent reporter applications. *Anal Biochem* **345**, 140-148 (2005).
9. Gammon, S.T., Leevy, W.M., Gross, S., Gokel, G.W. & Piwnica-Worms, D. Spectral unmixing of multicolored bioluminescence emitted from heterogeneous biological sources. *Anal Chem* **78**, 1520-1527 (2006).
10. Thorne, N., Inglese, J. & Auld, D.S. Illuminating insights into firefly luciferase and other bioluminescent reporters used in chemical biology. *Chem Biol* **17**, 646-657.
11. de Wet, J.R., Wood, K.V., DeLuca, M., Helinski, D.R. & Subramani, S. Firefly luciferase gene: structure and expression in mammalian cells. *Mol Cell Biol* **7**, 725-737 (1987).
12. Greer, L.F., 3rd & Szalay, A.A. Imaging of light emission from the expression of luciferases in living cells and organisms: a review. *Luminescence : the journal of biological and chemical luminescence* **17**, 43-74 (2002).
13. Crouch, S.P., Kozlowski, R., Slater, K.J. & Fletcher, J. The use of ATP bioluminescence as a measure of cell proliferation and cytotoxicity. *J Immunol Methods* **160**, 81-88 (1993).
14. Gross, S. & Piwnica-Worms, D. Spying on cancer: molecular imaging in vivo with genetically encoded reporters. *Cancer Cell* **7**, 5-15 (2005).
15. Li, X., Nakajima, Y., Niwa, K., Viviani, V.R. & Ohmiya, Y. Enhanced red-emitting railroad worm luciferase for bioassays and bioimaging. *Protein Sci* **19**, 26-33.
16. Caysa, H. et al. A redshifted codon-optimized firefly luciferase is a sensitive reporter for bioluminescence imaging. *Photochem Photobiol Sci* **8**, 52-56 (2009).
17. Rice, B.W. & Contag, C.H. The importance of being red. *Nat Biotechnol* **27**, 624-625 (2009).

18. Vilalta, M. et al. Dual luciferase labelling for non-invasive bioluminescence imaging of mesenchymal stromal cell chondrogenic differentiation in demineralized bone matrix scaffolds. *Biomaterials* **30**, 4986-4995 (2009).
19. Branchini, B.R., Southworth, T.L., DeAngelis, J.P., Roda, A. & Michelini, E. Luciferase from the Italian firefly *Luciola italica*: molecular cloning and expression. *Comparative biochemistry and physiology. Part B, Biochemistry & molecular biology* **145**, 159-167 (2006).
20. Michelini, E. et al. Spectral-resolved gene technology for multiplexed bioluminescence and high-content screening. *Analytical chemistry* **80**, 260-267 (2008).
21. Sena-Esteves, M., Tebbets, J.C., Steffens, S., Crombleholme, T. & Flake, A.W. Optimized large-scale production of high titer lentivirus vector pseudotypes. *J Virol Methods* **122**, 131-139 (2004).
22. Badr, C.E., Hewett, J.W., Breakefield, X.O. & Tannous, B.A. A highly sensitive assay for monitoring the secretory pathway and ER stress. *PLoS one* **2**, e571 (2007).
23. Tannous, B.A., Kim, D.E., Fernandez, J.L., Weissleder, R. & Breakefield, X.O. Codon-optimized Gaussia luciferase cDNA for mammalian gene expression in culture and in vivo. *Molecular therapy : the journal of the American Society of Gene Therapy* **11**, 435-443 (2005).
24. Tannous, B.A. Gaussia luciferase reporter assay for monitoring biological processes in culture and in vivo. *Nat Protoc* **4**, 582-591 (2009).
25. Villalobos, V., Naik, S. & Piwnicka-Worms, D. Current state of imaging protein-protein interactions in vivo with genetically encoded reporters. *Annu Rev Biomed Eng* **9**, 321-349 (2007).
26. Zhuang, F. & Liu, Y.H. Usefulness of the luciferase reporter system to test the efficacy of siRNA. *Methods Mol Biol* **342**, 181-187 (2006).
27. Craig, F.F., Simmonds, A.C., Watmore, D., McCapra, F. & White, M.R. Membrane-permeable luciferin esters for assay of firefly luciferase in live intact cells. *Biochem J* **276 (Pt 3)**, 637-641 (1991).
28. Baggett, B. et al. Thermostability of firefly luciferases affects efficiency of detection by in vivo bioluminescence. *Mol Imaging* **3**, 324-332 (2004).
29. Thompson, J.F. et al. Mutation of a protease-sensitive region in firefly luciferase alters light emission properties. *J Biol Chem* **272**, 18766-18771 (1997).
30. Michelini, E. et al. Combining intracellular and secreted bioluminescent reporter proteins for multicolor cell-based assays. *Photochem Photobiol Sci* **7**, 212-217 (2008).

CHAPTER VIII



A simple and sensitive assay for mycoplasma detection in mammalian cell culture

M. Hannah Degeling^{1,2,3}, M. Sarah S. Bovenberg^{1,2,3}, Casey A. Maguire¹ and Bakhos A. Tannous^{1,2}

¹Experimental Therapeutics and Molecular Imaging Laboratory, Neuroscience Center, Department of Neurology, ²Program in Neuroscience, Harvard Medical School, Boston, MA 02114 USA. ³Department of Neurosurgery, Leiden University Medical Center, Leiden, The Netherlands. ⁴Neuro-oncology Research Group, Department of Neurosurgery, VU Medical Center, Cancer Center Amsterdam, 1007 MB Amsterdam, The Netherlands. ⁵Faculty of Natural and Applied Sciences, Notre Dama University, Barsa, Lebanon.

ABSTRACT

Mycoplasma contamination in mammalian cell cultures is often overlooked yet is a serious issue, which can induce a myriad of cellular changes leading to false interpretation of experimental results. Here we present a simple and sensitive assay to monitor mycoplasma contamination (mycosensor) based on degradation of the *Gaussia* luciferase reporter in the conditioned medium of cells. This assay proved to be more sensitive as compared to a commercially available bioluminescent assay in detecting mycoplasma contamination in seven different cell lines. The *Gaussia* luciferase mycosensor assay provides an easy tool to monitor mammalian cells contaminants in a high-throughput fashion.

INTRODUCTION

Mycoplasmas, in the class mollicutes, are the smallest free-living organisms known. Small size combined with the absence of a rigid cell wall allows them to pass through most bacterial filters making them common pathogens in mammalian cell culture. Many contaminations go unnoticed, as there are often no overt signs of mycoplasma presence. This is in contrast to fungal or bacterial contamination where changes such as media pH, turbidity, odor, and direct microscopic visualization of organisms are observed. Mycoplasma contamination rates have been reported to be between 15-35% and could be as high as 70%¹⁻³ and are resistant to commonly used antibiotics such as Penicillin and Streptomycin. Several antibiotics which are known to kill mycoplasma are mostly effective in the extracellular media with intracellular mycoplasmas being somewhat sequestered from drugs¹. The effect of mycoplasma contamination depends on the particular species of mycoplasma as well as the contaminated cell type. Whereas some species may have no apparent effect on cell function, many others can produce severe cytopathic changes³. Due to a competition with their host cells for medium nutrients, mycoplasma can lead to significant changes in cell metabolism, proliferation, gene expression and function, leading to false data interpretation^{2,4-7}.

The ideal detection method for mycoplasma contamination would be simple to perform, sensitive, specific, rapid and inexpensive and can be used to test numerous cell cultures simultaneously and on a regular basis. Unfortunately, current mycoplasma assays have some but not all of these characteristics. For instance, classical microbiology culture assays are lengthy and can be unreliable due to the fastidious culture requirements for some species⁸. Polymerase chain reaction (PCR)-based detection of mycoplasma-specific nucleic acids is known to be the most reliable assay, however it is complex, time consuming and suffers from false positive and negative results if performed inadequately⁹. Other assays include fluorescent DNA staining, enzyme-linked immunosorbent assays and immunoblotting, with each having significant drawbacks¹⁰⁻¹².

Here, we describe a simple assay to monitor mycoplasma contamination in mammalian cell cultures based on degradation of the *Gaussia* luciferase (Gluc) reporter in the conditioned medium. This assay proved to be more sensitive in detecting mycoplasma as compared to a commercially available bioluminescent-based assay and is amenable to high-throughput applications.

EXPERIMENTAL SECTION

Cell culture. 293T human kidney fibroblast cells, HeLa human cervix adenocarcinoma cells and U87 human glioma cells were obtained from American Type Culture Collection (Manassas, VA). Gli36 human glioma cells were a kind gift from Dr. Anthony Capanogni, UCLA, CA. GBM11/5 and GBM20/3 glioblastoma cells were kindly provided from Dr. Xandra Breakefield, Massachusetts General Hospital, Boston, MA. MDA-MB-231 were obtained from ATCC. All cells were cultured in high glucose Dulbecco's modified Eagle's medium (Invitrogen, Carlsbad, CA) supplemented with 10% fetal bovine serum (FBS; Sigma, St Louis, MO) and 100 U/ml penicillin, 100 µg/ml streptomycin (Invitrogen) in a humidified atmosphere supplemented with 5% CO₂ at 37°C. 293T cells were engineered to stably express the naturally secreted Gluc by infecting these cells with a lentivirus vector expressing Gluc and GFP under the control of CMV promoter at a multiplicity of infection of 10

transducing units/cell in the presence of 10 µg/ml Polybrene® (Sigma) as we previously described¹³.

Standard mycoplasma contamination assays. The status of mycoplasma contamination of cultured cells was determined by MycoAlert® (Lonza Rockland, Rockland, ME) and where indicated by PCR PromoKine Mycoplasma Test KIT I/C (PromoCell, Heidelberg, Germany) according to the manufacturer's standard protocol. Mycoplasma contamination of cells was established by transferring media from cells which were tested positive by both MycoAlert® and PCR PromoKine to clean cells. Cells were intentionally contaminated 3 days prior to use in most experiments unless otherwise stated. Mycoplasma contamination status was monitored on a weekly basis for all cells using Lonza MycoAlert®. Cells treated with Plasmocin™ (InvivoGen, San Diego, CA) were cultured for 2 weeks in the presence of this drug according to the manufacturer's instructions, followed by 1 week without the drug and confirmed to be mycoplasma negative using MycoAlert®.

Recombinant Gluc protein. Recombinant Gluc protein was purified from bacterial extracts using a 6-histidine tag as we previously described¹⁴. Enzyme purity was determined using Commassie staining of purified Gluc after being resolved on SDS-PAGE Gel.

Gluc mycoplasma sensor assay. 1×10^5 mycoplasma clean or contaminated cells were plated in a 24 well plate. 16-24 h later, conditioned medium from cells expressing Gluc (previously aliquoted and frozen) or purified Gluc (35 ng/ml) was added to the media of these cells. Immediately following mixing Gluc with the media on these cells (time 0h) and 24 h later, 50 µl aliquots were collected and frozen at -80 °C. Twenty µl of these samples (in duplicates) were then transferred into a black 96 well microtiter plate (Greiner bio-one, Frickenhausen, Germany) and assayed for Gluc activity after the addition of 80 µl 20 µM coelenterazine (Nanolight, Pinetop, AZ) and acquiring photon counts for 10 sec using the Dynex MLX microtiter plate luminometer (McKinley Scientific, Sparta, NJ). Gluc stability is calculated as the RLU at time point B (e.g. 24 h)/ RLU at time point A (e.g. zero h). For the cell-free assay (Fig. 2a), conditioned media was removed from cells and cell debris removed by a 5-minute centrifugation at 300 x g. Cell-free media was then mixed in a 1:1 ratio with

Gluc-containing media and aliquots of media were collected at several time points before performing the Gluc bioluminescence assay.

Western blot analysis. Twelve microliter of conditioned medium from mycoplasma positive and negative cells containing Gluc were electrophoresed on 4-12 % gradient SDS-polyacrylamide gels (NuPAGE Bis-Tris, Invitrogen) and transferred to nitrocellulose membranes (Bio-Rad). Blots were stained with Ponceau to verify equal protein loading and blocked overnight at 4 °C using 10% non-fat dry milk in TBS-T. The membrane was then incubated with polyclonal rabbit anti-Gluc primary antibody (Nanolight technology, Pinetop, AZ) diluted 1:2000 in 2% milk/TBS-T for 1h at room temperature followed by washing using TBS-T. The blot was incubated with horseradish peroxidase (HRP) conjugated secondary anti-rabbit antibody (1:10,000; GE Healthcare; Little Chalfontbuckinghamshire, UK). Blots were developed using SuperSignal West Pico Chemiluminescent Substrate™ (Pierce, Rockford, IL) followed by exposure to HyBlot CL autoradiography film (Denville Scientific, South Plainfield NJ).

Purified mycoplasma experiments. The following mycoplasma species were purchased from Leibniz Institute DSMZ-German Collection of Microorganisms and Cell Cultures (Braunschweig, Germany): *Acholesplasma laidlawii*, *Mycoplasma arginini*, *Mycoplasma fermentans*, *Mycoplasma hominis*, *Mycoplasma hyorhinitis*, and *Mycoplasma orale*. Lyophilized mycoplasma pellets were sterilely rehydrated for 30 minutes in 500 µl of cell culture media. Next, 50 µl was mixed with 3 ml of complete cell culture media and transferred to a 10 cm² tissue culture well containing 3x10⁵ Gli36 cells. Successful mycoplasma growth was determined by Lonza MycoAlert® at 10 days post-infection. Cells were then plated into 24 well plates and mixed with Gluc-containing media and Gluc stability was calculated from 0 h and 72 h time points.

DNA sequence analysis of mycoplasma in contaminated media. Conditioned cell culture media (1.5 ml) from a contaminated HeLa culture was centrifuged at 500x g to remove cellular debris and then 15,000x g for 15 minutes to pellet mycoplasma. The pellet was resuspended in 100 µl of nuclease-free water and

mycoplasma DNA was amplified using PromoKine PCR Mycoplasma test kit I/C. The PCR reaction was desalted using Qiagen gel extraction columns (Qiagen, Valencia, CA) and specific amplification of the mycoplasma-specific PCR product was confirmed by agarose gel electrophoresis and ethidium bromide staining. The PCR product (~270 b.p.) was ligated into a subcloning plasmid (PCR®4-TOPO®) using the TOPO TA Cloning kit for Sequencing (Invitrogen) and transformed into electrocompetent DH10B bacteria (Invitrogen). Single bacteria colonies were isolated, cultured and plasmid DNA was purified using a QIAprep Miniprep kit (Qiagen). DNA sequencing was performed at the Massachusetts General Hospital DNA core facility using M13 forward and M13 reverse primers provided in the TOPO TA Cloning kit. The nucleotide sequence of each clone was compared to the DNA database on the National Center for Biotechnology Information website using basic local alignment search tool (BLAST®).

RESULTS AND DISCUSSION

We incidentally observed that the bioluminescent signal in conditioned media of different cell types expressing the naturally secreted *Gaussia* luciferase (Gluc)¹⁵ varied in stability over time (originally reported to be ~6 days in media¹³). Further analysis using commercially available tests revealed that cells with a decreased Gluc-catalyzed bioluminescent signal were contaminated with mycoplasma, while those with a more stable signal were mycoplasma-free. To further explore this phenomenon, we determined the stability of Gluc activity added to conditioned medium of seven different cell types. Initially, we confirmed that these cell lines were mycoplasma-free using both PCR and bioluminescence-based commercially available assays (see Experimental Section). Next, each cell line was divided into two groups in which one was maintained in mycoplasma-free environment and the other intentionally infected with mycoplasma-contaminated tissue culture media. Gluc-containing conditioned medium (from mycoplasma negative cell cultures) were added to these cells and the Gluc activity was measured immediately and twenty-four hours later. A decrease in Gluc signal (2-30 fold; $p < 0.0005$) was observed only in mycoplasma-contaminated cells as compared to mycoplasma-free cells (Fig. 1a).

To investigate the means by which Gluc enzymatic activity declines over time in mycoplasma-contaminated cells, we analyzed Gluc protein levels immediately and 24 h post-transfer of Gluc-containing medium on three mycoplasma-free and positive cells by Western blotting. While the level of Gluc protein remained stable in conditioned medium from mycoplasma-free cells over 24 hours, Gluc protein was undetectable in mycoplasma-contaminated conditioned medium from the same cell type (Fig. 1b). Equal loading of media was confirmed by Ponceau staining of transferred proteins (Supplementary Fig. 1). These data indicate that the decline in Gluc activity over time in mycoplasma-contaminated cells is likely caused by protease degradation of Gluc and not another mechanism of enzymatic inhibition.

To extend these findings and develop an assay to detect mycoplasma contamination (mycosensor), we purified 6xHistidine-tagged recombinant Gluc from bacteria and used it on 293T, U87, and HeLa cells. Recombinant Gluc (35 ng/ml) was added to cultured medium of mycoplasma-free and contaminated cells (1×10^5 cells plated in a 24 well plate) and the Gluc activity was analyzed immediately and twenty-four hours later in an aliquot of the conditioned medium. Again, a significant (8-100 fold; $p < 0.0005$) decrease in Gluc activity was observed only in mycoplasma-contaminated cells and not in uncontaminated cells confirming that recombinant Gluc can be used as a reporter to monitor mycoplasma contamination in mammalian cells (Fig. 1c).

In order to verify that the mycoplasma strain(s) we are using are one of the six most commonly (90-95%) found in contaminated mammalian cells¹, we performed PCR using primers specific to a region of DNA within the 16S rRNA operon coding region of these strains on U87, 293T, and HeLa cell lines and analyzed them by agarose gel electrophoresis. Specific bands of approximately 250 bp were observed in all mycoplasma-contaminated cultures while no bands were observed in negative cells (Fig. 1d). To ascertain which mycoplasma strain(s) were in our cultures, the PCR products were cloned into a bacterial plasmid and 10 individual clones were sequenced and their sequences were compared to entries in the public nucleotide database. Six clones aligned with 100% homology to *Acholeplasma laidlawii*, three clones aligned with sequence data from *Mycoplasma bovis genitalium*, and one clone which had highest sequence identity aligned with *Mycoplasma faucium*. This analysis indicated that our contaminated cell culture contained a mixture of

mycoplasma species, with the highest represented clone (*A. laidlawii*) being a common cell culture contaminant.

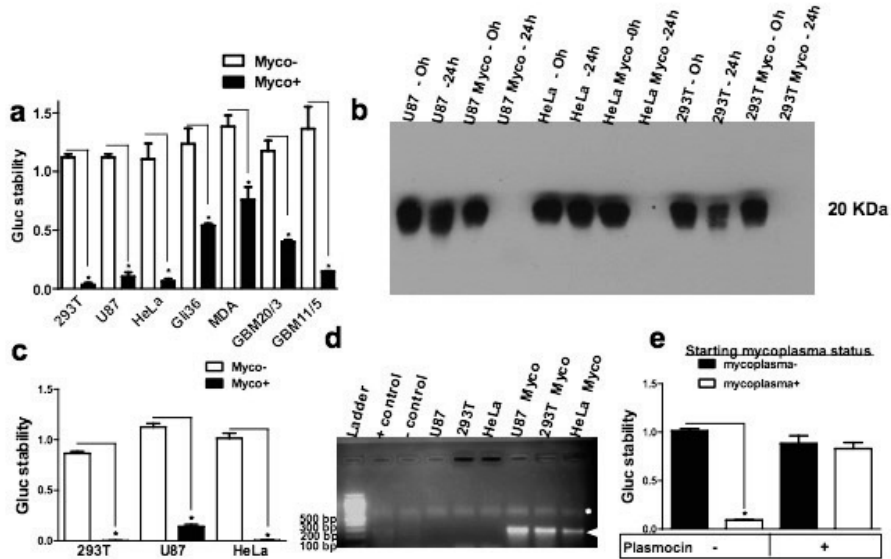


Figure 1. *Gaussia* luciferase (Gluc) reporter as a measure of mycoplasma contamination in mammalian cell culture. (a-b) conditioned medium from cells expressing Gluc were added on different mycoplasma clean or contaminated cells (1×10^5 cells plated in a 24-well plate) and the Gluc activity was detected immediately (0 h) and 24 h later either using a luminometer after addition of coelenterazine (a) or by Western blot analysis using anti-Gluc antibody and horse radish peroxidase-conjugated secondary antibody (b). (c) Purified recombinant Gluc (35 ng/ml) was added to mycoplasma positive or negative cells and Gluc activity was detected immediately and 24 h later using a luminometer. (d) A PCR assay, which specifically detects the most common strains of mycoplasma, was performed on all cell lines used. The smaller band (265-278 b.p., arrow head) results from the amplification of mycoplasma DNA. The larger band (479 b.p., asterisk) is an internal control indicating successful PCR amplification; it is not mycoplasma-specific. (e) Mycoplasma positive or negative cells were treated with Plasmocin for two weeks or left untreated. Three weeks post-treatment, a subculture of these cells was assayed using the Gluc mycoplasma assay. Activity data are presented as the average (from 3 independent experiment) of RLU ratios of 24 h over 0 h \pm standard deviation (* $P < 0.005$).

As the sequencing data revealed that our culture media was contaminated with at least three different types of mycoplasma, the decline in Gluc signal observed in the mycosensor assay could be due to one or more of these species. To ascertain that

the mycosensor assay is applicable for detection of individual and different mycoplasma species, we infected separate wells of uncontaminated Gli36 with three species of mycoplasma commonly found in cell culture contaminations (*Mycoplasma fermentans*, *Mycoplasma hominis*, and *Mycoplasma orale*). Infected cells were incubated with mycoplasma for several days. The presence of mycoplasma was initially confirmed using the MycoAlert® test. Next, cells were plated and the Gluc mycosensor assay was performed. Calculating Gluc stability from the 0 h and 72 h time points revealed that the Gluc mycosensor assay detected all three types of mycoplasma (Table 1). The decline in Gluc sensitivity ranged from 14% (*M. fermentans*) to 81% (*M. orale*), with *M. hominis* in between at 28% decline.

Table 1. Gluc Mycosensor Assay Detection of Purified Strains of Mycoplasma

mycoplasma strain	Gluc mycosensor assay ^a	MycoAlert assay
uncontaminated cells ^b	–	–
<i>Mycoplasma fermentans</i>	+	+
<i>Mycoplasma hominis</i>	+	+
<i>Mycoplasma orale</i>	+	+

^aA sample was considered to be mycoplasma positive when the Gluc signal declined by a statistically significant amount at 72 h as compared to time zero. ^bCells used were Gli36 human glioma cells. All mycoplasma strains in Table 1 were cultured in these cells.

To further confirm that the Gluc degradation was caused by mycoplasma, we treated both contaminated and uncontaminated 293T cell cultures with a well described anti-mycoplasma agent that contains both a macrolide and a quinolone (Plasmocin™). We also maintained the original mycoplasma-free or contaminated 293T cells without drug treatment. Three weeks later, the MycoAlert® mycoplasma assay was performed which showed the successful treatment of these cells (i.e. the treated cells tested negative for mycoplasma). The Gluc mycosensor assay was then performed as above. As expected, a significant decrease in Gluc activity over 24 h was observed in conditioned medium from contaminated/non-treated cells compared to mycoplasma-free cells (Fig. 1e; P<0.0001). More importantly, the anti-

mycoplasma treatment of contaminated cells restored Gluc stability to levels similar to mycoplasma-free cells showing that this assay can be used to monitor response of mycoplasma to different treatments. These results also confirm that the Gluc decline in these cells is indeed linked to mycoplasma contamination and not other cell culture artifacts.

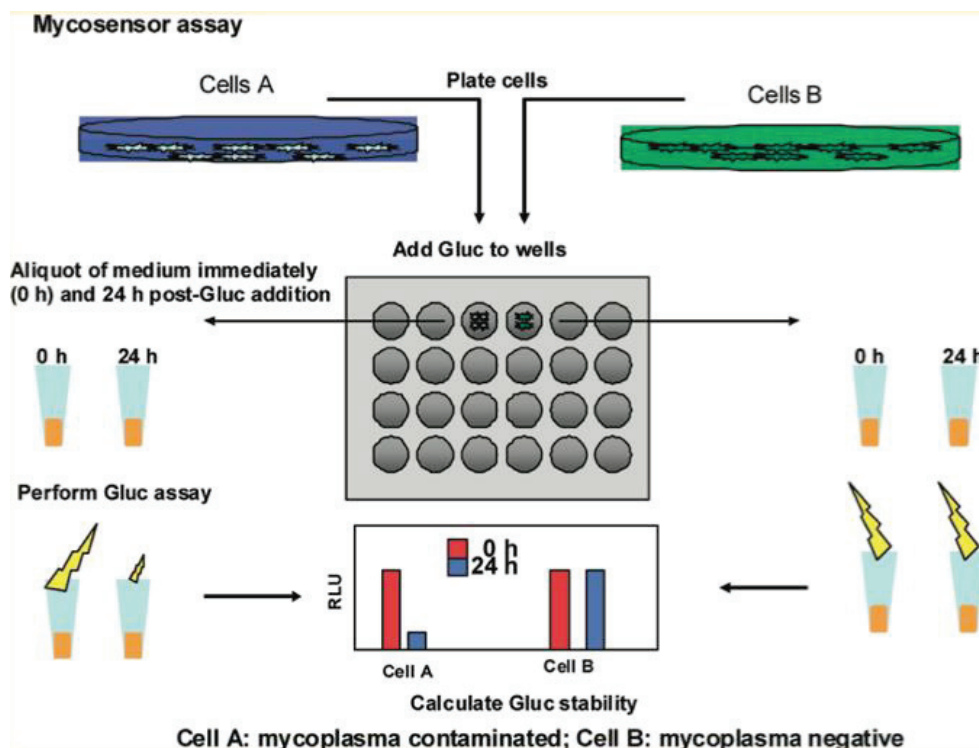


Image 1. Setup of the mycoplasma detection assay

As many mycoplasma are found in the extracellular conditioned media, we performed the Gluc mycoplasma assay in a simpler cell-free format. Conditioned medium was obtained from either mycoplasma-free or mycoplasma-contaminated HeLa cells and mixed with purified recombinant Gluc and activity was detected at different time points as above. As expected, no decline in Gluc activity was detected in medium from mycoplasma-free cells while a 38%, 81%, and 91% decline in Gluc activity was observed in medium from mycoplasma contaminated cells at 24 h, 48 h, and 72 h post-Gluc addition, respectively (Fig. 2a).

To evaluate the optimum time to perform the Gluc mycoplasma assay, highly-contaminated and non-contaminated 293T cells were plated in a 24-well plate and incubated with recombinant Gluc as above. Immediately and at different time points, the Gluc activity was measured on an aliquot of the conditioned medium. A linear decrease in Gluc activity was observed over time showing that highly-mycoplasma contaminated cells can be evaluated within one hour of incubation, being most sensitive at 24 hours (Fig. 2b).

To determine the linearity of Gluc mycosensor with respect to contaminated cell number, different amounts of mycoplasma-contaminated 293T cells were plated and analyzed using purified recombinant Gluc as above. Gluc stability was inversely proportional to cell number. The highest decline in activity over 24 h was observed with the highest concentration of cells (2×10^5 cells, 50-fold), followed by 1.0×10^5 cells (7-fold) and 5.0×10^4 cells (1.5-fold; Fig. 2c). No decline was observed at the lowest number of plated cells (1.0×10^4). These data indicate that at least 5.0×10^4 contaminated cells are required for the Gluc mycoplasma assay under the tested conditions.

To compare the sensitivity of our Gluc mycosensor to a commonly used commercially available bioluminescent-based assay (Lonza MycoAlert®), we performed dilutions of mycoplasma contaminated conditioned medium and added them to clean 293T cells. For a negative control, mycoplasma free 293T cells were used. One day post-contamination, equal amounts of cells were plated in a 24 well plate and recombinant Gluc was added to their conditioned medium 24 hrs later. At different time points (24, 48 and 72 hours), aliquots of conditioned medium were either assayed for Gluc activity or using the commercially available bioluminescent assay (Lonza MycoAlert®). For the Gluc-based mycoplasma assay, a significant decrease in Gluc activity was observed at all dilutions and all time points when compared to the respective negative control sample (Fig. 2d). In contrast, the commercially available assay was not able to detect any of the contaminated cells at the highest dilution (1:1600) at any of the time points (Fig. 2d, using a cut off of 2 as per manufacturer's instructions). This assay did detect mycoplasma lower dilutions of 1:200 (48h and 72h) and 1:800 (only at 72 h). These results indicate that the Gluc

mycoplasma assay is much more sensitive in detecting mycoplasma contamination and at earlier time point compared to the commonly used bioluminescent assay.

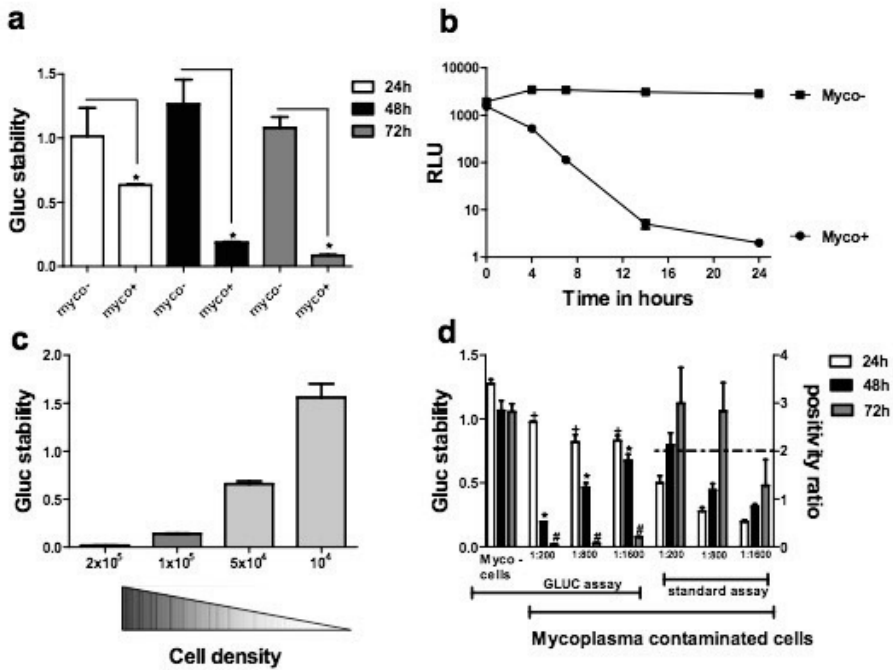


Figure 2. Gluc mycosensor assay optimization and sensitivity comparison. (a) Cell-free conditioned medium from mycoplasma free or contaminated HeLa cells were incubated with recombinant Gluc (35 ng/ml) and assayed immediately (0 h) and 24 h, 48 h, and 72 h later for Gluc activity using a luminometer. (b) Mycoplasma contaminated and non-contaminated 293T cells were plated in a 24 well plate and incubated with recombinant Gluc. Immediately (time zero) and at different time points, an aliquot of the conditioned medium were assayed for Gluc activity. (c) Recombinant Gluc was added to different amounts of cells plated in a 24 well plate. Immediately and 24 h later, aliquots of conditioned medium were assayed for Gluc activity. (d) Mycoplasma contaminated conditioned medium were diluted (1:200, 1:800, 1:1600) and added to clean 293T cells, which were plated the next day in a 24 well plate. Twenty-four h later, recombinant Gluc was added to each well. Immediately and at different time points, aliquots of conditioned medium were assayed for mycoplasma contamination using both the Gluc mycosensor assay and the commercially available MycoAlert® bioluminescent-based assay. The left y-axis corresponds to the Gluc assay results and the right y-axis corresponds to the commercially available assay results.

A cutoff ratio of 2 for mycoplasma contamination using the commercially available assay was used as per manufacturer's instructions.

In conclusion, we have developed a facile and sensitive assay for detection of mycoplasma contamination in mammalian cell cultures using *Gaussia* luciferase. Either conditioned medium from uncontaminated cells expressing Gluc or purified recombinant Gluc (which is commercially available) can be used for mycoplasma detection, making this assay simple and cost-effective. While the Gluc mycosensor assay detected mycoplasma from three separate types of mycoplasma, it remains to be seen if it can detect all strains of mycoplasma commonly found as cell culture contaminants. As recommended by Young *et al.*, screening of mycoplasma should be performed using two independent techniques to reduce the rate of false positives or false negatives⁸. We recommend using the Gluc mycosensor assay for screening purposes followed by PCR-based detection (which directly detects mycoplasma genomic DNA) for confirmational analysis. Since mycoplasma contamination degrades Gluc in the conditioned medium of cells, it could lead to false data interpretation when using Gluc as a reporter. These observations highlight the need for strict and frequent monitoring of mycoplasma contamination of all mammalian cell cultures.

REFERENCES

- 1 Drexler, H. G. & Uphoff, C. C. Mycoplasma contamination of cell cultures: Incidence, sources, effects, detection, elimination, prevention. *Cytotechnology* **39**, 75-90, doi:10.1023/A:1022913015916 (2002).
- 2 Hay, R. J., Macy, M. L. & Chen, T. R. Mycoplasma infection of cultured cells. *Nature* **339**, 487-488, doi:10.1038/339487a0 (1989).
- 3 Rottem, S. & Barile, M. F. Beware of mycoplasmas. *Trends Biotechnol* **11**, 143-151 (1993).
- 4 Logunov, D. Y. *et al.* Mycoplasma infection suppresses p53, activates NF-kappaB and cooperates with oncogenic Ras in rodent fibroblast transformation. *Oncogene* **27**, 4521-4531, doi:onc2008103 [pii] 10.1038/onc.2008.103 (2008).
- 5 Namiki, K. *et al.* Persistent exposure to Mycoplasma induces malignant transformation of human prostate cells. *PLoS One* **4**, e6872, doi:10.1371/journal.pone.0006872 (2009).
- 6 Zhang, S. *et al.* Mycoplasma fermentans infection promotes immortalization of human peripheral blood mononuclear cells in culture. *Blood* **104**, 4252-4259, doi:10.1182/blood-2004-04-1245 2004-04-1245 [pii] (2004).
- 7 Zinocker, S. *et al.* Mycoplasma contamination revisited: mesenchymal stromal cells harboring Mycoplasma hyorhinis potently inhibit lymphocyte proliferation in vitro. *PLoS One* **6**, e16005, doi:10.1371/journal.pone.0016005 (2011).
- 8 Young, L., Sung, J., Stacey, G. & Masters, J. R. Detection of Mycoplasma in cell cultures. *Nat Protoc* **5**, 929-934, doi:nprot.2010.43 [pii] 10.1038/nprot.2010.43 (2010).
- 9 Uphoff, C. C. & Drexler, H. G. Detection of mycoplasma in leukemia-lymphoma cell lines using polymerase chain reaction. *Leukemia* **16**, 289-293, doi:10.1038/sj.leu.2402365 (2002).
- 10 Kotani, H. & McGarrity, G. J. Rapid and simple identification of mycoplasmas by immunobinding. *J Immunol Methods* **85**, 257-267 (1985).
- 11 Masover, G. K. & Becker, F. A. Detection of mycoplasmas in cell cultures by fluorescence methods. *Methods Mol Biol* **104**, 217-226, doi:10.1385/0-89603-525-5:217 (1998).
- 12 Schmitt, M. & Pawlita, M. High-throughput detection and multiplex identification of cell contaminations. *Nucleic Acids Res* **37**, e119, doi:gkp581 [pii] 10.1093/nar/gkp581 (2009).
- 13 Wurdinger, T. *et al.* A secreted luciferase for ex vivo monitoring of in vivo processes. *Nature methods* **5**, 171-173, doi:10.1038/nmeth.1177 (2008).
- 14 Maguire, C. A. *et al.* Gaussia luciferase variant for high-throughput functional screening applications. *Analytical chemistry* **81**, 7102-7106, doi:10.1021/ac901234r (2009).
- 15 Tannous, B. A., Kim, D. E., Fernandez, J. L., Weissleder, R. & Breakefield, X. O. Codon-optimized Gaussia luciferase cDNA for mammalian gene expression in culture and in vivo. *Molecular therapy : the journal of the American Society of Gene Therapy* **11**, 435-443, doi:10.1016/j.ymthe.2004.10.016 (2005).

CHAPTER IX



Gaussia Luciferase-based mycoplasma detection assay in mammalian cell culture

M. Hannah Degeling^{1,3,4*}, M. Sarah S. Bovenberg^{1,3,4*} and Bakhos A. Tannous^{1,2,3}.

¹Experimental Therapeutics and Molecular Imaging Laboratory, Neuroscience Center, Department of Neurology,
²Center for Molecular Imaging Research, Department of Radiology, Massachusetts General Hospital, and
³Program in Neuroscience, Harvard Medical School, Boston, USA. ⁴Department of Neurosurgery, Leiden
University Medical Center, Leiden, The Netherlands.

* These authors contributed equally

Summary

Mycoplasma contamination in mammalian cell culture is a common problem with serious consequences on experimental data, and yet many laboratories fail to perform regular testing. In this chapter, we describe a simple and sensitive mycoplasma detection assay based on the bioluminescent properties of the *Gaussia* luciferase reporter.

Key words: Mycoplasma contamination, Mycoplasma detection assay, Gluc mycosensor, cell culture contamination, antibiotics, bioluminescence reaction

1. Introduction

Mycoplasmas are common contaminants of mammalian cell culture; due to their small size and the absence of a rigid cell wall, they have the ability to pass through most bacterial filters. In contrast to other contaminants such as fungi and bacteria, mycoplasma contamination is impossible to detect by eye, since the contamination does not influence the color of the cell culture medium, the pH, the turbidity, nor the odor. Mycoplasmas are also not visible under the regular light microscopes in cell culture laboratories. Furthermore, the fact that mycoplasma can grow both intracellular and extracellular greatly contributes to their resistance to several antibiotics in the extracellular cell culture medium, such as penicillin and streptomycin.¹ Due to these issues, mycoplasma contamination rates in mammalian cell culture laboratories have been found to be as high as 70%.¹⁻³

Mycoplasma contamination can have a tremendous effect on host cells. For instance, mycoplasma can interfere with numerous cellular processes including cell metabolism, proliferation, gene expression, and function.^{2,3,4,5,6,7} Therefore, all cell culture laboratories should test cell cultures for mycoplasma contamination on a regular basis. The ideal detection method for mycoplasma contamination should be simple to perform, sensitive, specific, rapid, inexpensive, and suitable for testing of numerous cell cultures simultaneously.

In this chapter, we describe a simple mycoplasma detection assay based on degradation of the *Gaussia* luciferase (Gluc) reporter protein. Typically, in conditioned medium of cells under regular culture conditions, Gluc has a half-life of >7 days.⁸ The half-life of Gluc is tremendously decreased in the presence of mycoplasma contamination, and therefore the level of decline in Gluc activity correlates to mycoplasma infection rate.⁹ This mycoplasma-specific decrease has been confirmed by several assays including Western blot analysis, which showed Gluc protein degradation over short period of time (2 - 24 hours) only in the presence of mycoplasma contamination. We reasoned that this phenomenon could be used as a sensitive and specific biosensor to monitor the mycoplasma contamination in mammalian cells (Mycosensor).⁹

Around 90-95% of all mycoplasma contamination in mammalian cell cultures is caused by either *M. orale*, *M. hyorhinitis*, *M. arginini*, *M. fermentans*, *M. hominis* or *A. laidlawii*.¹ The Gluc mycosensor has been confirmed on three of these commonly isolated mycoplasma strains including *Mycoplasma fermentans*, *Mycoplasma hominis*, and *Mycoplasma orale*. Importantly, this Mycosensor showed to be more sensitive in detecting mycoplasma contamination as compared to a commercially available bioluminescent-based assay and is amenable to high-throughput applications.⁹ Alternative Mycoplasma detection methods are available including mycoplasma DNA amplification by polymerase chain reaction, which is sensitive but prone to errors; by traditional bacterial cell culture, which is very time consuming;¹⁰ or by commercially-available kits which have low sensitivity and are costly. The Gluc Mycosensor however, is easy to use, sensitive, and especially suited for testing of numerous cell quantities simultaneously. Nevertheless, we recommend in all cases to combine two different detection methods to achieve and maintain total mycoplasma clearance in the cell culture hoods.

2. Materials

2.1. Gluc Recombinant Protein

1. Gluc recombinant protein (Nanolight)

Or, for the preparation of Gluc recombinant protein:

2. cDNA encoding Gluc (Nanolight), and N-terminal pelB periplasmic signal sequence, and a C-terminal 6-His tag in pET26b (+) vector (Novagen).
3. HMS174 competent bacterial cells and LB containing 30 µg/mL kanamycin.
4. IPTG Bugbuster Master Mix containing Benzonase (Novagen).
5. NJ45 µm syringe filter nickel charged resin column (Novagen).
6. Binding buffer: 0.5 M NaCl, 20mM Tris-HCl, 5 mM imidazole, pH 7.9
7. Wash buffer: 0.5 M NaCl, 20 mM Tris-HCl, 60 mM imidazole, pH 7.9
8. Elution buffer: 0.5 M NaCl, 20mM Tris-HCl, 1 M imidazole, pH 7.9
9. Coelenterazine and a luminometer
10. 3500 MW cut-off dialysis tubing (Fisher Scientific).
11. Bradford assay.
12. SDS-PAGE, NuPAGE, 10% Bis-Tris gel and coomassie blue staining (Invitrogen).

2.2. Gluc-containing medium

1. 293T human fibroblast cells.
2. Lentivirus vector expressing Gluc and the enhanced green fluorescent protein (GFP) under the control of CMV promoter
3. Polybrene.

2.3. Cell culture

1. High glucose Dulbecco's modified Eagle's medium. Supplemented with 10% fetal bovine serum, and 100 U/mL penicillin and 100 µg/mL streptomycin (**see note 1 and 2**).
2. Incubator with a humidified atmosphere supplemented with 5% CO₂ at 37 °C.
3. 24-well cell culture plates.

2.4. Bioluminescence reaction

1. A luminometer to measure the bioluminescence activity of Gluc (**see note 3**).
2. 20 µM coelenterazine (Nanolight). Diluted in phosphate buffer saline (PBS; **see note 4**).
3. Black 96 well microtiter plates (**see note 5**).

3. Methods

Be aware that all materials used for cell culture and the Mycosensor assay should be stored and used under sterile conditions to avoid contamination during the Gluc incubation period. An overview of the complete Gluc Mycosensor assay protocol is presented in Figure 1.

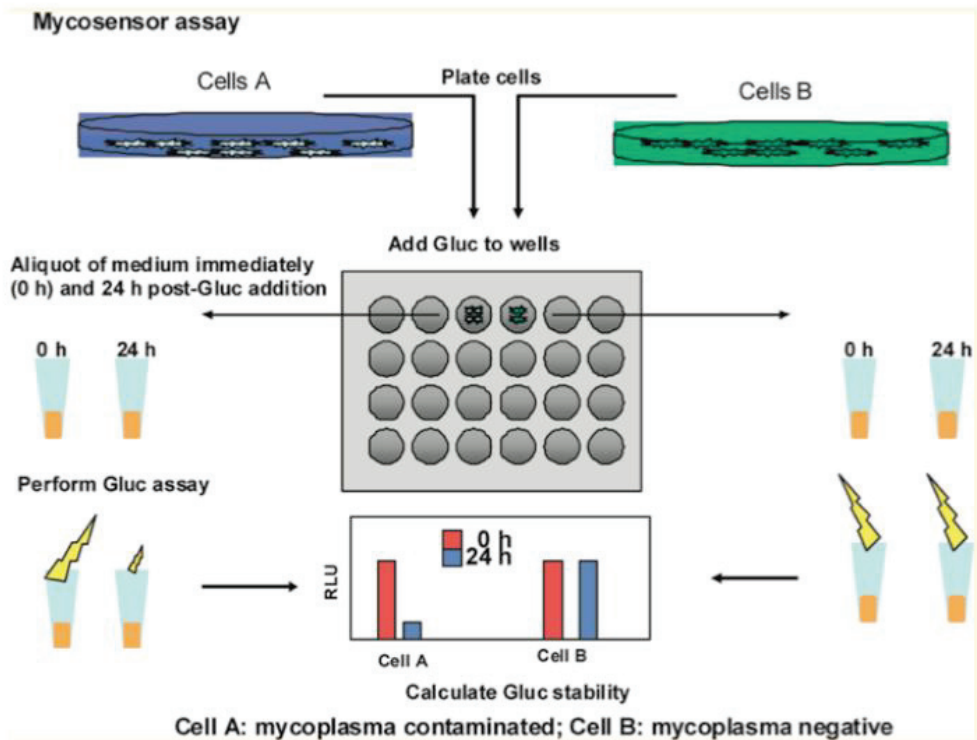


Figure 1. Setup of mycoplasma assay.

3.1. Gluc recombinant protein purification

In brief, the cDNA encoding Gluc is amplified by PCR using specific primers and cloned in-frame between an N-terminal pelB periplasmic signal sequence and a C-terminal 6-His tag in pET26b(+) vector using BamHI and XhoI sites. In this vector, gene expression is under the control of an isopropyl β -D-1-thiogalactopyranoside (IPTG)-inducible T7 RNA polymerase promoter. The vector is transformed into HMS174 competent bacterial cells and grown overnight in 200 mL LB containing 30 μ g/mL kanamycin. Once the culture reached an

OD₆₀₀ of 0.6, protein expression is induced by adding 20 μ M IPTG to the culture which is grown for 18 h at room temperature. Cells should be pelleted by centrifugation for 15 min at 10,000x g and resuspended in 10 mL Bugbuster Master Mix containing Benzonase. Insoluble debris is pelleted by another spin. The clarified lysate is then filtered through a 45 μ m syringe filter and loaded onto a nickel charged resin column equilibrated with binding buffer. The column should be rinsed with 20x volumes of binding buffer followed by 18x volumes of wash buffer. His-tagged Gluc is eluted from the column with 1.2 mL of elution buffer collecting 200 μ L fractions. The fraction containing the highest Gluc activity (as measured using coelenterazine and a luminometer) should be pooled and dialyzed against 30 mM Tris-HCl, pH 8.0 overnight using 3500 MW cut-off dialysis tubing. Glycerol is added to a final concentration of 10% and protein concentration is determined using the Bradford assay. Purity of protein can be analyzed by SDS-PAGE under reducing conditions using a NuPAGE[®] 10% Bis-Tris gel and coomassie blue staining.

3.2. Gluc-containing medium

As an alternative to recombinant Gluc, conditioned medium from mycoplasma-free cells stably expressing Gluc can be aliquoted and stored at -80 °C and can be used for the Mycosensor assay. In this chapter, we will take the widely used 293T human fibroblast cells as an example for the Mycosensor assay. 293T cells can be engineered to stably express the naturally secreted Gluc (**see note 1**) by infecting these cells with a lentivirus vector expressing Gluc and the enhanced green fluorescent protein (GFP) under the control of CMV promoter at a multiplicity of infection of 10 transducing units/cell in the presence of 10 μ g/mL Polybrene.⁸ The next day, cells are washed and maintained in regular growth medium. GFP can be used as a marker to monitor transduction efficiency and therefore Gluc expression.

3.3. Mycosensor assay

1. Culture the test cells for at least 72 hours under normal culture conditions as described above (**see note 2**).
2. Plate cells to be tested in triplicates in a 24 well plate at around 30% confluency; an ideal amount of 293T cells would be 1×10^5 cells/well, however, as low as

5×10^4 cells can be used. Cells should be plated in 500 μL of growth medium (**see note 6**). In order to save time, it is also possible to simply assay the cell-free conditioned medium of the test cells by transferring a small aliquot to the 24 well plate instead of re-plating the cells, In this case, the Gluc-containing medium or purified Gluc can be added immediately and step 3 can be skipped. One should take into consideration that this technique is much less sensitive than the standard protocol (**see note 7**).

3. The next day, add purified Gluc to a final concentration of 35 ng/mL to conditioned medium. Alternatively, if one chooses to use Gluc-containing medium, remove 250 μL of medium from cells to be tested and add 250 μL of Gluc-containing media (**see note 8**).
4. Mix by stirring the plate and immediately take a 50 μL aliquot from each well; this will be used as the time point zero. Samples can be frozen at $-80\text{ }^\circ\text{C}$ until further analysis (**see note 9**).
5. Return the plate to the cell culture incubator.
6. At 24 hours post-Gluc addition, take another 50 μL aliquot from each well and freeze at $-80\text{ }^\circ\text{C}$. If fast analysis is required, and if mycoplasma contamination is high, it is possible to detect a decrease in Gluc activity (and therefore mycoplasma contamination) after 4 hours. However, if mycoplasma contamination is low, 4 hours will not yield a significant degradation of Gluc and longer incubation time is needed. One may choose to perform time analysis by storing an aliquot of conditioned medium at different time points.
7. Do not discard the cells at the 24-hour time point since very low levels of mycoplasma can be detected after 48h or 72h, even if test results are negative at earlier time points (**see note 9**).
8. Assay these aliquots for Gluc activity using coelenterazine and a luminometer (see below).

3.4. The Mycosensor bioluminescence assay

9. Thaw aliquots from the different time points to room temperature (**see note 10**).
10. While waiting, dilute coelenterazine in PBS to a final concentration of 20 μM and incubate for 20-30 minutes in the dark (**see note 11**).
11. Transfer 20 μL of each aliquot into black 96 well microtiter plate.

12. Using a luminometer with a built-in injector, inject 80 μL of coelenterazine and acquire the signal immediately for 10 seconds (**see note 12**).

3.5. The Mycosensor assay results

Mycoplasma contamination is determined by comparing the Gluc signal at time point B (e.g., 24h) to the signal at time zero. A significant decrease in Gluc activity indicates mycoplasma contamination (**see note 13**). Typical results from a positive and negative mycoplasma assay are presented in Figure 2.

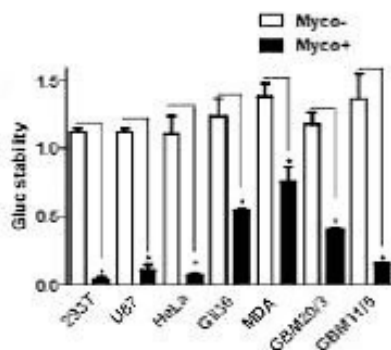


Figure 2. Gaussia luciferase as a measure of mycoplasma contamination in mammalian cell culture. Conditioned medium from cells expressing Gluc were added on different mycoplasma clean or contaminated cells (1×10^5 cells plated on 24-well plate) and the Gluc activity was detected immediately (0h) and 24 h later using a luminometer after addition of coelenterazine.

4. Notes

1. Be alert that the cells used to express Gluc, and from which the conditioned medium is used for the Mycosensor assay, are not contaminated with mycoplasma. We recommend to test these cells on a regular basis with two different mycoplasma detection assays such as: MycoAlert® (Lonza Rockland, Rockland, ME) and PCR PromoKine Mycoplasma Test KIT I/C (PromoCell, Heidelberg, Germany) according to the manufacturer's standard protocol.
2. Mycoplasma needs at least 48 – 72 hours to recover from frozen stocks and therefore cells should be cultured for at least 3 days after thawing from liquid nitrogen before testing for contamination.
3. Any plate reader with a built-in injector that can adequately measure bioluminescence can be used.
4. Other concentrations of CZN can be used, up to 100 μM ; however, the 20 μM concentration of CZN in combination with the luminometer used in our laboratory,

and the black microtiter plate will lead to the most optimum Gluc value under our assay conditions.

5. This note is also to some extent applicable to notes 3 and 4; be aware that the Gluc signal can reach saturation depending on the amount of Gluc used and the sensitivity of the luminometer. In the case that Gluc-containing conditioned medium is used for the Mycosensor assay, this problem is more likely to occur. The use of black plates could solve this problem as they typically yield up to one log lower signal as compared to white plates. As an alternative, one can dilute the medium before the assay.
6. Keep in mind that plating too many cells will result in overconfluency at 72 hours resulting in cell death and therefore the Mycosensor will not be accurate.
7. As an alternative to testing mycoplasma contamination on plated cells, recombinant Gluc can be added directly to an aliquot of conditioned medium from cells to be tested; however, this strategy is less sensitive as compared to testing the cells themselves. One may choose to do the assay on conditioned medium initially and if the results are negative, it can then be confirmed on plated cells.
8. Be careful when adding Gluc not to disrupt the cells, since some cell types are easily detached from the plate leading to false results.
9. It is of utmost importance to include a time point zero when performing the Mycosensor at a range of time points. It is recommended to take 2 different aliquots of conditioned medium at time point zero in case one chooses to run the 24 hour time point first. If test results are negative, the 48 and 72 hours time point can then be assayed and compared to the second aliquot of time point zero.
10. We observed that aliquots from the same sample but treated in a different manner (e.g. frozen versus not-frozen) can show some variation in Gluc signal intensity. It is important to treat all aliquots, including the ones from different time points, in the same manner.
11. Coelenterazine purchased should be first reconstituted in acidified methanol (1 drop of HCL to 10 mL of Methanol) to a final concentration of 5 mg/mL. Just before use, it is diluted in PBS to a final concentration of 20 μ M. Coelenterazine is prone to auto-oxidation and a decrease in bioluminescence signal over time can simply be observed due to this artifact. Incubating diluted coelenterazine for 20 min in the dark stabilizes the signal and will result in a stable bioluminescent output.

12. A luminometer with built-in injector is required to perform the Mycosensor assay, since Gluc catalyzes a flash-type bioluminescence reaction. Therefore, the reaction starts with a high signal, followed by a rapid decrease over the course of few seconds.¹¹ If a luminometer with built-in injection is not available, one can dilute coelenterazine in PBS containing 0.1% Triton X-100. We showed that this detergent yields some stability to the Gluc signal, especially when used in combination with GlucM43I mutant.¹² Alternatively, stabilization kits are available from Targeting Systems or Nanolight (GAR-reagents). The substrate should be diluted in the appropriate reagent and can be added manually to the medium and assayed using a luminometer.
13. We recommend testing cells for mycoplasma contamination on a regular basis using the Gluc Mycosensor. Confirm negative results with another type of assay, such as the PCR-based mycoplasma assay.

REFERENCES

- 1 Drexler, H. G. & Uphoff, C. C. Mycoplasma contamination of cell cultures: Incidence, sources, effects, detection, elimination, prevention. *Cytotechnology* **39**, 75-90, doi:10.1023/A:1022913015916 (2002).
- 2 Hay, R. J., Macy, M. L. & Chen, T. R. Mycoplasma infection of cultured cells. *Nature* **339**, 487-488, doi:10.1038/339487a0 (1989).
- 3 Rottem, S. & Barile, M. F. Beware of mycoplasmas. *Trends in biotechnology* **11**, 143-151 (1993).
- 4 Logunov, D. Y. *et al.* Mycoplasma infection suppresses p53, activates NF-kappaB and cooperates with oncogenic Ras in rodent fibroblast transformation. *Oncogene* **27**, 4521-4531, doi:10.1038/onc.2008.103 (2008).
- 5 Namiki, K. *et al.* Persistent exposure to Mycoplasma induces malignant transformation of human prostate cells. *PLoS one* **4**, e6872, doi:10.1371/journal.pone.0006872 (2009).
- 6 Zhang, S. *et al.* Mycoplasma fermentans infection promotes immortalization of human peripheral blood mononuclear cells in culture. *Blood* **104**, 4252-4259, doi:10.1182/blood-2004-04-1245 (2004).
- 7 Zinocker, S. *et al.* Mycoplasma contamination revisited: mesenchymal stromal cells harboring Mycoplasma hyorhinis potently inhibit lymphocyte proliferation in vitro. *PLoS one* **6**, e16005, doi:10.1371/journal.pone.0016005 (2011).
- 8 Wurdinger, T. *et al.* A secreted luciferase for ex vivo monitoring of in vivo processes. *Nature methods* **5**, 171-173, doi:10.1038/nmeth.1177 (2008).
- 9 Degeling, M. H., Maguire, C. A., Bovenberg, M. S. & Tannous, B. A. Sensitive assay for mycoplasma detection in mammalian cell culture. *Analytical chemistry* **84**, 4227-4232, doi:10.1021/ac2033112 (2012).
- 10 Uphoff, C. C. & Drexler, H. G. Detection of mycoplasma in leukemia-lymphoma cell lines using polymerase chain reaction. *Leukemia : official journal of the Leukemia Society of America, Leukemia Research Fund, U.K* **16**, 289-293, doi:10.1038/sj.leu.2402365 (2002).
- 11 Tannous, B. A., Kim, D. E., Fernandez, J. L., Weissleder, R. & Breakefield, X. O. Codon-optimized Gaussia luciferase cDNA for mammalian gene expression in culture and in vivo. *Molecular therapy : the journal of the American Society of Gene Therapy* **11**, 435-443, doi:10.1016/j.ymthe.2004.10.016 (2005).
- 12 Maguire, C. A. *et al.* Gaussia luciferase variant for high-throughput functional screening applications. *Analytical chemistry* **81**, 7102-7106, doi:10.1021/ac901234r (2009).

SUBMITTED

CHAPTER X



Multimodal targeted high relaxivity thermosensitive liposome for in vivo imaging

Maayke M P Kuijten^{1,4,5}, M. Hannah Degeling^{1,4,6}, John W. Chen^{2,3}, Gregory Wojtkiewicz³, Peter Waterman³, Ralph Weissleder³, Klaas Nicolay⁵ and Bakhos A Tannous^{1,4}.

¹Neuroscience Center and Molecular Neurogenetics Unit, Department of Neurology, ²Division of Neuroradiology, Department of Radiology, ³Center for Systems Biology, Massachusetts General Hospital, and ⁴Program in Neuroscience, Harvard Medical School, Boston, MA 02114 USA. ⁵Department of Biomedical Engineering, Biomedical NMR, Eindhoven University of Technology, Eindhoven, the Netherlands. ⁶Department of Neurosurgery, Leiden University Medical Center, Leiden, the Netherlands.

ABSTRACT

Liposomes are spherical, self-closed structures formed by lipid bilayers that can encapsulate drugs and/or imaging agents in their hydrophilic core or within their membrane moiety, making them suitable delivery vehicles. We have synthesized and characterized a new targeting, thermosensitive liposome, containing gadolinium-DOTA lipid bilayer, as a multimodal molecular imaging agent for magnetic resonance and optical imaging. We showed that this liposome has a much higher molar relaxivities r_1 and r_2 compared to a more conventional liposome containing gadolinium-DTPA-BSA lipid. By incorporating both gadolinium and rhodamine in the lipid bilayer as well as biotin on its surface, we used this agent for multimodal imaging and targeting of tumors through the strong biotin-streptavidin interaction. Since this new liposome is thermosensitive, it can be used for ultrasound-mediated drug delivery at specific sites, such as tumors, and can be guided by magnetic resonance imaging.

INTRODUCTION

Magnetic resonance imaging (MRI) is a routine diagnostic tool with many advantages compared to other imaging modalities including its noninvasive character, lack of radiation burden and its excellent spatial and temporal resolution^{1, 2}. Despite its many advantages, there are intrinsic limitations caused by MRI contrast agents, such as short vascular half-life circulation, which could lead to potential side effects. This drawback can be overcome by using liposomes which can incorporate a high payload of gadolinium-containing amphiphilic lipid in their bilayer resulting in a spectacular increase in effective longitudinal (r_1) relaxivity per particle³⁻⁵.

Liposomes are spherical, self-closed structures formed by one or more lipid bilayers and contain an aqueous phase inside and between bilayers⁶. The amphiphilic lipids used for the formation of liposomes are usually comprised of a hydrophilic head group and two hydrophobic fatty acyl chains. Their amphiphilic character results in spontaneous assembly into aggregates in aqueous environment. Hydrophilic drugs can be enclosed in the aqueous compartment while hydrophobic

drugs can be incorporated in the lipid bilayers core^{7, 8}. These characteristics together with their potential to invade the immune system, target cells, and reduce unwanted side-effects made them the drug delivery vehicle of choice^{3, 4, 6, 9}. Further, the surface of liposomes can be modified and grafted with different targeting moieties including antibodies or bioresponsive components like biosensitive lipids or polymers⁸. In addition to drug delivery, the success of liposomes has led to their use as carriers for imaging agents since they can either encapsulate a contrast agent, a fluorophore for optical imaging, or both within their interior or in their bilayer. This characteristic overcomes problems associated with these imaging agents such as rapid clearance, non-specific cellular interaction, and toxicity resulting in poor contrast and low resolution images^{3, 8}.

Multifunctional liposomes have been developed for image-guided drug delivery by incorporating both therapeutic drugs and contrast agents for MRI^{3, 4}. Typically, lipid-based contrast agents such as amphiphilic gadolinium(Gd)-DTPA derivatives are incorporated within the membrane moiety of the liposome, leaving the lumen to encapsulate therapeutic molecules^{2, 10}. The disadvantage of these liposomes is that they contain a single Gd-chelate moiety per molecule leading to lower MRI detectability. In an attempt to overcome these limitations, macromolecular Gd-chelates with several residues in the single molecular chain have been used, however, these polychelates could change the liposome structure, affecting its surface properties^{2, 11}. Thermosensitive liposomes have been developed for ultrasound-mediated drug delivery at specific sites, such as tumors¹²⁻¹⁴, and can be guided by imaging^{10, 15, 16}. These liposomes typically incorporate the contrast agent within their lumen for which relaxivity is low when the liposome is intact and only increases during phase transition¹⁷.

Given these limitations, an alternative strategy to enhance detectability with MRI is to increase the effective longitudinal relaxivity per Gd-chelate moiety. In this study, we synthesized and characterized a new liposome, named NLP, which contains Gd-DOTA lipid bilayer and is thermosensitive due to the addition of lipids with transition temperatures below 45 °C. We compared the activity of this liposome to a more conventional liposome (CLP; with a transition temperature of 60 °C) containing Gd-DTPA-BSA lipid and showed that NLP has a much higher efficacy as

a MRI contrast agent. By embedding the gadolinium imaging agent in the membrane of the liposome, this agent exhibits high intrinsic relaxivity when the liposome is intact, making it suitable for monitoring the delivery of drug carriers to the target. Further, we engineered a targeting multifunctional liposome based on NLP which carries both gadolinium and a fluorophore in the lipid bilayer as well as biotin on its surface, and demonstrated that it could be used for multimodal molecular imaging and targeting of tumors through the strong biotin-streptavidin interaction.

RESULTS

Synthesis and characterization of the NLP liposome formulation. We have synthesized a thermosensitive liposome with gadolinium containing lipids as a new contrast agent for MRI (**Fig. 1**). We compared the characteristics of this new formulation (NLP) to a more conventional DSPC-based Gd-containing liposome (CLP, **Fig. 1**). We first measured the mean average hydrodynamic diameter of the NLP liposome and showed it to be 86 nm, which is smaller than the conventional CLP liposome having a size of 109 nm (**Fig. 2a** and **Table 1**). The mean average diameter of the NLP liposome, stored at 4 °C, was again investigated after 5 weeks. We observed that both the size and size distribution of the liposome remained constant with an average hydrodynamic diameter of 85 nm (data not shown). The consistency of these results indicates a sterically-stabilized liposome preparation with a shelf lifetime of at least 5 weeks.

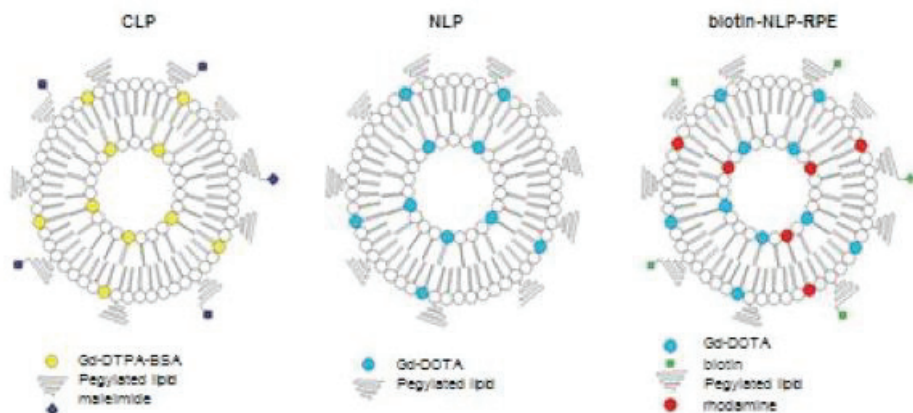


Figure 1. Schematic overview of CLP, NLP and NLP-biotin-RPE liposomes.

We synthesized a new DPPC-based liposome (NLP) containing gadolinium-DOTA lipid and compared its characteristics to more conventional DSPC-based liposome with gadolinium-DTPA-BSA (CLP). In order to make NLP multifunctional, a biotin and rhodamine containing lipid was added to the formulation so the liposome can be traced both with magnetic resonance and fluorescence imaging and can be targeted using the strong biotin-streptavidin interaction (NLP-biotin-RPE).

In order to determine the efficacy of the different liposomes as contrast agents, we determined the gadolinium ion concentration in both NLP and CLP. The Gd(III) concentration estimated by phosphate determination for CLP and NLP was 2.790 mM and 1.925 mM respectively (**Table 1**). The Gd(III) concentration in these liposomes were also precisely determined using inductively coupled plasma mass spectroscopy (ICP-MS) and found to be 2.920 mM and 2.238 mM, respectively, similar to the concentration found by phosphate determination (**Table 1**).

Table 1: Characterization CLP, NLP and biotin-NLP-RPE liposomes.

Characteristics	CLP	NLP	biotin-NLP-RPE
Size	109 nm	86 nm	93 nm
Concentration Gd(III) by phosphate determination	2.8 mM	1.9 mM	1.8 mM
Concentration Gd(III) by ICP	2.9 mM	2.2 mM	1.9 mM

Thermosensitivity of NLP liposome. To determine the thermosensitivity of the NLP liposome, calcein release during heating was investigated. The fluorescent signal of calcein is quenched due to its high concentration (30 mM) inside the aqueous lumen of the liposome. During phase transition, the lipids in the liposome rearrange and the liposome shell opens resulting in calcein release and hence increased fluorescence signal. Upon liposome heating, lipid rearrangement started at 38 °C resulting in leakage of its content (**Fig. 2b**).

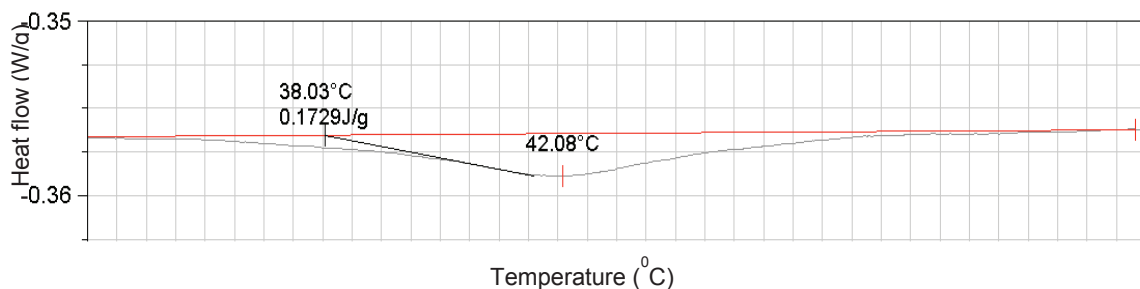
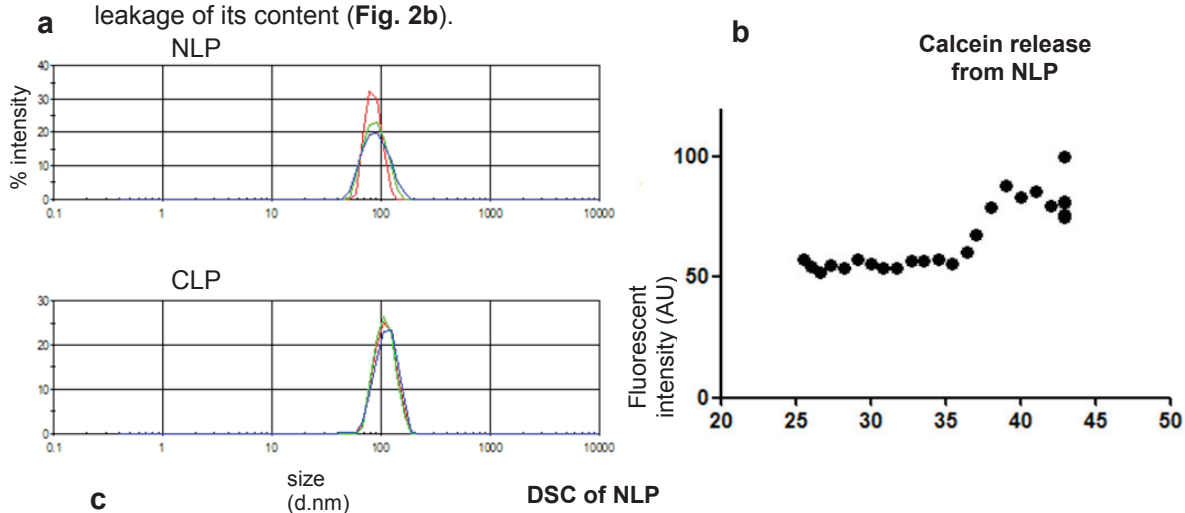


Figure 2. Size distribution and thermosensitivity of NLP and CLP liposomes. (a) The size of the liposome was measured with dynamic light scattering. Intensity plots showing the average hydrodynamic diameters of NLP and CLP to be 86 nm and 109 nm respectively. (b) NLP-containing calcein was heated at different temperatures. The fluorescent intensity starts to increase around 37 - 38 °C indicating lipid rearrangement and further increases until around 39 °C. No significant further increase is visible upon addition of the lysis reagent triton X-100. (c) Differential scanning calorimetry (DSC) showing that NLP has a transition temperature of 42 °C.

The fluorescent signal further increased until around 39 °C at which temperature all calcein appeared to be released. No further increase in fluorescence signal was visible upon the addition of the lysis reagent Triton X-100, showing that all calcein was already released during the 40 minutes heating period. The transition temperature of NLP defined as the temperature at the top of transition phase was determined with differential scanning calorimetry (DSC) and found to be 42 °C (**Fig. 2c**).

Relaxivity determination of NLP liposome. The measured Gd(III) concentration was used to determine the longitudinal (r_1) and the transversal (r_2) relaxivities of the different liposome formulations. Since NLP is thermosensitive (due to the incorporation of the DPPC and DMPC lipids), r_1 and r_2 relaxivities were determined at different temperatures to investigate the influence of hyperthermia on the imaging efficacy of this liposome. Longitudinal and transversal relaxivities of the liposome formulations at different temperatures were obtained from the slope of the linear fit of relaxation rates as a function of Gd(III) concentration. At higher temperature, both r_1 and r_2 relaxivities of the NLP decreased showing a negative influence of hyperthermia on imaging efficacy of NLP (**Fig. 3a**).

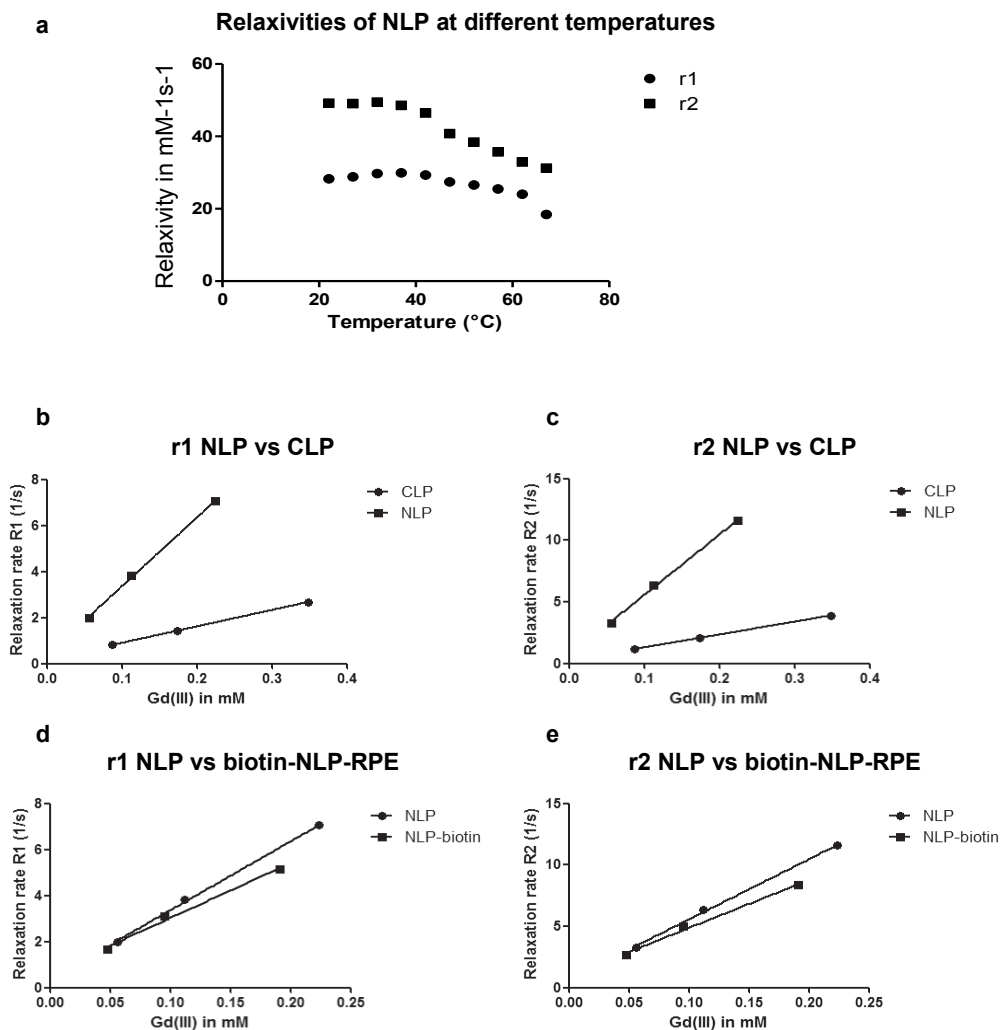


Figure 3. Longitudinal and transversal relaxivities of the different liposome formulations in $\text{mM}^{-1}\text{s}^{-1}$. Longitudinal (r_1) and transversal (r_2) relaxivities were obtained from NMR measurements at 60 MHz and 1.41 Tesla. **(a)** longitudinal and transversal relaxivities of NLP liposomes obtained at different temperatures ranging from 22 °C to 67 °C with 5 °C intervals. **(b,c)** Longitudinal and transversal relaxation rates of NLP as compared to CLP liposomes obtained at 37 °C. **(d,e)** Relaxation rates of NLP versus NLP-biotin-RPE are presented.

To determine the efficacy of NLP as a contrast agent, r_1 and r_2 relaxivities at 37 °C were compared to the conventional CLP liposome. T1 and T2 measurements were performed at 60 MHz corresponding to a magnetic field strength of 1.41 Tesla.

The Gd(III)DTPA-BSA-based CLP liposome exhibited a longitudinal r_1 relaxivity of $7.52 \text{ mM}^{-1}\text{s}^{-1}$ (**Table 2, Fig. 3b**), which is similar to values published for the same formulation ($7.5 \text{ mM}^{-1}\text{s}^{-1}$)¹⁸. The transversal r_2 relaxivity of CLP was found to be $10.6 \text{ mM}^{-1}\text{s}^{-1}$. On the other hand, the Gd(III)DOTA-DSPE based NLP liposome exhibited four-fold higher r_1 of $29.9 \text{ mM}^{-1}\text{s}^{-1}$ and five-fold higher r_2 of $49.0 \text{ mM}^{-1}\text{s}^{-1}$ as compared to CLP (**Table 2, Fig. 3b,c**). The longitudinal relaxivity of NLP was >2-fold higher compared to the published relaxivity for DSPC-based Gd(III)DOTA-DSPE containing liposome ($12.8 \text{ mM}^{-1}\text{s}^{-1}$)¹⁸. The reported relaxivities are the average relaxivities of the Gd(III) ions in the inner and outer leaflets of the lipid bilayer.

Table 2: Longitudinal (r_1) and transversal (r_2) relaxivities in $\text{mM}^{-1}\text{s}^{-1}$ of CLP, NLP and biotin-NLP-RPE liposome formulations at 37°C obtained from NMR measurements at 60 MHz at 1.5 Tesla.

Relaxivity at 37°C	CLP	NLP	Biotin-NLP-RPE
Relaxivity r_1	$7.5 \text{ mM}^{-1}\text{s}^{-1}$	$29.9 \text{ mM}^{-1}\text{s}^{-1}$	$23.9 \text{ mM}^{-1}\text{s}^{-1}$
Relaxivity r_2	$10.6 \text{ mM}^{-1}\text{s}^{-1}$	$49.0 \text{ mM}^{-1}\text{s}^{-1}$	$39.0 \text{ mM}^{-1}\text{s}^{-1}$
r_2/r_1	1.41	1.64	1.64

Synthesis and characterization of a targeted multimodal NLP liposome. In order to increase sensitivity and selectivity of the newly formulated contrast agent, targeted NLP was synthesized with a biotin on its surface (biotin-NLP). Further, to make NLP suited for multimodal imaging (fluorescence and MRI), rhodamine-PE (RPE) was added within the lipid bilayers of the liposome (biotin-NLP-RPE; **Fig. 1**). The addition of biotin and rhodamine to the NLP formulation did not affect its size (93 nm, **Table 1**). The gadolinium ion concentration as well as the longitudinal, and transversal relaxivities of biotin-NLP-RPE were found to be similar to the non-targeted NLP liposome (**Table 1,2; Fig. 3d,e**).

Targeting of cells with biotin-NLP-RPE in culture. To determine the functionality of the newly synthesized biotin-NLP-RPE liposome in targeting tumor cells, viable Gli36 human glioma cells overexpressing both the mutant EGFRvIII, a frequent genetic alteration in primary brain tumors¹⁹ and GFP, or plain Gli36 control cells were incubated with a biotinylated antibody against EGFRvIII followed by Streptavidin-Alexa647 and finally by biotin-NLP-RPE and analyzed by fluorescence microscopy.

A distinct surface staining of both Alexa647 (indicative of streptavidin binding) and rhodamine-PE (liposome) was observed, showing the functionality of this liposome in targeting tumor cells (**Fig. 4a**). The plain Gli36 cells did not show any surface staining (data not shown).

To evaluate the usefulness of the biotin-NLP-RPE in targeting tumor cells in a different model, Gli36 human glioma cells were engineered by a lentivirus vector to express both GFP (marker for transduction efficiency) as well as a fusion protein between a biotin acceptor peptide (BAP), preceded by a signal sequence, and the transmembrane domain (TM) of the PDGFR receptor (BAP-TM)²⁰. Upon gene transfer and expression, the biotin ligase will tag the BAP peptide with a single biotin moiety which is presented on the cell surface through TM. These cells as well as control cells were then labeled with streptavidin-Alexa647 followed by incubation with biotin-NLP-RPE and analyzed by fluorescence microscopy. A distinct cell surface staining was found on cells expressing BAP-TM for both Alexa647 and RPE proving the specific targeting of biotin-NLP-RPE (**Fig. 4b**). Control cells did not show any surface staining (data not shown).

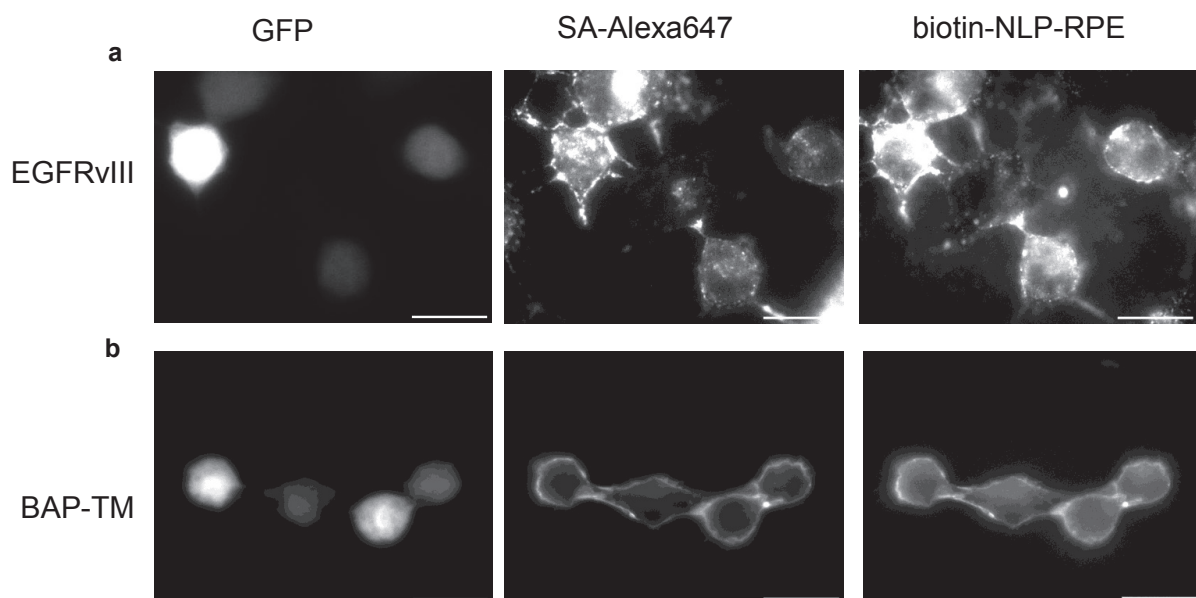


Figure 4. Targeting of cells with biotin-NLP-RPE liposome. (a) Gli36 human glioma cells expressing the EGFRvIII receptor and GFP were labeled with a biotinylated-antibody against EGFRvIII followed by streptavidin-Alexa647 and biotin-NLP-RPE, and analyzed by fluorescence microscopy for both Alexa647 and RPE. (b) Gli36 cells were infected with

lentivirus vector expressing BAP-TM and GFP. These cells were labeled with Streptavidin-Alexa647 followed by biotin-NLP-RPE and analyzed as in (a).

Targeted multimodal *in vivo* imaging of tumors using biotin-NLP-RPE. To confirm the functionality of biotin-NLP-RPE in an *in vivo* model, Gli36 cells engineered by gene transfer to express BAP-TM or plain Gli36 control cells were injected subcutaneously in the flanks of nude mice (n=5) at two different locations. Two-weeks later, mice were i.v. injected with either biotin-NLP-RPE or a complex consisting of biotin-NLP-RPE and streptavidin-Alexa750 (Alexa750-SA-NLP-RPE) and imaged first with fluorescence-mediated tomography (FMT; 4 hrs post-injection) for Alexa750 confirming streptavidin targeting. Significant accumulation (*p<0.001) of Alexa750 signal was observed in tumors expressing biotin on their surfaces as compared to control tumors in mice injected with Alexa750-SA-NLP-RPE and not the non-targeted biotin-NLP-RPE (without the use of streptavidin), showing efficient targeting of this NLP complex to biotin expressing tumors (**Fig. 5a,b**). The same mice were also imaged with T1w MRI at 4 and 24 hrs post-injection. Significantly higher accumulation (*p<0.001) of NLP liposome over time was observed in tumors expressing biotin on their surfaces as compared to control tumors only in mice injected with targeted Alexa750-SA-NLP-RPE complex showing that tumors can be targeted and imaged with MR using this liposome complex (**Fig. 5c,d**). Mice injected with non-targeted biotin-NLP-RPE liposome showed similar and lower accumulation in both tumors.

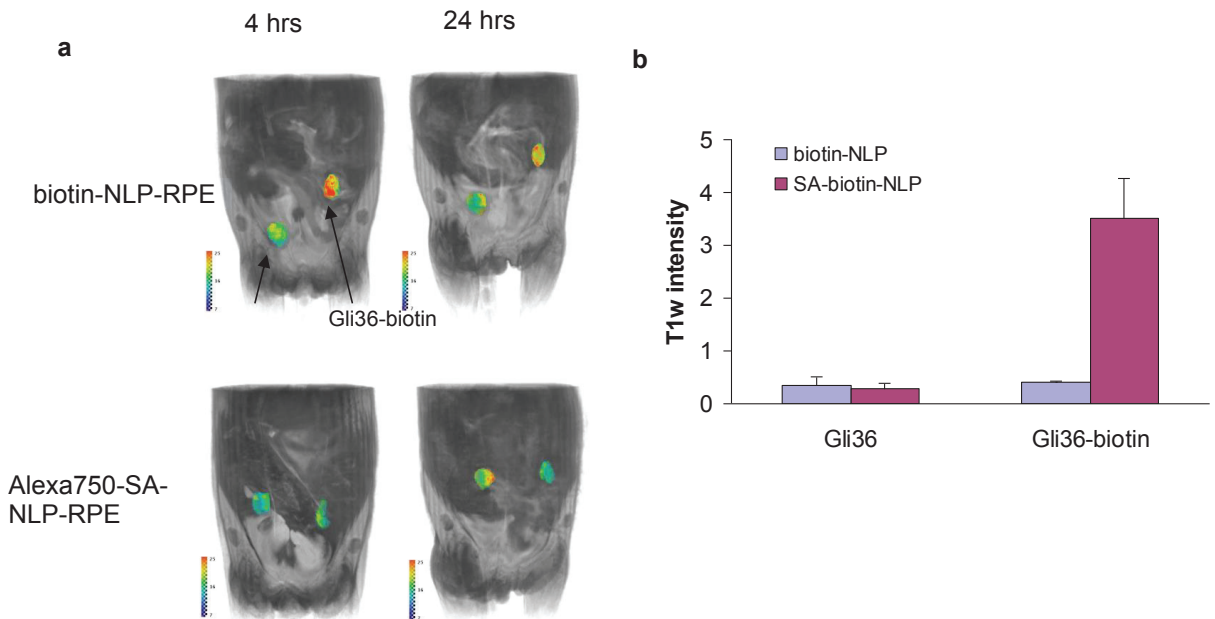
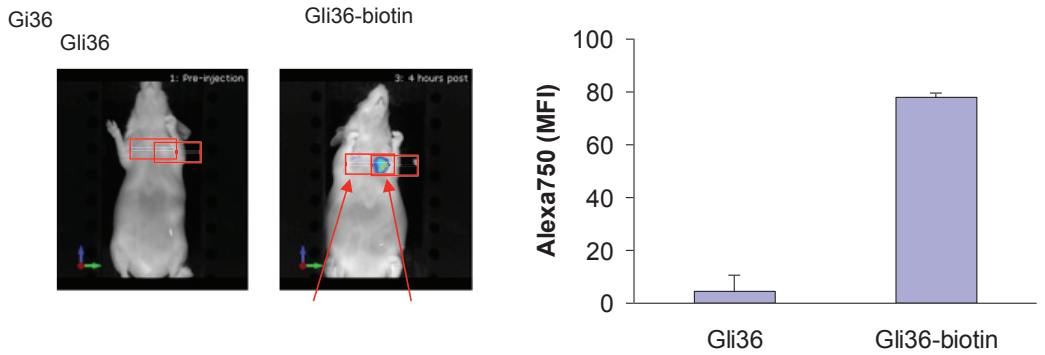


Figure 5. Targeting and in vivo imaging of tumors with biotin-NLP-RPE. Gli36 human glioma cells or same cells expressing biotin on their surfaces (through BAP-TM) were implanted subcutaneously in nude mice (n=5) at 2 different sites. Two-weeks later, mice were i.v. injected with either biotin-NLP-RPE or a complex consisting of biotin-NLP-RPE and streptavidin-Alexa750 (Alexa750-SA-NLP-RPE) and imaged 4 hrs later with FMT Alexa750. (a-b) a representative mouse from each group is shown in (a) and quantitation of fluorescent accumulation in each tumor in (b). (c-d) The same mice were also imaged with T1w MRI at 4 and 24 hrs post-injection (c). T1w intensities at 24 hrs were normalized to 4 hrs for each tumor (d). *p<0.001 as calculated by student's t-test.

DISCUSSION

In this study, we synthesized a new liposome and characterized it by comparing its efficacy as a contrast agent to a more conventional liposome. We showed that the new liposome NLP exhibited four-fold higher longitudinal and five-fold higher transversal relaxivity compared to a conventional liposome CLP. Further, the longitudinal relaxivity (at 1.41 Tesla) of NLP was >2-fold higher compared to a published liposome formulation with the same Gd-DOTA containing lipid ($29.9 \text{ mM}^{-1} \text{ s}^{-1}$ compared to $12.8 \text{ mM}^{-1} \text{ s}^{-1}$)¹⁸. Since the NLP formulation is thermosensitive, we observed a temperature dependency for both longitudinal and transversal relaxivities being lower at higher temperature. Recent studies showed that an increase in temperature leads to an increase in longitudinal relaxivity for DSPC-based Gd(III)DOTA-DSPE containing liposomes ($12.8 \text{ mM}^{-1} \text{ s}^{-1}$ at 37°C compared to over $14 \text{ mM}^{-1} \text{ s}^{-1}$ at 67°C)¹⁸. A potential explanation for these differences between typical liposomes and NLP could be the increased water exchange across the liposomal membrane at higher temperature resulting in larger contribution of Gd(III)DOTA-DSPE in the inner leaflet of the liposome to the overall longitudinal relaxivity²¹⁻²⁴. The unique composition of the NLP liposome could possibly positively affect the water exchange across the liposomal membrane and explain its high relaxivities compared to both CLP and Gd(III)DOTA-DSPE containing liposome. To further increase the sensitivity and selectivity of the NLP contrast agent, and to make it useful for multimodal imaging, we synthesized the NLP liposome with biotin on its surface and rhodamine within the lipid bilayer. The Gd(III) inside the liposome can serve as a contrast agent for MRI and the rhodamine can be used for imaging at the single cell level with fluorescence. This biotin-NLP-RPE showed to have three to four-fold higher relaxivities compared to CLP¹⁸. Further, we showed that streptavidin can serve as a bridge between biotin-NLP-RPE and biotinylated antibody to target specific receptors overexpressed on tumor cells.

In vivo optical imaging has limited use due to the problem of light absorption by pigmented molecules such as hemoglobin and scattering by mammalian tissues, leading to a decrease in the detection limit. The biotin-NLP-RPE was synthesized with a rhodamine-containing lipid in the bilayer, which was shown to be useful in targeting tumor cells at the single cell level in culture using fluorescence imaging. This same complex would be useful for single cell detection *in vivo* using intravital

microscopy and could be extended for intraoperative fluorescence imaging²⁵. Further, the rhodamine can be replaced with any fluorophore emitting in the near infra-red region of the spectrum, which can then be used for FMT imaging in deep tissues *in vivo*²⁶. The biotin on the NLP surface makes these liposomes universal targeted contrast agents for which practically any peptide/antibody specific to a cell of interest can be complexed to it through the strong interaction of biotin with streptavidin. The specificity of biotin to streptavidin has been exploited for several medical and scientific applications including drug or toxin targeting, *in vivo* imaging of targeted cells, and antibody-guided radioimmunotherapy in humans^{20, 27, 28}.

The use of biotin-NLP-RPE liposome can be extended and applied for drug delivery. The combination of imaging with drug delivery is very valuable in the search for new therapeutic strategies. Further, the thermosensitive characteristic of this liposome does not only have a positive effect on the relaxivity, but could also be used as a delivery strategy for drugs, for instance to solid tumors. Our *in vitro* data shows that a temperature of 39 °C can lead to an increase in calcein release from NLP liposomes. This thermosensitive feature of NLP has a high clinical impact in which NLP liposome can encapsulate a therapeutic drug which can be released specifically on the tumor site by ultrasound-induced hyperthermia, similar to previously published methods^{10, 15, 16}. Further, by including Gd(III) in these liposomes, MRI can be used for guided drug release at the specific site¹⁰.

In conclusion, we have synthesized a new liposome with higher r1 and r2 relaxivities as compared to conventional liposome and showed it to be useful for targeting and multimodal imaging of tumors. Since this liposome is thermosensitive, it can be used for ultrasound-mediated drug delivery at specific sites, such as tumors, which can be guided by MRI or catheter based optical imaging²⁹⁻³²

MATERIALS AND METHODS

Materials for liposome preparation. 1,2-Dipalmitoyl-sn-glycero-3-phosphocholine (DPPC), 1,2-ditetradecanoyl-sn-glycero-3-phosphocholine (DMPC), 1,2-distearoyl-sn-glycero-3-phosphoethanolamine-N-[methoxy(polyethylene glycol)-2000] (PEG2000-DSPE), 1,2-distearoyl-sn-glycero-3-phosphoethanolamine-N-[biotinyl(polyethylene glycol)2000] (Biotin-PEG2000-DSPE), 1,2-Dioleoyl-sn-Glycero-

3-Phosphoethanolamine-N-(Lissamine Rhodamine B Sulfonyl) (Rhodamine PE), 1,2-distearoyl-sn-glycero-3-phosphoethanolamine-N-[maleimide(polyethylene glycol)-2000] (PEG2000-DSPEmal), 1,2-Distearoyl-sn-glycero-3-phosphocholine (DSPC) and cholesterol were purchased from Avanti Polar Lipids (Alabaster, AL). Gd(III)DOTA-DSPE and Gd(III)-DTPA-bis(stearylamide) (Gd(III)-DTPA-BSA) were obtained from Gateway Chemical Technology (St. Louis, MO).

Preparation of liposome formulations. Liposomes were prepared according to three different formulations: the more conventional liposome DSPC-Gd(III)DTPA-BSA (CLP), the new formulation DPPC-Gd(III)DOTA (NLP) and the new formulation biotinylated and rhodamine-labeled: DPPC-Gd(III)DOTA-biotin (biotin-NLP-RPE). NLP liposome was prepared with DPPC, DMPC, Gd(III)DOTA-DSPE and PEG2000-DSPE at a molar ratio of 50:20:25:5 (**Table 3**). As a control, CLP liposome were used containing DSPC, Gd(III)DTPA-BSA, PEG2000-DSPE, PEG 2000-DSPEmal and cholesterol in a molar ratio of 36.7: 25:2.5:2.5:33.3 (**Table 3**). The biotin-NLP-RPE liposome was prepared with DPPC, DMPC, Gd (III)DOTA-DSPE, PEG2000-DSPE, Biotin-PEG2000-DSPE and Rhodamine PE at a molar ratio of 50:20:25:2.5:2.5:0.1 (**Table 3**). These liposomes were prepared by lipid film hydration followed by extrusion⁵. The lipid film was prepared by dissolving the lipid mixture (50 μ mol) in 3:1 v/v $\text{CHCl}_3/\text{MeOH}$ in a 250 ml round-bottomed flask. The solution was evaporated using rotation evaporation for 15 minutes at 200 mbar and 30 °C and at 150 mbar till dryness. In order to assure complete dryness, rotation evaporation was pursued at 0 mbar for 15 more minutes and the film was subsequently put under a nitrogen flow for at least one hour. The NLP and biotin-NLP-RPE films were dried over night. The films were hydrated with 4 ml HEPES buffered saline (HBS) (20 mM HEPES and 135 mM NaCl at pH 7.4) at 60 °C for NLP and biotin-NLP-RPE and 65 °C for the CLP liposomes after heating the film to 65 °C. The films of the NLP and biotin-NLP-RPE liposomes were not heated before addition of the HBS. The lipid dispersions were extruded (Lipofast Extruder, Avestin, Ottawa, Ontario) at 60 °C and 65 °C for the NLP and CLP liposomes respectively. The lipid dispersions were extruded through polycarbonate membrane filters (Whatman, Maidstone, UK) with a pore diameter of 400 nm (1 time), through filters with a pore diameter of 200 nm (6 times) and through filters with a pore diameter of 100 nm (6 times).

Table 3. Formulations of CLP, NLP and biotin-NLP-RPE liposomes.

CLP	Mol %	NLP	Mol %	NLP-biotin-RPE	Mol %
DSPC	36.67	DPPC	50	DPPC	50
Gd(III)DTPA-BSA	25	DMPC	20	DMPC	20
Cholesterol	33.33	Gd(III)-DOTA-DSPE	25	Gd(III)-DOTA-DSPE	25
PEG2000-DSPE	2.5	PEG2000-DSPE	5	PEG2000-DSPE	2.5
PEG2000-DSPEmal	2.5			Biotin-PEG2000-DSPE	2.5
				Rhodamine PE	0.1

Liposome characterization. The size and size distribution of liposomes were measured using dynamic light scattering (DLS) at 25, 37 or 41 °C on a Malvern Zetasizer Nano S apparatus (Malvern, UK) equipped with a 633 nm laser. These measurements were performed in sextuple using three different concentrations of liposome suspension in 400 µl HBS (20 mM HEPES and 135 mM NaCl at pH 7.4).

Total lipid and gadolinium [Gd(III)] concentrations of liposome suspensions were calculated using phosphate determination, performed according to Rouser after destruction of the samples with perchloric acid at 180 °C³³. The amount of phospholipids in the sample was determined using a calibration curve between 0 and 80 nmol phosphate. The total amount of lipids and the amount of gadolinium containing lipids in the sample was calculated based on the measured amount of phospholipids.

The gadolinium ion concentration was determined for NLP and biotin-NLP-RPE liposomes using inductively coupled plasma mass spectroscopy (ICP-MS;

DRCII Perkin-Elmer, Philips Research Material Analysis, Eindhoven, The Netherlands). From each sample, 150 μ l was taken, weighed and sent in for ICP.

Determination of thermosensitivity

The thermosensitivity of NLP liposome was determined based on calcein release experiment and differential scanning calorimetry. In order to measure calcein release, NLP liposome films (25 μ mol) were hydrated with 2 ml of 30 mM calcein 100 mM NaCl solution in HBS (pH 6.8). Extrusion was performed according to the same protocol as for the NLP liposome. Free calcein was separated from calcein-containing liposome using PD-10 column (GE-healthcare). Liposome was then dissolved in HBS (20 mM HEPES and 135 mM NaCl; pH 7.4). The fluorescent intensity of the calcein-containing liposome was measured with a fluorometer (excitation wavelength: 494 nm; emission wavelength: 517 nm). As a control, the fluorescent intensity of the liposome was measured at room temperature before and after addition of 10% triton-X in water. The fluorescent intensity was measured every minute for 40 minutes. The first measurement was performed at 25 $^{\circ}$ C and the temperature of the water bath increased by 1 $^{\circ}$ C every minute. The temperature of the sample was measured every two minutes. After 40 minutes, 10% triton-X in water was added to the sample to determine the maximal fluorescent intensity. The phase transition temperature of NLP liposome was measured with differential scanning calorimetry (DSC, Universal V4 5A TA Instruments).

Determination of relaxivity. To determine the longitudinal and transversal relaxivities of the liposomes, spin-lattice relaxation time (T1) and spin-spin relaxation time (T2) measurements were performed on a Bruker (Rheinstetten, Germany) Minispec mq60 NMR analyzer (60 MHz) with a magnetic field of 1.41 Tesla. T1 relaxation times were obtained using the standard inversion recovery method with a recycle delay of 20 s, inversion time ranging from 5 ms to 10 seconds, the inversion sequence was repeated ten times and four averages. T2 times were measured using a Carr-Purcell-Meiboom-Gill (CPMG) sequence with a recycle delay of 20 s, interecho time of 0.4 ms, 10,000 echoes and 16 averages.

The longitudinal r_1 and the transversal r_2 relaxivities were obtained from the slope of the linear fit of relaxation rates as a function of gadolinium ion concentration described in equation 1 and 2 respectively (below). The relaxation rates R_1 and R_2

are the inverse of T1 and T2 respectively. The longitudinal and transversal relaxivities are a measure for the efficacy of the contrast agent.

$$\frac{1}{T1} = \frac{1}{T1_{tissue}} + r1[CA] \quad (1)$$

$$\frac{1}{T2} = \frac{1}{T2_{tissue}} + r2[CA] \quad (2)$$

[CA] is the concentration of the contrast agent, in this case the Gd(III) concentration in mM and r1 and r2 the longitudinal and transversal relaxivity respectively³⁴. In order to determine the relaxivities of the CLP, NLP and biotin-NLP-RPE liposomes, T1 and T2 measurements were performed at 37°C. Since NLP liposome is thermosensitive, relaxivities were determined at different temperatures. T1 and T2 measurements were performed within a temperature range of 22 °C to 67 °C with 5 °C intervals.

Cell culture. Gli36 human glioma cells were obtained from Dr. Anthony Capanogni, UCLA, CA. Gli36 cells were transduced with a retrovirus vector expressing the mutant EGFRvIII and puromycin resistant gene (obtained from Dr. Miguel Sena-Esteves, Department of Neurology, University of Massachusetts Medical Center, Worcester). The cells were selected by culturing the cells in conditioned media with 1 mg/l puromycin. Gli36 cells were also infected with a lentivirus vector expressing a biotin acceptor peptide, preceded by a signal sequence followed by the transmembrane domain of PDGFR (BAP-TM) as previously described²⁰. As a control, Gli36 cells were infected with similar empty lentivirus vector. All cells were cultured in Dulbecco's modified Eagle's medium (DMEM) supplemented with 10% fetal bovine serum (Sigma, St. Louis, MO) and 100 U penicillin and 0.1 mg streptomycin (Sigma) per milliliter at 37 °C in a 5% CO₂ humidified incubator.

In vitro targeting of glioma cells with biotin-NLP-RPE. Seventy five thousand cells were plated in 1.5 ml conditioned media on coverslips (Fisher Scientific) in a 24 well plate. Twenty-four hours later, cells were incubated with 250 ng/ml of biotinylated anti-EGFRvIII antibody for 5 min (in phosphate buffer saline, PBS, a kind gift from Dr. Darell D. Bigner, Duke University Medical Center) at room temperature. Cells were then washed and incubated with streptavidin-Alexa647 (1:200; Molecular Probes) for 5 min. Cells were washed again and incubated with biotin-NLP-RPE (70 μM) for 5 min. Cells were then washed, fixed with 4% paraformaldehyde, mounted on coverslips and analyzed by fluorescence

microscopy. For cells expressing BAP-TM, similar protocol was followed without the use of the antibody.

Targeting and Multimodal imaging of tumors with biotin-NLP-RPE *in vivo*. All animal studies were approved by the Subcommittee on Research Animal Care at Massachusetts General Hospital and were performed in accordance to their guidelines and regulations. Mice were kept on biotin-deficient diet throughout the study. One million Gli36 cells (in 50 μ l) expressing BAP-TM or control cells were mixed with similar volume of Matrigel (Becton Dickinson) and implanted subcutaneously in the flanks of nude mice in 2 different locations. Two weeks later, mice (n=5) were injected with a complex of streptavidin-Alexa750 (200 μ g) and biotin-NLP-RPE (200 μ l of 7 mM) pre-incubated for 15 min. Mice were then imaged with fluorescence-mediated tomography and magnetic resonance at different time points.

Magnetic resonance imaging. MRI was performed using an animal 4.7 T MRI scanner (Bruker, Billerica, MA) consisting of coronal and axial T1w images (rapid acquisition with refocused echoes (RARE) sequence, TR=900 ms, TE=14.1 ms, field of view=5.4 cm x 4.0 cm, matrix size=256 x 256, slice thickness=1 mm, 16-18 slices) obtained before and after intravenous administration of Alexa750-SA-NLP-RPE or biotin-NLP-RPE as control as above. Post contrast images were obtained at 4 and 24 hrs post injection. Image analysis and segmentation was performed using the OsiriX™ DICOM viewer. Contrast-to-noise ratios were computed as $(ROI_{\text{tumor}} - ROI_{\text{muscle}})/STD(\text{noise})$, where ROI=region of interest drawn to encompass the tumor on the slice where the tumors are the largest or a region of flank muscle, and STD=standard deviation. For the 3D MRI image, the tumors were segmented out manually in the Amira environment (Visage Imaging, Inc., San Diego, CA). This was volume rendered in pseudocolor. The rest of the body was volume rendered in gray scale.

Fluorescence-mediated tomography. Quantitative fluorescent tomographic imaging was carried out on a commercial imaging system (FMT2500, Perkin Elmer, Waltham MA). Prior to imaging, mice received an intravenous injection of imaging agent. Four hours after injection, mice were non-invasively imaged under general

isoflurane anesthesia (1-1.5% at 2l/min). Paired absorption and fluorescent data sets were collected using a scanning laser, and 3-dimensional reconstructions were generated utilizing the TrueQuant FMT software.

ACKNOWLEDGEMENTS

This work was supported by grant from NIH/NCI 4R00CA126839 (BAT), and P50CA86355 (RW and BAT), as well as NIH/NINDS R01-NS070835 (JWC), R01-NS072167 (JWC), and P30NS045776 (BAT). The authors would like to thank Dr. Darell D. Bigner (Duke University Medical Center) for providing the antibody against EGFRvIII, Dr. Casey Maguire (MGH) for biotinylation of this antibody and Dr. Miguel Sena Esteves (Universisty of Massachusetts Medical Center) for providing the retrovirus vector expressing EGFRvIII.

REFERENCES

1. Weissleder R. (2002). Scaling down imaging: Molecular mapping of cancer in mice. *Nature Reviews Cancer*.2(1):11-18.
2. Hu FQ, Joshi HM, Dravid VP, Meade TJ. (2010). High-performance nanostructured MR contrast probes. *Nanoscale*.2(10):1884-1891.
3. Bae KH, Chung HJ, Park TG. (2011). Nanomaterials for cancer therapy and imaging. *Mol Cells*.31(4):295-302.
4. Barreto JA, O'Malley W, Kubeil M, Graham B, Stephan H, Spiccia L. (2011). Nanomaterials: applications in cancer imaging and therapy. *Adv Mater*.23(12):H18-40.
5. Mulder WJM, Strijkers GJ, Griffioen AW, van Bloois L, Molema G, Storm G, et al. (2004). A liposomal system for contrast-enhanced magnetic resonance imaging of molecular targets. *Bioconjugate Chemistry*.15(4):799-806.
6. Torchilin VP. (2005). Recent advances with liposomes as pharmaceutical carriers. *Nat Rev Drug Discov*.4(2):145-160.
7. Kozłowska D, Foran P, MacMahon P, Shelly MJ, Eustace S, O'Kennedy R. (2009). Molecular and magnetic resonance imaging: The value of immunoliposomes. *Adv Drug Deliv Rev*.61(15):1402-1411.
8. Mody VV, Nounou MI, Bikram M. (2009). Novel nanomedicine-based MRI contrast agents for gynecological malignancies. *Adv Drug Deliv Rev*.61(10):795-807.
9. Srikanth M, Kessler JA. (2012). Nanotechnology-novel therapeutics for CNS disorders. *Nat Rev Neurol*.8(6):307-318.
10. Kono K, Nakashima S, Kokuryo D, Aoki I, Shimomoto H, Aoshima S, et al. (2011). Multi-functional liposomes having temperature-triggered release and magnetic resonance imaging for tumor-specific chemotherapy. *Biomaterials*.32(5):1387-1395.
11. Shiraishi K, Kawano K, Minowa T, Maitani Y, Yokoyama M. (2009). Preparation and in vivo imaging of PEG-poly(L-lysine)-based polymeric micelle MRI contrast agents. *J Control Release*.136(1):14-20.
12. Fossheim SL, Il'yasov KA, Hennig J, Bjornerud A. (2000). Thermosensitive paramagnetic liposomes for temperature control during MR imaging-guided hyperthermia: in vitro feasibility studies. *Acad Radiol*.7(12):1107-1115.
13. Kielar F, Tei L, Terreno E, Botta M. (2010). Large relaxivity enhancement of paramagnetic lipid nanoparticles by restricting the local motions of the Gd(III) chelates. *J Am Chem Soc*.132(23):7836-7837.
14. Yatvin MB, Weinstein JN, Dennis WH, Blumenthal R. (1978). Design of liposomes for enhanced local release of drugs by hyperthermia. *Science*.202(4374):1290-1293.
15. de Smet M, Langereis S, van den Bosch S, Grull H. (2010). Temperature-sensitive liposomes for doxorubicin delivery under MRI guidance. *Journal of Controlled Release*.143(1):120-127.
16. Tagami T, Foltz WD, Ernsting MJ, Lee CM, Tannock IF, May JP, et al. (2011). MRI monitoring of intratumoral drug delivery and prediction of the therapeutic effect with a multifunctional thermosensitive liposome. *Biomaterials*.32(27):6570-6578.

17. Grull H, Langereis S. (2012). Hyperthermia-triggered drug delivery from temperature-sensitive liposomes using MRI-guided high intensity focused ultrasound. *J Control Release*.161(2):317-327.
18. Hak S, Sanders H, Agrawal P, Langereis S, Grull H, Keizer HM, et al. (2009). A high relaxivity Gd(III)DOTA-DSPE-based liposomal contrast agent for magnetic resonance imaging. *European Journal of Pharmaceutics and Biopharmaceutics*.72(2):397-404.
19. Peri S, Navarro JD, Amanchy R, Kristiansen TZ, Jonnalagadda CK, Surendranath V, et al. (2003). Development of human protein reference database as an initial platform for approaching systems biology in humans. *Genome Res*.13(10):2363-2371.
20. Tannous BA, Grimm J, Perry KF, Chen JW, Weissleder R, Breakefield XO. (2006). Metabolic biotinylation of cell surface receptors for in vivo imaging. *Nature Methods*.3(5):391-396.
21. Laurent S, Vander Elst L, Thirifays C, Muller RN. (2008). Relaxivities of paramagnetic liposomes: on the importance of the chain type and the length of the amphiphilic complex. *Eur Biophys J*.37(6):1007-1014.
22. Wang T, Hossann M, Reinl HM, Peller M, Eibl H, Reiser M, et al. (2008). In vitro characterization of phosphatidylglycerol-based thermosensitive liposomes with encapsulated 1H MR T1-shortening gadodiamide. *Contrast Media Mol Imaging*.3(1):19-26.
23. Koenig SH, Ahkong QF, Brown RD, 3rd, Lafleur M, Spiller M, Unger E, et al. (1992). Permeability of liposomal membranes to water: results from the magnetic field dependence of T1 of solvent protons in suspensions of vesicles with entrapped paramagnetic ions. *Magn Reson Med*.23(2):275-286.
24. Hak S, Sanders HM, Agrawal P, Langereis S, Grull H, Keizer HM, et al. (2009). A high relaxivity Gd(III)DOTA-DSPE-based liposomal contrast agent for magnetic resonance imaging. *Eur J Pharm Biopharm*.72(2):397-404.
25. van Dam GM, Themelis G, Crane LM, Harlaar NJ, Pleijhuis RG, Kelder W, et al. (2011). Intraoperative tumor-specific fluorescence imaging in ovarian cancer by folate receptor-alpha targeting: first in-human results. *Nat Med*.17(10):1315-1319.
26. Deliolanis NC, Dunham J, Wurdinger T, Figueiredo JL, Tannous BA, Ntziachristos V. (2009). In-vivo imaging of murine tumors using complete-angle projection fluorescence molecular tomography. *J Biomed Opt*.14(3):030509.
27. Axworthy DB, Reno JM, Hylarides MD, Mallett RW, Theodore LJ, Gustavson LM, et al. (2000). Cure of human carcinoma xenografts by a single dose of pretargeted yttrium-90 with negligible toxicity. *Proceedings of the National Academy of Sciences of the United States of America*.97(4):1802-1807.
28. Sakahara H, Saga T. (1999). Avidin-biotin system for delivery of diagnostic agents. *Advanced Drug Delivery Reviews*.37(1-3):89-101.
29. Hara T, Bhayana B, Thompson B, Kessinger CW, Khatri A, McCarthy JR, et al. (2012). Molecular imaging of fibrin deposition in deep vein thrombosis using fibrin-targeted near-infrared fluorescence. *JACC Cardiovasc Imaging*.5(6):607-615.
30. Yoo H, Kim JW, Shishkov M, Namati E, Morse T, Shubochkin R, et al. (2011). Intra-arterial catheter for simultaneous microstructural and molecular imaging in vivo. *Nat Med*.17(12):1680-1684.

31. Staruch R, Chopra R, Hynynen K. (2011). Localised drug release using MRI-controlled focused ultrasound hyperthermia. *Int J Hyperthermia*.27(2):156-171.
32. Carignan CS, Yagi Y. (2012). Optical endomicroscopy and the road to real-time, in vivo pathology: present and future. *Diagn Pathol*.7(1):98.
33. Rouser G, Fleische.S, Yamamoto A. (1970). 2 dimensional thin layer chromatographic separation of polar lipids and determination of phospholipids by phosphorus analysis of spots. *Lipids*.5(5):494-&.
34. Burtea CL, S.; Vander Elst, L.; and Muller, R. N. Contrast Agents: Magnetic Resonance. Molecular Imaging I, Handbook of Experimental Pharmacology. Vol 185(1):135-165. Springer Berlin Heidelberg; 2008.

CHAPTER XI



Advances in stem cell therapy against gliomas

M. Sarah S. Bovenberg^{1,2,3*}, M. Hannah Degeling^{1,2,3*}, and Bakhos A. Tannous^{1,2}

¹Experimental Therapeutics and Molecular Imaging Laboratory, Neuroscience Center, Department of Neurology, ²Program in Neuroscience, Harvard Medical School, Boston, MA 02114 USA. ³Department of Neurosurgery, Leiden University Medical Center, Leiden, The Netherlands. * These authors contributed equally

ABSTRACT

Malignant gliomas are one of the most lethal cancers, and despite extensive research very little progress has been made in improving prognosis. Multimodality treatment combining surgery, radiation, and chemotherapy is the current golden standard, but effective treatment remains difficult due to the invasive nature and high recurrence of gliomas. Stem cell-based therapy using neural, mesenchymal, or hematopoietic stem cells may be an alternative approach because it is tumor selective and allows targeted therapy that spares healthy brain tissue. Stem cells can be used to establish a long-term antitumor response by stimulating the immune system and delivering prodrug, metabolizing genes, or oncolytic viruses. In this review, we discuss current trends and the latest developments in stem cell therapy against malignant gliomas from both the experimental laboratory and the clinic.

Stem cell-based therapy against gliomas

Gliomas account for about 60% of all primary central nervous system tumors with a very poor prognosis. Glioblastoma (GBM), the most malignant type of glioma, has a median survival of approximately 12-18 months ^{1, 2}. The characteristics of this malignancy include uncontrolled cellular proliferation, invasiveness with both long root-like processes and single invasive cells, areas of necrosis, resistance to apoptosis, extensive angiogenesis, and multiple genetic alterations (Figure 1) ³. Standard-of-care treatment includes maximal surgical resection of the tumor followed by radiation and chemotherapy (temozolomide); however, as the poor survival rate indicates, these treatments have not been effective in preventing disease progression. Most patients die within a year of diagnosis from a new secondary tumor foci forming within 2 cm of the resected area ^{4, 5}. The location of the tumor (the brain) and its invasive nature prevent complete surgical removal, while radiotherapy cannot be given in a high enough dosage due to inevitable damage to the normal brain parenchyma. Since chemotherapeutics cannot efficiently cross the blood brain barrier (BBB), and glioma cells have a high tendency to develop resistance against these agents, the efficacy of this approach is limited. The heterogeneous nature of GBM cells, and the complex interaction between different types of tumor cells, stromal cells within the tumor, vasculature, and extracellular matrix (ECM), complicates matters even further since no clear target can be identified, and multiple

interlinked pathways exist, severely decreasing treatment efficacy. Recently, it has been shown that a small population of tumor cells, called cancer stem cells, is responsible for tumor/glioma growth, resistance and recurrence. These neural stem-like cells (also called glioma stem cells; GSC) have the ability of self-renewal and differentiation into a diverse population of cells, both tumorigenic and non-tumorigenic, and display a profound interaction with the endothelial vascular niche. Although the working mechanism is not exactly clear, it is thought that GSCs promote microvascular angiogenesis through secretion of vascular endothelial growth factor (VEGF), while secreted factors from this same vascular niche allow them to maintain their undifferentiated state ⁶. Once implanted in immunogenic mice, GSCs have the ability to recapitulate a phenocopy of the original malignancy ⁷. Further, GSCs appear to be more resistant to conventional therapy as compared to their non stem-like cells counterpart due to their relative quiescence, and will remain at the tumor site, eventually causing a relapse ^{8,9}.

Over the past decade, stem cells (SC) have become increasingly popular as an alternative therapy for treating malignant gliomas. In 2000, Aboody *et al.* described the unique intrinsic capacity of neural stem cells (NSC) to “home” to the tumor site and migrate along metastatic/invasive tumor borders far from their initial site of transplantation, thereby raising the possibility of using NSCs as a therapeutic delivery vehicle in the brain ¹⁰. Many research groups followed this example and, as of today, a wide variety of stem cell-based therapeutics has been tested. Aside from the homing mechanism that selectively targets tumor cells, some stem cells can effortlessly cross the BBB, are easily modified to carry therapeutic genes, have immunosuppressive properties that prevent a host immunoreaction after implantation, and seem capable of shielding therapeutics such as oncolytic viruses from the host immune response, thereby ensuring long term reservoirs of therapeutic virus at the tumor site.

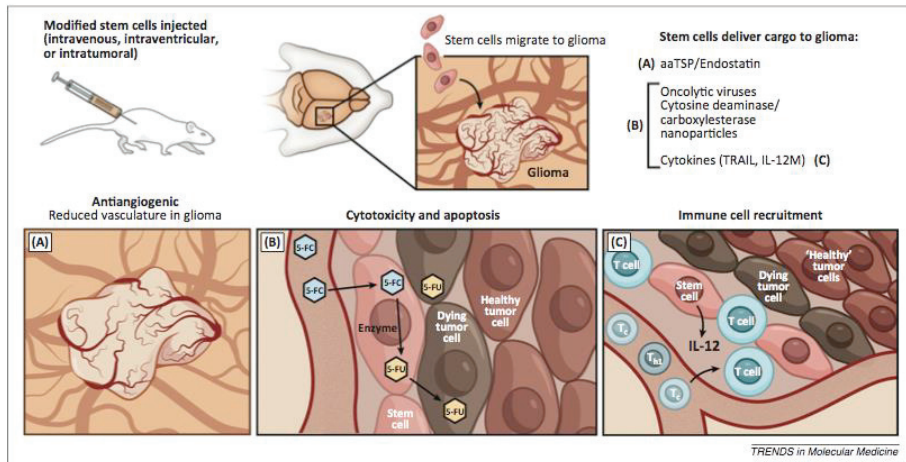


Figure 1. Overview of stem cell-based delivery of different therapeutics to gliomas. Several forms of therapy can be delivered by modified stem cells, including antiangiogenic factors such as aaTSP or endostatin (A), oncolytic viruses or enzymes capable of processing prodrugs such as 5-FC to cytotoxic compounds (B), and immune regulatory factors such as interleukin (IL)-12 that can recruit antitumor immune cells (C). Abbreviations: aaTSP, antiangiogenic protein thrombospondin; TRAIL, tumor necrosis factor-related apoptosis-inducing ligand; T_{h1}, T helper 1 cell; T_{Cx}, cytotoxic T cell.

NSCs are the stem cell type most commonly used for glioma therapy. They are the precursor cells of the central nervous system (CNS) and the only endogenous stem cells to the brain. These cells can self-renew and, due to their multipotent nature, can differentiate into neurons, astrocytes, and oligodendrites. NSCs have a very strong glioma tropism, especially targeting tumor border and hypoxic zones, and can cross the BBB, making excellent carriers for therapeutics such as viral particles, prodrugs, and cytokines¹⁰. An interesting feature of NSCs is their ability in targeting not only the primary tumor mass, but also the invasive GSCs, providing a chance in eliminating the driving factor of glioma progression and recurrence. NSCs not only target gliomas, but have also shown an equal tropism for breast cancer and melanoma brain metastases^{11, 12}. The mechanism underlying this tumor tropism is not yet fully understood, but it is assumed that various chemo attractants and cytokines released by the tumor microenvironment are critical. Because NSCs do not display major histocompatibility complex type II (MHCII) on their cell surface, no host immunoresponse is evoked upon transplantation¹³. In addition, the secretion of

immunomodulating cytokines such as interleukin 10 (IL-10) further suppresses the local immune response, allowing the optimal delivery of a therapeutic payload with minimal neuro-inflammation¹⁴. NSCs could potentially be harvested from the adult brain, but this process is very complicated and time consuming. As an alternative, most studies use stable cell lines of immortalized NSCs originally obtained from embryonic cells, which often makes their use controversial due to ethical, regulatory, and political concerns.

Mesenchymal stem cells (MSC) are the most often studied alternative to NSCs for glioma therapy. These adult stem cells retain their stem cell characteristics, display similar tropism to glioma, and can cross the BBB. They can differentiate into any cell of the mesenchymal lineage including osteoblasts, chondrocytes, myocytes, and adipocytes¹⁵. MSCs are easily obtained from bone marrow, adipose tissue, peripheral blood, umbilical cord (UC) blood, or the placenta, and can be isolated by their expression of the surface markers CD73, CD90, CD105, CD146, CD271, STRO-1, and lack of expression of the hematopoietic markers CD34 and CD45¹⁶. As with NSCs, local immunosuppression can be observed upon implantation¹⁷.

Less frequently used cell types include embryonic stem cells (ESCs) and hematopoietic stem cells (HSCs). The use of ESCs is heavily disputed due to their origin; they can only be obtained from embryonic or fetal tissue¹⁸. Unlike other cell types, ESCs can be modified by homologous recombination, not only eliminating the use of (often inefficient) viral transduction, but further allowing for very specific genetic alterations yielding lines of cells that are stable and identical, ideal for clinical use^{19, 20}. HSCs on the other hand are adult stem cells that can be easily obtained from peripheral blood or bone marrow. HSCs display tropism to brain tumors and therefore are becoming of interest for malignant glioma therapy²¹. Homing of these cells to the tumor site is mediated through attraction to two cytokines, tumor necrosis factor beta (TNF β) and stromal derived factor alpha (SDF1 α)²². Furthermore, the expression of E-selectin by glioma endothelial cells helps adhere circulating HSCs to the tumor tissue.

Currently, a wide range of stem cell-based therapeutic strategies is being investigated pre-clinically while a small portion of this research is being transitioned

to the clinic (Figure 2; Table 1). In this review, we summarize recent advances in the field of stem cell therapy for malignant gliomas and discuss future directions and challenges.

Box 1. Cell types used for glioma stem cell therapy

NSCs are the only adult stem cells endogenous to the human brain. They can differentiate into neurons, astrocytes, and oligodendrites. The subventricular zone (SVZ) of the forebrain is the area richest in NSC, but they can also be found in the striatum and the dentate gyrus of the hippocampus. NSCs are problematic to isolate and expand because only small numbers are available in the mature brain. A wide range of surface markers has been associated with NSCs, as well as expression of sox-1 and -2, pax-6 and nestin. A recent study shows selection based on expression of the surface markers CD133⁺/CD184⁺/CD271⁺/CD44⁺/CD24⁺ allows for highly pure cultures of NSCs²³. NSCs tend to grow in neurospheres *in vitro* and are cultured in specialized NSC growth medium containing Dulbecco's modified Eagle medium (DMEM)/glutamax, B27, insulin, glucose, penicillin/streptomycin, bGFG and EGF. Differentiation is promoted by epidermal growth factor (EGF) and fibroblast growth factor (FGF)²⁴.

MSCs are non-hematopoietic bone marrow (BM)-derived adult stem cells with the capacity to differentiate into cells of the mesenchymal lineage including osteocytes, chondrocytes, myocytes and adipocytes. Compared to NSCs, they are relatively easily isolated from BM, umbilical cord (UC) blood, placenta, adipose tissue and peripheral blood. Once cells are aspirated from BM, they are cultured in DMEM and fetal bovine serum (FBS) at 37 °C and 5% CO₂. MSCs, in contrast to the hematopoietic progenitor cells that are also derived from BM, adhere to tissue culture plastic within 24-48h. Isolation and selection occurs based on their adherent growth in culture, expression of the surface markers CD73, CD90, CD105, CD146, CD271 and STRO1 and lack of expression of CD34 and CD45 and HLA-DR.¹⁶

HSCs are bone marrow derived adult stem cells that give rise to blood cells of both the myeloid and lymphoid lineage, including thrombocytes, erythrocytes, monocytes, neutrophils, basophils, eosinophils, macrophages, dendritic cells (myeloid) and B- and T lymphocytes and Natural Killer (NK) cells (lymphoid). Cells can be obtained from the BM, umbilical cord, and peripheral blood. Pretreatment with granulocyte colony stimulating factor (GSCF) stimulates migration of HSCs to the blood and is often used. Selection takes place based on surface markers and is subject to ongoing debate. Currently the markers most widely accepted for human MSCs are CD34⁺/CD59⁺/Thy-1⁺/CD38⁻/c-kit⁺ combined with a lack of lineage markers²⁵, but for mice MSCs different expression markers are used.

ESCs are pluripotent. They are the only stem cells with unlimited plasticity and replication

potential, which makes them highly attractive for research purposes. However, their use is highly disputed due to the source of origin. ESCs are derived from the inner mass of the blastocyst 4 to 5 days after *in vitro* fertilization (IVF) by immunosurgery and plated onto a layer of support cells consisting of mouse embryonic fibroblast (MEF) in special hESC medium consisting of DMEM with 20% KSR, bFGF, glutamine, non essential amino acids, penicillin/streptomycin and β -mercaptoethanol. This allows the embryonic cells to attach and to expand without the risk of differentiation. Differentiation occurs once the embryonic cells are removed from their support cells and are allowed to form embryoid bodies. Nanog and Oct4 transcription factors are often used to determine the phase of differentiation. As of lately, several protocols using synthetic polymers are now available culturing ESC in the absence of feeder cells or serum. However, Higuchi et al showed that none of these protocols have been able to prevent differentiation and pluripotency of ESCs in the long term, limiting their current value for the stem cell therapy field.²⁶

iPSCs are somatic cells that are reprogrammed to become ESC-like through introduction of embryonic genes including Sox 3 and 4, Oct-4, myc and Klf4/LIN28 by viral vectors in a process that takes between 15 and 30 days. The infected cells are then cultured in ESC medium, and after 10 to 15 days colonies will appear, which can be expanded. These new stem-like cells express ESC markers are capable of differentiating into cells of the endoderm, mesoderm, and ectoderm and can replicate indefinitely.

Stem cells for cargo delivery

Genetic manipulation is one of the research strategies most often investigated for glioma, because it has an almost unlimited range of potential targets. Therapeutic genes stimulating the immune system, inducing tumor cell death, inhibiting angiogenesis, and limiting metastatic potential, have been extensively studied, and many different approaches and gene combinations have been used. However, gene therapy (and/or viral therapy) alone has not been able to live up to its full potential, due to activation and elimination by the host immune system, low transduction efficiency and gene expression, and a lack of even distribution throughout the target tissue. Since stem cells are known to display strong tropism to glioma, are capable of crossing the blood brain barrier, suppress the host immune system, and are easily genetically modified, they make ideal delivery vehicles for therapeutic agents, including genes. Most therapeutic strategies for malignant gliomas using stem cells involve the delivery of mainly four different types of cargos: cytokines, enzymes or prodrugs, oncolytic viruses, and nanoparticles.

i. Cytokine-based glioma therapy

Tumor necrosis factor-related apoptosis-inducing ligand (TRAIL) is one of the most commonly explored cancer therapeutics because it binds to death receptors found specifically on tumor cells, causing a widespread apoptotic effect with minimal cytotoxic effects on normal tissues (Figure 2); however, some cancer types, including GBM, display resistance to TRAIL-mediated apoptosis (Box 2)²⁷⁻³¹. Three recent studies have used NSCs as a delivery vehicle for the secreted soluble variant of TRAIL (sTRAIL) by fusing the N-terminus of Flt3L (a ligand for Flt3L tyrosine kinase receptor) to the extracellular domain of TRAIL. Hingtgen *et al* designed a reporter system to non-invasively monitor the delivery, fate, and therapeutic effect of sTRAIL to GBM by fusing a luciferase reporter to sTRAIL²⁷. NSCs delivered the fusion protein to the tumor site, and luciferase bioluminescence imaging allowed tracking of both NSCs and the delivery of sTRAIL to glioma tumors. With the continuous delivery of sTRAIL by NSCs, a decreased glioma burden was observed as soon as six days post-implantation. Given that glioma cells are known to develop resistance to TRAIL (Box 2), new ways are being explored to sensitize GBM to this therapeutic agent. Balyasnikova *et al.* explored the possibility of combining sTRAIL therapy with the proteasome inhibitor bortezomib and showed that survival significantly increases with this dual treatment³². NSC-mediated delivery of sTRAIL has also been combined with the kinase inhibitor PI-103, which inhibits the PI3 kinase (PI3K)–Akt–mTOR pathway and thus inhibits proliferation and tumor growth³¹. Inhibition of this pathway antagonizes the effect of sTRAIL, resulting in a more efficient induction of apoptosis and cell death. Both studies highlight the need for therapeutics capable of sensitizing glioma to TRAIL. Recently, Badr *et al.* characterized a family of cardiac glycosides, including lanatoside C, an FDA-approved compound that sensitizes GBM cells to TRAIL and showed that the combination of recombinant TRAIL and lanatoside C yielded an enhanced therapeutic effect^{33, 34}. Given that this family of compounds is known to penetrate the brain, they can be easily applied in combination with the NSC-sTRAIL strategy for GBM therapy. Three additional studies used MSCs for sTRAIL delivery. In 2009, Sasportas *et al.* assessed the potential for using MSCs for treating glioma by investigating the cell fate, therapeutic efficacy, and genetic engineering of these cells²⁸. In a proof of principle study, MSCs were engineered *ex vivo* to express sTRAIL³⁵. These engineered MSCs migrated towards glioma, retained their stem-like

properties, and showed prolonged survival in the tumor surroundings, providing a basis to further develop MSC-based therapies for glioma (Figure 2). MSCs engineered to secrete sTRAIL also appear to be resistant to its cytotoxic effect, whereas a caspase-mediated apoptosis was induced in glioma cells. Shortly after, Menon *et al.* confirmed these findings²⁹ using MSCs transduced to express both sTRAIL and the mCherry fluorescent protein, demonstrating tumor specificity and retention in glioma cells both *in vitro* and *in vivo*. Moreover, significant survival was observed in the treated group as compared to control animals, suggesting that MSCs expressing sTRAIL could provide an interesting approach for anti-glioma therapy. Choi *et al.* applied the same strategy using human adipose tissue derived MSCs (hAT-MSCs) engineered to express sTRAIL and reported similar results³⁶.

Genetically modified MSCs can also be used to secrete molecules that do not directly target glioma, but which attract innate immune cells to the tumor, as shown by Ryu *et al.*³⁷. MSCs engineered to express modified interleukin 12 (IL-12M), a proinflammatory cytokine that induces T-helper 1 and cytotoxic T cell immunity, yielded prolonged survival of glioma-bearing mice when injected intratumorally. Remarkably, control mice injected with USB-MSC-IL12M showed resistance to new tumorigenesis, suggesting a tumor-specific T cell immunity.

ii. Enzyme/prodrug-based glioma therapy

As an alternative strategy to the use of active drugs, which have the risk of targeting normal tissue, many studies have focused on the use of prodrugs that are activated exclusively at the tumor site, thereby increasing tissue selectivity. One of the most popular suicide gene therapy approaches relies on the herpes simplex virus type I thymidine kinase (HSV-TK) and the prodrug ganciclovir (GCV). Although excellent results have been reported in experimental settings, a lack of efficacy was observed in clinical trials³⁸⁻⁴¹. Low transduction efficiency and the absence of a bystander effect are thought to be the main causes for this lack of success. To overcome these limitations, Ryu *et al.* designed a protocol using MSCs expressing HSV-TK (MSC-TK) combined with valproic acid (VPA), which upregulates gap junction proteins between MSCs and glioma cells, yielding an enhanced bystander effect⁴². This combined treatment significantly inhibited tumor growth and prolonged survival compared with mice treated with MSC-TK in the absence of VPA. Several studies

have tested a rat glioma model with NSCs (HB1.F3) transduced with the gene for cytosine deaminase (CD), which converts the prodrug 5-fluorocytosine (5-FC) into the active, inhibitory compound 5-fluorouracil (5-FU; Figure 2)^{43,44}. In contrast to the active drug 5-FU, the prodrug 5-FC can cross the BBB. Two separate studies have reported reduced tumor volumes and increased survival in CD/5-FC treated rats with glioma.⁴⁵⁻⁴¹ Joo *et al.* demonstrated both migration and homing of the HB1.F3 NSCs expressing CD to the tumor site as well as reduced tumor volume after breast cancer cells were implanted in one hemisphere of the mouse brain and CD-expressing NSCs were implanted into the contralateral hemisphere, followed by injection of the prodrug 5-FC¹¹. Beyond demonstrating the feasibility of this treatment, this experiment showed that NSCs can not only home to primary brain tumors, but can also migrate towards metastases. However, the survival of animals was not significantly prolonged, suggesting that repeated administration of NSCs and prodrug is required. Further, a combination of NSC-encoding different therapeutic genes or the addition of conventional anticancer therapies to this treatment strategy might be needed. Two other studies reported the use of MSCs to deliver CD to brain tumors and showed an increased mice survival upon intratumoral injection of MSC-CD cells followed by 5-FC therapy (Table 1)^{43,44}.

Lim *et al.* modified NSCs to express the rabbit carboxylesterase enzyme rCE, which converts the prodrug CTP-11 (irinotecan) into the active chemotherapeutic agent SN-38 (7-ethyl-10-hydroxycamptothecin), a potent topoisomerase I inhibitor⁴⁶. Given that intratumoral injection is not favorable when multiple lesions are involved, as in the case for glioma, NSCs were administered systemically. After intravenous injection, rCE-expressing NSCs efficiently penetrated the brain targeting both the primary glioma site as well as infiltrating glioma cells (containing GSCs) that are known to be the source of tumor recurrence and patient death. However, the accumulation of NSCs in non-brain organs was also observed, but did not lead to any tissue damage or tumor formation, although follow-up studies might be needed to evaluate these effects on the long term.⁴⁶ The authors speculate that the use of tumor trophic modulating agents and/or the use of multiple injections could enhance NSCs delivery to the tumor site, thereby increasing specificity and therapeutic effect. Using the same enzyme/prodrug therapy, Zhao *et al.* explored the use of NSCs engineered to secrete rCE enzyme and showed that this strategy yielded 200-fold

higher bystander effect on tumor cells in vitro and enhanced therapeutic effect on metastatic breast cancer in vivo⁴⁷. This strategy should provide an enhanced therapeutic effect for malignant gliomas as compared to NSCs expressing endogenous rCE.

A hallmark of malignant gliomas is extensive angiogenesis with glioma stem cells needing a vascular niche for optimal functioning^{6, 8, 48}. Yin *et al.* used MSCs to express the anti-angiogenesis factor (endostatin), the prodrug-activating enzyme rCE (activates CTP-11 into SN-38), or a combination of both⁴⁹. *In vivo*, MSCs expressing endostatin and rCE led to the highest antitumor response, including reduced angiogenesis, increased cell death, and a reduced GSCs population. Choi *et al.* evaluated the characteristics and therapeutic potential of human adipose tissue-derived MSCs (hAT-MSCs) in a rat brainstem glioma model and found, similar to NSCs, that hAT-MSCs modified to express rCE has tumor tropism, drug activation, and increased life span⁵⁰. In another attempt to target angiogenesis, van Eekelen *et al.* modified NSCs to express antiangiogenic protein thrombospondin (aaTSP-1)⁵¹. aaTSP-1 was shown to target glioma vasculature and to significantly reduce vessel density in a glioma brain co-culture containing endothelial cells, established glioma cells, and glioma stem cells. The decrease in tumor vessel density correlated with decrease in tumor progression and increased survival, most likely due to the disrupted interaction between endothelial cells and glioma stem cells.

iii. Oncolytic virus-based glioma therapy

Theoretically, oncolytic viruses have a significant potential for glioma therapy due to their specificity and high efficiency in killing tumor cells. However, current viral therapeutic strategies have not yet reached their full potential due to poor distribution at the tumor site, low infectivity of tumor cells, and the host immune response (Box 2). To overcome these limitations, Ahmed *et al.* evaluated NSCs as carriers for the targeted delivery of CRAD-S-pk7, a glioma restricted oncolytic adenovirus¹⁴. NSCs loaded with CRAD-S-pk7 injected intracranially inhibited tumor growth and increased median survival by 50%, as compared to animals treated with CRAD-S-pk7 alone, suggesting that NSCs can shield the virus from the host immune system before delivery to the tumor. Interestingly, the oncolytic virus seemed to enhance

NSCs migration towards the tumor site. In a follow up study by the same group, the FDA-approved NSC line HB1.F3-CD was loaded with CRAD-S-pk7 and a thorough characterization of this carrier system was performed ⁵². NSCs loaded with CRAD-S-pk7 retained tumor tropism, continued to replicate CRAD-S-pk7 for over a week after injection, and effectively distributed the CRAD-S-pk7 virus among glioma cells *in vivo*. Nonspecific delivery of adenovirus in the brain was drastically reduced and, due to local injection of NSCs, no migration of NSCs to distant organs was observed, showing that this oncolytic virus carrier system holds a great potential for glioma therapy.

iv. Nanoparticle-based glioma therapy

Following a different approach, several groups are using MSCs to deliver to gliomas nanoparticles, which can carry different therapeutic agents incorporated into the particle or attached to the surface. MSCs can circumvent the problem that nanoparticles have in crossing the BBB, typically yielding low targeting efficiency to brain tumors. In a proof of principle study, Roger *et al.* used poly-lactic acid nanoparticles or lipid nanocapsules loaded with coumarin-6, a lipophilic fluorescent dye used to assess the intracellular uptake of nanoparticles by stem cells that was successfully delivered to the tumor site ⁵³. In a follow up study, MSCs loaded with lipid nanocapsules containing the organometallic complex ferrociphenol (Fc-diOH), a drug with demonstrated cytotoxic effect on glioma cells both *in vitro* and *in vivo*, were shown to have an effective anti-cancer treatment ⁵⁴. Li *et al.* designed a high-efficacy targeting approach for nanoparticle drug delivery using MSCs expressing silica nanorattle doxorubicin (dox) on the cell surface ⁵⁵. The drug was efficiently delivered and resulted in a wider distribution and longer retention of dox at the tumor site, with subsequent enhanced glioma apoptosis as compared with free dox and silica-encapsulated dox control groups.

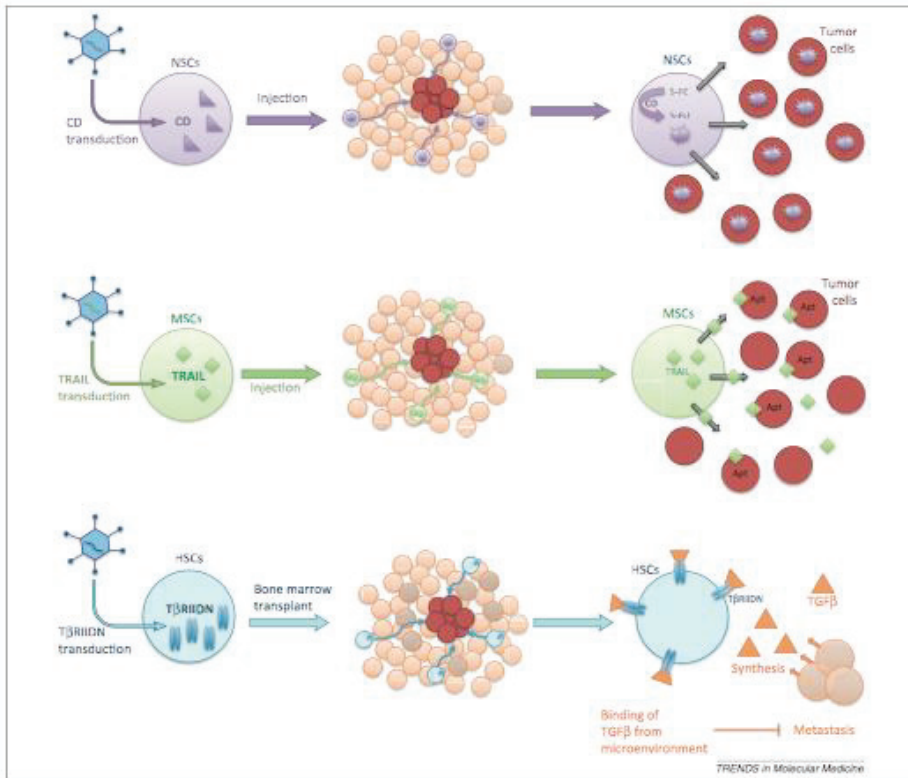


Figure 2. Examples of stem cell-based therapies against gliomas. Many variations on stem cell therapy are possible, and three are depicted here using mesenchymal, neuronal and hematopoietic stem cells (MSCs, NSCs, and HSCs, respectively). Abbreviations: TGF β , transforming growth factor β ; Apt, apoptosis; CD, cytosine deaminase; TRAIL, tumor necrosis factor apoptosis-inducing ligand; T β RIIDN, dominant negative mutant of transforming growth factor β receptor II.

Routes of administration and enhancement of the stem cell model

Several studies have focused on developing alternative strategies to increase the therapeutic effect of SC-based therapy to brain tumors by enhancing delivery mode, tumor tropism, and cellular delivery vehicles (Table 1 and Box 2).

i. Routes of administration

Successful administration of stem cells is crucial for their antitumor efficacy. Both intratumoral or intravenous injections can effectively deliver stem cells, and either injection route is used in the majority of studies⁵⁶. Panciani *et al.* proposed a different delivery route using injections into ventricles or spaces of the brain speculating that this injection mode may lead to the formation of a reservoir of therapeutic cells⁵⁷. This study confirmed that intraventricular transplanted MSCs do create a niche in the subventricular space and can be triggered to migrate to the site of tumor formation. A follow up study investigating the life span of implanted MSCs and their potential for finding and attacking GSCs and tumor recurrence is planned. Meanwhile, Bexell *et al.* studied long distance tropism and migration of MSCs after intratumoral and extratumoral implantations in a rat glioma model⁵⁸. No evidence of long distance MSC migration to the tumor site through either the corpus callosum to the contralateral hemisphere or through the striatum to the ipsilateral hemisphere was observed, suggesting the use of MSCs is limited to certain delivery routes. Intratumoral injection resulted in a dense and tumor specific distribution, as previously reported⁵⁹.

Biodegradable synthetic extracellular matrices (sECMs) have been used in various rodent models to provide mechanical support that promotes stem cell survival and differentiation into neurons^{60, 61}. Kauer *et al.* have evaluated the implantation of NSCs expressing sTRAIL encapsulated in sECM at the tumor cavity following tumor resection and found that the washout of NSCs by cerebrospinal fluid was reduced drastically³⁰. Both migratory stem cells and sTRAIL could leave the ECM environment and reach the tumor site, but increased retention at the tumor site and a subsequent increase in sTRAIL secretion was observed, suggesting that coating stem cells with ECM may be a highly successful strategy for treating GBM⁶².

ii. Factors that regulate glioma tropism

Stem cells are particularly attractive for glioma therapy due to their tropism to the tumor site. It is still not clear how this “homing mechanism” works, but growth factors and chemokines secreted or expressed by glioma cells are known to be important. Park *et al.* designed MSCs to overexpress the alpha chemokine receptor CXCR4⁶³, a receptor that specifically binds SDF1 α , a key cytokine mediator of glioma tropism

^{64, 65}. CXCR4 overexpression enhances the migratory capacity of MSCs to gliomas both *in vitro* and *in vivo*; inhibition of either SDF1 α or CXCR4 completely blocks migration. Kim *et al.* followed a similar approach and showed that upregulating of interleukin 8 (IL-8) secretion by glioma, or overexpression of the IL-8 receptor CXCR1 on the MSC surface, enhanced the migration capability of MSCs to the tumor. Inhibiting IL-8 significantly reduced migration, suggesting that CXCR1 is a major regulator in glioma tropism ⁶⁶. Velpula *et al.* showed that multiple cytokines are involved in recruiting MSCs to the glioma site, including IL-8, GRO, GRO α , MCP-1, and MCP-2 ⁶⁷, but more research is needed to completely unravel the mechanism of tumor site homing.

iii. Improved cellular vehicles

To date, the experimental use of ESCs for glioma therapy has been limited to the delivery of sTRAIL, owing to ethical, regulatory, and political concerns, and no recent studies have been published (Table 1) ⁶⁸. Recently, Lee *et al.* reported on the use of induced pluripotent stem cells (iPSCs) to generate NSCs ⁶⁹ and showed that in this context, iPSCs and ESCs are functionally equivalent, but iPSCs can be relatively easy to generate from somatic cells and are not burdened by the ethical concerns. In this study, iPSCs cells were generated by transducing primary mouse embryonic fibroblasts with four transcription factors, Oct-4, Sox 2, c-Myc and Klf4; by culturing iPSCs in monoculture, NSCs were generated. To test the functionality and potential use for glioma therapy, these NSCs were transduced with a baculovirus containing the HSV-TK gene and injected in the contralateral hemisphere of tumor-bearing mice. Prolonged survival and inhibition of tumor growth was observed, indicating that iPSC-derived NSCs possess all characteristics required to serve as a cellular carrier for glioma therapy. The same research group recently published a new study evaluating the use of human embryonic stem cells to generate NSCs ⁷⁰ in which the authors speculate that ESC-derived NSCs have the potential to produce limitless amounts of identical NSCs, while at the same time eliminating variability in the quality of therapeutic cells, allowing for better comparative analysis of different studies.

Endothelial progenitor cells are a subpopulation of hematopoietic stem cells that are known to migrate towards the neovasculature of certain cancers and integrate at the

tumor site and have also been studied as gene carriers for the treatment of glioma ⁷¹. Because EPCs can be easily collected from peripheral blood and display the appropriate tumor tropism, they make an interesting candidate for glioma stem cell-based therapy. Accumulation of EPCs at the tumor site has been confirmed by non-invasive imaging: Tc-99 single photon emission computed tomography (SPECT) and magnetic resonance imaging (MRI) imaging of EPCs transformed with the human sodium iodide symporter (hNIS) gene or ferumoxides-protamide sulphate (FePro), respectively. Using a novel inducible lentivirus expression system under the stress controlled HSP70B promoter, Noyan *et al.* reported a proof of principle study that used a HSC-based gene therapy method to treat solid tumors using immunotherapy ⁷². Hematopoietic stem and progenitor cells (HSPCs) were genetically modified to express the dominant negative mutant of the transforming growth factor-beta receptor II (T β RIIDN), which is known to neutralizes TGF- β signaling in the tumor microenvironment and can thereby suppress tumor cell metastasis (Figure 2) ⁷³. Mice received a bone marrow (BM) transplant with the modified HSPCs followed by subcutaneous injection of glioma cells. A massive antitumor immune response was reported and glioma tumor cell growth was prevented completely.

Table 1. Stem cell therapy against malignant gliomas

SC function	Approach	Transgene/modificati on strategy	Application	Refs
Cargo delivery	Cytokine	Expression of sTRAIL-luciferase fusion; NSC	Visualization of TRAIL-mediated therapy	27
		sTRAIL plus bortezomib; NSC	Glioma sensitization to TRAIL	32
		sTRAIL plus mTor inhibitor; NSC	Glioma sensitization to TRAIL	31
		sTRAIL; MSC	Proof of principle MSC-mediated TRAIL therapy	28, 29, 36
		IL-12 expression; MSC	Immunotherapy	37
	Enzyme/prodrug activation	aaTSP-1 expression; NSC	Anti-angiogenesis therapy	51
		rCE expression; NSC	SN-38 mediated therapy	46
		rCE expression; MSC	SN-38 mediated therapy	50
		Endostatin and/or carboxylesterase 2; MSC	Anti-angiogenesis therapy	49
		CD expression; NSC	5-FC therapy	45, 41, 11
		CD expression; MSC	5-FC therapy	43, 44
		HSV-TK and VPA; MSC	Enhanced efficacy of HSV-TK mediated therapy	42
		Oncolytic virus	CRAD-S-pk7 expression; NSC	Proof of principle
			Enhanced carrier system	52
	Nanoparticles	NP's loaded with coumarin 6; MSC	Proof of principle NP-mediated delivery system	53
		NP's loaded with Fc-diOH; MSC	NP delivery	54
NP's carrying silica nanorattle dox; MSC		NP delivery	55	
NSC delivery to glioma	Coating with sECM; NSC	Improved NSC delivery	30	
Enhancement of the SC model	Routes of administration	Intraventricular injections	Improved delivery mode	57
		Intratumoral vs extratumoral injections; MSC	Proof of principle; improved delivery mode	58
	Factors regulating tropism	CXCR 4 overexpression; MSC	Enhanced glioma tropism	63
		IL-8 and/or CXCR 1 overexpression; MSC	Enhanced glioma tropism	66
		Overexpression of various cytokines; MSC	Enhanced glioma tropism	67
	Improved cellular vehicles	IPSCs generated from embryonic fibroblasts; ESC	Proof of principle	69
		NSC differentiation; ESC	Proof of principle	70
		EPC; hNIS and FePro expression; HSC	Proof of principle; imaging	71
		TβRIIDN expression; HSC	Proof of principle; Immunotherapy	72

Abbreviations: MSC mesenchymal stem cell; NSC neural stem cell; ESC embryonic stem cell; HSC hematopoietic stem cell; NP nanoparticle; sTRAIL secretable tumor necrosis factor apoptosis-inducing ligand; IL-12 interleukin 12; Fc-diOH ferrociphenol; dox doxorubicin; HSV-TK herpes simplex virus thymidine kinase; VPA valproic acid; CD cytosine deaminase; rCE rabbit carboxylesterase; IL-8 interleukin 8; aaTSP-1 antiangiogenic protein thrombospondin; sECM synthetic extracellular matrix; iPSCs induced pluripotent stem cells; FePro ferumoxides-protamide sulphate; TβRIIDN Growth factor β-receptor II; 5-FC 5-fluorocytosine

Box 2. Glioma stem cell therapy in the clinic

City of Hope Hospital, NCT 01172964

In July 2010 the very first clinical trial using stem cells as therapeutics for malignant gliomas was started at the City of Hope Hospital, California. Patients with histologically confirmed grade III or IV glioma, or patients diagnosed with grade II glioma and radiographic findings of grade III/IV glioma were enrolled and had their tumor mass removed by craniotomy. At the time of debulking, they received intracranial injections with HB1F3.CD genetically modified neural stem cells (day zero). In the absence of disease progression or intolerance to the injected cells, patients received on day 4–10 oral dosages of 5-FC every six hours. Response to therapy, and adverse effects were evaluated by MRI on day 32, 60 and for every 2 months onwards. No results have been published yet, and as for now, 30 patients have been enrolled.

Study details as described on www.clinicaltrials.gov

- Primary Outcome Measures: determination of the safety and feasibility of intracerebral administration of genetically-modified neural stem cells (NSCs) in combination with oral 5-fluorocytosine.
- Secondary Outcome Measures: Relationship between intracerebral and systemic concentrations of 5-FC and 5-FU with increasing NSC dose level; Presence of 5-FU in the brain using 19F-MRS; Assessment of development of immunogenicity against NSCs; Obtain preliminary imaging data regarding perfusion permeability parameters and imaging characteristics as shown on magnetic resonance imaging (MRI) studies due to the presence of NSCs in the brain; Assessment of the fate of NSCs at autopsy when feasible

Clinical transition and/or obstacles to translation*i. Glioma stem cell therapy in the clinic*

Although a vast amount of interesting and exciting research is being explored using stem cells as a therapeutic strategy for malignant gliomas, most of these studies are being performed in the laboratory setting. This indicates that although the bench results are promising, translating these therapeutic strategies to the clinic remains difficult with only a single clinical trial in progress (Box 2, 3).

Box 3. Barriers to glioma therapy

Blood-brain barrier (BBB): The BBB consists of a lining of tight junctions between the endothelial cells of the brain capillaries. These tight junctions restrict the passage of molecules from the blood to the brain extra cellular matrix, allowing only certain substances to pass. Antibodies, antibiotics, chemotherapeutic agents, and some stem cells are unable to cross, severely limiting the potential of systemic therapy for glioma.

Blood-tumor barrier: Angiogenesis with leaky vessel formation, necrosis, and the highly heterogeneous character of the glioma cell population makes it very difficult to establish consistent distribution of vectors and other agents. Further, certain areas of the tumor are almost inaccessible, resulting in only a very limited effect of the applied therapeutics.

Tumor cells invasion in the brain: As gliomas progress and invade the brain, an extensive modulation of the extracellular matrix occurs. This phenomenon complicates curative surgery and radiotherapy considerably and results in tumor recurrence after surgical resection, often leading to patient death.

Secretion of local cytokines and growth factors that might induce malignant transformation in stem cells: Glioma cells are known to secrete a wide variety of chemokines and GF such as matrix metalloproteinases (MMPs), plasminogen tissue inhibitor 1 (PTI1), VEGF, EGF, FGF insulin growth factor 2 (IGF2), hepatocyte growth factor (HGF), and IL6 that are capable of initiating malignant transformation of nearby stem cells, recruiting them for contribution to tumor proliferation and growth. This is of particular concern when one actively introduces SC at the tumor site for glioma therapy and therefore extensive research needs to be done to address these safety issues.⁷⁴

Escaping immune surveillance: Glioma surface markers such as MCH surface expression are often downregulated allowing glioma cells not only to escape the host immune response, but also to protect themselves from newly designed drugs targeted specifically to glioma cells.⁷⁵

Resistance to therapies such as TRAIL: Malignant gliomas such as glioblastoma are known to acquire resistance to therapies. In the case for TRAIL-based therapy, upregulation of the Bcl2 associated Athanoge (BAG3) genes and multiple other genes have been described to cause resistance at various points along the apoptotic pathway. New research is focused at finding molecules that sensitize GBM cells to TRAIL.^{31, 32, 34}

Secretion of local immunosuppressants: This problem does not only hinder the efficacy of the host immune system against the tumor cells, but also makes it increasingly difficult to use immunotherapy for anti-glioma treatment.

At the City of Hope (California) by Aboody *et al.*, NSCs (HB1.F3-CD) genetically modified to express *E. coli* cytosine deaminase, which will convert the oral pro-drug 5-FC into the chemotherapeutic agent 5-FU at the tumor site, are being tested as was done in various animal models (Table 1) ^{11, 41, 43-45}. The modified NSCs are injected directly at the tumor site after surgical resection of the tumor mass. Oral 5-FC will be given every six hours between day 4 and day 10. Because NSCs have a strong tropism for glioma ^{10, 76}, no toxicity to normal brain cells is expected while efficient elimination of GBM cells is expected. The primary aim of this trial is to test the safety and feasibility of the NSC-CD system in humans, with secondary objective to evaluate immunogenicity and pharmacokinetics.

ii. Improving techniques for clinic/trials

A major limitation of stem cell therapy in general is safety. Stem cells possess many characteristics that make them well suited as cellular transport vehicles but their capacity for unlimited self-renewal raises several concerns regarding patient safety. Spontaneous tumor formation in longstanding MSC cultures has recently been reported, and it was shown that after implantation, a small fraction of immortalized NSCs continue to proliferate ^{10, 77}. A 2009 clinical trial by Amariglio *et al.* for the treatment of ataxia telangiectasia with NSC injection reported the formation of multiple brain tumors in a patient four years after treatment ⁷⁸. The standardized use of suicide genes such as CD for each stem cell line would theoretically minimize this risk.

Aside from malignant transformation of stem cells, the secretion of growth factors and chemokines, and the direct local immunosuppressive effect of stem cells may modify the tumor microenvironment in such a way that tumor growth is promoted. The latter has been reported in other solid tumors after injection with MSCs ^{74, 79, 80}, and MSCs have been shown to enhance the metastatic potential of breast cancer cells ⁸¹. The tumor promoting role of MSCs, however, remains in dispute; several studies report a glioma-suppressing effect of implanted MSCs ^{82, 83}, and MSCs used in the clinic to treat neurodegenerative diseases and stroke have been well tolerated with limited side effects. The discrepancy between various studies is yet another issue that needs to be solved before stem cell-based therapy can be successfully applied to glioma treatment in the clinic. For now, it remains very difficult to interpret study results and to compare data between various study groups,

given the large variability between the stem cells themselves and the methods employed by different groups. Better ways of cell selection and preparation are absolutely essential to design stable and identical cell lines that can create reproducible datasets and optimally functioning cell carrier systems, a characteristic that might be attributable to subgroups rather than the stem cell population as a whole. Furthermore, systematic comparison of stem cell migratory potential, the ability to target GSCs, survival, and efficacy of delivery are needed to identify the optimal carrier system and delivery route. Ahmed *et al.* recently reported that effective oncolytic virus delivery by NSCs was clearly superior to MSCs, although equivalent migration capacity was displayed⁸⁴. However, although many groups make use of the enzyme/prodrug combination of CD/5-FC in either NSCs or MSCs, no comparative studies have been performed, which is a missed opportunity in the quest for an optimal carrier system. Many more examples could be discussed, and until these issues are resolved, it seems to be overly optimistic to expect an easy transition of stem cell glioma therapy to the clinic. The ability to target glioma stem cells rather than glioma cells in general might prove to be a crucial point since these cells are thought to be the cause of tumor recurrence and patient death.

Translation is also slowed by concerns regarding several limitations of current glioma models used to test these strategies in the laboratory. Although many pathophysiological similarities between the rodent glioma model and human tumors are observed, many models are based on xenografts in immunocompromised mice. Implanted tumor cells will not mimic the process of *de novo* tumorigenesis, and tumor-associated immunosuppression and immune-modulating events are not likely to be accurately reflected, resulting in a slightly different tumor microenvironment. Doucette *et al.* have proposed overcoming this limitation by using an RCAS/Ntv-a glioma model in which endogenous glioma develop and acquire tumor and stromal features similar to human tumors⁸⁵. This may be an improvement over existing glioma models, but this study was also performed using immunocompromised mice, implying that many variables will remain unknown until clinical testing is completed.

To resolve some of these issues and obtain a true understanding of the working mechanism and antitumor effect of stem cell-based therapy, the development of adequate imaging tools is of the utmost importance. Not only do we need these tools to increase treatment efficacy, but the ability to track single stem cells and determine their fate, tropism, migration, interaction with the tumor

environment, and mechanism of action will answer important questions regarding safety and efficacy. Several imaging tools capable of tracking stem cells are currently available preclinically (e.g., bioluminescence imaging, fluorescence), but these techniques are not yet available for use in humans due to several concerns including (substrate) toxicity and sensitivity. Recently, Thu *et al.* developed a method to visualize NSCs by magnetic resonance imaging (MRI), using iron labeling (ferumoxide-protamine sulfate complex) of NSCs ⁸⁶, and Menon *et al.* reported similar results after labeling human MSCs with ferumoxide ⁸⁷; tumor tropism remained unaltered. Similar approaches might provide a solution that is easily translated to the clinic; however, more research is needed to fine tune these techniques for application in humans.

Whereas new imaging tools are necessary to develop stem cell therapy, the availability and efficacy of stem cells and whether they serve as vehicles for therapy or have a direct therapeutic effect are issues that also remain to be addressed. Malignant gliomas are a rapidly progressing and ever changing cancer, and if too much time is needed to obtain a certain number of stem cells, the tumor might have acquired resistance to the therapy being explored (e.g., chemotherapeutics, TRAIL, etc.). Furthermore, when stem cells are passaged too many times during expansion, differentiation and phenotypic changes may occur that limit their therapeutic potential. The use of stem cells might also be disputed due to ethical concerns. Limited availability hinders not only research opportunities but also limits the benefit of the potential approach, given that a working strategy that is not readily available cannot provide a cure. Techniques that allow for the rapid growth and expansion of cells while maintaining their characteristics are of extreme importance, as is optimal cell delivery to the tumor site. Whereas clinical studies opt for a direct intratumoral injection, preclinical experiments are testing intranodal, intradermal, intraventricular, or systemic injections in an attempt to enhance delivery success.

iii. Appropriate patient selection - when will this method work?

Patient selection may play an important role in the efficacy of the chosen therapeutic approach. More and more evidence suggest that specific genetic mutations in glioma cells respond to different therapies, and therefore genotyping or discovery of new biomarkers for personalized medicine could yield to an enhanced treatment success. An example would be the status of O6- methylguanine DNA transferrase or MGMT,

a DNA repair enzyme that protects cells from damage caused by ionizing radiation and alkylating agents. The MGMT promoter is methylated in 40 to 45% of GBMs, which means the cells are unable to properly repair DNA damage^{88, 89}. This group might benefit much more from a prodrug/enzyme-based approach as compared to patients without a methylated MGMT promoter tumor. Also, it is known that patients with an EGFR amplification rarely respond to chemotherapy at all, suggesting that the benefit of a CD/5-FC approach in this group will be minimal. This may not only potentially downplay the overall efficacy of this therapy, but may also falsely disqualify a successful approach by showing that results obtained in experimental studies cannot be repeated in the clinic.

TRAIL plays an important role in the experimental design of stem cell-based therapy against gliomas, however, the use of this therapeutic is not (yet) reflected in clinical trials. Some clinical studies using TRAIL for treating various cancers can be found, but, except for a small subset of patients, the therapeutic results of administering TRAIL have been disappointing and do not reflect the results obtained in animal models^{90, 91}. Finding ways to identify the subgroup of patients that are responsive to TRAIL therapy or the discovery of adjuvants that help sensitize gliomas and other cancer cells to TRAIL might be needed before taking additional steps towards the clinic. With the discovery of lanatoside C as a TRAIL sensitizer, one of these hurdles has been overcome and since both agents are FDA-approved and have been used in the clinic separately, we expect a short transition to the first clinical trial. However, a proper comparison between carrier types and injection routes in experimental setting will be necessary to give this strategy a fair shot.

Conclusions

Stem cells provide a highly promising and innovative approach for the treatment of malignant gliomas. Provided that some of the discussed issues/limitations can be addressed, this therapeutic strategy could become of tremendous value in the search for a cure for tumors as heterogeneous and as difficult to reach as glioblastoma. Other exciting strategies such as gene therapy and oncolytic viral therapy, which by themselves have failed to establish clinically-relevant antitumor effects, are now given a second chance to prove their value for the treatment of brain

tumors. The combined approach of stem cells and gene/viral therapy has the potential to be of great benefit for glioma patients, and in this role, stem cell therapy could be used alongside surgery, chemotherapy, and radiation therapy, complementing each other to create a highly effective, integral antitumor therapy.

ACKNOWLEDGEMENTS

Dr. Tannous is supported by grants from the National Institutes of Health, the *National Institute of Neurological Disorders and Stroke*_([1R01NS064983](#)). The authors would like to thank Mr. Romain Amante for assistance in drawing Figure 2.

REFERENCES

1. Johnson DR, Ma DJ, Buckner JC, Hammack JE. (2012). Conditional probability of long-term survival in glioblastoma: A population-based analysis. *Cancer*.
2. Grossman SA, Ye X, Piantadosi S, Desideri S, Nabors LB, Rosenfeld M, et al. (2010). Survival of patients with newly diagnosed glioblastoma treated with radiation and temozolomide in research studies in the United States. *Clin Cancer Res*.16(8):2443-2449.
3. Furnari FB, Fenton T, Bachoo RM, Mukasa A, Stommel JM, Stegh A, et al. (2007). Malignant astrocytic glioma: genetics, biology, and paths to treatment. *Genes Dev*.21(21):2683-2710.
4. Hochberg FH, Pruitt A. (1980). Assumptions in the radiotherapy of glioblastoma. *Neurology*.30(9):907-911.
5. Okamoto Y, Di Patre PL, Burkhard C, Horstmann S, Jourde B, Fahey M, et al. (2004). Population-based study on incidence, survival rates, and genetic alterations of low-grade diffuse astrocytomas and oligodendrogliomas. *Acta Neuropathol*.108(1):49-56.
6. Calabrese C, Poppleton H, Kocak M, Hogg TL, Fuller C, Hamner B, et al. (2007). A perivascular niche for brain tumor stem cells. *Cancer Cell*.11(1):69-82.
7. Singh SK, Clarke ID, Terasaki M, Bonn VE, Hawkins C, Squire J, et al. (2003). Identification of a cancer stem cell in human brain tumors. *Cancer Res*.63(18):5821-5828.
8. Bao S, Wu Q, Sathornsumetee S, Hao Y, Li Z, Hjelmeland AB, et al. (2006). Stem cell-like glioma cells promote tumor angiogenesis through vascular endothelial growth factor. *Cancer Res*.66(16):7843-7848.
9. Chalmers AJ. (2007). Radioresistant glioma stem cells--therapeutic obstacle or promising target? *DNA Repair (Amst)*.6(9):1391-1394.
10. Aboody KS, Brown A, Rainov NG, Bower KA, Liu S, Yang W, et al. (2000). Neural stem cells display extensive tropism for pathology in adult brain: evidence from intracranial gliomas. *Proc Natl Acad Sci U S A*.97(23):12846-12851.
11. Joo KM, Park IH, Shin JY, Jin J, Kang BG, Kim MH, et al. (2009). Human neural stem cells can target and deliver therapeutic genes to breast cancer brain metastases. *Mol Ther*.17(3):570-575.
12. Aboody KS, Bush RA, Garcia E, Metz MZ, Najbauer J, Justus KA, et al. (2006). Development of a tumor-selective approach to treat metastatic cancer. *PLoS One*.1:e23.
13. Einstein O, Ben-Hur T. (2008). The changing face of neural stem cell therapy in neurologic diseases. *Arch Neurol*.65(4):452-456.
14. Ahmed AU, Thaci B, Alexiades NG, Han Y, Qian S, Liu F, et al. (2011). Neural stem cell-based cell carriers enhance therapeutic efficacy of an oncolytic adenovirus in an orthotopic mouse model of human glioblastoma. *Mol Ther*.19(9):1714-1726.
15. Picinich SC, Mishra PJ, Mishra PJ, Glod J, Banerjee D. (2007). The therapeutic potential of mesenchymal stem cells. Cell- & tissue-based therapy. *Expert Opin Biol Ther*.7(7):965-973.

16. Caplan AI. (2009). Why are MSCs therapeutic? New data: new insight. *J Pathol.*217(2):318-324.
17. Jones BJ, McTaggart SJ. (2008). Immunosuppression by mesenchymal stromal cells: from culture to clinic. *Exp Hematol.*36(6):733-741.
18. Keller G. (2005). Embryonic stem cell differentiation: emergence of a new era in biology and medicine. *Genes Dev.*19(10):1129-1155.
19. Germano IM, Uzzaman M, Keller G. (2008). Gene delivery by embryonic stem cells for malignant glioma therapy: hype or hope? *Cancer Biol Ther.*7(9):1341-1347.
20. Gerecht-Nir S, Itskovitz-Eldor J. (2004). Human embryonic stem cells: a potential source for cellular therapy. *Am J Transplant.*4 Suppl 6:51-57.
21. Tabatabai G, Bahr O, Mohle R, Eyupoglu IY, Boehmler AM, Wischhusen J, et al. (2005). Lessons from the bone marrow: how malignant glioma cells attract adult haematopoietic progenitor cells. *Brain.*128(Pt 9):2200-2211.
22. Tabatabai G, Herrmann C, von Kurthy G, Mittelbronn M, Grau S, Frank B, et al. (2008). VEGF-dependent induction of CD62E on endothelial cells mediates glioma tropism of adult haematopoietic progenitor cells. *Brain.*131(Pt 10):2579-2595.
23. Yuan SH, Martin J, Elia J, Flippin J, Paramban RI, Hefferan MP, et al. (2011). Cell-surface marker signatures for the isolation of neural stem cells, glia and neurons derived from human pluripotent stem cells. *PLoS One.*6(3):e17540.
24. Zhang SC, Wernig M, Duncan ID, Brustle O, Thomson JA. (2001). In vitro differentiation of transplantable neural precursors from human embryonic stem cells. *Nat Biotechnol.*19(12):1129-1133.
25. Miller JS, McCullar V, Punzel M, Lemischka IR, Moore KA. (1999). Single adult human CD34(+)/Lin-/CD38(-) progenitors give rise to natural killer cells, B-lineage cells, dendritic cells, and myeloid cells. *Blood.*93(1):96-106.
26. Higuchi A, Ling QD, Ko YA, Chang Y, Umezawa A. (2011). Biomaterials for the feeder-free culture of human embryonic stem cells and induced pluripotent stem cells. *Chem Rev.*111(5):3021-3035.
27. Hingtgen SD, Kasmieh R, van de Water J, Weissleder R, Shah K. (2010). A novel molecule integrating therapeutic and diagnostic activities reveals multiple aspects of stem cell-based therapy. *Stem Cells.*28(4):832-841.
28. Sasportas LS, Kasmieh R, Wakimoto H, Hingtgen S, van de Water JA, Mohapatra G, et al. (2009). Assessment of therapeutic efficacy and fate of engineered human mesenchymal stem cells for cancer therapy. *Proc Natl Acad Sci U S A.*106(12):4822-4827.
29. Menon LG, Kelly K, Yang HW, Kim SK, Black PM, Carroll RS. (2009). Human bone marrow-derived mesenchymal stromal cells expressing S-TRAIL as a cellular delivery vehicle for human glioma therapy. *Stem Cells.*27(9):2320-2330.
30. Kauer TM, Figueiredo JL, Hingtgen S, Shah K. (2012). Encapsulated therapeutic stem cells implanted in the tumor resection cavity induce cell death in gliomas. *Nat Neurosci.*15(2):197-204.
31. Bagci-Onder T, Wakimoto H, Anderegg M, Cameron C, Shah K. (2011). A dual PI3K/mTOR inhibitor, PI-103, cooperates with stem cell-delivered TRAIL in experimental glioma models. *Cancer Res.*71(1):154-163.
32. Balyasnikova IV, Ferguson SD, Han Y, Liu F, Lesniak MS. (2011). Therapeutic effect of neural stem cells expressing TRAIL and bortezomib in mice with glioma xenografts. *Cancer Lett.*310(2):148-159.

33. Badr CE, Niers JM, Morse D, Koelen JA, Vandertop P, Noske D, et al. (2011). Suicidal gene therapy in an NF-kappaB-controlled tumor environment as monitored by a secreted blood reporter. *Gene Ther.*18(5):445-451.
34. Badr CE, Wurdinger T, Tannous BA. (2011). Functional drug screening assay reveals potential glioma therapeutics. *Assay Drug Dev Technol.*9(3):281-289.
35. Shah K, Tung CH, Yang K, Weissleder R, Breakefield XO. (2004). Inducible release of TRAIL fusion proteins from a proapoptotic form for tumor therapy. *Cancer Res.*64(9):3236-3242.
36. Choi SA, Hwang SK, Wang KC, Cho BK, Phi JH, Lee JY, et al. (2011). Therapeutic efficacy and safety of TRAIL-producing human adipose tissue-derived mesenchymal stem cells against experimental brainstem glioma. *Neuro Oncol.*13(1):61-69.
37. Ryu CH, Park SH, Park SA, Kim SM, Lim JY, Jeong CH, et al. (2011). Gene therapy of intracranial glioma using interleukin 12-secreting human umbilical cord blood-derived mesenchymal stem cells. *Hum Gene Ther.*22(6):733-743.
38. Takamiya Y, Short MP, Ezzeddine ZD, Moolten FL, Breakefield XO, Martuza RL. (1992). Gene therapy of malignant brain tumors: a rat glioma line bearing the herpes simplex virus type 1-thymidine kinase gene and wild type retrovirus kills other tumor cells. *J Neurosci Res.*33(3):493-503.
39. Rath P, Shi H, Maruniak JA, Litofsky NS, Maria BL, Kirk MD. (2009). Stem cells as vectors to deliver HSV/tk gene therapy for malignant gliomas. *Curr Stem Cell Res Ther.*4(1):44-49.
40. Ezzeddine ZD, Martuza RL, Platika D, Short MP, Malick A, Choi B, et al. (1991). Selective killing of glioma cells in culture and in vivo by retrovirus transfer of the herpes simplex virus thymidine kinase gene. *New Biol.*3(6):608-614.
41. Lee SJ, Kim Y, Jo MY, Kim HS, Jin Y, Kim SU, et al. (2011). Combined treatment of tumor-tropic human neural stem cells containing the CD suicide gene effectively targets brain tumors provoking a mild immune response. *Oncol Rep.*25(1):63-68.
42. Ryu CH, Park KY, Kim SM, Jeong CH, Woo JS, Hou Y, et al. (2012). Valproic acid enhances anti-tumor effect of mesenchymal stem cell mediated HSV-TK gene therapy in intracranial glioma. *Biochem Biophys Res Commun.*421(3):585-590.
43. Fei S, Qi X, Kedong S, Guangchun J, Jian L, Wei Q. (2012). The antitumor effect of mesenchymal stem cells transduced with a lentiviral vector expressing cytosine deaminase in a rat glioma model. *J Cancer Res Clin Oncol.*138(2):347-357.
44. Kosaka H, Ichikawa T, Kurozumi K, Kambara H, Inoue S, Maruo T, et al. (2012). Therapeutic effect of suicide gene-transferred mesenchymal stem cells in a rat model of glioma. *Cancer Gene Ther.*19(8):572-578.
45. Kim JH, Kim JY, Kim SU, Cho KG. (2012). Therapeutic effect of genetically modified human neural stem cells encoding cytosine deaminase on experimental glioma. *Biochem Biophys Res Commun.*417(1):534-540.
46. Lim SH, Choi SA, Lee JY, Wang KC, Phi JH, Lee DH, et al. (2011). Therapeutic targeting of subdural medulloblastomas using human neural stem cells expressing carboxylesterase. *Cancer Gene Ther.*18(11):817-824.
47. Zhao D, Najbauer J, Annala AJ, Garcia E, Metz MZ, Gutova M, et al. (2012). Human neural stem cell tropism to metastatic breast cancer. *Stem Cells.*30(2):314-325.

48. Folkins C, Shaked Y, Man S, Tang T, Lee CR, Zhu Z, et al. (2009). Glioma tumor stem-like cells promote tumor angiogenesis and vasculogenesis via vascular endothelial growth factor and stromal-derived factor 1. *Cancer Res.*69(18):7243-7251.
49. Yin J, Kim JK, Moon JH, Beck S, Piao D, Jin X, et al. (2011). hMSC-mediated concurrent delivery of endostatin and carboxylesterase to mouse xenografts suppresses glioma initiation and recurrence. *Mol Ther.*19(6):1161-1169.
50. Choi SA, Lee JY, Wang KC, Phi JH, Song SH, Song J, et al. (2012). Human adipose tissue-derived mesenchymal stem cells: characteristics and therapeutic potential as cellular vehicles for prodrug gene therapy against brainstem gliomas. *Eur J Cancer.*48(1):129-137.
51. van Eekelen M, Sasportas LS, Kasmieh R, Yip S, Figueiredo JL, Louis DN, et al. (2010). Human stem cells expressing novel TSP-1 variant have anti-angiogenic effect on brain tumors. *Oncogene.*29(22):3185-3195.
52. Thaci B, Ahmed AU, Ulasov IV, Tobias AL, Han Y, Aboody KS, et al. (2012). Pharmacokinetic study of neural stem cell-based cell carrier for oncolytic virotherapy: targeted delivery of the therapeutic payload in an orthotopic brain tumor model. *Cancer Gene Ther.*19(6):431-442.
53. Roger M, Clavreul A, Venier-Julienne MC, Passirani C, Sindji L, Schiller P, et al. (2010). Mesenchymal stem cells as cellular vehicles for delivery of nanoparticles to brain tumors. *Biomaterials.*31(32):8393-8401.
54. Roger M, Clavreul A, Huynh NT, Passirani C, Schiller P, Vessieres A, et al. (2012). Ferrociphenol lipid nanocapsule delivery by mesenchymal stromal cells in brain tumor therapy. *Int J Pharm.*423(1):63-68.
55. Li L, Guan Y, Liu H, Hao N, Liu T, Meng X, et al. (2011). Silica nanorattle-doxorubicin-anchored mesenchymal stem cells for tumor-tropic therapy. *ACS Nano.*5(9):7462-7470.
56. Ahmed AU, Lesniak MS. (2011). Glioblastoma multiforme: can neural stem cells deliver the therapeutic payload and fulfill the clinical promise? *Expert Rev Neurother.*11(6):775-777.
57. Panciani PF, Fontanella M, Tamagno I, Battaglia L, Garbossa D, Inghirami G, et al. (2012). Stem cells based therapy in high grade glioma: why the intraventricular route should be preferred? *J Neurosurg Sci.*56(3):221-229.
58. Bexell D, Gunnarsson S, Svensson A, Tormin A, Henriques-Oliveira C, Siesjo P, et al. (2012). Rat multipotent mesenchymal stromal cells lack long-distance tropism to 3 different rat glioma models. *Neurosurgery.*70(3):731-739.
59. Bexell D, Gunnarsson S, Tormin A, Darabi A, Gisselsson D, Roybon L, et al. (2009). Bone marrow multipotent mesenchymal stroma cells act as pericyte-like migratory vehicles in experimental gliomas. *Mol Ther.*17(1):183-190.
60. Pan L, Ren Y, Cui F, Xu Q. (2009). Viability and differentiation of neural precursors on hyaluronic acid hydrogel scaffold. *J Neurosci Res.*87(14):3207-3220.
61. Teng YD, Lavik EB, Qu X, Park KI, Ourednik J, Zurakowski D, et al. (2002). Functional recovery following traumatic spinal cord injury mediated by a unique polymer scaffold seeded with neural stem cells. *Proc Natl Acad Sci U S A.*99(5):3024-3029.
62. Flight MH. (2012). Drug delivery: Encapsulation improves therapeutic stem cell action. *Nat Rev Drug Discov.*11(2):106.

63. Park SA, Ryu CH, Kim SM, Lim JY, Park SI, Jeong CH, et al. (2011). CXCR4-transfected human umbilical cord blood-derived mesenchymal stem cells exhibit enhanced migratory capacity toward gliomas. *Int J Oncol.*38(1):97-103.
64. Luo Y, Cai J, Xue H, Miura T, Rao MS. (2005). Functional SDF1 alpha/CXCR4 signaling in the developing spinal cord. *J Neurochem.*93(2):452-462.
65. Bakondi B, Shimada IS, Peterson BM, Spees JL. (2011). SDF-1alpha secreted by human CD133-derived multipotent stromal cells promotes neural progenitor cell survival through CXCR7. *Stem Cells Dev.*20(6):1021-1029.
66. Kim SM, Kim DS, Jeong CH, Kim DH, Kim JH, Jeon HB, et al. (2011). CXCR4 chemokine receptor 1 enhances the ability of human umbilical cord blood-derived mesenchymal stem cells to migrate toward gliomas. *Biochem Biophys Res Commun.*407(4):741-746.
67. Velpula KK, Dasari VR, Rao JS. (2012). The homing of human cord blood stem cells to sites of inflammation: Unfolding mysteries of a novel therapeutic paradigm for glioblastoma multiforme. *Cell Cycle.*11(12):2303-2313.
68. Germano IM, Uzzaman M, Benveniste RJ, Zaurava M, Keller G. (2006). Apoptosis in human glioblastoma cells produced using embryonic stem cell-derived astrocytes expressing tumor necrosis factor-related apoptosis-inducing ligand. *J Neurosurg.*105(1):88-95.
69. Lee EX, Lam DH, Wu C, Yang J, Tham CK, Ng WH, et al. (2011). Glioma gene therapy using induced pluripotent stem cell derived neural stem cells. *Mol Pharm.*8(5):1515-1524.
70. Zhao Y, Lam DH, Yang J, Lin J, Tham CK, Ng WH, et al. (2012). Targeted suicide gene therapy for glioma using human embryonic stem cell-derived neural stem cells genetically modified by baculoviral vectors. *Gene Ther.*19(2):189-200.
71. Varma NR, Janic B, Iskander AS, Shankar A, Bhuiyan MP, Soltanian-Zadeh H, et al. (2012). Endothelial progenitor cells (EPCs) as gene carrier system for rat model of human glioma. *PLoS One.*7(1):e30310.
72. Noyan F, Diez IA, Hapke M, Klein C, Dewey RA. (2012). Induced transgene expression for the treatment of solid tumors by hematopoietic stem cell-based gene therapy. *Cancer Gene Ther.*19(5):352-357.
73. Shah AH, Tabayoyong WB, Kundu SD, Kim SJ, Van Parijs L, Liu VC, et al. (2002). Suppression of tumor metastasis by blockade of transforming growth factor beta signaling in bone marrow cells through a retroviral-mediated gene therapy in mice. *Cancer Res.*62(24):7135-7138.
74. Spaeth EL, Dembinski JL, Sasser AK, Watson K, Klopp A, Hall B, et al. (2009). Mesenchymal stem cell transition to tumor-associated fibroblasts contributes to fibrovascular network expansion and tumor progression. *PLoS One.*4(4):e4992.
75. Tran CT, Wolz P, Egensperger R, Kosel S, Imai Y, Bise K, et al. (1998). Differential expression of MHC class II molecules by microglia and neoplastic astroglia: relevance for the escape of astrocytoma cells from immune surveillance. *Neuropathol Appl Neurobiol.*24(4):293-301.
76. Brown AB, Yang W, Schmidt NO, Carroll R, Leishear KK, Rainov NG, et al. (2003). Intravascular delivery of neural stem cell lines to target intracranial and extracranial tumors of neural and non-neural origin. *Hum Gene Ther.*14(18):1777-1785.

77. Liu J, Zhang Y, Bai L, Cui X, Zhu J. (2012). Rat bone marrow mesenchymal stem cells undergo malignant transformation via indirect co-cultured with tumour cells. *Cell Biochem Funct.*
78. Amariglio N, Hirshberg A, Scheithauer BW, Cohen Y, Loewenthal R, Trakhtenbrot L, et al. (2009). Donor-derived brain tumor following neural stem cell transplantation in an ataxia telangiectasia patient. *PLoS Med.*6(2):e1000029.
79. Djouad F, Plence P, Bony C, Tropel P, Apparailly F, Sany J, et al. (2003). Immunosuppressive effect of mesenchymal stem cells favors tumor growth in allogeneic animals. *Blood.*102(10):3837-3844.
80. Houghton J, Stoicov C, Nomura S, Rogers AB, Carlson J, Li H, et al. (2004). Gastric cancer originating from bone marrow-derived cells. *Science.*306(5701):1568-1571.
81. Karnoub AE, Dash AB, Vo AP, Sullivan A, Brooks MW, Bell GW, et al. (2007). Mesenchymal stem cells within tumour stroma promote breast cancer metastasis. *Nature.*449(7162):557-563.
82. Kucerova L, Matuskova M, Hlubinova K, Altanerova V, Altaner C. (2010). Tumor cell behaviour modulation by mesenchymal stromal cells. *Mol Cancer.*9:129.
83. Nakamura K, Ito Y, Kawano Y, Kurozumi K, Kobune M, Tsuda H, et al. (2004). Antitumor effect of genetically engineered mesenchymal stem cells in a rat glioma model. *Gene Ther.*11(14):1155-1164.
84. Ahmed AU, Tyler MA, Thaci B, Alexiades NG, Han Y, Ulasov IV, et al. (2011). A comparative study of neural and mesenchymal stem cell-based carriers for oncolytic adenovirus in a model of malignant glioma. *Mol Pharm.*8(5):1559-1572.
85. Doucette T, Rao G, Yang Y, Gumin J, Shinojima N, Bekele BN, et al. (2011). Mesenchymal stem cells display tumor-specific tropism in an RCAS/Ntv-a glioma model. *Neoplasia.*13(8):716-725.
86. Thu MS, Najbauer J, Kendall SE, Harutyunyan I, Sangalang N, Gutova M, et al. (2009). Iron labeling and pre-clinical MRI visualization of therapeutic human neural stem cells in a murine glioma model. *PLoS One.*4(9):e7218.
87. Menon LG, Pratt J, Yang HW, Black PM, Sorensen GA, Carroll RS. (2012). Imaging of human mesenchymal stromal cells: homing to human brain tumors. *J Neurooncol.*107(2):257-267.
88. Louis DN, Pomeroy SL, Cairncross JG. (2002). Focus on central nervous system neoplasia. *Cancer Cell.*1(2):125-128.
89. Cairncross G, Macdonald D, Ludwin S, Lee D, Cascino T, Buckner J, et al. (1994). Chemotherapy for anaplastic oligodendroglioma. National Cancer Institute of Canada Clinical Trials Group. *J Clin Oncol.*12(10):2013-2021.
90. Aboody K, Capela A, Niazi N, Stern JH, Temple S. (2011). Translating stem cell studies to the clinic for CNS repair: current state of the art and the need for a Rosetta Stone. *Neuron.*70(4):597-613.
91. Tabatabai G, Wick W, Weller M. (2011). Stem cell-mediated gene therapies for malignant gliomas: a promising targeted therapeutic approach? *Discov Med.*11(61):529-536.

CHAPTER XII



Cell-based immunotherapy against gliomas: from bench to bedside

M. Sarah S. Bovenberg^{1,2,3*}, M. Hannah Degeling^{1,2,3*}, and Bakhos A. Tannous^{1,2}

¹Experimental Therapeutics and Molecular Imaging Laboratory, Neuroscience Center, Department of Neurology,
²Program in Neuroscience, Harvard Medical School, Boston, MA 02114 USA. ³Department of Neurosurgery,
Leiden University Medical Center, Leiden, The Netherlands. * These authors contributed equally

ABSTRACT

Glioblastoma (GBM) comprises 51% of all gliomas and is the most malignant form of brain tumors with a median survival of 18-21 months. Standard-of-care treatment includes maximal surgical resection of the tumor mass in combination with radiation and chemotherapy; however, as the poor survival rate indicates, these treatments have not been effective in preventing disease progression. Cellular Immunotherapy is currently being explored as an adjuvant experimental therapeutic approach to treat malignant brain tumors. In this review, we discuss advances in active, passive, and vaccine immunotherapeutic strategies for gliomas both at the bench and in the clinic.

INTRODUCTION

Gliomas account for about 60% of all primary central nervous system tumors. Glioblastoma (GBM) which comprises 51.2% of all gliomas is the most malignant form with a 2 years survival rate of 40% and a median survival of 18-21 months.^{1, 2} Current standard of care includes surgical debulking of the tumor mass, followed by radiation and chemotherapy (temozolomide);³ however, as the poor survival rate indicates, these treatments have not been effective in preventing disease progression. The location of malignant gliomas (the brain) and their invasive properties cause complete surgical resection of the tumor mass nearly impossible, while high doses of radiotherapy cannot be delivered due to potential damage to the normal brain. Chemotherapeutics often cannot cross the blood-brain barrier efficiently and gliomas are known to develop resistance along these treatment regimen.⁴⁻⁸

Cellular therapy is based on the idea of introducing a specific cell type into a particular tissue to treat the disease. Its earliest application can be dated back into the fifties where it was used in the bone marrow transplantation field.^{9, 10} Currently, a broader spectrum of cellular therapy application is pursued. Different cell types are used in replacement therapies, taking over the function of diseased cells in the target organ, as can be seen in diabetes where insulin producing cells are injected in order to replace their malfunctioning originals in the pancreas.^{11, 12} Tissue engineering in

which *ex vivo* whole organs are recreated out of cells is in its early phase but holds a tremendous potential for the future.¹³ An example that found its way to the clinic is artificial skin grown from collagen scaffolds seeded with the patient's own epidermal skin cells.¹⁴ This technique is FDA-approved and has shown to drastically improve the life of patients with burn injuries. While both replacement therapy and tissue engineering focus on the use of cells for their inherent function (e.g. myoblast for the generation of muscle tissue), other research is focusing on the application of cells for tasks outside of their preprogrammed function profile. For instance, stem cells or immune cells can be used for immunotherapy or as carriers of therapeutic genes or pro-drugs that gets activated at a specific location in the body. This cell-based therapy provides a new and interesting strategy for the treatment of cancer including brain tumors. Cellular Immunotherapy in particular has the potential to both specifically target brain tumor cells (and thereby limiting brain damage), and to establish a long term antitumor response by stimulating the immune system, and thus is being explored as an alternative therapy for gliomas. Currently, a wide range of strategies is investigated at the bench, while slowly but steadily a small portion of this research is transitioned to the clinic. In this review, we cover recent advances in the field of Immuno-cellular therapy for malignant gliomas both in the early experimental phase as well as in the clinical setting.

EXPERIMENTAL IMMUNO-CELL THERAPY

Over the last decade, extensive studies have been performed evaluating the use of modified immune cells as a potential therapeutic approach for gliomas. *In vivo* glioma xenografts of intracranial or subcutaneously-injected cells as well as spontaneously-induced gliomas are widely used and commonly accepted models that depict an accurate and reproducible tumor environment in rodents. Histopathological changes as pseudopallisade necrosis, glomeruloid vascular hyperplasia, and infiltrating cells mimic those found in human gliomas.¹⁵ In this section, we discuss experimental approaches using a variety of cells to boost the immune system and to establish a potent immune response against malignant brain tumors.

Overview of immuno-cell therapy. Cellular immunotherapy is based on the use of cells from the innate and adaptive immune system to elicit an antitumor response. Either passive or active immunotherapy can be pursued. Passive immunotherapy involves the *ex vivo* activation of immune cells, which are subsequently injected back into the patient to attack the tumor directly. Often, these cells are not only activated, but also genetically modified to have enhanced antitumor properties. This approach has proven to be successful, but has the limitation of lacking prolonged or continuous antitumor response. Recent studies are focusing towards active immunotherapy or a combination of both. Active immunotherapy relies on the activation of the endogenous immune system either by vaccines or *ex vivo* activated cells. This approach allows for long-term antitumor effect, which not only enhances the likelihood of the tumor being eradicated, but also decreases the risk of tumor recurrence. T-cells, dendritic cells, and macrophages are the cells of choice for this therapeutic strategy (Table1; Box1).

Cell type	Transgene/modification strategy	Application	References
T cells	Anti-HER2 receptor	Anti-glioma immunotherapy, evaluation of associated autoimmune pathology	16
	HER2-CAR	Anti-glioma immunotherapy; evaluation of enhanced CAR-mediated tumor cell recognition.	17
	IL13Ra2	Anti-GSC immunotherapy	18
Dendritic cells (DC)	IL13Ra2	Anti-GSC immunotherapy; more efficient expression of antigens at MHC level	19
	Ad-Fit3L/Ad-TK	Anti-glioma viral therapy; more efficient delivery and enhanced viral distribution at the tumor site.	20
	CSC antigen load	Anti-glioma immunotherapy; enhanced antitumor response	21
Macrophages	Nanoshell load	Photothermal-mediated glioma therapy; proof of concept of macrophage as delivery vehicles for NS	22

Table 1 Overview of experimental immuno-cell therapy against gliomas

Abbreviations: HER2, human epidermal growth factor receptor 2; CAR, chimeric antigen receptor; IL13Ra2, interleukin-13 zetakine 2; Ad-Fit3L/Ad-TK, adenovirus expressing Fit3L/TK; CSCs, cancer stem cells; NS, nanoshell

Box 1 Cells used for immune-cellular therapy

T Cells or T-lymphocytes are part of the white blood cell compartment and play an important role in the cell-mediated immunity. Hallmark of these cells is expression of the T Cell Receptor (TCR) on their surface. Several subtypes of T Cells do exist, all with a different role in the adaptive immune response. **CD4 lymphocytes**, or T helper lymphocytes are the mediators of the immune system. Once activated by encounter of antigen presenting cells (APCs) expressing antigens in the MHC class II, they start secreting cytokines that in turn activate cytotoxic T lymphocytes (CTL) and macrophages, helping differentiation of B cells into plasma cells, initiating a humoral immune response. CTLs, or **CD8 T Lymphocytes** are responsible for direct cell mediated killing. They recognize their target by binding to antigens expressed by MCH class I complex, found on the surface of virtually every cell in the body. Their main targets are cells infected with virus, transplants, and tumor cells. The last group of T lymphocytes are the **Natural Killer T Cells** (NKTs). These cells are very similar to NK cells (natural killer cells) of the innate immune system. Their job is to recognize glycolipid antigen expressed by CD1d. Once activated, they can differentiate into either T helper lymphocytes or cytotoxic T lymphocytes, initiating both a cytokine mediated and direct cytolytic immune response.

Macrophages play an important role in the immune response. They can be recognized by surface expression of CD14, CD40, CD11b, lysozyme M, Mac1/3 and CD68. They originate from monocytes, which, once activated through local inflammatory factors, starts differentiating. Macrophages play a role in both in innate and adaptive immune system, in which they have three distinct roles. They phagocytose pathogens and cellular debris, cleaning the inflammation site; these cells present the digested pathogens in MHC class II, thereby stimulating CD4 lymphocytes, and they secrete various local monokines and interleukins, creating a strong chemotactic environment for T cells.

Dendritic Cells function as APCs, just like macrophages. Their hallmark is expression of the toll like receptor (TLR). They are present in skin, respiratory and gastro-intestinal tract, patrolling all tissues in contact with the external environment. Once a pathogen is encountered, migration towards the lymph nodes occurs, where they present their pathogen to B and T lymphocytes. DCs are the only APCs capable of presenting antigens both through the MHC class I and class II pathways, thereby stimulating B cells, CD4 T lymphocytes and CD8 lymphocytes. Additionally, these cells are capable of secreting cytokines that further enhance differentiation of surrounding immune cells.

T cell-based immunotherapy. T cells are often used as cellular vehicles for the treatment of different types of cancer, typically resistant to conventional therapy. These cells can be easily modified with tumor-specific antigens to target tumor cells. An interesting strategy in T cell-based immunotherapy is the use of chimeric antigen receptors (CARs). CARs combine the antigen-binding domain of antibodies with the ζ chain of T cell receptors, creating an increased binding between the T cell and the tumor antigen. In a proof-of-concept study, Wang et al.,¹⁶ showed that CD8⁺ T cells can become tumor-specific when directed towards a tumor epitope such as the human epidermal growth factor receptor 2 (HER2), overexpressed in tumors versus normal tissues. Gene-engineered T-cells to express anti-HER2 chimeric receptor were intravenously transferred in combination with lymph ablation and interleukin-2 (IL-2). The autoimmune effect had no significant toxicity on normal mammary and brain tissues expressing HER2, while antitumor effect could be demonstrated, indicating that the modified T cells were specific to the tumor. Nakazawa et al.,¹⁷ similarly combined HER2 and CARs to modify a T cell population, creating a functional HER2 chimeric antigen receptor (HER2-CAR). Although HER2 is overexpressed by many different tumors, including malignant gliomas, the expression is often too low to be recognized by T cells. Intratumoral injection of CARs demonstrated efficient killing of tumor cells *in vivo*, including the CD133-positive glioma stem-like cells (GSC; also known as tumor initiating cells-resistant to chemo- and radiotherapy), and increased survival rate.²³ The challenge of this therapeutic strategy is to establish stable expression of the activated antigen while achieving enough expansion with nonspecific activated T cells (ATC; known to be intolerant to transfection) as well as persistent antitumor effect. To overcome these limitations, the same group used Epstein-Bar virus (EBV) to stimulate T cells (EBV-CTLs), a method known to elicit an enhanced immune response.²⁴ EBV-CTLs outperformed the ATCs in both expansion and antitumor persistence.²⁵⁻²⁷ Further, the nonviral piggybac (PB) transposon system was evaluated for HER2-CAR gene delivery to T cells. While this model has been successfully applied in mouse primary cells, human cell lines, and inducible pluripotent stem cells (iPSC), PB has not been evaluated for *in vivo* immunotherapeutic model. No preferential integration near or into oncogenes was observed, as typically the case with retrovirus and lentivirus-based transduction method. PB gene transfer was highly effective and the transduced cells could be maintained for >100 days in culture, while retaining stable

transgene expression and T cell properties. Since transposons are less expensive than viral vectors, and easier to produce, this method provides an interesting new approach for gene delivery.

Dendritic cell and macrophage-based therapy. Dendritic Cells (DCs) are the most potent antigen-presenting cells (APCs) of the human body, sensitizing T cells to all acquired antigens. In contrast to activation of T cells *ex vivo*, dendritic cells activation and stimulation induce a long-term immune response and is therefore considered active immunotherapy. Dendritic cells can be loaded with tumor antigens *ex vivo* that can subsequently activate the endogenous immune system upon injection. Although this technique is safe, clinical efficiency is still to be improved to achieve high expression of the antitumor antigen at the major histocompatibility complex (MHC) on the dendritic cell surface and to expand the subgroup of these cells that primes naïve T cells. Saka et al.,¹⁹ designed a DC vaccine-based strategy aimed at targeting the interleukin-13 zetakine (IL13Ra2), overexpressed in gliomas. Since proper expression of this antitumor antigen at the DC MHC was problematic, a late endosomal/lysosomal sorting signal was added to the IL13ra2 plasmid. DCs were transduced with this plasmid and injected intraperitoneally in glioma-bearing mice on day 3 and 10 post-tumor implantation. A significant increase in the number of CD4+ and CD8+ T lymphocytes in the IL13ra2-DC-treated tumor environment was observed, resulting in an increased survival rate.¹⁹ In a model in which gene therapy is effective but dendritic cell vaccination is not-effective, Mineharu et al.,²⁰ demonstrated that combining *in situ* Ad-Flt3L/Ad-TK-mediated gene therapy (an FDA-approved adenoviral vector expressing either fms-like tyrosine kinase 3 ligand or thymidine kinase) with dendritic cell vaccination increases therapeutic efficacy and antitumor immunity as compared to *in situ* Ad-Flt3L/Ad-TK-mediated gene therapy alone. Ad-Flt3L and Ad-TK were intratumorally injected, followed by systemic administration of the prodrug ganciclovir (GCV). Flt3L causes dendritic cells to migrate, differentiate, and expand within the tumor microenvironment of mice and rats. TK at the tumor site converts GCV into a highly toxic phosphorylated drug causing the death of dividing tumor cells. Further, tumor treated with GCV releases high mobility group 1 protein (HMGB1), which serves as an adjuvant of the innate immune system by stimulating Toll like receptor 2 in signaling bone marrow-derived DCs (BMDCs) confirming previous studies.^{28, 29} To achieve enhanced proliferation

and antitumor effect, the dendritic cells were conditioned *ex vivo* with Fl3t and interleukin-6 (IL-6).²⁰

As an alternative of loading DCs with regular tumor antigens, Xu et al.,²¹ explored the use of cancer stem cells (CSC) antigens as a source for DC anti-glioma vaccination. CSCs are thought to play an important role in the onset, progression, and recurrence of malignant gliomas and are known to express high levels of MHCs and tumor associated antigens (TAA). A sufficient T cell response against CSCs and an increase in survival of mice bearing 9L gliosarcoma CSCs tumors was observed as compared to DCs loaded with daughter or conventionally cultured 9L cells after intradermal injection of the vaccine. Albeit conventional loading and CSCs antigen loading of DCs require further comparison in DC maturation and memory T cell generation *in vivo*, the authors speculate that CSC antigens might indeed be more suited for DCs loading as compared to conventional tumor antigens. A clinical trial evaluating DCs vaccines using CSCs is being considered and will start shortly.²¹

Another antigen-presenting cells used for immuno-cell therapy are macrophages. The advantage of these cells is their ability to easily travel across the blood-brain barrier, which often remains a great limitation for effective brain tumors therapy. Tumor-associated macrophages are often observed in glioma microenvironment, and intravenously injected macrophages targets the brain tumor site.³⁰ In a recent study, Baek et al.,²² used macrophages loaded with gold-coated nanoshells for the treatment of human multicellular glioma spheroids, an *in vitro* model with similar characteristics in both resistance to radio- and chemotherapy, and in growth and metabolic rates of glioma tumors *in vivo*, while simulating the tumor before vascularization. Nanoshells are spherical nanoparticles consisting of a di-electric core (called the silica), and an outer layer coated with a thin metallic shell (often made of gold) that converts the absorbed light to heat with great efficiency. Nanoshells are relatively small and can thereby easily be taken up by macrophages. In this study, using the glioma spheroids model, the authors compared macrophages loaded with empty nanoshells to macrophages with gold-coated nanoshells and found that the latter were able to inhibit tumor growth by photo-thermal therapy, while no response was observed with the empty control group.

IMMUNO-CELL THERAPY IN THE CLINIC

Despite an abundance of experimental research, only a small number of clinical trials is currently in progress focusing on the safety, efficacy, and feasibility of immuno-cellular therapeutic approach in a phase I/II setting. While experimental therapies show a wide variety of strategic approaches, the clinic reflects a somewhat more conservative approach with dendritic cell vaccines and modified T lymphocytes dominating the picture (Table 2). Recently, two clinical trials showed the potential of immuno-cell therapy for the treatment of cancer. A study led by Professor Carl June at the University of Pennsylvania showed the success of adoptive CAR T cell therapy in treating chronic lymphocytic leukemia (CLL), where 2 out of 3 patients underwent complete remission after CAR-CD19 therapy and are remaining so for >1 year after treatment.^{31, 32} Another trial led by Drs. Renier Brentjens and Michel Sadelain at the Memorial Sloan Kettering Cancer Institute showed that the same CAR strategy can successfully treat patients with CLL and B cell acute lymphoblastic leukemia (ALL), two forms of blood cancer.^{33, 34} These successful trials prove the significance of immuno-cellular therapeutic strategies for treating different tumors, including gliomas.

Table 2. Current immuno-cell therapy in clinical Trials

Therapy	Cell/vaccine type	Transgene/modification strategy	Application	Phase	Clinicaltrial.gov Identifier #	Ref		
Cellular immunotherapy	CD 8+ T lymphocytes	Expression of IL-13 zetakine chimeric immunoreceptor, Hy/TK selection/suicide fusion protein	Assessment of the feasibility and safety of ex vivo expanded and genetically modified autologous CD8+ T lymphocytes in patients with recurrent or refractory high-grade malignant glioma.	Pilot	NCT00730613 (completed)	18, 35		
	T cells	Expression of EGFRvIII CAR (PG13-139-CD8-CD28BBZ (F10)	Evaluation of the safety and feasibility of administering T Cells expressing Anti-EGFRvIII Chimeric Antigen Receptor to patients with malignant Gliomas expressing EGFRvIII	Phase I/II	NCT01454596	36, 37		
Vaccine cell therapy	CTL	BTIC antigen load	Evaluation of the feasibility of administering of Imiquimod/BTIC Lysate-Based therapy for Diffuse Intrinsic Pontine Glioma in children and young adults	Pilot	NCT01400672	38		
	Dendritic cells (DCs)	ICT-107		Evaluation of the safety and efficacy of ICT-107 in newly diagnosed patients with GBM following resection and chemo-radiation.	Phase II	NCT01280552	39	
		205-NY-ESO-1 fusion protein		Evaluation of the side effects and best schedule of dendritic vaccine therapy with/without sirolimus in treating patients with NY-ESO-1 expressing solid tumors.	Phase I	NCT01522820	40, 41	
		WT1 protein		Evaluation of the immunogenicity and clinical efficacy of WT1-specific CD8+ T cell antitumor response after intradermal vaccination with autologous WT1 mRNA-transfected DC	Phase I/II	NCT01291420	42, 43	
		A2B5+ antigen load		Evaluation of the efficacy of vaccination with DCs loaded with Glioma Stem-like Cells Associated Antigens against GBM	Phase II	NCT01567202	44	
		Autogenic GBM cell lysate			Evaluation of the adverse and therapeutic effects of a postoperative autologous dendritic cell tumor vaccine in patients with malignant glioma	Phase I/II	Published	45
					Evaluation of the immunologic response to cervical intranodal vaccination with autologous tumor lysate-loaded DCs in patients with GBM after radiation therapy and TEM	Phase I	Published	46
	IMA 950	TUMAPs: multi-peptide vaccine (IMA 950) containing 11 TUMAPs found in a majority of GBMs designed to activate TUMAP-specific T cells		Evaluation of the safety and tolerability of IMA950 when given with cyclophosphamide, granulocyte macrophage-colony stimulating factor (GM-CSF) and imiquimod in patients with GBM	Phase I	NCT01403285	47	
		TUMAPs		Evaluation of the side effects of IMA 950 vaccine therapy when given together with temozolomide and radiation therapy in treating patients with newly diagnosed GBM	Phase I	NCT01222221	48, 49	
	GBM cells	Autologous tumor cells treated with ILGFR1 antisense oligodeoxynucleotide ex vivo and re-implanted in diffusion chambers to stimulate the native immune system		Evaluation of the safety of rectus sheath implantation of diffusion chambers encapsulating autologous malignant Glioma cells treated with ILGFR1 antisense Oligodeoxynucleotide in patients with recurrent GBM	Phase I	NCT01550523	50	

Cellular vaccine and immunotherapy combined	TVI Brain I glioma cells; Killer T cells	<ul style="list-style-type: none"> Autologous glioma cells <i>ex vivo</i> neutralized to elicit a Killer T cell response <i>in vivo</i> Autologous DC stimulated Killer T cell precursors cultured and stimulated <i>ex vivo</i> to reach a higher activity level. 	Evaluation of the safety and efficacy of TVI-Brain-1 as a treatment for recurrent GBM	Phase II	NCT01290692	51
	Glioma vaccine, DC; DCIK	<ul style="list-style-type: none"> Dendritic cells pulsed with tumor lysate CIK cells activated by DCs stimulation (DCIKs) 	Evaluation of DCIK Combined With DC Treatment for Glioma	Phase I/II	NCT01235845	52
	DCs; CTL	<ul style="list-style-type: none"> CMV presenting DCs Cytotoxic T lymphocytes stimulated by CMV and EBV 	Evaluation of the safety and persistence of escalating doses of autologous CMV-specific CTL in patients with CMV-positive GBM.	Phase I	NCT01205334	53, 54
		<ul style="list-style-type: none"> CMV presenting DCs Cytotoxic T-lymphocytes stimulated by CMV and modified to express CARs targeting the HER2 molecule (FRP5.CD28.CAR) 	Evaluation of the safety, persistence and antitumor efficacy of escalating doses of autologous CMV-specific CTL expressing FRP5.CD28.CAR in patients with HER2-positive recurrent GBM	Phase I/II	NCT01109095	23, 53

Abbreviations: BTIC, brain tumor initiating cell; CTL, cytotoxic T lymphocyte; DCIK, dendritic cell (DC) activated cytokine induced killer cell (CIK); 06BG, 06-Benzylguanidine; EGFR, epidermal growth factor receptor; CAR, chimeric antigen receptor; HER2, human epidermal growth factor receptor 2; TUMAP, tumor-associated peptides; ILGFR1, Insulin-like Growth Factor Receptor-1

T cell immunotherapy in the clinic. With malignant gliomas being known for their immune evasive strategies, barely any immune response is provoked. However, the immune cells could be of tremendous value in the fight against brain tumors; they could provide a very efficient elimination mechanism of the tumor bulk and metastatic/invasive cells, without the need to undergo quality of life impairing as in the case for chemo- or radiotherapeutic paradigms. Many of the current strategies are exploring methods to overcome the lack of immune response to glioma cells by artificially stimulating the immune system either by passive or active immunization. The use of T cells is one of the most popular strategies in the clinic, often used in combination with dendritic cell vaccines. Two clinical trials focus on *ex vivo*-stimulation of T cells to boost a passive immune response are currently in progress.

In one trial by Forsman et al., at the City of Hope Medical Center, autologous peripheral blood mononuclear cells (PBMC) are collected and genetically modified to express the membrane-tethered IL13 cytokine chimeric T cell receptor (TCR) targeting the IL13 receptor $\alpha 2$ (IL13R $\alpha 2$) present in over 80% of malignant gliomas. This IL13 zetakine has an E13Y mutation, which enhances its specificity for the IL13 $\alpha 2$ receptor by >50-fold, as compared to the normal IL13 receptor expressed by

the healthy brain tissue.^{18, 35} In addition to the IL13 zetakine, the cytotoxic T lymphocytes (CTL) were further modified to express the thymidine kinase suicide gene (HyTK) under the control of the constitutively active cytomegalovirus (CMV) promoter in case immediate ablation of CTL activity is required. Repeated CTL infusion was performed over 2 weeks (3 times/week) followed by an injection every 3 weeks in the absence of disease progression and signs of autoimmunity. Recently, an experimental study from the same group was published discussing the use of the IL13 zetakine in an orthotopic mouse tumor model.^{18, 35} The authors showed that IL13R α 2 is expressed by both glioma stem cells and the more differentiated tumor cell population, and that IL13R α 2 zetakine therapy ablates the tumor initiating activity of IL13R α 2 positive GSCs. At time of writing, the pilot study has been completed, however, the results have not been published yet.

Rosenberg et al., at the National Institutes of Health Clinical Centre takes on a similar approach by genetically modifying peripheral blood lymphocytes to express the anti-EGFRvIII chimeric antigen receptor. As in the case for IL13R α 2, the mutant EGFRvIII receptor is overexpressed in 30-70% of glioblastoma, while no expression is seen in the normal brain.⁵⁵ After *ex vivo* preparation, the autologous modified cells will be intravenously injected and safety, feasibility, and progression-free interval will be monitored.

Vaccine therapy in the clinic. With 9 clinical trials either in progress or recently completed, vaccine therapy is the most popular clinical immuno-cellular therapeutic approach for malignant gliomas. Vaccine therapy is based on active immunization of the body against glioma, resulting in a permanent and sustained attack of the tumor by the immune system. In five out of the nine trials, autologous dendritic cells are used to stimulate the patient immune system to evoke an antitumor immune response. Dendritic cells are the most potent antigen-presenting cells with the capability of presenting antigenic material not only by the MHC II pathway (stimulating CD4+ T lymphocytes), but also by MHC I pathway (stimulating a CD8+ Lymphocyte response) through a process called 'cross presenting', which results in a diversification of the immune response.^{39, 56} ImmunoCellular therapeutics, LTD., recently initiated a phase II study using the immunotherapeutic vaccine ICT-107 composed of synthetically purified antitumor antigens corresponding to epitopes found on GBM cells. Autologous dendritic cells are *ex vivo* pulsed with ICT-107 and

injected intradermally upon completion of tumor removal and 6 weeks of temozolomide therapy. An earlier Phase I study demonstrated safety and efficacy of this therapeutic strategy. Earlier this year, Odumsi et al., at the Roswell Park Cancer Institute initiated a large phase I study evaluating the safety and feasibility of a new vaccine aimed at NY-ESO-1 expressing solid tumors in combination with Sirolimus, an mTOR inhibitor.⁴⁰ Autologous dendritic cells are *ex vivo* pulsed with the 205-NY-ESO-1 fusion protein and intranodally injected. The investigators hope that this strategy will elicit a stronger immune response yielding to enhanced tumor killing. At the same time, Berneman et al., at the University Hospital (Antwerp, Belgium) are evaluating immunogenicity and efficacy of intradermal vaccination with autologous dendritic cells genetically modified to express WT1 protein, overexpressed in a variety of solid tumors. A previous phase I study in patients with acute myeloid leukemia demonstrated the vaccine is well tolerated and elicits a CD8+ T lymphocyte response.^{42, 43} In China, Zhou et al., at the Huashan Hospital initiated a Phase II study evaluating the overall survival of patients with primary and/or secondary GBM after treatment with autologous dendritic cells loaded with autogenic glioma stem cells (A2B5+). A study investigating the adverse and therapeutic effect of post-operative dendritic cells-derived tumor vaccine was recently published by Chang et al.,⁴⁵ in the Journal of Clinical Neuroscience reporting an increase in the median survival to 525 days and a 5 year survival rate to 18.8% as compared to the historical control group (380 days and 0%). Patients underwent surgery to debulk the tumor mass and the vaccine was prepared using cells from the surgical specimen. Autologous dendritic cells were administered using a 6 months-10 injections course. The authors report that 47% of the enrolled patients developed a transient elevation in alanine aminotransferase (ALT)/aspartate aminotransferase (AST) levels, which correlated with the vaccination schedule and high doses of dendritic cells vaccine. At lower levels of dendritic cells vaccine, no increase in serum ALT/AST was observed suggesting the safe upper limit of 2×10^7 dendritic cells/dose.

Another recently completed study by Fadul et al.,⁴⁶ was reported in the Journal of Immunotherapy focusing on the immune response, progression free survival (PFS), and overall survival (OS) of GBM patients treated with intranodal autologous tumor lysate dendritic cells vaccination. CTL tumor specific activation was measured and correlated with both PFS and OS. All patients were still alive 6 months after diagnosis and a PFS of 9.5 months was reported. Median OS was 28

months, which is significantly higher than the OS of 18-21 months in GBM patients receiving standard therapy.²

As an alternative to the standard dendritic cells approach, Andrews et al., at the Thomas Jefferson University (Philadelphia) initiated a pilot study evaluating the possibility of stimulating the dendritic cells population *in vivo*. *In vivo* stimulation is thought to be more effective and is expected to elicit a stronger and longer immune response as compared to *ex vivo* stimulation.⁵⁷ Diffusion chambers containing autologous tumor cells treated *ex vivo* with insulin-like growth factor receptor-1 (IGFR-1) antisense oligodeoxynucleotide were re-implanted in the rectus sheet to stimulate the native immune system. Loss of IGFR-1 is expected to result in apoptosis with subsequent release of tumor antigen containing exosomes (microvesicles), which will allow the diffusion chamber to act as a slow-release antigen depot.⁵⁰ Since a wound containing a foreign body is created upon implantation of the diffusion chamber, high levels of dendritic cells are expected to be present in the immediate surroundings, enhancing the efficacy of antitumor activation of the immune system.

Three studies demonstrated that the use of dendritic cells for vaccine therapy is not the only way to go. A pilot study by Moertel et al., at the Masonic Cancer Centre (University of Minnesota) developed a cell-based cancer vaccine composed of glioma stem-like associated antigens found in the brain tumor initiating cell line GBM6 (BTICs).^{58, 59} Upon administration, the BTIC vaccine is thought to stimulate an antitumor CTL response against both GSCs and the more proliferated tumor bulk. Since GSCs have the ability of self-renewal and seem to drive tumor growth and initiation, elimination of this specific group of glioma cells would be of tremendous benefit. Vaccine administration will start following radiation therapy and will be given every 2 weeks for 4 weeks in combination with the drug imiquimod, which acts as an immune response modifier.

Two separate groups are conducting a phase I study to test the safety and feasibility of IMA 950, a therapeutic multi-peptide vaccine containing 11 tumor-associated peptides (TUMAPs) found in a majority of GBMs designed to activate TUMAP-specific T cells. Rumpling et al., (Cancer Research UK) are testing the vaccine in combination with granulocyte-macrophage colony-stimulating factor (GM-CSF) and radiation and chemotherapy (temozolomide) for patients with newly diagnosed gliomas.⁶⁰ Sul et al., (Immatic Biotechnologies GmbH in collaboration

with the National Cancer Institute) follow a similar approach to test IMA 950 with GM-CSF and locally-applied imiquimod, 20 min after each vaccination. Patients will further be treated with one dose of cyclophosphamide prior to the first vaccination.

Vaccine and cellular therapy combined. Two clinical trials using the combined approach of vaccine and immunotherapy are being performed by Ahmed et al., at the Baylor College of Medicine. In the first trial, autologous CTLs are *ex vivo* stimulated with human β herpes cytomegalovirus (h-CMV) presenting dendritic cells. CMV-specific antigens can be detected in 70-90% of malignant glioma cells, but not the normal brain.^{61, 62} The CMV-specific CTLs are then cultured in the presence of EBV-infected cells, to boost a stronger immune response upon intravenous administration.²⁴ The second trial goes a step further and genetically modifies the CMV-specific CTLs to express the chimeric antigen receptor targeting HER2, which is associated with 70% of GBM malignancies.⁶³ Both trials are still in their initial phase I stage; however, a recently published pilot study by the same group evaluated the use of CMV-specific T cells and demonstrated that autologous T cells could successfully be activated and expanded, are able to recognize the CMV antigens pp65 and IE1, and are capable of killing CMV-infected autologous GBM cells.⁵³ In the meantime, Wood et al., (TVAX Biomedical) are testing in a phase II trial (supported by positive safety and efficacy study in a phase I trial) a brain cancer vaccine called TVI-Brain I, consisting of neutralized autologous tumor cells. Upon vaccination, an immune response of killer T cells is expected yielding a highly effective antitumor activity. Yao et al., at Quindao University use a somewhat similar approach in a phase I/II trial combining intranodal dendritic cells vaccination with subsequent *ex vivo* expansion of activated T cells in patients with recurrent glioma. The study is specifically aimed at a group of T cells, called cytokine-induced killer cells (CIK), which are known to express a very potent antitumor activity.^{52, 64} Cells will be selected by expression of the cell markers CD3 and CD56.

LIMITATIONS AND FUTURE PROSPECTS OF IMMUNO-CELL THERAPY

Although a wide range of potential targets and immuno-cellular therapeutic strategies are investigated experimentally, only the most successful are transitioned to the

clinic. The translation from the laboratory to the clinic remains a difficult phase, with dendritic cells vaccine strategy being the most successful example. Dendritic cell therapy has proven safe with some therapeutic success; however, no breakthrough has been achieved using this therapeutic strategy for gliomas. The clinical outcome did not reflect the expected results on the bench, showing perhaps a limitation in the existing glioma models. For dendritic cell therapy to be effective in animal models, vaccination is mostly given before tumor implantation. This of course is impossible in human patients. While many pathophysiological similarities between the rodent glioma models and the human tumors can be observed, many models are performed in immunocompromised mice. Therefore, tumor-associated immunosuppression and immune modulating events are not likely to be reflected accurately and their usefulness as models for evaluating immuno-cellular therapy might be limited. Further, tumor xenografts will not mimic the process of tumorigenesis *de novo*, resulting in a slightly different tumor microenvironment. The use of rodents with intact immune system, and the development of genetically-induced glioma models could help optimizing preclinical studies, leading to a more predictable transition to the clinic.

Another difficulty in assessing the efficacy and success of dendritic cells vaccination (or any other strategy) in the clinic is the relatively low number of glioma patients per trial group often leading to a weak statistical significance. Further, it is difficult to compare study outcomes from different trials, since inclusion criteria and injection route differ from one group to another, which can have a substantial effect on patient survival. The use of corticosteroids and other co-medication, as often seen in malignant glioma patients such as GBM, impairs objective assessment even further as efficacy of treatment might be limited, side effects might get masked, and differentiation of immune cells is halted. In the case of vaccination, improvements have only been seen when compared to historical controls, which are improper controls to use for glioma studies. When compared to standard of care, no clinical significant benefits have been reported. Furthermore, caution has to be exerted when interpreting effects on immune function following vaccination. In most if not all clinical trials of vaccination, brain inflammation has never been detected. Although this is usually (wrongly) interpreted as the vaccines being safe, the absence of any adverse effects in hundreds of immunized patients, most likely speaks of the ineffective vaccination. Thus, at this stage, we remain unable to differentiate the

absence of side effects as a result of non-effective vaccination, or, actual safety. So far, only a single study combining gene/vaccine therapy in dogs showed physiologically effective immune activation associated with brain inflammation, which resulted in clinical benefits.⁶⁵ This study is the only objective description supporting the idea that under the right conditions, it is possible to stimulate a systemic immune response that can attack the brain and brain tumors.

To undermine some of these problems, and to get a true understanding of the working mechanism and antitumor effect of immuno-cellular therapies, the development of adequate imaging tools is of uttermost important. The ability to track immune cells and to determine their fate, tropism, migration, interaction with the surroundings, and mechanism of action will answer important questions regarding safety and efficacy. Several imaging tools are currently available in the preclinical setting (e.g. bioluminescence and fluorescence); however, these techniques are not (yet) translatable for use in humans due to several concerns including (substrate) toxicity and sensitivity. Labeling of stem cells with ferumoxide, which allows them to be tracked *in vivo* by magnetic resonance imaging (MRI) has been successfully reported to monitor in real-time migration and distribution of these cells at the tumor site.⁶⁶ Similar approaches might be translated to the clinic to track immune cells, however, additional studies are required to fine tune this technique and increase its sensitivity to make it suited for *in human* use. While new imaging tools are a necessity to further develop the immuno-cell therapy field, another issue that needs to be addressed is the availability and efficacy of the cells themselves. High passage number of effector cells *in vitro*, in order to reach adequate levels, could lead to differentiation and change of phenotype, limiting their therapeutic potential. New techniques that allow rapid growth and expansion of these cells while maintaining their characteristics will be of extreme importance for the cellular Immunotherapy field. Similar problems can be seen in the clinic where lack of *in vivo* expansion and inability to maintain high expression levels over a sufficient period of time could limit treatment efficacy. This may result not only in unsuccessful clinical trials, but also in the abandonment of a potentially successful strategy. The success of the CAR-CD19 adoptive T cell therapy study for CLL and ALL shows that once the immune cells are manipulated, extensive *in vivo* expansion and high levels of gene expression could be maintained over time, therefore, immunotherapy can indeed be an effective strategy in the battle against cancer. In order to stimulate cell survival

and proliferation, a 4-1 BB co-stimulatory domain was added to the CAR construct, resulting in >1000-fold higher proliferation rate of T cells once injected *in vivo*, with each T cell killing approximately 1000 CLL cells. Three out of three CLL patients showed clinical activity lasting for over 6 months, with 2 out of 3 patients reaching complete remission.^{31, 32} Kloss et al., demonstrated a similar successful approach in a prostate cancer model using a chimeric co-stimulator receptor (CCR) together with CARs, with increased selectivity of the modified T cells for prostate cancer cells.⁶⁷ Although still at the experimental level, this strategy may greatly increase efficacy and safety of T cell adaptive immunotherapy. Both approaches could easily be adapted to T cells glioma therapy (similar to the Nakazawa¹⁷ and Wang¹⁶ studies), potentially in combination with EBV-CLT.

Several studies are exploring different strategies to deliver immune cells to the tumor. While many choose a direct injection route, others are exploring intranodal, intradermal, or systemic injection, in an attempt to enhance the delivery success. Direct comparison of these delivery strategies should be performed in order to reach the optimal injection route for effective glioma therapy. Other research groups argue that *ex vivo* cell manipulation is time consuming and may result in cellular differentiation and an increased risk of infection. Thus, the focus should not be on “how to deliver the manipulated cells”, but on “how to manipulate the cells *in vivo*”. The studies being performed by Andrews et al., at the Thomas Jefferson University will shed new light on these possibilities.

Finally, when discussing treatment efficacy and success of new clinical strategies, it is important to bear in mind the current prognosis and treatment options available for glioma patients. While the results of CAR-CD19 trial showed that 2 out of the 3 CLL patients are in remission for over a year, which is extraordinary, one must realize that with a median survival of 8 to 10 years, the CLL population is not comparable to glioma patients. We advocate that in a patient population where the 2 years survival rate is only 40%, and in the past 25 years, the median survival rate has only increased by 3 months, our expectation on efficacy should be as equally moderate.^{1, 2} Further, the gain of months rather than years should be valued as well as the decrease in side effects and/or increase in patient’s well-being. The aim of trials should therefore not only be directed against increased survival, but also for better “quality of life”. Hopefully, optimizing some of the strategies discussed here will eventually turn the wheel and allow us to increase our goals and expectations.

For now, it is difficult to conclude the role and effect of immuno-cellular therapy on malignant gliomas. If some of the discussed issues can be addressed, and current clinical trials show promising results, this therapeutic strategy has the potential to give a tremendous value in the search for a cure for tumors as heterogeneous as GBM, complementing current standard therapy.

Box 2 Cell isolation and preparation for immunotherapy

T lymphocytes can be obtained from several sources, including thymus, lymphnodes, spleen and peripheral blood, the latter being the most accessible. Cells are separated from the whole blood samples by Ficol isopaque-based density gradient separation. Since lymphocytes are less dense than erythrocytes, they can easily be extracted after centrifugation. Distinction between B and T lymphocytes can then be made based on differences in growth patterns, with T lymphocytes forming rosettes in the presence of sheep erythrocytes and B lymphocytes being non rosette forming. Nylon fiber column separation is an alternative approach, allowing to specifically select for adherent T lymphocytes. Several commercial kits are available to specifically purify T lymphocyte subtypes (CD4, CD8, NKT) based on monoclonal antibody reactions. To generate CTLs against specific antigens (for instance expressed on tumor cell surface), the CTLs can be cultured in the presence of APCs loaded with the desired antigen. Cells are cultured in basal medium containing RPMI 1640, 10% fetal calf serum, penicillin/streptomycin, L-glutamate, phytohaemagglutinin and a buffer solution. New studies are focusing on the development of serum free medium, in order to standardize T cell populations and eliminate confounders.

Macrophages can be isolated from various tissues. One strategy involves isolation of these cells from peripheral blood. Blood-derived macrophages are isolated based on the very same Ficol-gradient centrifugation protocol described for T lymphocytes. Antibody-based cell separation kits selecting the CD14 monocyte fraction are available. Subsequent culture of these cells in the presence of macrophage colony stimulating factor 1 (M-CSF-1) will result in macrophage differentiation. The same RPMI culture media is used as described for T lymphocytes.

Dendritic cells can be generated through various protocols. One technique involves DCs separation from the whole blood samples by Ficol gradient centrifugation. B-lymphocytes and monocytes are then subtracted from the cell suspension using monoclonal antibodies directed towards CD19 and CD14. Dendritic cells are then isolated from the remaining (B and monocyte depleted) mixture by CD304, CD141 and CD1c directed antibodies. Selected cells are cultured in RPMI media containing M-CSF-1 yielding to DCs differentiation.

REFERENCES

1. Johnson DR, Ma DJ, Buckner JC, Hammack JE. (2012). Conditional probability of long-term survival in glioblastoma: A population-based analysis. *Cancer*.
2. Grossman SA, Ye X, Piantadosi S, Desideri S, Nabors LB, Rosenfeld M, et al. (2010). Survival of patients with newly diagnosed glioblastoma treated with radiation and temozolomide in research studies in the United States. *Clin Cancer Res*.16(8):2443-2449.
3. Stupp R, Hegi ME, Mason WP, van den Bent MJ, Taphoorn MJ, Janzer RC, et al. (2009). Effects of radiotherapy with concomitant and adjuvant temozolomide versus radiotherapy alone on survival in glioblastoma in a randomised phase III study: 5-year analysis of the EORTC-NCIC trial. *Lancet Oncol*.10(5):459-466.
4. Albesiano E, Han JE, Lim M. (2010). Mechanisms of local immunoresistance in glioma. *Neurosurg Clin N Am*.21(1):17-29.
5. Haar CP, Hebbar P, Wallace GCt, Das A, Vandergrift WA, 3rd, Smith JA, et al. (2012). Drug Resistance in Glioblastoma: A Mini Review. *Neurochem Res*.
6. Wu A, Wei J, Kong LY, Wang Y, Priebe W, Qiao W, et al. (2010). Glioma cancer stem cells induce immunosuppressive macrophages/microglia. *Neuro Oncol*.12(11):1113-1125.
7. Stupp R, Pica A, Mirimanoff RO, Michielin O. (2007). [A practical guide for the management of gliomas]. *Bull Cancer*.94(9):817-822.
8. Stupp R, Roila F. (2009). Malignant glioma: ESMO clinical recommendations for diagnosis, treatment and follow-up. *Ann Oncol*.20 Suppl 4:126-128.
9. Gale RP. (1979). Bone marrow transplantation in acute leukemia: current status and future directions. *Haematol Blood Transfus*.23:71-78.
10. Santos GW, Eifenbein GJ, Tutschka PJ. (1979). Bone marrow transplantation-present status. *Transplant Proc*.11(1):182-188.
11. Joglekar MV, Hardikar AA. (2012). Isolation, expansion, and characterization of human islet-derived progenitor cells. *Methods Mol Biol*.879:351-366.
12. Efrat S, Russ HA. (2012). Making beta cells from adult tissues. *Trends Endocrinol Metab*.23(6):278-285.
13. Vacanti JP. (2012). Tissue engineering and the road to whole organs. *Br J Surg*.99(4):451-453.
14. Wain RA, Shah SH, Senarath-Yapa K, Laitung JK. (2012). Dermal substitutes do well on dura: comparison of split skin grafting +/- artificial dermis for reconstruction of full-thickness calvarial defects. *Clin Plast Surg*.39(1):65-67.
15. Jones TS, Holland EC. (2011). Animal models for glioma drug discovery. *Expert Opin Drug Discov*.6(12):1271-1283.
16. Wang LX, Westwood JA, Moeller M, Duong CP, Wei WZ, Malaterre J, et al. (2010). Tumor ablation by gene-modified T cells in the absence of autoimmunity. *Cancer Res*.70(23):9591-9598.
17. Nakazawa Y, Huye LE, Salsman VS, Leen AM, Ahmed N, Rollins L, et al. (2011). PiggyBac-mediated cancer immunotherapy using EBV-specific cytotoxic T-cells expressing HER2-specific chimeric antigen receptor. *Mol Ther*.19(12):2133-2143.
18. Brown CE, Starr R, Aguilar B, Shami A, Martinez C, D'Apuzzo M, et al. (2012). Stem-like tumor initiating cells isolated from IL13Ralpha2-expressing

- gliomas are targeted and killed by IL13-zetakine redirected T cells. *Clin Cancer Res.*
19. Saka M, Amano T, Kajiwara K, Yoshikawa K, Ideguchi M, Nomura S, et al. (2010). Vaccine therapy with dendritic cells transfected with Il13ra2 mRNA for glioma in mice. *J Neurosurg.*113(2):270-279.
 20. Mineharu Y, King GD, Muhammad AK, Bannykh S, Kroeger KM, Liu C, et al. (2011). Engineering the brain tumor microenvironment enhances the efficacy of dendritic cell vaccination: implications for clinical trial design. *Clin Cancer Res.*17(14):4705-4718.
 21. Xu Q, Liu G, Yuan X, Xu M, Wang H, Ji J, et al. (2009). Antigen-specific T-cell response from dendritic cell vaccination using cancer stem-like cell-associated antigens. *Stem Cells.*27(8):1734-1740.
 22. Baek SK, Makkouk AR, Krasieva T, Sun CH, Madsen SJ, Hirschberg H. (2011). Photothermal treatment of glioma; an in vitro study of macrophage-mediated delivery of gold nanoshells. *J Neurooncol.*104(2):439-448.
 23. Ahmed N, Salsman VS, Kew Y, Shaffer D, Powell S, Zhang YJ, et al. (2010). HER2-specific T cells target primary glioblastoma stem cells and induce regression of autologous experimental tumors. *Clin Cancer Res.*16(2):474-485.
 24. Quintarelli C, Savoldo B, Dotti G. (2010). Gene therapy to improve function of T cells for adoptive immunotherapy. *Methods Mol Biol.*651:119-130.
 25. Pule MA, Savoldo B, Myers GD, Rossig C, Russell HV, Dotti G, et al. (2008). Virus-specific T cells engineered to coexpress tumor-specific receptors: persistence and antitumor activity in individuals with neuroblastoma. *Nat Med.*14(11):1264-1270.
 26. Woltjen K, Hamalainen R, Kibschull M, Mileikovsky M, Nagy A. (2011). Transgene-free production of pluripotent stem cells using piggyBac transposons. *Methods Mol Biol.*767:87-103.
 27. Woltjen K, Michael IP, Mohseni P, Desai R, Mileikovsky M, Hamalainen R, et al. (2009). piggyBac transposition reprograms fibroblasts to induced pluripotent stem cells. *Nature.*458(7239):766-770.
 28. Ali S, King GD, Curtin JF, Candolfi M, Xiong W, Liu C, et al. (2005). Combined immunostimulation and conditional cytotoxic gene therapy provide long-term survival in a large glioma model. *Cancer Res.*65(16):7194-7204.
 29. Curtin JF, Liu N, Candolfi M, Xiong W, Assi H, Yagiz K, et al. (2009). HMGB1 mediates endogenous TLR2 activation and brain tumor regression. *PLoS Med.*6(1):e10.
 30. Shinonaga M, Chang CC, Suzuki N, Sato M, Kuwabara T. (1988). Immunohistological evaluation of macrophage infiltrates in brain tumors. Correlation with peritumoral edema. *J Neurosurg.*68(2):259-265.
 31. Porter DL, Levine BL, Kalos M, Bagg A, June CH. (2011). Chimeric antigen receptor-modified T cells in chronic lymphoid leukemia. *N Engl J Med.*365(8):725-733.
 32. Kalos M, Levine BL, Porter DL, Katz S, Grupp SA, Bagg A, et al. (2011). T cells with chimeric antigen receptors have potent antitumor effects and can establish memory in patients with advanced leukemia. *Sci Transl Med.*3(95):95ra73.
 33. Brentjens RJ, Santos E, Nikhamin Y, Yeh R, Matsushita M, La Perle K, et al. (2007). Genetically targeted T cells eradicate systemic acute lymphoblastic leukemia xenografts. *Clin Cancer Res.*13(18 Pt 1):5426-5435.

34. Brentjens RJ, Riviere I, Park JH, Davila ML, Wang X, Stefanski J, et al. (2011). Safety and persistence of adoptively transferred autologous CD19-targeted T cells in patients with relapsed or chemotherapy refractory B-cell leukemias. *Blood*.118(18):4817-4828.
35. Kahlon KS, Brown C, Cooper LJ, Raubitschek A, Forman SJ, Jensen MC. (2004). Specific recognition and killing of glioblastoma multiforme by interleukin 13-zetakine redirected cytolytic T cells. *Cancer Res*.64(24):9160-9166.
36. Stroncek DF, Berger C, Cheever MA, Childs RW, Dudley ME, Flynn P, et al. (2012). New directions in cellular therapy of cancer: a summary of the summit on cellular therapy for cancer. *J Transl Med*.10(1):48.
37. Stupp R, Mason WP, van den Bent MJ, Weller M, Fisher B, Taphoorn MJ, et al. (2005). Radiotherapy plus concomitant and adjuvant temozolomide for glioblastoma. *N Engl J Med*.352(10):987-996.
38. Finocchiaro G, Pellegatta S. (2011). Immunotherapy for glioma: getting closer to the clinical arena? *Curr Opin Neurol*.24(6):641-647.
39. Kim W, Liao LM. (2010). Dendritic cell vaccines for brain tumors. *Neurosurg Clin N Am*.21(1):139-157.
40. Tsuji T, Matsuzaki J, Kelly MP, Ramakrishna V, Vitale L, He LZ, et al. (2011). Antibody-targeted NY-ESO-1 to mannose receptor or DEC-205 in vitro elicits dual human CD8+ and CD4+ T cell responses with broad antigen specificity. *J Immunol*.186(2):1218-1227.
41. Wadle A, Mischo A, Strahl S, Nishikawa H, Held G, Neumann F, et al. (2010). NY-ESO-1 protein glycosylated by yeast induces enhanced immune responses. *Yeast*.27(11):919-931.
42. Van Driessche A, Van de Velde AL, Nijs G, Braeckman T, Stein B, De Vries JM, et al. (2009). Clinical-grade manufacturing of autologous mature mRNA-electroporated dendritic cells and safety testing in acute myeloid leukemia patients in a phase I dose-escalation clinical trial. *Cytotherapy*.11(5):653-668.
43. Van Tendeloo VF, Van de Velde A, Van Driessche A, Cools N, Anguille S, Ladell K, et al. (2010). Induction of complete and molecular remissions in acute myeloid leukemia by Wilms' tumor 1 antigen-targeted dendritic cell vaccination. *Proc Natl Acad Sci U S A*.107(31):13824-13829.
44. Hua W, Yao Y, Chu Y, Zhong P, Sheng X, Xiao B, et al. (2011). The CD133+ tumor stem-like cell-associated antigen may elicit highly intense immune responses against human malignant glioma. *J Neurooncol*.105(2):149-157.
45. Chang CN, Huang YC, Yang DM, Kikuta K, Wei KJ, Kubota T, et al. (2011). A phase I/II clinical trial investigating the adverse and therapeutic effects of a postoperative autologous dendritic cell tumor vaccine in patients with malignant glioma. *J Clin Neurosci*.18(8):1048-1054.
46. Fadul CE, Fisher JL, Hampton TH, Lallana EC, Li Z, Gui J, et al. (2011). Immune response in patients with newly diagnosed glioblastoma multiforme treated with intranodal autologous tumor lysate-dendritic cell vaccination after radiation chemotherapy. *J Immunother*.34(4):382-389.
47. Sul J, Fine HA. (2010). Malignant gliomas: new translational therapies. *Mt Sinai J Med*.77(6):655-666.
48. Brada M, Stenning S, Gabe R, Thompson LC, Levy D, Rampling R, et al. (2010). Temozolomide versus procarbazine, lomustine, and vincristine in recurrent high-grade glioma. *J Clin Oncol*.28(30):4601-4608.

49. Gorlia T, Stupp R, Brandes AA, Rampling RR, Fumoleau P, Ditttrich C, et al. (2012). New prognostic factors and calculators for outcome prediction in patients with recurrent glioblastoma: A pooled analysis of EORTC Brain Tumour Group phase I and II clinical trials. *Eur J Cancer*.
50. Andrews DW, Resnicoff M, Flanders AE, Kenyon L, Curtis M, Merli G, et al. (2001). Results of a pilot study involving the use of an antisense oligodeoxynucleotide directed against the insulin-like growth factor I receptor in malignant astrocytomas. *J Clin Oncol*.19(8):2189-2200.
51. Sloan AE, Dansey R, Zamorano L, Barger G, Hamm C, Diaz F, et al. (2000). Adoptive immunotherapy in patients with recurrent malignant glioma: preliminary results of using autologous whole-tumor vaccine plus granulocyte-macrophage colony-stimulating factor and adoptive transfer of anti-CD3-activated lymphocytes. *Neurosurg Focus*.9(6):e9.
52. Li H, Wang C, Yu J, Cao S, Wei F, Zhang W, et al. (2009). Dendritic cell-activated cytokine-induced killer cells enhance the anti-tumor effect of chemotherapy on non-small cell lung cancer in patients after surgery. *Cytotherapy*.11(8):1076-1083.
53. Ghazi A, Ashoori A, Hanley PJ, Brawley VS, Shaffer DR, Kew Y, et al. (2012). Generation of polyclonal CMV-specific T cells for the adoptive immunotherapy of glioblastoma. *J Immunother*.35(2):159-168.
54. Hoa N, Ge L, Kuznetsov Y, McPherson A, Cornforth AN, Pham JT, et al. (2010). Glioma cells display complex cell surface topographies that resist the actions of cytolytic effector lymphocytes. *J Immunol*.185(8):4793-4803.
55. Hatanpaa KJ, Burma S, Zhao D, Habib AA. (2010). Epidermal growth factor receptor in glioma: signal transduction, neuropathology, imaging, and radioresistance. *Neoplasia*.12(9):675-684.
56. Rodriguez A, Regnault A, Kleijmeer M, Ricciardi-Castagnoli P, Amigorena S. (1999). Selective transport of internalized antigens to the cytosol for MHC class I presentation in dendritic cells. *Nat Cell Biol*.1(6):362-368.
57. Tacke PJ, de Vries IJ, Torensma R, Figdor CG. (2007). Dendritic-cell immunotherapy: from ex vivo loading to in vivo targeting. *Nat Rev Immunol*.7(10):790-802.
58. Hu Y, Fu L. (2012). Targeting cancer stem cells: a new therapy to cure cancer patients. *Am J Cancer Res*.2(3):340-356.
59. Selvan SR, Carbonell DJ, Fowler AW, Beatty AR, Ravindranath MH, Dillman RO. (2010). Establishment of stable cell lines for personalized melanoma cell vaccine. *Melanoma Res*.20(4):280-292.
60. Zhan Y, Xu Y, Lew AM. (2012). The regulation of the development and function of dendritic cell subsets by GM-CSF: More than a hematopoietic growth factor. *Mol Immunol*.52(1):30-37.
61. Dziurzynski K, Chang SM, Heimberger AB, Kalejta RF, McGregor Dallas SR, Smit M, et al. (2012). Consensus on the role of human cytomegalovirus in glioblastoma. *Neuro Oncol*.14(3):246-255.
62. Lucas KG, Bao L, Bruggeman R, Dunham K, Specht C. (2011). The detection of CMV pp65 and IE1 in glioblastoma multiforme. *J Neurooncol*.103(2):231-238.
63. Potti A, Forseen SE, Koka VK, Pervez H, Koch M, Fraiman G, et al. (2004). Determination of HER-2/neu overexpression and clinical predictors of survival in a cohort of 347 patients with primary malignant brain tumors. *Cancer Invest*.22(4):537-544.

64. Mesiano G, Todorovic M, Gammaitoni L, Leuci V, Giraud Diego L, Carnevale-Schianca F, et al. (2012). Cytokine-induced killer (CIK) cells as feasible and effective adoptive immunotherapy for the treatment of solid tumors. *Expert Opin Biol Ther.* 12(6):673-684.
65. Pluhar GE, Grogan PT, Seiler C, Goulart M, Santacruz KS, Carlson C, et al. (2010). Anti-tumor immune response correlates with neurological symptoms in a dog with spontaneous astrocytoma treated by gene and vaccine therapy. *Vaccine.* 28(19):3371-3378.
66. Thu MS, Najbauer J, Kendall SE, Harutyunyan I, Sangalang N, Gutova M, et al. (2009). Iron labeling and pre-clinical MRI visualization of therapeutic human neural stem cells in a murine glioma model. *PLoS One.* 4(9):e7218.
67. Kloss CC, Condomines M, Cartellieri M, Bachmann M, Sadelain M. (2012). Combinatorial antigen recognition with balanced signaling promotes selective tumor eradication by engineered T cells. *Nat Biotechnol.* 31(1):71-75.

CHAPTER XIII



DISCUSSION

Part 1: Sarah Bovenberg
Part 2: Hannah Degeling

I. CREATING THE IDEAL ANTI GLIOMA AGENT

As has been highlighted throughout this thesis, brain tumors, and GBM in particular, are very difficult types of cancer to treat. A quick search on PubMed will reveal a wide range of strategic approaches that are currently being explored, ranging from new chemotherapeutic agents and/or dose schemes, drugs, surgical techniques, antibodies, to cell- and gene therapy. Even though it is beyond the scope of this thesis to discuss all of these approaches, it can be concluded that many exciting research is being done, based on ideas that theoretically should be able to destroy the tumor mass completely. However, what works on paper does not necessarily work in the lab, let alone in clinical settings. Other strategies seem to work just fine – without anyone fully understanding what causes their success. When thinking about the ideal anti-glioma agent, the following characteristics should be present:

- 1) The agent is highly selective to glioma cells, while causing minimal damage to the normal brain tissue
- 2) The agent has the ability to track down single invasive cells
- 3) The agent should attack the glioma cells through a range of pathways, thereby blocking tumor escape mechanisms and accounting for the heterogeneous nature of the glioma cell population
- 4) Its action should be continuous, until the eradication of all tumor cells is completed
- 5) The agent should contain a biological marker that allows for monitoring of the effect of treatment over time
- 6) The agent should be able to cross the blood-brain barrier
- 7) The agent is tailored to the individual patient

Objectively, stem cell therapy seems to hold all the right cards. However, as can be concluded from our reviews in **Chapter XI** and **XII**, we still have a long way to go before all issues are resolved. This raises the following questions:

- What is needed to improve treatment efficacy?
- What is needed to bridge the gap to the clinic?

The primary aim of this thesis was to gain better understanding of both glioma biology and anticancer mechanisms by visualizing what happens at cellular and molecular level. Imaging tools will be of the utter most importance to get a true understanding of the working mechanisms and antitumor effect of cellular therapies. The ability to track single cells, to monitor cell differentiation, tropism, migration, interactions with the environment and mechanisms of action will allow us to answer important questions regarding safety and efficacy.

To create this ideal anti-glioma agent, in this thesis we have developed several tools. First, we focused on secreted blood reporters, since they allow for sensitive, fast detection, quantification and non invasive, *ex vivo* monitoring of *in vivo* processes, with the generation of multiple data sets without the need to sacrifice the animal. Therefore, we developed an enhanced Gluc blood assay (**Chapter III**), in which Gluc is captured from the blood by an antibody-mediated reaction before bioluminescence reaction takes place. This procedure prevented signal quenching by pigmented molecules like hemoglobin, and resulted in an over one order in magnitude increase in sensitivity, allowing the detection of few circulating cells and early tumor metastases by the simple measurement of a few drops of blood.

Second, we selected an agent that is highly specific to glioma cells, while leaving healthy brain tissue unaffected. Through an extensive drug screen the Tannous lab recently discovered how the cardiac glycoside lanatoside C seems to sensitize glioma cells to anti cancer agent TRAIL. In **Chapter V** we describe how the combined treatment of sTRAIL and lanatoside C is highly effective in eradicating glioma cells and avoiding resistance and/or recurrence *in vivo*. Since TRAIL cannot cross the blood brain barrier, we decided to circumvent this problem by delivering sTRAIL directly to brain tumor environment by AAV-mediated gene delivery. By engineering the normal brain to synthesize and secrete sTRAIL, we created a zone of resistance against newly developed glioma, which can be treated with lanatoside C therapy. While treatment with sTRAIL by itself resulted in an initial decrease in tumor progression, followed by regrowth through resistant cells, no regrowth took place in the presence of lanatoside C. Further, since sTRAIL binds selectively to death receptors found only on tumor cells, no additional damage to healthy brain tissue was observed.

Third, to measure the effect of combined lanatoside C and TRAIL treatment, we developed the first triple luciferase bioluminescence imaging system for *in vivo* use (**Chapter V**). The reporter system allowed us to sequentially monitor the changes at cellular level once therapy was initiated, with *Vargula* luciferase being used as a marker of efficient gene transfer of sTRAIL to healthy brain tissue, *Gaussia* luciferase as marker of TRAIL binding to the death receptor on Glioma cells and firefly luciferase as a marker of tumor volume and therefore therapeutic response.

Fourth, since tumorigenesis is an intricate and dynamic process and GBM cells in particular are known for their ability to escape cell death and change characteristics, we developed the first multiplex blood reporter based on secreted alkaline phosphatase (SEAP), *Gaussia* and *Vargula* luciferases (**Chapter IV**). This multiplex system differs from the triple imaging system as described in Chapter V in that here all reporters are secreted. As a result, tumor changes can be followed in real time (by simply taking an aliquot of blood), whereas the reporter from chapter V does not allow for real time imaging. Since *Vargula* has not been previously used as a blood reporter we first characterized it as a secreted blood reporter. As a proof of concept we monitored the response of three different subsets of glioma cells to the chemotherapeutic agent Temozolomide (TMZ) in the same animal. U87 glioma parent cells (sensitive to TMZ) were engineered by a lentivirus vector to express Gluc (U87-Gluc), while U87R1 (resistant to TMZ) were engineered to express Vluc (U87R1-Vluc) and U87R2 (resistant to TMZ) were engineered to express both SEAP and Fluc (U87-SEAP/Fluc). All cell lines were mixed equally and intracranially implanted. One week later mice were either injected with TMZ or DMSO (control) and blood was collected at different time points. As expected, a continuous decrease in Gluc signal was observed over time in the TMZ group, while an increase in signal was observed in the control group. Both Vluc and SEAP levels increased over time in both treatment and control group, showing that U87R1 and U87R2 cells are indeed resistant to TMZ. No signal bleeding or substrate cross reaction was observed, proving that these 3 reporters can be used simultaneously in the same animal. This new multiplex reporter system can be extended and applied to many different fields for simultaneous monitoring of multiple biological parameters in real time.

II. FUTURE APPLICATION

All together, these systems create the tools to develop a highly effective therapeutic/diagnostic anti-glioma agent. Since viral therapy is known to have its limitations in terms of distribution and delivery (as discussed throughout this thesis), and stem cells intrinsically possess quite some of the characteristics needed for the ideal glioma agent (tropism, penetrating the blood brain barrier, ability to track metastasis), stem cells would be the ideal carrier for our toolbox. In this case, the combined sTRAIL/lanatoside C therapy approach could be applied to stem cell carrier system, in which stem cells will be modified to express sTRAIL. These cells can either be injected in the tumor cavity after surgery or even be given systemically. The genetically modified stem cells can be tracked using the enhanced Gluc blood assay, visualizing patterns of migration and tropism over time. Since the assay is sensitive enough to pick up signals from as little as 10 cells, the ability of the modified stem cells to invade the healthy brain parenchyma to capture single invasive glioma cells can be evaluated, as well as the specificity of the stem cells to glioma. Simultaneously, *Vargula* luciferase under the control of NFκB responsive elements, which can be detected either in the blood or by means of BLI, can be used to monitor delivery and binding of sTRAIL to the death receptors on glioma cells, while Fluc imaging (or the SEAP blood assay) can be used to evaluate the tumor response to TRAIL and lanatoside C. This approach will for the first time allow monitoring of several biological processes in response to therapy, giving new insight in the complex interactions of therapeutics to cancer cells. Obviously, other parameters can be chosen, since this system is applicable to any biological process of interest. Further, since lanatoside C, AAV vectors, stem cells and TRAIL have been previously used in the clinic separately, this combined therapeutic approach should be easily adaptive to the clinical setting.

III. CREATING THE IDEAL LUCIFERASE

Once working on optimizing BLI reporters to monitor several tumor processes simultaneously, a second issue came to mind. While *Gaussia* Luciferase possesses many favorable characteristics needed in a reporter, including high signal intensity, favorable enzyme stability and a secretion signal, and is thereby the luciferase of

choice for many BLI applications, its use for *in vivo* imaging is limited due to its emission of blue light which is absorbed by pigmented molecules such as hemoglobin and scattered by mammalian tissues. Furthermore, its flash type bioluminescence reaction, which makes the signal decrease in intensity shortly after the substrate is added, makes it unsuited for high-throughput applications such as drug screens. Therefore, in **Chapter VI**, we started a directed evolution mediated screen for Gluc mutants with more favorable characteristics, which resulted in the generation of multiple clones with higher signal intensity, glow-like kinetics (suited for high-throughput applications) and a shift in the emission towards the red region of the spectrum (suited for *in vivo* applications). Although more work needs to be done to further optimize these clones, the first step towards a red-shifted *Gaussia* Luciferase has been made. This is not only interesting for laboratory work, but in a time where optical guided surgery is on the verge of break through, a luciferase with good tissue penetration can become of tremendous value.

IV. FUTURE APPLICATIONS

Stable Gaussia

Since the ‘discovery’ of the alkylating agent temozolomide no real improvement has been made in the development of anti-glioma drugs. One approach to solve this problem is the screening of small molecule libraries for potential anti-glioma hits. This process is a time-consuming and costly as thousands of molecules must be screened. *Gaussia* luciferase is commonly used as cell viability marker as it is secreted, allowing functional analysis of drug kinetics over time by sampling of the conditioned media. As described above, its flash like luminescence, requiring each well to be injected with substrate before the read – instead of reading complete plates at a time – severely limited the amount of data that could be obtained in a certain time. The new Gluc clones with glow type BLI will be able to simplify and speed up the current process, allowing more clones to be screened and thereby increasing the chance of finding a hit. One could also imagine the benefit of using multiple luciferase reporters at the same time (e.g., the multiplex reporter systems as developed in this thesis), in order to develop a multi-parameter high throughput screening. This would provide valuable information with regards to drug working mechanisms and gene/pathway activation - thereby eventually allowing mapping of tumor response and prediction of outcome.

Red Gaussia

Optical guided surgery, which hypothetically allows for real time visualization of tumor borders, metastatic cells and nearby vulnerable structures, could potentially create a revolution in oncologic surgery. As for now, it comprises various modalities, including PET, CT, MRI and near infrared (NIR) fluorescence. While PET, MRI and CT are great diagnostic tools, they are less suitable to translate their findings to mark sharp borders of “sick” and “healthy” tissue in the operation field. Further, they are costly and not always available in OR setting. Fluorescence imaging is based on a fluorescent probe that has the ability to absorb light at a particular wavelength and subsequently emits light at a longer wavelength. Where the original fluorescent markers were not quite suitable for *in vivo* use, due to poor tissue penetration and high signal to noise ratio's (SNR), near infra red (NIR) fluorescence (with an emission spectrum of 650-900nm) has overcome these problems. A recent pilot study in the Netherlands using the fluorescent probe fluorescein isothiocyanate (FITC) in patients with ovarian cancer was highly successful in identifying the tumor mass and metastasis < 0.5 mm, while no benign masses were colored (*Van Dam GM, Themelis G, Crane LM, et al. Intraoperative tumor-specific fluorescence imaging in ovarian cancer by folate receptor-alpha targeting: first in-human results. Nat Med. 2011;17:1315-9*). NIR fluorescence is both cost efficient and easy to use and therefore makes a good candidate for optical-guided surgery. If instead of fluorescence probes, a red-shifted *Gaussia* Luciferase could be developed, it would have the additional advantage that no external light source is needed, resulting in a further reduction of the SNR and the generation of even higher sensitivity. In animal settings, BLI is preferred over fluorescence due to this higher sensitivity. However, since *Gaussia* needs its substrate coelenterazine in order to emit light, toxicity concerns related to the substrate and immunogenicity of the *Gaussia* protein should be evaluated before the step to the clinic is made.

V. ENHANCING TISSUE CULTURE RELIABILITY

Tissue culture is the foundation for glioma research. Human glioma cell lines are differentiated, expanded, and manipulated in order to develop reliable glioma models that will increase our insight in tumor biology and give us the opportunity to test various strategies. The more reliable the tumor model, the more reliable the outcome

of the experiment and the more likely the obtained results will be reproducible in clinical setting. However, when cells are passaged over a long period of time, differentiation and phenotypic changes may occur, as well as contamination with bacteria, fungi and/or other organisms. Whereas some types of contamination are easily detected and therefore solved, others go unnoticed and severely compromise results. The latter can be said for Mycoplasma, the smallest type of free-living organism known. In order to enhance tissue culture reliability we developed a *Gaussia*-luciferase based mycoplasma detection assay, in which the rate of Gluc degeneration corresponds with the amount of Mycoplasma in the tissue culture media.

VI. FUTURE APPLICATION

Our current assay is more sensitive and cheaper than currently available commercial assays and will help researchers to work more efficient and accurate.

VII. CURRENT LIMITATIONS AND FUTURE DIRECTIVES: THE BIG PICTURE

In the beginning of this chapter two questions were raised:

- What is needed to improve treatment efficacy?
- What is needed to bridge the gap to the clinic?

Chapter-wise we discussed what actions were taken to overcome some of the limitations faced in our specific field of glioma research, in order to increase both efficacy and the likelihood of the approach being successful in clinical settings. Now it's time to look at the big picture. When looking at the glioma research field an sich one can't help but notice that very little research is able to – successfully - cross the gap between experimental setting and the clinic. Considering the amount of time (and results) that is required to 'prepare' a strategy for FDA approved clinical testing, this is remarkable.

One important limitation slowing the translation from experimental setting to clinic can be attributed to the current *glioma models*. Although many pathophysiological

similarities between the rodent glioma model and human tumors are observed, many models are based on xenografts in immunocompromised mice. Implanted tumor cells will not mimic the process of *de novo* tumorigenesis, and tumor-associated immunosuppression and immune-modulating events are not likely to be accurately reflected, resulting in a slightly different tumor microenvironment. Especially when testing immunotherapeutic approaches that require activation of the body's immune system to attack the tumor cells, this situation is less than optimal and might confound results severely. The use of rodents with an intact immune system and genetic induction of the tumorigenesis might circumvent these problems.

A second limitation arises at the level of the clinical trial itself. Since glioblastoma is a relatively 'rare' disease and since survival is poor, there's only a *limited number of patients* that can be enrolled. This results in trials with less than optimal numbers for statistical analysis. Further, since inclusion criteria differ between study groups, substantially influencing survival rates and outcome, it is hard to compare results. Also, patients often use of co-medication including corticosteroids, which impairs objective assessment even further, as efficacy of the treatment may be limited, side effects may be masked and tumor differentiation may be halted.

A third limitation is caused by difficulties related to acquiring *proper expression levels* of the to be tested therapy. Viral gene transduction levels tend to be low or decline steadily over a sufficient period of time. In both scenarios treatment efficacy is limited. This may result not only in unsuccessful clinical trials, but also in the abandonment of a potentially successful strategy. Targeting healthy brain tissue instead of the tumor itself has shown to result in more effective gene expression and might be an alternative to the current approach. In experimental setting stem- and immuno-cell carriers have shown impressive results with regards to tracking tumor cells and delivering oncolytic viruses, enzymes, cytokines, activated immune cells and other lethal substances directly to the tumor cells. However, this has yet to be demonstrated on larger scale in the clinic.

A fourth issue, closely related to the third, is appropriate *patient selection*. As discussed extensively throughout this thesis, GBM is a highly heterogeneous tumor on both molecular and genetic level. More and more evidence suggest that specific

genetic mutations in glioma cells respond to different therapies, and therefore genotyping or discovery of new biomarkers for personalized medicine could yield to an enhanced treatment success. Patient selection will not only increase patient quality of life (QoL) - withholding chemotherapy when genetic profiling will predicted the tumor is not responsive to this type of therapy - but will also give new therapeutic approaches a fair shot. Including patients with a EGFRIII mutation –which is often unresponsive to chemotherapy- for a clinical trial to test a new alkylating agent may not only potentially downplay the overall efficacy of this therapy, but may also falsely disqualify a successful approach by showing that results obtained in experimental studies cannot be repeated in the clinic.

A fifth issue is *safety*. The use of stem and/or immuno-cells, with the capacity of unlimited self-renewal, raises concerns with regards to malignant transformation. Further, the secretion of cytokines and growth factors and the local immuno-suppressive effects of stem cells could hypothetically promote tumor growth. The standard inclusion of a suicide gene in the DNA of each stem cell might help creating a safer experience. Besides safety matters, ethical issues need to be addressed. These questions do not only concern the glioma research field, but are applicable to the research community as a whole.

From the above one conclusion can be drawn: to undermine these problems and to get a true grip on a tumor as diverse as GBM a multi angle approach is needed. It is highly unlikely that – for a tumor this diverse - a single agent approach will yield the desired results. An integrated therapy based on genetic profiling that blocks several tumor escape mechanisms at once, has much more chances of succeeding.

The same can be said for the approach towards glioma research in general. A multidisciplinary, multi-angle approach is much more likely to yield results than isolated, singular attempts. To stimulate this process, the National Brain Tumor Society recently launched the DREAM Cancer Prediction Challenge, a campaign in which researchers from all backgrounds are asked to work together to attack Glioma. A virtual database, containing all available preclinical data from research groups over the world, will be generated and made accessible to participating researchers. The challenge is to design a computational model that can screen small molecule/drug

libraries against glioma, and can predict tumor response to the selected agent. If such a program can be developed, the benefit will be enormous. Not only will we be able to screen millions of compounds in a time- and cost-effective manner, it will also drastically reduce the amount of animal sacrifices needed. The data obtained by multiplex reporter systems to map the various pathways activated by certain drugs or involved in tumor escape mechanisms might play a crucial role in this project.

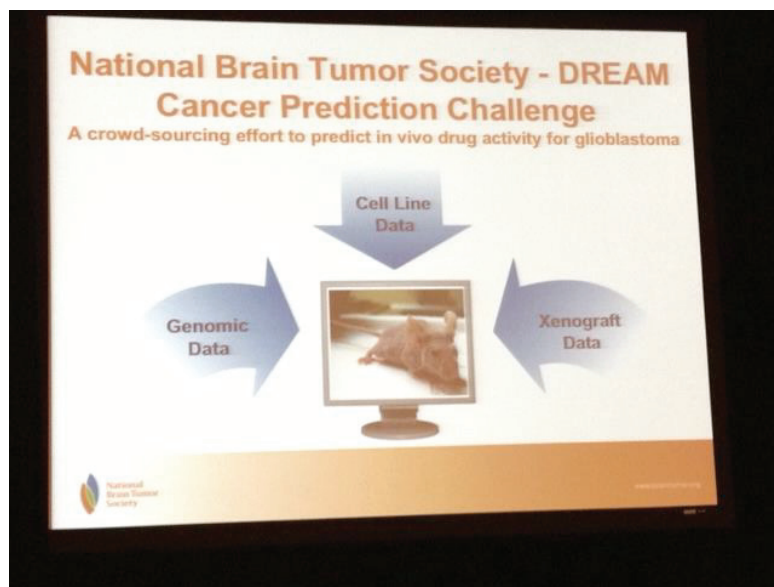


image obtained from the National Brain Tumor Society.

VII. IN CONCLUSION

In conclusion, in this thesis we have developed several tools for the road towards a better understanding of glioma biology and more effective therapy. In order to justify the importance of this work, in **Chapter XI** and **XII** we give an overview of the research being done in the neuro-oncology community and the difficulties encountered. The tools we developed (including a therapeutic agent specifically selective for glioma cells, two new multiplex imaging modalities and more sensitive assays and luciferase imaging agents) will eventually help us to translate experimental setups to the clinic, since a better understanding of the 'what' at molecular level, will result in a 'how' in a broader setting. The triple BLI and blood

assays will be of enormous value in this understanding, since they will allow us to study interactions – of tumor cells, growth factors, intrinsic pathways and therapeutics – *in vivo*; mimicking the ‘real’ situation as close as possible, and giving us new clues on how to increase efficacy, select new targets, prevent safety issues and eventually, to bridge the gap to the clinic.

Part 2: Discussion by Hannah Degeling

In The Netherlands, **cancer** is the leading cause of death and surpassed cardiovascular diseases in 2008. Of the 136.058 people that died in 2010, 32% of all the deaths were caused by cancer.² Even though great achievements are made in the battle against cancer, with a cure rate of 90% for testicular cancer as a good example, numerous cancer types are still difficult to treat:⁶ patients diagnosed with glioblastoma multiforme will have a life expectancy of around 1 year.⁷ The treatment of cancer remains a critical issue in our society.

The battle against cancer continues and we carry on developing new molecular imaging modalities to diagnose and monitor cancer growth. We screen for new drugs to improve chemotherapy⁸, we use radio-isotopes in the field of nuclear medicine, and we even isolate the DNA gene sequence coding for the light emission in the copepod *Gaussia princeps*. We know the 'light proteins' better as luciferases and use them for bioluminescence imaging.

Bioluminescence imaging (BLI) has greatly contributed to developments in cancer research. BLI allows for monitoring of real-time tumor processes in animal models without disturbing the natural dynamics. This led to the use of BLI in xenogeneic, orthotopic, and genetically engineered animals and provided for great insight in tumor processes.⁹ Even more, BLI is not only used to evaluate the characteristics of an already existing tumor, it can also provide us of more information about the onset of cancer.¹⁰ Evidently, BLI has conquered an indispensable place in experimental research for cancer.

Nevertheless, the different luciferases used for BLI each have their disadvantages. *Gaussia* luciferase (Gluc) has a high light output, an enzymatic half-life of around 5 days, and is secreted out of the cells into the blood stream, making *ex vivo* applications possible.¹¹ However, Gluc has a light emission in the blue spectrum, which is, during *in vivo* imaging, mostly absorbed by pigmented molecules such as hemoglobin and is scattered by mammalian tissues before even reaching the camera.¹² Further, Gluc has a flash light emission, which can on one hand be useful for real-time monitoring, on the other hand, it makes high-throughput screening for drugs impossible. Hence, we screened for a Gluc with better characteristics in **chapter VI** and found mutants with a peak shift towards the red region of the spectrum, opening the path for further screen. The shift in wavelength is not enough

for more sensitivity during *in vivo* experiments. However, it does provide information about which part of Gluc is associated with the wavelength of the light emission, which will be useful for future attempts in Gluc wavelength engineering. Moreover, we found a Gluc mutant which yields stable light output without the need of a detergent such as of Triton-X 100¹³, suited for high-throughput screening. High-throughput screening requires a stable signal of the luciferase in order to compare the signal of the first reading with the last one. Gluc is of great advantage for such drug-screens since it is naturally secreted out of the cells and simply measuring signal in the media is sufficient. Until now Gluc needed the addition of Triton-X 100¹³ to provide a stable signal, while obviously no additional supplements to screening media are preferred. A downside of the stable mutant is its low signal intensity, making the luciferase less sensitive. Finally, we observed that all Gluc mutants contained mutations in a specific region and thereby we revealed the active site of Gluc. Once more, a better understanding of the structure of Gluc protein is very important for future Gluc engineering.

When measuring Gluc signal in the blood *ex vivo*, instead of searching for a red-spectrum Gluc, another approach to overcome Gluc signal quenching in the blood is to optimize the actual assay. In **Chapter III**, by capturing Gluc from blood using specific antibody, we developed a Gluc blood assay that showed a ten-fold higher sensitivity compared to assaying Gluc signal directly in the blood.¹² In the case of tumor, the Gluc signal in the blood can be detected at a much earlier time point and requires less tumor load.⁴

However, the antibody assay does have certain limitations. First of all the preparations and the actual assay are time consuming compared to simply assaying Gluc directly in the blood. Further, Gluc antibody has certain costs; this could be a limitation when many animals need to be monitored on a regular basis.

Nevertheless, Gluc signal in the blood is often at the low side and a more sensitive assay will be of great value. This high sensitivity will give us the opportunity to monitor very small or slow growing tumors and to detect only a few circulating tumor cells, as in the case of metastasis, which was until now difficult to achieve with Gluc. Hence, the Gluc antibody assay makes it possible to obtain more accurate information about apoptosis and the actual tumor growth.^{12, 14, 15} Perhaps, this assay decreases the urgency of finding a red-light Gluc variant for *in vivo*

applications. On the other hand, the assay could also serve as a temporarily tool for more sensitivity until research found the red Gluc.

Different secreted reporters can be multiplexed together to monitor several processes in the blood at the same time *ex vivo*, given that each reporter utilizes a different substrate. ¹⁶ **Chapter IV** evaluates the potential to multiplex three different blood reporters, Gluc, secreted embryonic alkaline phosphatase (SEAP), and *Vargulla* luciferase (Vluc), and explores the possibility of a triple blood system for future research applications. Experimental research will benefit from these novel blood reporter combinations, especially when there is no need to sacrifice the animal. A downside of the reporter system is that it will take some effort to achieve a high transduction efficiency of the tumor cells and to read each time point with the three different reporters requiring three different assay procedures. .

Theoretically, an *ex vivo* blood reporter assay would have the potential for future clinical application, nonetheless, the genes coding for the blood reporters will still have to be incorporated into the DNA of our tumor cells.

As for blood reporters, research has also focused on discovering and constructing different variants for different luciferases. Not only to optimize the specific characteristics of each luciferase, but also to expand the diversity of luciferases for imaging multiple processes simultaneously. In the case of the Italian firefly luciferase (liFluc) from *Luciola italica*, a green and a red light emission variant was characterized as described in **chapter VII**. ¹⁷ Since Fluc is due to its beneficial characteristics a popular luciferase in experimental research, it will be of great use to have different variants. Nevertheless, Fluc is partly popular due to its red light emission and the green Italian variant will most likely serve as a second marker.

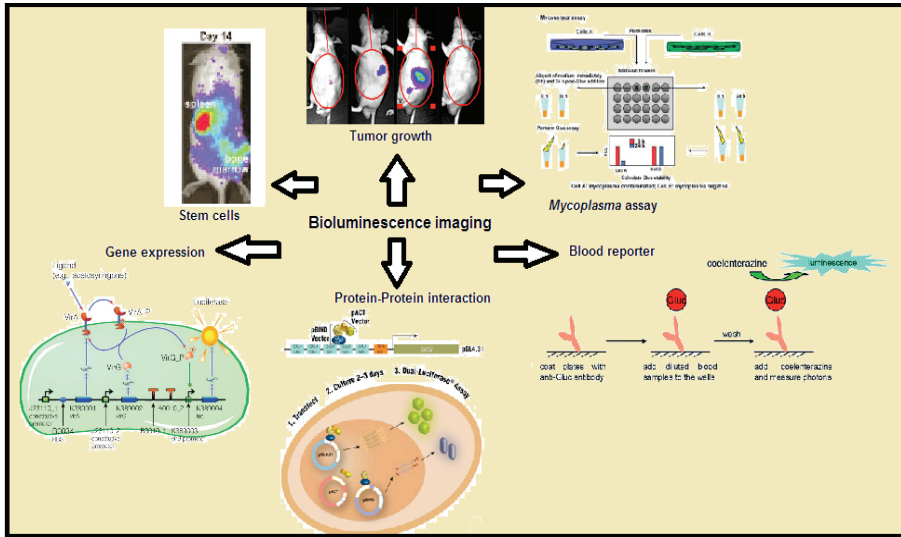


Figure 1. Bioluminescence and applications. 1 4 3 4 5
 , , , , ,

The clinical application of luciferases is still far from being established. Even though BLI appears to be of great use in experimental animal models, a gap between these models and humans remains. What milestones should be conquered?

First of all, the human genome does not encode for the luciferases as used in experimental setting. This means that our immune system will try to eliminate the luciferase protein once expressed. Besides a potential immuno-reaction, we have not determined yet whether these foreign proteins are safe to our body, and, most importantly, what the long term effect is of expressing these foreign molecules. Secondly, luciferases require a substrate to emit light. Even if it would be safe to have cells in human expressing *Gaussia* luciferase, the necessity remains to deliver a substrate to those cells. One delivery option would be an injection into the bloodstream. However, since this substrate would bypass all our body tissues, we should be absolutely certain that no side-effects will occur.

To generate an experimental animal model orthotropic tumor cells are first transduced with the gene encoding for the luciferase, afterwards injected into the animals, and once the tumor has grown we try to eliminate it again. Obviously, in a clinical setting the tumor is already present and our main purpose is only to remove the tumor cells: the opposite principle. First of all, in contrast to experimental research, in humans we are not able to decide on the type of Glioblastoma; with a

biopsy we are merely able to observe the specific type. Secondly, when a biopsy of the tumor mass of the patient is taken and the treatment is started, we can't be sure whether the entire tumor, including the microsatellites, of the patient remains genetically identical.¹⁸ Besides, high grade gliomas differ genetically for different individuals, limiting the possibility of finding a common molecular treatment for multiple patients.¹⁹ ²⁰Thirdly, it is relatively simple to manipulate the tumor cells *in vitro* before injecting them *in vivo*, while in humans the manipulation would be performed *in vivo*, with for example viral vectors, which is much more difficult to perform successfully. Further, in public opinion, manipulation of the human genome is still controversial.

To circumvent the problems mentioned above is to use luciferases for cellular therapy against cancer, as described in the experimental part of the review of **chapter XI**. Since these stem cells are first modified *ex vivo* to carry i.a. certain drugs, theoretically it should be possible to image the migration and the production of these cells and their drugs in a clinical setting with bioluminescence. Perhaps, one day through cellular therapy, BLI can be introduced into humans.

Whereas bioluminescence imaging is nowadays restricted to experimental use, fluorescence imaging is already applied in clinical setting. Fluorescence is used for endoscopic diagnostics, for example the exploration of gastric and colonic mucosae, and can even be used during surgeries.²¹ During surgery, fluorescence can provide information about the tumor edge and the distinction between normal tissue and tumor tissue. An example is 5-aminolevulinic acid, an optical dye that specifically adheres to brain tumor cells and thereby serves as a useful tool during malignant glioma resection.²² One limitation for clinical use of fluorescence is a limited tissue penetration. Radioisotopes provide much greater depth tissue penetration. However, for surface diagnostics, such as endoscopic diagnostics, less penetration is necessary and fluorescence appears to be very useful.²² Another limitation is the exact quantification of the signal, since different tissues absorb the light in different quantities and different tissues show different background fluorescence, resulting in a bias of the measured fluorescence signal.²¹ Bioluminescence, on the contrary, is only measured when the luciferase and the substrate are actually present, which would provide more accurate results compared to fluorescence. Certainly, bioluminescence is not introduced into humans yet. Even so, with fluorescence each

dye also needs to be proven safe separately for clinical application, which definitely slows down the progress of fluorescence for clinical purposes.²¹

Another approach for the treatment of cancer, which is widely used in experimental setting and also useful for clinical purposes, is the use of **liposomes**. Liposomes provide for selective target delivery and can carry a sufficient amount of drugs. Since they are currently widely used in pharmaceutical setting, and thus approved for clinical purposes, they are of great interest.²³ An example of a successful liposomal drug is a target specific liposome containing doxorubicin to treat breast cancer metastasis.²⁴ However, also in the field of liposomes certain drawbacks remain, such as the quick elimination of liposomes from the blood. In the last decade, liposomes have been a popular topic in research resulting in the creation of many different variants, including long-circulating liposomes and immuno-specific liposomes.²³ One can theorize that the combination of an optimized liposome that is target specific, that can cross the blood-brain-barrier, and only releases the effective drug at the site of tumor, would be ideal for the treatment of the glioblastoma. And if we continue to speculate about future possibilities, we might even be able to incorporate the gene sequence for Gluc combined with an effective drug or an apoptotic gene sequence into a cationic liposome, and we will be able to monitor the tumor of the patient weekly by BLI.

Nonetheless, even in experimental research it would be difficult to create a liposome with all the structures mentioned above incorporated in its body. Moreover, a liposome is not like a viral vector, it doesn't incorporate into the human genome for stable expression, which means that a liposome carrying solely the gene sequence of Gluc wouldn't be of any use. The liposome would have to carry a viral vector with the Gluc sequence for Gluc expression.

Further, it would be important that the liposome has optimal MRI contrast to determine the correct location before releasing its viral vector. Still, once experimental research will have a solid and relatively simple protocol for the creation of such liposomes, they will be of great use for pre-clinical research.

Since we can find liposomes in many different shapes and formats, it is reasonable to speculate about all the different treatment possibilities with liposomes. Liposomes are not only drug carriers or DNA delivery vehicles for cancer treatment; on the contrary, liposomes are also interesting for the treatment of, for example,

neurodegenerative diseases, such as Duchenne muscular dystrophy. And liposomes have already been investigated for the delivery of a variety of agents, including nucleic acids and prednisolone, in the fight against this disease.^{25 26} Ideally in numerous of diseases, liposomes would adhere at the location of preference and locally produce our enzyme of interest. And most remarkably, research did already develop liposomes that are able to produce proteins themselves, resulting in a combined delivery and production system.²⁷ Therefore, what remains is the necessity of finding a perfect liposome that is very sensitive for camera detection to follow its track, it adheres specifically to the tissue of preference, and it will solely at that location release the drugs or secrete the produced protein. Conceivably, progress will be made with liposomes as protein producing vehicles and we will improve the use of essential cellular elements within a liposome.

In chapter X, we developed a liposome that is very well detectable with MRI; the liposome is target specific due to the presence of biotin at its surface and thermo-sensitive for the release of its contents. This liposome will be very suitable for the delivery of drugs to tumor cells. And hopefully, due to the possibility of tracking its faith accurately by MRI and its target specificity, this liposome will be able to serve as a promising model for a combined delivery and production system.

Many roads lead to Rome and liposomes are not the only drug delivery vehicles that can be modified for target specificity. In **chapter XI**, the use of stem cells for the treatment against brain cancer has been reviewed. Even though only one clinical trial so far is making use of these vehicles, the experimental data provide an interesting perspective. Besides serving as drug vehicles, stem cells can also deliver gene and oncolytic viral therapy at the tumor site. A prospect for experimental research would be a luciferase coupled to a virus and carried by stem cells. And theoretically, oncolytic viruses have a significant potential for glioma therapy due to their specificity and high efficiency in killing tumor cells. However, current viral therapeutic strategies have not yet reached their full potential due to poor distribution at the tumor site, low infectivity of tumor cells, and the host immune response. Therefore the strategy of hiding the virus within a stem cell has great potential.²⁸ Moreover, in experimental research a luciferase was coupled to TRAIL and delivered by neural stem cells.²⁹ Aside from stem cells, immune cells are useful as well as described in **chapter XII**. Glioma tumor cells are clever in evading the innate immune system; immune cell

therapy can trigger an immune response instead. And since dendritic cells are potent antigen presenting cells, they emerge as promising vaccine cells in clinical trials.^{30,31} For both stem and immune cell therapy, experimental research widely explores the possibilities while the clinical application advances more gradually. The translation from experimental to clinical application remains a difficult phase. The use of rodents with intact immune system, and the development of genetically-induced glioma models could help optimizing preclinical studies, leading to a more predictable transition to the clinic.

Since this thesis is about Cancer and Luciferases, the luciferases are mainly evaluated for the use in cancer research and the revelation of tumor processes. However, their value in experimental research is much broader than that and even to the extent that a disturbing *Mycoplasma* contamination can be revealed by Gluc. Gluc protein in cell culture is degraded in the presence of *Mycoplasma* and in such a stable manner that we created a Gluc Mycoplasma assay as described in **chapter VIII** and **IX**.³

The assay is more sensitive and less expensive than other often used *Mycoplasma* assays. A limitation is that most research doesn't make use of transduction techniques with viral vectors, and definitely not a Gluc vector, which means that Gluc media will either have to be ordered from other laboratories or a great number of cells need to be transformed with Gluc protein for a sufficient stock.

Even so, once a solid Gluc containing media stock is acquired, the assay is simple to perform and in sensitivity and expenses it is superior to a popular mycoplasma assay.³ Therefore, it might just be a matter of time before this assay becomes the standard Mycoplasma detection assay at most cell culture laboratories.

Notably, *Mycoplasma sp.* do not only occur in cell culture; on the contrary, they are known to give for example pneumonia in humans.³² With this knowledge, one can speculate that Gluc in clinical setting would be degraded by *Mycoplasma* as well. Even more, if *Mycoplasma* contamination has such a significant effect on Gluc, wouldn't we be able to construct a Gluc sensitive to a particular biological substance of interest? This would be of great value for future experimental research. We did speculate the possibility of this idea and constructed a Gluc protein which contains a MMP sensitive cleavage sequence. MMPs are well known biological cleavage

proteins produced by almost every cell. The constructed Gluc was expected to show a greatly reduced half-life in the presence of MMPs; however, no decrease in half-life was observed in the presence of MMPs. An explanation for this can be sought in the folding structure of Gluc, which would conceal the sensitive cleavage spot from the MMPs.

Bioluminescence and cancer: experimental perspectives

Long ago, in the nineteenth century, seamen and fishermen saw lights on the water and realized that these lights were from organisms in the water emitting them: this was called **bioluminescence**. Only about 45 years ago, various luciferases began to be characterized.^{33 34 35} Nowadays bioluminescence is widely used in experimental research.

Novel luciferase variants are still discovered and created, which gives rise to even more imaging possibilities, such as dual/triple/quadruple imaging. Research reveals the structure of luciferases and provides thereby a manual for future luciferase engineering, resulting in optimal luciferase variants. In the last decades luciferases became important tools in experimental research.

What is it that makes luciferases valuable?

First of all, molecular cancer research needs solid tools that reveal tumor processes and monitor treatment effects. Luciferases serve as these tools; they can be attached to many different vehicles for numerous of research applications. Secondly, the variety in different kinds of luciferases creates the opportunity to use them for a wide spectrum of services; they can, for example, be used for the monitoring of gene expression, but also for tracking stem cell therapy.²⁹ Thirdly, certain luciferases can serve as secreted blood reporters and the *in vivo* tumor biologics can be measured *ex vivo* by these reporters. This is very useful for experimental *in vivo* research, since the animals don't need to be sacrificed for every single time point. Obviously, not all diagnostic agents require the animal to be sacrificed for the desired information and the tumor can, for example, be made visible under a camera. However, if the animals receive anesthetics before imaging it will definitely take a considerable amount of time to image all the animals for every single time point and simply withdrawing some blood will have an advantage. Besides, one of the great utilities of blood reporters is that they can provide detailed information about the

different biological processes of the tumor. Moreover, since multiple blood reporters exists, we are able to monitor the tumor response to therapy of different kinds of tumor cells at the same time, as shown in **chapter IV**. And, since blood reporters can be coupled to different genes expressed by the same tumor, our triple reporter system will make it possible to monitor noninvasively three different biological processes of the same tumor. Further, since luciferases can be expressed by all kinds of tumor cells, their value is not restricted to brain cancer research. And lastly, the lack of signal background makes them very specific compared to other imaging modalities.

Even so, luciferases could be applied in research to a much greater extent. Why the hesitation?

In the last decades molecular research has had a high focus on discovering and developing novel reporters, resulting in the availability of different reporters suited for the same purposes. Fluorescence, for example, can mark tumor cells and with the use of a laser it can easily be seen by eye. Or, for example liposomes with MRI contrast in their bilayer, they can be tracked by MRI and don't need a luciferase for monitoring. Besides, the contrast doesn't require a substrate to light up under the camera. Since current glioblastoma diagnostics and follow-up are MRI-guided, research has a relatively high focus at optimizing and developing new MRI applications. This brings us to the understanding that if bioluminescence would be introduced into humans, luciferases would not only serve as optimal tools for basic experimental research but their value would also be extended to preclinical experiments. .

Another practical limitation of bioluminescence is that a sensitive and quick reading luminometer needs to be acquired, which doesn't belong to standard laboratory equipment. However, once a luminometer is purchased it doesn't require much expertise and since the bioluminescence readings are often quick a single machine would serve for a couple of laboratories. Further, for monitoring gene expression in mammalian cells, viral vectors are needed to transduce the BLI genes, which is also not a technique every laboratory is familiar with. However, luciferases can be purchased as purified protein, they can be expressed by bacteria, and mammalian cells can easily be transformed with the protein. And even if stable transduction of the mammalian cells is required, BLI expressing cells can be provided by other laboratories or the technique of transduction can obviously be learned.

Regarding the limitations, for the expansion of luciferases in experimental research we need to continue the work of optimizing the existing variants and the creation of novel reporter systems. Further, it will be essential to have simple protocols for the usage of different BLI constructs for different applications. Luciferases do require special handling; however, with the correct equipment and techniques, they definitely have the potential of becoming valuable tools for every day laboratory use.

In conclusion, molecular research is indispensable for the understanding of cancer and luciferases play an important role in revealing these tumor processes. Therefore, in this thesis, we contributed to a better understanding of luciferases and their applicability in experimental cancer research. For (pre-) clinical purposes we expanded our field to the creation of a liposome that is susceptible for a biotin-streptavidin complex by biotin on its surface and highly sensitive for MRI. Moreover, we evaluated cellular vehicles to efficiently reach and treat the tumor target. Hopefully, in the battle against cancer, luciferases will continue to contribute to a better understanding of cancer and serve as useful guidance tools in the development of new cancer treatment.

REFERENCES

1. Hwang RF. Tumor-stromal interactions assessed by co-injection of pancreatic stellate and cancer cells. *pancreapedia*. Available at: <http://www.pancreapedia.org/tools/methods/tumor-stromal-interactions-assessed-by-co-injection-of-pancreatic-stellate-and-cancer->
2. . *Iavireport*. Available at: [http://www.iavireport.org/Back-Issues/Documents/Figure 1 Testing for gene expression in humanized mice.htm](http://www.iavireport.org/Back-Issues/Documents/Figure_1_Testing_for_gene_expression_in_humanized_mice.htm).
3. Degeling MH, Maguire CA, Bovenberg MS, Tannous BA. (2012). Sensitive assay for mycoplasma detection in mammalian cell culture. *Anal Chem*.84(9):4227-4232.
4. Bovenberg MS, Degeling MH, Tannous BA. (2012). Enhanced gaussia luciferase blood assay for monitoring of in vivo biological processes. *Anal Chem*.84(2):1189-1192.
5. Promega.
6. society Ac. (2011). Can testicular cancer be found early?
7. Freedman RA, Partridge AH. (2011). Adjuvant therapies for very young women with early stage breast cancer. *Breast*.20 Suppl 3:S146-149.
8. Badr CE, Niers JM, Tjon-Kon-Fat LA, Noske DP, Wurdinger T, Tannous BA. (2009). Real-time monitoring of nuclear factor kappaB activity in cultured cells and in animal models. *Mol Imaging*.8(5):278-290.
9. O'Neill K, Lyons SK, Gallagher WM, Curran KM, Byrne AT. (2010). Bioluminescent imaging: a critical tool in pre-clinical oncology research. *J Pathol*.220(3):317-327.
10. Badr CE, Tannous BA. (2011). Bioluminescence imaging: progress and applications. *Trends Biotechnol*.29(12):624-633.
11. Tannous BA, Kim DE, Fernandez JL, Weissleder R, Breakefield XO. (2005). Codon-optimized Gaussia luciferase cDNA for mammalian gene expression in culture and in vivo. *Mol Ther*.11(3):435-443.
12. Wurdinger T, Badr C, Pike L, de Kleine R, Weissleder R, Breakefield XO, et al. (2008). A secreted luciferase for ex vivo monitoring of in vivo processes. *Nat Methods*.5(2):171-173.
13. Maguire CA, Deliolanis NC, Pike L, Niers JM, Tjon-Kon-Fat LA, Sena-Esteves M, et al. (2009). Gaussia luciferase variant for high-throughput functional screening applications. *Anal Chem*.81(16):7102-7106.
14. Chung E, Yamashita H, Au P, Tannous BA, Fukumura D, Jain RK. (2009). Secreted Gaussia luciferase as a biomarker for monitoring tumor progression and treatment response of systemic metastases. *PLoS One*.4(12):e8316.
15. Niers JM, Kerami M, Pike L, Lewandrowski G, Tannous BA. (2011). Multimodal in vivo imaging and blood monitoring of intrinsic and extrinsic apoptosis. *Mol Ther*.19(6):1090-1096.
16. Tannous BA, Teng J. (2011). Secreted blood reporters: insights and applications. *Biotechnol Adv*.29(6):997-1003.
17. Maguire CA, van der Mijn JC, Degeling MH, Morse D, Tannous BA. (2011). Codon-Optimized *Luciola italica* Luciferase Variants for Mammalian Gene Expression in Culture and In Vivo. *Mol Imaging*.

18. Haar CP, Hebbar P, Wallace GC, Das A, Vandergriff WA, 3rd, Smith JA, et al. (2012). Drug resistance in glioblastoma: a mini review. *Neurochem Res.*37(6):1192-1200.
19. Wang Y, Jiang T. (2013). Understanding high grade glioma: molecular mechanism, therapy and comprehensive management. *Cancer Lett.*331(2):139-146.
20. Sulman EP, Guerrero M, Aldape K. (2009). Beyond grade: molecular pathology of malignant gliomas. *Semin Radiat Oncol.*19(3):142-149.
21. Taruttis A, Ntziachristos V. (2012). Translational optical imaging. *AJR Am J Roentgenol.*199(2):263-271.
22. Napp J, Mathejczyk JE, Alves F. (2011). Optical imaging in vivo with a focus on paediatric disease: technical progress, current preclinical and clinical applications and future perspectives. *Pediatr Radiol.*41(2):161-175.
23. Torchilin VP. (2005). Recent advances with liposomes as pharmaceutical carriers. *Nat Rev Drug Discov.*4(2):145-160.
24. Symon Z, Peyser A, Tzemach D, Lyass O, Sucher E, Shezen E, et al. (1999). Selective delivery of doxorubicin to patients with breast carcinoma metastases by stealth liposomes. *Cancer.*86(1):72-78.
25. Weller C, Zschuntzsch J, Makosch G, Metselaar JM, Klinker F, Klinge L, et al. (2012). Motor performance of young dystrophic mdx mice treated with long-circulating prednisolone liposomes. *J Neurosci Res.*90(5):1067-1077.
26. Negishi Y, Hamano N, Shiono H, Akiyama S, Endo-Takahashi Y, Suzuki R, et al. (2012). [The development of an ultrasound-mediated nucleic acid delivery system for treating muscular dystrophies]. *Yakugaku Zasshi.*132(12):1383-1388.
27. Murtas G, Kuruma Y, Bianchini P, Diaspro A, Luisi PL. (2007). Protein synthesis in liposomes with a minimal set of enzymes. *Biochem Biophys Res Commun.*363(1):12-17.
28. Ahmed AU, Thaci B, Alexiades NG, Han Y, Qian S, Liu F, et al. (2011). Neural stem cell-based cell carriers enhance therapeutic efficacy of an oncolytic adenovirus in an orthotopic mouse model of human glioblastoma. *Mol Ther.*19(9):1714-1726.
29. Hingtgen SD, Kasmieh R, van de Water J, Weissleder R, Shah K. (2010). A novel molecule integrating therapeutic and diagnostic activities reveals multiple aspects of stem cell-based therapy. *Stem Cells.*28(4):832-841.
30. Rodriguez A, Regnault A, Kleijmeer M, Ricciardi-Castagnoli P, Amigorena S. (1999). Selective transport of internalized antigens to the cytosol for MHC class I presentation in dendritic cells. *Nat Cell Biol.*1(6):362-368.
31. Kim W, Liao LM. (2010). Dendritic cell vaccines for brain tumors. *Neurosurg Clin N Am.*21(1):139-157.
32. Denny FW, Glezen WP. (1971). Mycoplasma pneumoniae disease: clinical spectrum, pathophysiology, epidemiology, and control. *J Infect Dis.*Jan(123(1)):74-92.
33. Greer LF, 3rd, Szalay AA. (2002). Imaging of light emission from the expression of luciferases in living cells and organisms: a review. *Luminescence.*17(1):43-74.
34. Johnson FH, Shimomura O. (1972). Enzymatic and nonenzymatic bioluminescence. *Photophysiology.*(7):275-334.

35. McElroy WD, Seliger HH, White EH. (1969). Mechanism of bioluminescence, chemiluminescence and enzyme function in the oxidation of firefly luciferin. *Photochem Photobiol.*10(3):153-170.

CHAPTER XIX



SUMMARY

GLIOMA

Glioblastoma multiforme (GBM) is the most malignant variant of glioma. This tumor does not only display an extremely aggressive, invasive growth pattern, but is also very difficult to treat. With a two-year survival rate of 40% and a median survival of 12-18 months after treatment, prognosis is poor. Factors contributing to this outcome can be divided in two groups. First, current treatment options are not successful in halting tumor progression. The current standard of care includes surgical debulking of the tumor mass, followed by radiation and chemotherapy (temozolomide). However, the location of the tumor (the brain) and its invasive, root like growth pattern limit the results that can be achieved by surgery. The same limitations apply to radiotherapeutic treatment, with the nature of the surrounding tissue not allowing high enough doses of radiation to be delivered. Chemotherapeutics cannot cross the blood brain barrier efficiently and often resistance develops before the tumor is eradicated. While treatment has prolonged lifespan from 4-6 months to 12-18 months, we seem to book less progression than seen in other cancer fields.

The second complicating factor, which is closely related to minimal improvements in treatment modalities, is the highly complex and aggressive behavior of GBM tumor cells. GBM tumors are highly heterogeneous, display all kinds of anti-apoptotic escape routes, suppress the immune system, invade the surrounding parenchyma with unmatched aggressiveness and possess a whole array of tools to rearrange the extra tumoral environment to their advantage. Glioma stem cells (GSC) seem to drive this process, and, as recent research has shown, can reestablish a copy of the original tumor when transplanted into immunocompromised mice. Studies investigating the genetic profile of GBM have demonstrated further that the heterogeneity has a strong genetic component. Several genetic alterations can occur, each predisposing its bearer to a certain growth pattern and level of invasiveness and, most importantly, response to therapy. The complexity and crosstalk of intracellular pathways contribute even more to the difficulty of finding an effective treatment.

Whereas for example patients with a loss of chromosome 1p respond to a chemotherapy regimen of PVC (procarbazine, CCNU and vincristine) combined with

temozolomide, GBMs with EGFR-III amplification rarely respond to chemotherapy at all. O6- methylguanine DNA transferrase or MGMT, a DNA repair enzyme that protects cells from damage caused by ionizing radiation and alkylating agents, is currently the most powerful molecular predictor of outcome and benefit of temozolomide treatment. If MGMT methylation is present, the cells are unable to properly repair DNA damage, resulting in a relatively good response to treatment.

Based on current state of matter it can be concluded that new interventions are needed. Gene therapy was long thought to be the magical approach to cure all kind of diseases, including cancer. However, clinical trials have shown this approach has yet to overcome some major limitations in order to make a difference in the medical field. Some mayor successes have been reported, however, many attempts still fail to make a clinically relevant impact. Lack of efficient gene delivery and transfer, and the inability to achieve high enough levels of gene expression are some of the major limitations of this approach. The patient's own immune response against the allogeneic gene and its viral vector is partly responsible for this. Since inadequate expression will confound results, it is hard to judge on the efficacy of certain therapeutic gene strategies and this may partly explain the inconsistency that exists between animal studies and clinical trials.

BIOLUMINESCENCE IMAGING

In order to get a better understanding of glioma tumor biology, and to develop a more successful therapeutic approach, it is important to be able to visualize the processes taking place on cellular, molecular, and even genetic level. Bioluminescence imaging (BLI) is a technique that uses the enzymatic activity of luciferases to visualize all kind of intra- and extracellular processes. In order to emit light, a chemical conversion of the luciferase by its substrate is needed. *American Firefly luciferase* (Fluc), *Gaussia Princeps* (Gluc), *Renilla reniformis* (Rluc) and *Vargulla hilgendorfi* (Vluc) have all successfully been used as mammalian cell reporters.

BLI is extensively used in cancer. Due to the high complexity, the interactions between cells and their environment, intracellular crosstalk and the invasive nature

of GBM tumors, it is highly desirable to be able to label tumor cells and detect cancer pathways. BLI can help understanding these complex processes by visualizing “what happens” during tumorigenesis, by assessing gene activation, cell growth and behavior, tracking of cancer stem cells (CSC) and metastasis and recurrence following chemotherapy. Further, it can potentially visualize tumor cell response to certain therapeutic compounds, allowing us to see which pathways and escape mechanisms are activated and where intervention is needed. Since BLI can be used both *in vitro* and *in vivo*, it can help identifying new cancer treatments by validating experimental drugs in animal models, bridging the gap between the laboratory and the clinic.

OUTLINE

In this thesis we developed reporters, diagnostics and a 'curative strategy' for Glioma, based on the joint forces of BLI and gene therapy.

In **Chapter III** we describe the development of a new antibody based *Gaussia* luciferase blood assay. *Gaussia* luciferase differs from other luciferases in that it is secreted from the cell and can be detected in the circulation. The advantages of this characteristic are huge. Instead of having to measure BLI signal by either using a CCD camera (which is time consuming and static) or by sacrificing the animal, one can simply take an aliquot of blood and measure the Gluc signal. This allows for the *ex vivo* monitoring of *in vivo* processes in real time, which is extremely valuable when studying tumorigenesis. However, Gluc emits blue light, which is partly absorbed by pigmented molecules as hemoglobin. This limits the sensitivity of the assay, as a part of the signal is lost. To overcome this problem, we developed an alternative assay in which Gluc is captured from the blood in an antibody-mediated reaction before the signal is acquired. By elimination of the signal quenching molecules the assay showed to be over one order of magnitude more sensitive in detecting the Gluc signal. The new sensitivity standard will allow us to detect small numbers of circulating cells, early tumor metastasis and apoptosis.

In **Chapter IV** the development of a multiplex *ex vivo* blood reporter system based on the secreted alkaline phosphatase (SEAP), *Gaussia* luciferase and a secreted variant of *Vargula hilgendorfi* is described. We first characterized VLuc as a blood

reporter and multiplexed it with Gluc and SEAP to develop a triple blood reporter system to monitor three distinct biological processes. As a proof of concept, we successfully monitored the response of three different subsets of glioma cells to the chemotherapeutic agent temozolomide in the same animal. This multiplex system can be extended and applied to many different fields for simultaneous monitoring of multiple biological parameters in the same biological system.

In **Chapter V** the development of an *in vivo* triple reporter system based on *Vargula*, *Gaussia* and *Firefly* luciferases for sequential imaging of three different biological processes is described. We applied this system to monitor the effect of the apoptosis-inducing ligand sTRAIL (soluble Tumor necrosis factor-Related Apoptosis-Inducing Ligand) on GBM tumor cells using an adeno-associated viral AAV vector. TRAIL is only toxic to cancer cell since only these cells overexpress TRAIL death receptors. However, there also appears to be a group of tumors, including GBM, that is resistant to TRAIL-mediated apoptosis. To overcome this limitation, we identified a molecule that sensitized GBM cells for TRAIL, called lanatoside C, which is a known cardiac glycoside. Since TRAIL cannot cross the blood brain barrier, we engineered the normal brain to synthesize and secrete sTRAIL. Thereby, we created a zone of resistance against newly developed glioma, which can be treated with lanatoside C therapy. We used Vluc to monitor AAV gene delivery of sTRAIL to the healthy brain parenchyma, Gluc to monitor the binding of sTRAIL to the glioma death receptor on the tumor cells and the consequential activation of downstream events, and Fluc to measure tumor response to combined sTRAIL and lanatoside C treatment. Binding of sTRAIL on tumor cells activated downstream events leading to an initial decrease in glioma proliferation. However, this was followed by tumor re-growth through resistant cells. Co-treatment with lanatoside C sensitized the resistant subpopulation of glioma to sTRAIL-induced apoptosis as monitored by the triple reporter system. Since AAV vectors, TRAIL, and cardiac glycosides have already been used in a clinical setting, though in uncombined administration strategies, this therapeutic strategy could be easily adapted for use in humans. This work is the first demonstration of triple *in vivo* bioluminescence imaging and will have broad applicability in different fields.

In **Chapter VI** the development of better variants of *Gaussia* luciferase, that can be used in the multiplex reporter systems of **Chapter III, IV** and **V**, or by themselves, are described. *Gaussia* luciferase has many advantageous properties over other luciferases, including high signal intensity, favorable enzyme stability and a secretion signal, which allows for signal detection in the blood. However, current limitations of Gluc as a reporter include signal quenching and absorption by pigmented molecules (as discussed in **Chapter IV**) and its flash type light emission, which results in rapid light decay and makes Gluc less suitable as cell viability marker in drug screens. When thousands of compounds need to be tested, stable light emission is required. To overcome these limitations, a library of Gluc variants was generated using directed molecular evolution and screened for relative light output, a shift in emission spectrum, and glow-type (stable) emission kinetics. Several variants with a 10-15nm shifts in emission spectrum were identified, as well as a Gluc variant yielding over 10 minutes of stable light output that can be used in high throughput applications.

Different variants of the same luciferase can be used simultaneously as long as there is enough difference in their range of light emission. In **chapter VII** we characterized a codon-optimized variant of Italian firefly luciferase (liFluc) for mammalian gene expression and used the green and red light emission variants for *in vivo* tumor imaging. The red shifted variant showed to be a useful marker for *in vivo* tumor growth over time.

In **Chapter VIII** and **IX** a simple and sensitive assay to monitor mycoplasma contamination is described. Mycoplasma contamination in mammalian cell culture is often overlooked, yet is a serious issue that can induce a myriad of cellular changes and thereby confound results. Since glioma research heavily relies on cell culture and the effects of mycoplasma can set research projects back for years, we developed a mycoplasma detection assay based on the degradation of Gluc in the conditioned medium of contaminated cells. Whereas Gluc has a half life of > 7 days in the conditioned media of mycoplasma free cells, the half life of Gluc is tremendously decreased in the presence of mycoplasma contaminations, with the level of decline correlating to the mycoplasma infection rate. Our Gluc based mycoplasma assay proved to be more sensitive as compared to commercially available BLI assays.

In **chapter X** we took a different approach for the treatment of brain cancer: we developed a liposome as a contrast agent for MRI with a higher efficiency than the conventional liposome. Liposomes are spherical, self-closed structures formed by one or several concentric lipid bilayers with an aqueous phase inside and between the lipid bilayers. They are proven effective for the delivery of drugs and imaging agents to the tumor site. Our liposome can target cells by its biotin inclusion, it can be monitored by MRI, and the therapeutic agent can be released by ultra sound, due to its thermo-sensitivity.

In **Chapter XI** and **XII** we provided an overview of the Glioma research field, placing the work developed in this thesis in a broader setting. We reviewed current research strategies, both in experimental setting and in the clinic, discussed the translational gap that exists between those two worlds and reflected on possible future directions. Cellular therapeutic strategies (including stem cells and immuno cells) seem to provide a solution for the problems that currently halt the advances in gene therapy. Stem cells have the ability to specifically target glioma cells, both invasive and located in the tumor. Aside from the homing mechanism that selectively targets tumor cells, stem cells can effortlessly cross the BBB, are easily modified to carry therapeutic genes, have immunosuppressive properties that prevent a host immunoreaction after implantation, and seem capable of shielding therapeutics such as oncolytic viruses from the host immune response, thereby ensuring long term reservoirs of therapeutic virus at the tumor site.

Immunocells are used as vaccines to stimulate an antitumor response by the patient's own immune system. The advantage of this approach is the establishment of a sustainable tumor attack, theoretically not only eradicating the tumor, but also protecting the patient against the development of recurrences. Both stem- and immuno cell therapies are now carefully introduced in the clinic, and first results seem to indicate they are well tolerable and safe. The efficacy of these approaches is not yet optimal, but examples in other fields show that when optimization steps are taken, current limitations can be overcome. Suggestions for improvement of the field and the role for BLI in this process are discussed in **Chapter XI, XII** and **XIII**.

CHAPTER XV



SAMENVATTING

GLIOM TUMOREN

Glioblastoma multiforme (GBM) is de meest maligne variant van de glioom tumoren. Deze tumor staat niet alleen bekend om zijn extreem agressieve, invasieve groeipatroon, maar is daarnaast zeer moeilijk te behandelen. Met een 2-jaars overleving van 40% en een mediane overleving van 12 tot 18 maanden is de prognose somber. Factoren die hieraan bijdragen zijn onder te verdelen in twee groepen. Ten eerste zijn de huidige behandelopties niet in staat tumor progressie een halt toe te roepen. Het standaard behandelplan voor GBM tumoren bestaat uit chirurgische resectie van de tumor, gevolgd door bestraling en temozolomide chemotherapie. De locatie van de tumor (het brein) en zijn invasieve, grillige groeipatroon maken het echter praktisch onmogelijk de tumor in zijn totaliteit te verwijderen, terwijl radiotherapie niet in optimale dosering kan worden toegediend door mogelijke schade aan het omliggende weefsel. Verder is de waarde van chemotherapeutica beperkt, doordat de bloed-hersenbarrière efficiënte opname verhindert. Hoewel bestaande behandelingen de levensverwachting van patiënten met GBM hebben verlengd van 4-6 maanden naar 12-18 maanden, lijken de ontwikkelingen en ziekte winst achter te blijven bij de progressie die op andere terreinen van kankeronderzoek geboekt wordt.

De tweede complicerende factor in het GBM onderzoek, die nauw gerelateerd is aan de minieme ontwikkelingen op therapeutisch gebied, is de biologische complexiteit van de GBM tumor formatie. GBM tumoren zijn bijzonder heterogeen, brengen verschillende anti-apoptose mechanismen tot expressie, onderdrukken het immuunsysteem, groeien volgens een zeer invasief patroon diep in het omringende weefsel, en bezitten daarnaast een hele gereedschapskist aan mogelijkheden om het extratumorale weefsel naar hun voordeel te moduleren. Glioma stem cellen (GSC) lijken de drijvende kracht in dit proces. Recent onderzoek heeft aangetoond dat deze cellen in staat zijn een exacte kopie van de originele tumor te genereren, wanneer ze getransplanteerd worden in immuungecompromitteerde muizen. Verder kunnen verschillende genetische veranderingen worden aangetoond, die corresponderen met een specifiek groeipatroon, de mate van invasiviteit en, belangrijkste van al, respons op behandeling.

Waar patiënten met verlies van chromosoom 1p goed reageren op een chemotherapie schema van temozolomide en PVC (procarbazine, CCNU en vincristine), heeft dezelfde behandeling bij patiënten met een EGFR-III mutatie geen enkel effect. O6-methylguanine DNA transferase (MGMT) status is momenteel de meest accurate voorspeller van een goede reactie op temozolomide behandeling. MGMT is een DNA herstel eiwit dat cellen beschermt tegen schade ten gevolge van straling en alkaliserende middelen. In een bepaald percentage GBM tumoren is MGMT gemethyleerd, wat leidt tot een onvermogen temozolomide geïnduceerde DNA schade te herstellen, resulterend in celdood.

Nieuw interventies zijn gezien de huidige stand van zaken meer dan gewenst. Gen therapie werd lange tijd beschouwd als de magische oplossing voor de genezing van velerlei ziekten, waaronder kanker. In klinische studies is echter naar voren gekomen dat deze strategie nog flink wat hindernissen te overwinnen heeft, voordat we kunnen spreken van een doorbraak in de geneeskunde. Hoewel enkele grote successen zijn gerapporteerd, is het percentage studies dat een klinisch relevant resultaat behaalt, nog altijd laag. Een gebrek aan adequate gen overdracht en distributie, en het onvermogen om hoge expressie waarden te bewerkstelligen, zijn enkele van de problemen die overwonnen moeten worden. Het immuunsysteem van de patiënt, dat het gen en bijbehorende virus vector als lichaamsvreemd beschouwd, speelt hierin een belangrijke rol. Aangezien inadequate gen expressie confounding van studie resultaten kan opleveren, waarbij men onterecht aanneemt dat de gekozen therapie niet werkt, is het lastig oordelen over de daadwerkelijke effectiviteit van gen therapie. Dit biedt mogelijk ook een verklaring voor de inconsistentie tussen resultaten verkregen in diermodellen en in klinische studies.

BIOLUMINESCENCE IMAGING

Om een beter inzicht te krijgen in de processen die een rol spelen bij de GBM tumorformatie en om een aanknopingspunt te vinden voor een succesvolle therapeutisch benadering, is het van groot belang om de gebeurtenissen die op cellulair, moleculair en genetisch niveau plaats vinden, te begrijpen. Bioluminescence imaging (BLI) is een techniek die de enzymatische activiteit van luciferases gebruikt om intra- en extracellulaire processen- letterlijk- zichtbaar te

maken. Wanneer een luciferase in contact komt met zijn substraat, wordt licht uitgezonden. Koppeling van het luciferase gen aan het gen dat men wil onderzoeken (gene of interest, GOI), leidt tot het ontstaan van een Bioluminescence signaal op het moment dat het GOI actief wordt (bijvoorbeeld in respons op een bepaald medicijn), terwijl geen signaal gedetecteerd kan worden wanneer activatie niet plaats vindt. *American Firefly* luciferase (Fluc), *Gaussia princeps* (Gluc), *Renilla reniformis* (Rluc) en *Vargulla hilgendorfi* (Vluc) zijn voorbeelden van luciferases die met succes gebruikt zijn als reporters in verscheidene cel systemen.

BLI is een techniek die meer en meer gebruikt wordt in het kankeronderzoek. Door de hoge mate van complexiteit van GBM tumoren, de vele interacties tussen tumorcellen en het omringend weefsel, de intracellulaire crosstalk en het invasieve groeipatroon, is het bijzonder waardevol om cellen te kunnen labelen en vervolgen. Ook de identificatie van de intracellulaire pathways die dit gedrag bewerkstelligen is een cruciaal onderdeel van de zoektocht naar een therapeutische interventie. BLI kan ons helpen deze complexe processen te begrijpen door zichtbaar te maken 'wat er nou precies gebeurt' tijdens de tumorigenese. De activatie van specifieke genen, de groei en gedragsveranderingen van cellen, de effecten van Kanker Stam Cellen (cancer stem cells, CSC) en hun patroon van metastase en recidief formatie na chemotherapie kan theoretisch allemaal gevolgd worden via BLI. Ook de tumor cel respons op bepaalde middelen, met activatie van bepaalde pathways en escape routes, zou via BLI in beeld gebracht moeten kunnen worden, met een 'map' van mogelijke interventiepunten als resultaat. Aangezien BLI zowel *in vitro* als *in vivo* toepasbaar is, kan het tevens een belangrijke 'tool' worden voor de validatie van experimentele anti kanker medicijnen in diermodellen, daarmee een brug slaand tussen cel modellen en de kliniek.

In dit proefschrift hebben we de krachten van genterapie en Bioluminescence imaging gecombineerd voor de ontwikkeling van nieuwe reporters, diagnostische tools en een potentieel therapeutische interventie voor GBM.

OVERZICHT

In dit proefschrift hebben we reporters, diagnostische tools en een “curatieve strategie” ontwikkeld voor de behandeling van Glioom tumoren, op basis van gen therapie en BLI.

In **Hoofdstuk III** beschrijven we de ontwikkeling van een nieuwe assay voor de detectie van Gluc in het bloed, gebaseerd op een antilichaam reactie. *Gaussia* luciferase verschilt van andere luciferases in feit dat het gesecreteerd wordt door de cellen die het Gluc gen tot expressie brengen en in de circulatie terecht komt. De voordelen van deze eigenschap zijn enorm. In plaats van meting van het BLI signaal door middel van een CCD camera (wat een tijdrovend en statisch proces is) of door opoffering van het proefdier, kan worden volstaan met het afnemen van enkele druppels bloed waaruit vervolgens het Gluc signaal bepaald kan worden. Dit stelt men in staat om *ex vivo in vivo* processen te vervolgen op het moment dat deze ook daadwerkelijk plaatsvinden (en niet pas minuten, uren of dagen later). Voor het ontrafelen van tumorgeneese is dat van onvoorstelbaar belang. Een limiterende factor in deze strategie werd gevormd door het feit dat Gluc blauw licht uitstraalt. Blauw licht wordt geabsorbeerd door gepigmenteerde moleculen als hemoglobine, wat de sensitiviteit van de assay sterk doet afnemen, aangezien een deel van het signaal verdwijnt. Om dit probleem te omzeilen hebben we een alternatieve assay ontwikkeld, waarin Gluc wordt ‘gevangen’ uit het bloed door een antilichaam, voordat de Bioluminescence reactie plaatsvindt. Doordat de reactie nu plaats kan vinden in de afwezigheid van signaal absorberende moleculen, is de sensitiviteit van het bloed assay met meer dan een orde van grootte toegenomen en zijn we in staat om een tiental circulerende cellen en beginnende metastasen te detecteren.

In **Hoofdstuk IV** beschrijven we de ontwikkeling van een multiplex reporter in het bloed gebaseerd op secreted alkaline phosphatase (SEAP), *Gaussia* luciferase en *Vargula hilgendorfi*, voor het *ex vivo* analyseren van gebeurtenissen *in vivo*. Vluc was nog niet eerder gebruikt als reporter in het bloed en moest daarom eerst gekarakteriseerd worden. Vervolgens zijn Vluc, Gluc en SEAP gebruikt voor de ontwikkeling van een reporter die gebruikt kan worden voor het gelijktijdig meten van drie verschillende biologische parameters in het bloed. Waar in de praktijk de CCD

camera gebruikt wordt om de activiteit van luciferases te monitoren, volstaat voor deze nieuwe reporter het afnemen van enkele druppels bloed op de door de onderzoeker gewenste tijdstippen. Dit heeft niet alleen het voordeel dat de procedure zo een stuk minder tijd in beslag neemt, maar daarnaast stelt het de onderzoeker in staat in real time cellulaire processen te vervolgen, zonder rekening te hoeven houden met de halfwaarde van een eventueel eerder gemeten signaal. Om de reporter te testen werd de reactie van 3 verschillende glioma cel lijnen op het chemotherapeuticum temozolomide gelijktijdig gemeten in hetzelfde proefdier. De drie verschillende signalen waren goed van elkaar te onderscheiden en leken niet met elkaar te reageren. Dit systeem kan op heel veel verschillende gebieden worden toegepast.

In **Hoofdstuk V** beschrijven we de ontwikkeling van een drievoudig reporter systeem, gebaseerd op *Vargula*, *Gaussia* en *Firefly* luciferase, voor het gelijktijdig vervolgen van drie verschillende biologische processen *in vivo*. Dit systeem is vervolgens gebruikt om het effect van soluble tumor necrosis factor-related apoptosis-inducing ligand (sTRAIL, verpakt in een AAV vector) gecombineerd met de cardiac glycoside Lanatoside C in verschillende glioom modellen te evalueren. De TRAIL death-receptor wordt alleen tot expressie gebracht door tumor cellen, waardoor gezonde cellen geen schade ondervinden van de toediening van TRAIL. Er lijkt echter ook een groep tumoren te bestaan, die niet gevoelig is voor door TRAIL gemedieerde celdood. Gliomen behoren helaas tot deze groep. In een poging deze resistentie te overwinnen, hebben we een screen gedaan naar moleculen die glioomcellen gevoelig maken voor TRAIL, leidend tot de identificatie van Lanatoside C.

Aangezien TRAIL niet instaat is de bloed hersen barriere te passeren, hebben we eerst het gezonde hersenweefsel gemodificeerd om sTRAIL tot expressie te brengen. Dit resulteerde in de formatie van een 'zone of resistance' rondom de tumor cellen. Lanatoside C werd vervolgens gebruikt als therapeuticum. Om een inzicht te krijgen in het precieze werkingsmechanisme van ons systeem is VLuc expressie gekoppeld aan het AAV-sTRAIL gen, waardoor gen-transfer en expressie gekwantificeerd kon worden. Daarnaast is Gluc expressie gekoppeld aan activatie van de glioma death receptor en de daaropvolgende activatie van intracellulaire cascades, terwijl Fluc als maat dient voor de reactie van de tumor op de

gecombineerde behandeling van sTRAIL en Lanatoside C. Hierdoor konden we zien dat de binding van TRAIL aan de tumorcellen (Vluc) leidde tot de activatie van verschillende intracellulaire pathways (Gluc) en een initiële afname van de glioom cel proliferatie (Fluc). Dit werd echter gevold door een fase van hergroei door therapie resistente cellen (Fluc). Wanneer we echter sTRAIL tegelijk met Lanatoside C toedienden, bleek dat ook de subpopulatie van resistente cellen werd geëlimineerd. Aangezien AAV-vectoren, TRAIL en Lanatoside C allen onafhankelijk van elkaar al enkele jaren met goedkeuring van de FDA in de kliniek gebruikt worden, zou het relatief eenvoudig moeten zijn om deze combinatietherapie voor GBM voor patiënten beschikbaar te maken. Het drievoudige *in vivo* BLI reporter systeem dat wij ontwikkeld hebben voor deze studie is het eerste in zijn soort, en heeft een brede toepasbaarheid in vele onderzoeksgebieden.

In **Hoofdstuk VI** beschrijven we de ontwikkeling van nieuwe en betere varianten van *Gaussia* luciferase, die zowel gebruikt kunnen worden in de boven beschreven reportersystemen (Hoofdstuk 3, 4 en 5) als op zichzelf. *Gaussia* luciferase heeft vele eigenschappen die het de luciferase van keuze maakt voor velerlei toepassingen, zoals een hoge signaal intensiteit, gunstige enzym stabiliteit en een secretie sequentie, die detectie in het bloed mogelijk maakt. Echter, de emissie van licht in de blauwe zone van het spectrum (zoals besproken in hoofdstuk III) en een flash-type bioluminescence reactie, maken dat Gluc niet voor alle toepassingen even geschikt is. De flash-type bioluminescence, waarbij snelle afname van het signaal volgt na contact met het substraat, is vooral onhandig wanneer grote hoeveelheden data geanalyseerd dienen te worden, zoals bij een high throughput drug screen. De waarde van Gluc als cell viability marker is in die situatie beperkt, aangezien er, puur door de tijd die het kost het signaal te lezen, afname van de signaal intensiteit ontstaat, en het begin en einde van de screen daardoor niet goed met elkaar vergeleken kunnen worden. In een poging deze eigenschap te veranderen, hebben wij een middels 'directed molecular evolution' een library van > 5000 Gluc varianten gegenereerd. Al deze varianten zijn gescreend voor signaal intensiteit, een shift in emissiespectrum, en glow-type (stabiele) licht emissie. De screen heeft verschillende varianten met een 10 tot 15nm shift in emissie spectrum opgeleverd en een Gluc variant met een licht output die stabiel bleef gedurende 10 minuten. Deze laatste variant is daarmee bijzonder geschikt voor high throughput applicaties.

Het is ook mogelijk verschillende varianten van dezelfde luciferase tegelijk toe te passen, zolang ze maar verschillen in lichtemissie. In **hoofdstuk VII** hebben we een codon geoptimaliseerde variant van de Italian Firefly luciferase (liFluc) gekarakteriseerd voor genexpressie in zoogdiercellen. Bovendien hebben we de rood-lichtemissie variant toegepast in *in vivo* tumor beeldvorming. De rode variant bleek een succesvolle marker voor het in tijd volgen van tumorgroei.

In **Hoofdstuk VIII** en **IX** beschrijven we het ontstaan van een eenvoudige en sensitieve assay voor het detecteren van mycoplasma contaminatie. Mycoplasma contaminatie in celkweek wordt vaak niet opgemerkt, maar is een ernstig probleem dat een scala aan cellulaire veranderingen veroorzaakt en daarmee onderzoeksresultaten in sterke mate kan beïnvloeden. Aangezien celkweek de fundatie vormt voor glioomonderzoek en mycoplasmacontaminatie kan leiden tot het weggooien van jaren van onderzoek, hebben we een mycoplasma detectie assay ontwikkeld gebaseerd op de degradatie van Gluc in het medium van gecontamineerde cellen. Onder normale omstandigheden heeft Gluc een halfwaardetijd van > 7 dagen. Echter, in de aanwezigheid van Mycoplasma wordt Gluc afgebroken met een snelheid die direct correspondeert met de hoeveelheid mycoplasma contaminatie. Ons op Gluc gebaseerde mycoplasma detectie assay is daarmee sensitiever dan de detectie kits die momenteel commercieel verkrijgbaar zijn.

Ons onderzoek naar de therapie en diagnostiek naar hersentumoren neemt een andere wending in **hoofdstuk X**: we hebben een liposoom ontworpen die over een hogere contrastintensiteit voor MRI onderzoek beschikt dan de conventionele liposoom. Liposomen zijn sferische, afgesloten structuren die uit een dubbele lipide buitenlaag bestaan met daartussen en in het centrum van de liposoom een waterachtige substantie. Ze zijn bewezen effectief voor het vervoer van drugs en beeldvormende stoffen naar de tumorcellen. Onze liposoom kan vanwege zijn biotin doelgericht specifieke cellen bereiken, zijn baan kan worden gevolgd met MRI, en vanwege zijn thermosensitiviteit kan de therapeutische inhoud op de gewenste locaties worden vrijgelaten met behulp van Ultra Sound.

In **Hoofdstuk XI** en **XII** geven we tot slot een overzicht van de huidige stand van zaken in het glioom onderzoek, waardoor het werk van dit proefschrift in een breder kader geplaatst kan worden. We bespreken verschillende onderzoeksstrategieën, zowel in experimentele setting als in de kliniek, en evalueren het gat dat tussen beide werelden bestaat. Verder gaan we in op stappen die ons in ziens ondernomen moeten worden om het onderzoeksveld op een hoger plan te tillen. Cel therapie (zowel stam cel therapie als immunocell therapie) lijkt een oplossing te bieden voor veel van de problemen die de effectiviteit en progressie van het genterapie onderzoek momenteel belemmeren. Stam cellen kunnen gebruikt worden als transport middel voor therapeutische genen en zijn in staat specifiek glioom cellen op te sporen, zelfs wanneer het metastasen betreft, bestaande uit slechts enkele cellen. Ze passeren zonder moeite de bloed –hersenbarrière en hebben een lokaal immunosuppressieve werking, wat voorkomt dat er een immuunreactie volgt na transplantatie. Ook schermen ze het therapeutische gen af van het immuunsysteem, wat leidt tot een vele male effectievere gen-transfer en een langdurige antitumor respons. Immuun cellen daarentegen worden vaak gebruik als cel vaccins en maken juist gebruik van het immuunsysteem van de patiënt. Het voordeel van deze aanpak is dat het eigen immuunsysteem van de patiënt wordt gestimuleerd om de tumor aan te vallen, wat niet alleen leidt tot eradicatie van de tumor, maar de patiënt in theorie ook zou moeten beschermen tegen het ontstaan van recidieven. Zowel stamcel- als immunotherapie vindt langzaam de weg naar de kliniek, waar de eerste trials laten zien dat ze (in ieder geval op korte termijn) veilig zijn en goed getolereerd worden. De resultaten uit experimentele studies heeft men nog niet kunnen evenaren, maar voorbeelden uit andere onderzoeksgebieden laten zien dat met de nodige optimalisatie veel van de huidige problematiek overwonnen kan worden. Suggesties voor verbeteringen, en de potentiële rol van BLI hierin, worden besproken in hoofdstuk XI en XII en XIII.

ACKNOWLEDGEMENTS

Writing a dissertation is by no means a solitary accomplishment. Here we would like to name the many inspiring people that contributed along our journey.

First and foremost, we would like to express our sincere gratitude to Prof. Tannous for his guidance, patience, motivation, immense knowledge, and above all for his invaluable support as a mentor and a friend. Dear Bakhos, it was an honor to work with you!

Dr. Vleggeert-Lankamp, dear Carmen, thank you for introducing us to research in such an early stage of our medical studies and showing us what women can accomplish in the academic world. You have been a source of inspiration throughout and your advice and input have greatly contributed to our dissertation.

Prof. Peul, thank you for supporting this collaboration between Boston and Leiden and for your valuable input in our PhD trajectory.

Dr. Maguire, dear Casey, you taught us all the skills required in a lab and made researchers out of us. Thank you for your patience, dedication and expertise. Our gratitude applies to all our fellow lab mates in the Tannous and Breakefield lab; you all have made our time in Boston unique. Many thanks for all the help and shared knowledge. Regarding our laboratory skills we are also grateful to Prof. ten Dijke, who provided us with a basic training in Molecular Biology.

We would like to thank both the consecutive Deans of the Leiden University Medical Center, Prof. Klasen and Prof. Hogendoorn, for their valuable support and guidance in our medical career paths, and the members of our PhD committee. Thank you for your interest and willingness to take a seat in the committee.

Personal Acknowledgements by Sarah Bovenberg

To my dear friends, in Leiden, Boston or anywhere in the world: thank you for all the support, laughs and unforgettable moments. You are the antidote for too many hours in the lab or library.

Daan en Lau, mijn maatjes. Ik ben trots en dankbaar dat jullie mij vandaag bij staan als paranimfen; moge het symbolisch zijn voor hoe belangrijk jullie voor mij zijn in het gewone leven. Dank voor alle support, interesse en bovenal voor het vermogen om overal de draak mee te steken. Jullie humor plaatst zaken in het juiste perspectief, en dat is onmisbaar.

Julian, een wijs man zei ooit: 'The world needs dreamers and the world needs doers. But above all, the world needs dreamers who do.' Jij bent er een uit die unieke laatste categorie. Dank voor je kijk op het leven en de kleur die je overal aan geeft. Jouw liefde en 'passie for life' maken dat iedere dag een gouden randje heeft.

Lieve pap en mam, jullie zijn de laatsten op de lijst, want zoals ze zeggen: 'save the best for last.' Jullie betrokkenheid, enthousiasme en onvoorwaardelijk vertrouwen is goud waard. Pap, jij bent een steunpilaar in alles. Als ik ooit maar half zo veel weet als jij ben ik een gezegend mens. Mam, jouw zorgzaamheid en behulpzaamheid zijn zelfs aan de andere kant van de oceaan te voelen. Al ben ik vaak ver weg, er is altijd een warm huis om naar terug te keren. Ik kan jullie niet genoeg bedanken.

Personal Acknowledgements by Hannah Degeling

Waar anders te beginnen dan bij mijn goede vrienden? Ik wil mijn vrienden bedanken omdat ik ze kan vertrouwen, omdat ze mij kracht en moed geven en omdat ze me altijd bijstaan. Jaren heb ik van huis gewoond, maar mijn vrienden waren dichtbij.

Ik ben mijn paranimf Nadia Atai dankbaar. Iedere keer als ik met haar praat over het onderzoek, over onze levenspaden, of eigenlijk over alles wat het leven omvat dan geeft ze mij energie en ideeën.

Matthijs, mijn wijze broer en paranimf, is van jongs af aan mijn maatje. Niet alleen heeft hij overal een antwoord op en oplossing voor, maar met zijn scherpe geest en pragmatisme waakt hij ook nog eens over zijn kleine zusje.

Tenslotte bedank ik mijn ouders voor hun onvoorwaardelijke liefde en steun.

OVERVIEW PUBLICATIONS SARAH BOVENBERG

Bovenberg M.S.S, Degeling MH, Vleggeert CLAM, Wurdinger T and Bakhos A Tannous **Multiplex blood reporters for simultaneous monitoring of cellular processes.** May 2013, *Analytical Chemistry*, 2013 Nov 5;85(21):10205-10

Bovenberg MSS*, Degeling MH* and Bakhos A. Tannous **Cell-based immunotherapy against Glioma: from bench to bedside.** *Molecular Therapy*, 2013 Jul;21(7):1297-305 * These authors contributed equally.

Bovenberg MSS*, Degeling MH* and Bakhos A. Tannous **Advances in the development of stem cell therapy for Glioma.** *Trends in Molecular Medicine*, 2013 May 19;(5) 281-291 * These authors contributed equally.

Bovenberg MSS*, Degeling MH*, Lewandrowski G, de Gooijer MC, Vleggeert CLAM and Bakhos A. Tannous **Directed molecular evolution reveals *Gaussia* luciferase variants with enhanced light output stability.** *Anal Chem.* 2013 Mar 5;85(5):3006-12 * These authors contributed equally.

Bovenberg MSS*, Degeling MH* and Bkayos A Tannous **Enhanced *Gaussia* luciferase blood assay for monitoring of in vivo biological processes.** *Anal Chem.* 2012 Jan 17; 84(2):1189-92. * These authors contributed equally.

Bovenberg M.S.S*, Degeling MH*, Tannous M, Bakhos A Tannous ***Gaussia* luciferase-based mycoplasma detection assay in mammalian cell culture** *Methods Mol. Biol.* 2014; 1098:47-55 * These authors contributed equally.

Maguire CA, Bovenberg MSS, Tannous BA. **Novel triple bioluminescence imaging system for monitoring of glioma response to combined soluble TRAIL and lanatoside C therapy.** *Mol Ther Nucleic Acids*, 2013 June 18; 2e99

M. Hannah Degeling, M. Sarah S. Bovenberg and Bakhos A. Tannous. **Sensitive assay for Mycoplasma detection in Mammalian cell culture.** *Anal Chem.* 2012 May 1; 84(9):4227- 32.

Bovenberg M.S.S*, Degeling MH*, de Ruiter GC, LAKke EA and Vleggeert CLAM **Type grouping in rat skeletal muscle after crush injury.** *J Neurosurgery.* 2011;114(5):1449-56 1098:47-55 * These authors contributed equally

CURRICULUM VITAE SARAH BOVENBERG

Maria Sarah Sophie Bovenberg was born in Utrecht, the Netherlands, on the 22nd of August, 1987. She graduated the Erasmiaans Gymnasium in 2005 and started medical school at Leiden University in September of that same year. During her second year in medical school she spent a semester at Karolinska Institutet in Stockholm, Sweden, which triggered her interest in research. Upon return to Leiden she participated in the Leiden Medical School Honors Class and was invited to join the Excellent Student Program, which provided her with the opportunity to work as a student-researcher at the Neurosurgery Department under Dr. Carmen Vleggeert. The collaboration resulted in a publication in a peer reviewed medical journal and a written grant/study proposal. After completing the first part of her medical studies in early 2009, Sarah started a 2-month internship at the Leiden Molecular Cell Biology department and afterwards moved to Boston for a PhD trajectory at the Tannous Lab of Experimental Therapeutics and Molecular Imaging, an affiliation of Harvard Medical School. Under the supervision of Prof. Tannous she conducted several studies on Bioluminescence and Gene Therapy for Glioblastoma Multiforme and attended classes on Neurobiology, Gene Therapy and Developmental Neurobiology at Harvard Medical School. After her return to the Netherlands in 2012, Sarah continued her medical training at Leiden University. She also completed 2 internships in primary care and dermatology at the John Burns School of Medicine in Hawaii, USA, and is busy setting up a company aimed at the American medical education market. She will graduate medical school in the fall of 2014.

OVERVIEW PUBLICATIONS HANNAH DEGELING

M. Hannah Degeling*, M. Sarah S. Bovenberg*, and Bakhos A. Tannous
* These authors contributed equally. **Cell-based immunotherapy against gliomas: from bench to bedside.** *Molecular therapy*, May 2013

M. Hannah Degeling*, M. Sarah S. Bovenberg*, and Bakhos A. Tannous
* These authors contributed equally. **Advances in the development of stem cell therapy against gliomas.** *Trends in Molecular Medicine*, March 25, 2013

M. Hannah Degeling*, M. Sarah S. Bovenberg*, Grant K. Lewandrowski, Mark C. de Gooijer, Carmen L.A.M. Vleggeert-Lankamp, Marie Tannous, Casey A. Maguire, and Bakhos A. Tannous* * These authors contributed equally. **Directed molecular evolution reveals *Gaussia* luciferase putative core region and variants with emission spectral shift and enhanced light stability.** *Analytical Chemistry*, March 5 2013

M. Hannah Degeling, M. Sarah S. Bovenberg and Bakhos A. Tannous
A simple assay for mycoplasma detection in mammalian cell culture. *Analytical Chemistry*, 16th April 2012

M. Hannah Degeling*, M. Sarah S. Bovenberg*, and Bakhos A. Tannous.
*These authors contributed equally. ***Gaussia* luciferase-based mycoplasma detection assay in mammalian cell culture.** *Methods in Molecular biology*, Humana Press, USA

M. Hannah Degeling*, M. Sarah S. Bovenberg* and Bakhos A. Tannous * equal contribution. **An enhanced *Gaussia* luciferase blood assay for monitoring of in vivo biological processes.** *Analytical Chemistry*, Dec 27th, 2011

Maguire CA, Casey, van der Mijl JC, Degeling MH, Morse D and Tannous BA.
Codon optimized *Luciola italica* luciferase variants for mammalian gene expression in culture and in vivo. *Mol imaging*, 2011 June 9

Degeling MH*, Bovenberg MS*, de Ruiter GC, Feirabend HK, Lakke EA, Vleggeert Lankamp CL. *equal contribution. **Type grouping in skeletal muscle after crush injury.** *J. Neurosurgery* 114:1449-1456, 2011

Kuijten MMP, Degeling MH, Chen J, Weissleder R, Nicolay K and Tannous BA.
Multimodal targeted high relaxivity liposome for in vivo imaging. Submitted to *Analytical chemistry*

M. Sarah S. Bovenberg, M. Hannah Degeling, Sayedali Hejazi, Romain Amante, Marte van Keulen, Judith W.M. Jeuken, Sepideh Akbaripanihi, Carmen L.A. Vleggeert-Lankamp, Marie Tannous⁵, Pieter Wesseling, Thomas Wurdinger, and Bakhos A. Tannous. **Multiplex blood reporters for simultaneous monitoring of cellular processes.** *Analytical Chemistry*, Oct 11 2013

CURRICULUM VITAE HANNAH DEGELING

Hannah Degeling was born in Amsterdam, The Netherlands on the 2nd of December in 1986. In 2005 she obtained her high school Gymnasium diploma with credit at Laar en Berg in Laren. Subsequently she enrolled for the Leiden University Medical School. In her second year of studies she attended an exchange program for a full semester in Stockholm at Karolinska Institutet. After returning to Leiden she retrieved interest in the combination of research and neurosurgery and started a research project at the Neurosurgery department of Leiden under surveillance of dr. C.L.A.M Vleggeert-Lankamp. She obtained her doctorate of Leiden Medical School in 2009 and moved to Boston to start a PhD program at Massachusetts General Hospital and Leiden Neurosurgery department with prof. W.C. Peul as her promoter. Next to the research at the Harvard neuroscience laboratory she attended two courses at Harvard Medical School: Development Neurobiology and Neurobiology. After 3 years of laboratory work she returned to The Netherlands in June 2012 to start her medical internships at Leiden University. During this period she also completed the remaining writing work for the thesis and composed lectures for an Education company to prepare nurses for their Hesi and NCLEX exams. In 2013 she lived for 3 months in Suriname to fulfill her gynecology internship. And from January 2014 until July 2014 she will conclude her medical training by internships of plastic surgery and general surgery at the VU Medical center and the Antoni van Leeuwenhoek hospital.

Hannah dedicates much of her time to sport activities and is currently a member of the Flakkee athletics club.